

World Journal of *Gastroenterology*

World J Gastroenterol 2019 March 21; 25(11): 1289-1431



**REVIEW**

- 1289** Emerging role of ^{18}F -fluorodeoxyglucose positron emission tomography for guiding management of hepatocellular carcinoma
Lee SM, Kim HS, Lee S, Lee JW
- 1307** Noninvasive evaluation of nonalcoholic fatty liver disease: Current evidence and practice
Zhou JH, Cai JJ, She ZG, Li HL

ORIGINAL ARTICLE**Basic Study**

- 1327** Economic evaluation of the hepatitis C elimination strategy in Greece in the era of affordable direct-acting antivirals
Gountas I, Syrsa V, Papatheodoridis G, Souliotis K, Athanasakis K, Razavi H, Hatzakis A
- 1341** Clinical assessment and identification of immuno-oncology markers concerning the 19-gene based risk classifier in stage IV colorectal cancer
Lee JL, Roh SA, Kim CW, Kwon YH, Ha YJ, Kim SK, Kim SY, Cho DH, Kim YS, Kim JC
- 1355** Hemodynamic changes in hepatic sinusoids of hepatic steatosis mice
Fan J, Chen CJ, Wang YC, Quan W, Wang JW, Zhang WG

Case Control Study

- 1366** Diffusion-weighted magnetic resonance imaging and micro-RNA in the diagnosis of hepatic fibrosis in chronic hepatitis C virus
Besheer T, Elalfy H, Abd El-Maksoud M, Abd El-Razek A, Taman S, Zalata K, Elkashef W, Zaghloul H, Elshahawy H, Raafat D, Elemshaty W, Elsayed E, El-Gilany AH, El-Bendary M

Retrospective Study

- 1378** Early gastric cancer diagnostic ability of ultrathin endoscope loaded with laser light source
Suzuki T, Kitagawa Y, Nankinzan R, Yamaguchi T
- 1387** Clinical outcomes of ampullary neoplasms in resected margin positive or uncertain cases after endoscopic papillectomy
Sakai A, Tsujimae M, Masuda A, Iemoto T, Ashina S, Yamakawa K, Tanaka T, Tanaka S, Yamada Y, Nakano R, Sato Y, Kurosawa M, Ikegawa T, Fujigaki S, Kobayashi T, Shiomi H, Arisaka Y, Itoh T, Kodama Y
- 1398** Serum Mac-2 binding protein glycosylation isomer level predicts hepatocellular carcinoma development in E-negative chronic hepatitis B patients
Mak LY, To WP, Wong DKH, Fung J, Liu F, Seto WK, Lai CL, Yuen MF

Observational Study

- 1409** Gluten immunogenic peptide excretion detects dietary transgressions in treated celiac disease patients
Costa AF, Sugai E, Temprano MDLP, Niveloni SI, Vázquez H, Moreno ML, Domínguez-Flores MR, Muñoz-Suano A, Smecuol E, Stefanolo JP, González AF, Cebolla-Ramírez A, Mauriño E, Verdú EF, Bai JC

Randomized Clinical Trial

- 1421** Khubchandani's procedure combined with stapled posterior rectal wall resection for rectocele
Shao Y, Fu YX, Wang QF, Cheng ZQ, Zhang GY, Hu SY

ABOUT COVER

Editorial board member of *World Journal of Gastroenterology*, Jia-Xu Chen, MD, PhD, Professor, Traditional Chinese Medicine Diagnostics, School of Pre-Clinic Medicine, Beijing University of Chinese Medicine, Beijing 100029, China

AIMS AND SCOPE

World Journal of Gastroenterology (*World J Gastroenterol*, *WJG*, print ISSN 1007-9327, online ISSN 2219-2840, DOI: 10.3748) is a peer-reviewed open access journal. The *WJG* Editorial Board consists of 642 experts in gastroenterology and hepatology from 59 countries.

The primary task of *WJG* is to rapidly publish high-quality original articles, reviews, and commentaries in the fields of gastroenterology, hepatology, gastrointestinal endoscopy, gastrointestinal surgery, hepatobiliary surgery, gastrointestinal oncology, gastrointestinal radiation oncology, etc. The *WJG* is dedicated to become an influential and prestigious journal in gastroenterology and hepatology, to promote the development of above disciplines, and to improve the diagnostic and therapeutic skill and expertise of clinicians.

INDEXING/ABSTRACTING

The *WJG* is now indexed in Current Contents®/Clinical Medicine, Science Citation Index Expanded (also known as SciSearch®), Journal Citation Reports®, Index Medicus, MEDLINE, PubMed, PubMed Central, Scopus and Directory of Open Access Journals. The 2018 edition of Journal Citation Report® cites the 2017 impact factor for *WJG* as 3.300 (5-year impact factor: 3.387), ranking *WJG* as 35th among 80 journals in gastroenterology and hepatology (quartile in category Q2).

RESPONSIBLE EDITORS
FOR THIS ISSUE

Responsible Electronic Editor: Yan Huang

Proofing Editorial Office Director: Ze-Mao Gong

NAME OF JOURNAL

World Journal of Gastroenterology

ISSN

ISSN 1007-9327 (print) ISSN 2219-2840 (online)

LAUNCH DATE

October 1, 1995

FREQUENCY

Weekly

EDITORS-IN-CHIEF

Subrata Ghosh, Andrzej S Tarnawski

EDITORIAL BOARD MEMBERS

<http://www.wjgnet.com/1007-9327/editorialboard.htm>

EDITORIAL OFFICE

Ze-Mao Gong, Director

PUBLICATION DATE

March 21, 2019

COPYRIGHT

© 2019 Baishideng Publishing Group Inc

INSTRUCTIONS TO AUTHORS

<https://www.wjgnet.com/bpg/gerinfo/204>

GUIDELINES FOR ETHICS DOCUMENTS

<https://www.wjgnet.com/bpg/GerInfo/287>

GUIDELINES FOR NON-NATIVE SPEAKERS OF ENGLISH

<https://www.wjgnet.com/bpg/gerinfo/240>

PUBLICATION MISCONDUCT

<https://www.wjgnet.com/bpg/gerinfo/208>

ARTICLE PROCESSING CHARGE

<https://www.wjgnet.com/bpg/gerinfo/242>

STEPS FOR SUBMITTING MANUSCRIPTS

<https://www.wjgnet.com/bpg/GerInfo/239>

ONLINE SUBMISSION

<https://www.f6publishing.com>



Emerging role of ^{18}F -fluorodeoxyglucose positron emission tomography for guiding management of hepatocellular carcinoma

Sang Mi Lee, Hong Soo Kim, Sangheun Lee, Jeong Won Lee

ORCID number: Sang Mi Lee (0000-0002-7943-3807); Hong Soo Kim (0000-0003-3966-9302); Sangheun Lee (0000-0002-7884-1622); Jeong Won Lee (0000-0002-2697-3578).

Author contributions: All authors equally contributed to this paper with conception and design of the study, literature review, drafting, revision, editing of the paper, and approval of the final version.

Supported by the Soonchunhyang University Research Fund.

Conflict-of-interest statement: No potential conflicts of interest.

Open-Access: This is an open-access article that was selected by an in-house editor and fully peer-reviewed by external reviewers. It is distributed in accordance with the Creative Commons Attribution Non Commercial (CC BY-NC 4.0) license, which permits others to distribute, remix, adapt, build upon this work non-commercially, and license their derivative works on different terms, provided the original work is properly cited and the use is non-commercial. See: <http://creativecommons.org/licenses/by-nc/4.0/>

Manuscript source: Invited manuscript

Received: January 24, 2019

Peer-review started: January 24, 2019

First decision: February 21, 2019

Revised: February 25, 2019

Accepted: March 1, 2019

Article in press: March 1, 2019

Sang Mi Lee, Department of Nuclear Medicine, Soonchunhyang University Cheonan Hospital, Cheonan, Chungcheongnam-do 31151, South Korea

Hong Soo Kim, Department of Internal Medicine, Soonchunhyang University Cheonan Hospital, Cheonan, Chungcheongnam-do 31151, South Korea

Sangheun Lee, Division of Hepatology, Department of Internal medicine, Catholic Kwandong University College of Medicine, International St. Mary's Hospital, Incheon 22711, South Korea

Sangheun Lee, Institute for Health and Life Science, Catholic Kwandong University College of Medicine, International St. Mary's Hospital, Incheon 22711, South Korea

Jeong Won Lee, Department of Nuclear Medicine, Catholic Kwandong University College of Medicine, International St. Mary's Hospital, Incheon 22711, South Korea

Corresponding author: Jeong Won Lee, MD, PhD, Associate Professor, Department of Nuclear Medicine, Catholic Kwandong University College of Medicine, International St. Mary's Hospital, 25, Simgok-ro 100 beon-gil, Seo-gu, Incheon 22711, South Korea.

jwlee223@ish.ac.kr

Telephone: +82-32-2902975

Fax: +82-32-2903128

Abstract

Hepatocellular carcinoma (HCC) is one of major causes of cancer mortality worldwide. For decades, ^{18}F -fluorodeoxyglucose (FDG) positron emission tomography (PET) has been widely used for staging, predicting prognosis, and detecting cancer recurrence in various types of malignant diseases. Due to low sensitivity of FDG PET for detecting intrahepatic HCC lesions, the clinical value of FDG PET in HCC patients has been limited. However, recent studies with diverse analytic methods have shown that FDG PET has promising role in aiding management of HCC patients. In this review, we will discuss the clinical role of FDG PET for staging, predicting prognosis, and evaluating treatment response in HCC. Further, we will focus on recent clinical studies regarding implication of volumetric FDG PET parameters, the significance of FDG uptake in HCC for selecting treatment and predicting treatment response, and the use of radiomics of FDG PET in HCC.

Key words: Hepatocellular carcinoma; Fluorodeoxyglucose F18; Positron emission tomography; Staging; Prognosis

Core tip: Because of low sensitivity, clinical use of ^{18}F -fluorodeoxyglucose (FDG) positron emission tomography (PET) has been limited in patients with hepatocellular carcinoma (HCC). However, recent studies have shown clinical significance of FDG PET in various ways. The objective of this review is to provide an overview of the current literature regarding FDG PET in HCC and discuss emerging role of FDG PET in aiding management of HCC patients.

Citation: Lee SM, Kim HS, Lee S, Lee JW. Emerging role of ^{18}F -fluorodeoxyglucose positron emission tomography for guiding management of hepatocellular carcinoma. *World J Gastroenterol* 2019; 25(11): 1289-1306

URL: <https://www.wjgnet.com/1007-9327/full/v25/i11/1289.htm>

DOI: <https://dx.doi.org/10.3748/wjg.v25.i11.1289>

INTRODUCTION

In 2018, approximately 841000 new cases of liver cancer and 782000 associated deaths occurred worldwide, with liver cancer being the second leading cause of cancer death for males^[1]. Hepatocellular carcinoma (HCC) is the most common primary liver cancer, accounting for 75%-85% of cases of liver cancer^[1]. HCC is well-known as a highly lethal cancer, showing similar numbers of new cases and cancer deaths^[1,2]. Hepatitis B virus (HBV), hepatitis C virus (HCV), and alcohol intake are leading causes of HCC. In developed countries, obesity is an emerging risk factor for HCC^[2,3]. The Barcelona Clinical Liver Cancer (BCLC) staging system, endorsed by the European Association for the Study of the Liver and the European Organization for Research and Treatment of Cancer (EASL-EORTC), has been considered as the standard staging system for HCC in clinical practice because it links tumor stage to treatment strategy and has been validated in various different clinical situations^[4]. For HCC patients with stage 0 (single tumor < 2 cm) and stage A (single tumor > 2 cm or 3 tumor nodules < 3 cm), curative treatments including surgical resection, liver transplantation, and local ablation have been indicated^[4]. For HCC patients with stage B (multinodular tumors), transarterial chemoembolization (TACE) is primarily recommended^[4]. For HCC patients with stage C (tumors with portal vein invasion and/or extrahepatic spread), sorafenib is recommended as the first-line treatment^[4].

^{18}F -fluorodeoxyglucose (FDG), a glucose analog, is carried into viable cells by glucose transporter and subsequently phosphorylated by hexokinase, which has the same metabolic pathway as glucose^[5]. Therefore, FDG on positron emission tomography (PET) has been widely used as an imaging marker of glucose metabolism of normal organs and cancer tissue^[6-8]. Since cancer cells show high rates of glycolysis, FDG uptake is increased in cancer tissue^[5]. Thus, FDG PET has shown incremental value for diagnosing, staging, predicting prognosis, and restaging diverse kinds of malignant diseases^[5,9-11]. In contrast, FDG uptake in HCC varies according to the differentiation of HCC lesion^[12,13]. Earlier studies with FDG PET have shown a low diagnostic ability for detecting intrahepatic HCC lesions^[12-14], leading to a preconception that FDG PET has limited clinical value in patients with HCC. Nevertheless, diverse attempts have been performed to establish clinical role of FDG PET in HCC and recent studies have shown encouraging results of FDG PET in aiding management of patients with HCC.

In this review, we first summarized characteristics of HCC cells related with FDG uptake and results of studies regarding diagnostic and prognostic values of FDG PET in HCC. We then overviewed recent studies that dealt with volumetric FDG PET parameters, the significance of FDG uptake in HCC for selecting treatment and predicting treatment response, and radiomics of FDG PET in patients with HCC.

RELATIONSHIP BETWEEN HCC CHARACTERISTICS AND FDG UPTAKE

Because cancer cells have higher glycolytic rates than normal cells, higher amounts of glucose transporter and hexokinase expression are observed in tumor cells, resulting

in increased FDG uptake in cancer lesions^[15,16]. However, HCC cells show different expression patterns of proteins related to FDG uptake. HCC has lower level of glucose transporter-1 expression than cholangiocarcinoma and hepatic metastatic lesion^[17,18]. Furthermore, high expression of glucose-6-phosphatase which hydrolyzes FDG-6-phosphate to FDG that can be transported out of the cell has been observed in HCC^[19]. These different expression patterns contribute to low accumulation of FDG uptake in HCC, thereby reducing sensitivity for detecting HCC lesions^[19,20]. Nevertheless, increased glucose transporter expression and hexokinase activity have been demonstrated in high-grade HCC which is positively correlated with FDG uptake^[19,21]. Therefore, diverse degrees of FDG uptake have been shown according to the histopathological grade of HCC^[12,13,20]. Well-differentiated HCC reveals tumor-to-non-tumor liver uptake ratio (TLR) of around 1.1, indicating difficulty of differentiating FDG uptake of well-differentiated HCC lesion from that of normal liver tissue^[20]. Meanwhile, TLR of poorly-differentiated HCC lesion is more than 2.0^[20]. A previous study has shown that, by using the degree of FDG accumulation in HCCs, FDG PET could differentiate poorly-differentiated type from well-differentiated type with a sensitivity of 84% and a specificity of 75%^[22].

Recent studies have assessed the relationship between HCC characteristics and its FDG uptake at molecular level. Lee *et al*^[18] have compared gene expression profiles between HCCs with low FDG uptake and HCCs with high FDG uptake using surgical specimens of 10 HCC patients. In their study, HCCs with high FDG uptake demonstrated different gene expression profiles compared to those with low FDG uptake, showing increased expression of 11 genes particularly related to tumor cell adhesion, invasion, metastasis, anti-tumoral immunity, and chemotherapeutic response. They suggested that HCCs with high FDG uptake might have a more aggressive nature than those with low FDG uptake and that FDG uptake pattern of HCC could reflect potential of tumor progression and metastasis. Another recent study has evaluated the association between FDG uptake and expression of epithelial-mesenchymal transition markers in HCC^[21]. Epithelial-mesenchymal transition is the formation process of motile cells from immotile epithelial cells and is known to be involved in the formation of metastatic cancer cells^[23]. During epithelial-mesenchymal transition processes, expression levels of mesenchymal markers such as N-cadherin and vimentin increased, while expression of E-cadherin, an epithelial cell junction protein, is lost^[21,23]. The recent study demonstrated that, in HCCs with high FDG uptake, expression levels of N-cadherin and vimentin were up-regulated and the expression of E-cadherin was repressed^[21]. These significant associations between FDG uptake and expression of epithelial-mesenchymal transition-related proteins in HCC provides a basis for hypothesis that FDG PET might be useful for predicting the risk of extrahepatic metastasis in HCC patients^[21].

FDG PET IN STAGING HCC

Due to reduced FDG uptake in low-grade HCCs, previous studies have consistently reported a low sensitivity of FDG PET for detecting primary HCC lesions, ranging from 36% to 70%^[12-14,20,24-26]. A previous study by Teefey *et al*^[27] even reported that FDG PET detected none of cancer lesions in nine patients with HCC who underwent imaging examinations for work-up of liver transplantation. Based on results of these studies, EASL-EORTC guidelines has mentioned that FDG PET scan is not accurate for early diagnosis of HCC^[4]. In contrast, FDG PET has shown promising results for detecting extrahepatic metastasis. Because poorly-differentiated HCCs tend to metastasize more frequently, a positive statistical correlation between FDG avidity of primary HCCs and tendency of extrahepatic metastasis has been shown, suggesting that metastatic HCC lesions would also have increased FDG uptake^[28]. Extrahepatic metastasis is not an unusual finding in HCC. During staging work-up of HCC, extrahepatic metastases have been found in up to 37% of patients, with the most frequent site of metastasis being the lung, followed by lymph node, bone, and adrenal gland^[29,30]. In previous studies, FDG PET has demonstrated high sensitivities of 77%-100% for detecting extrahepatic metastasis^[28,31-34]. FDG PET has also shown superior diagnostic ability for detecting bone metastasis compared to bone scintigraphy and incomparable diagnostic accuracy for detecting lymph node metastasis compared to conventional computed tomography (CT) scan^[31,32]. However, FDG PET has a low sensitivity of 20% for detecting pulmonary metastases of less than 1 cm^[31]. Therefore, the diagnostic accuracy of chest CT was superior to that of FDG PET for detecting pulmonary metastasis^[31].

Clinical utility of imaging modality in staging malignant disease depends on whether the imaging examination can make further shift in cancer staging compared

to conventional examinations, thereby, changing treatment modality^[35]. In this respect, high diagnostic ability of FDG PET for detecting extrahepatic metastasis might not justify the clinical use of FDG PET in staging HCC. Delineation of additional extrahepatic metastatic lesion by FDG PET might have no significant effect on staging and selecting treatment in HCC patients whose extrahepatic metastases are already found by conventional imaging modalities^[35]. The clinical role of FDG PET in staging HCC should be evaluated in terms of ability to change cancer stage and treatment. However, only a small number of studies have assessed this ability of FDG PET in HCC patients, which are summarized in **Table 1**. In previous studies, FDG PET changed stage and treatment modalities in 1.5%-25% of HCC patients, mainly due to additional detection of extrahepatic metastases^[26,34,35]. A recent study by Cho *et al*^[35] has enrolled the largest number of patients (457 consecutive patients with HCC) among the studies. In their study, 5.0% of patients with BCLC stage A (6 out of 119 patients) and 1.4% of patients with BCLC stage B (1 out of 71 patients) were upstaged to stage C by FDG PET while none of patients with BCLC stage 0, C, or D had a shift in stage by FDG PET. Furthermore, additional extrahepatic metastases detected by FDG PET were found only in patients with T2 (3 out of 111 patients, 2.7%) and T3 (4 out of 78 patients, 5.1%) classifications of HCC. They suggested that routine staging FDG PET could have the clinical utility in patients with BCLC stage A and B or with T2 and T3 classifications.

FDG UPTAKE OF HCC AS A PREDICTOR FOR PROGNOSIS

Because FDG uptake of HCC is associated with tumor differentiation and aggressiveness, it is reasonable to assume that FDG uptake of HCC might have significant association with prognosis^[18,19,21]. Therefore, most studies on FDG PET in HCC patients have assessed the prognostic value of FDG PET for predicting clinical outcomes. These studies are summarized in **Tables 2-4**. In previous studies, visual analysis, maximum FDG uptake of tumor expressed as standardized uptake value (SUV), and TLR have been the most commonly used FDG PET parameters for evaluating FDG uptake of HCCs. Visual assessment and SUV are also commonly used as PET parameters in studies on other malignant diseases^[36,37]. TLR has been preferred in studies with HCC patients because TLR is known to correlate more closely with HCC doubling time and represent metabolic activities of HCCs more precisely than SUV^[38-40].

In previous studies on HCC patients who underwent curative surgical resection (**Table 2**), FDG uptake of HCC showed significant association with tumor recurrence, especially early recurrence after surgery, and overall survival, demonstrating worse survival in patients with high FDG uptake^[41-46]. However, several studies have failed to show the relationship between FDG PET findings and clinical outcomes on multivariate analysis^[47-49]. A recent study by Kim *et al*^[49] has retrospectively enrolled 226 patients with HBV-related HCC and evaluated the prognostic value of FDG PET findings. Results of that study revealed that, although positive FDG uptake of HCCs was significantly associated with overall survival, there was no significant difference in disease-free survival according to findings of FDG PET, suggesting that FDG PET could not predict the exact prognosis in patients with HBV-related HCC, because recurrence of HBV-related HCC also included intrahepatic metastasis or *de novo* recurrence. A retrospective multicenter study including 526 patients from nine Korean institutions has made a prognostic prediction model by combining alpha-fetoprotein (AFP)-des-gamma-carboxy prothrombin-tumor volume (ADV) score and FDG PET findings that are all available on staging work-up before surgical resection^[50]. The prognostic prediction model exhibited significant differences in tumor recurrence rates and overall survival rates according to ADV scores and PET findings, showing recurrence rate of 67.9% and survival rate of 70.6% in patients with high ADV score and hypermetabolic HCCs while the recurrence rate and survival rate in patients with low ADV score and isometabolic HCCs were 21.1% and 96.6%, respectively. The authors of that study suggested that, by using a combination of ADV scores and FDG PET findings, the risk of HCC recurrence could be reliably predicted.

In previous studies on HCC patients who underwent liver transplantation (**Table 3**), FDG PET findings consistently showed significant associations with recurrence-free survival and overall survival, demonstrating high recurrence rates after liver transplantation in patients with high FDG uptake^[39,51-61]. To select candidates for liver transplantation, the Milan criteria (a solitary tumor no more than 5 cm in diameter or 2 to 3 tumors no more than 3 cm in diameter) and the University of California San Francisco (UCSF) criteria (a solitary tumor up to 6.5 cm in diameter or up to 3 tumors

Table 1 Current literature evaluating the role of ^{18}F -fluorodeoxyglucose positron emission tomography in staging hepatocellular carcinoma

First author	Year	No. of patients	Study design	Staging system	No. of patient with a change of stage by FDG PET	No. of patients with a change of treatment by FDG PET
Yoon <i>et al</i> ^[34]	2007	87	Not specified	TNM	4 patients (4.6%), 3 patients TNM IVa to IVb, 1 patient TNM III to IVa	Not specified
Kawamura <i>et al</i> ^[26]	2014	64	Retrospective	BCLC	16 patients (25%), 6 patients BCLC 0 to C, 7 patients BCLC A to C, 3 patients BCLC B to C	16 patients (25%)
Cho <i>et al</i> ^[35]	2014	457	Retrospective	BCLC and TNM	7 patients (1.5%), 6 patients BCLC A to C, 1 patient BCLC B to C	7 patients (1.5%)

FDG: ^{18}F -fluorodeoxyglucose; PET: Positron emission tomography; HCC: Hepatocellular carcinoma; BCLC: Barcelona Clinic Liver Cancer.

no more than 4.5 cm with a total diameter up to 8 cm) have been commonly used^[62,63]. Therefore, most studies have compared the prognostic value of FDG PET with the conventional criteria or combined FDG PET findings with the conventional criteria to further stratify recurrence risk after liver transplantation^[51-58,61]. In previous studies, patients beyond the Milan criteria, but, showing negative finding on FDG PET had clinical outcomes comparable to those within the Milan Criteria^[52,53,55,61]. Furthermore, even if patients met the Milan criteria, higher recurrence rate was found in those with high FDG uptake of HCCs than that in those with low FDG uptake^[39,51]. A previous study by Lee *et al*^[58] has proposed new selection criteria with FDG PET finding and total tumor size (10 cm). The new criteria had similar area under the receiver operating characteristic curve value for predicting disease-free survival compared to the Milan criteria or the UCSF criteria^[58]. Takada *et al*^[60] have performed a retrospective multicenter study with 182 HCC patients who underwent living donor liver transplantation from 16 Japanese medical centers. In that study, FDG PET finding was found to be an independent predictive factor for tumor recurrence along with the Milan criteria and serum AFP level. Patients beyond the Milan criteria but with low serum AFP level and negative FDG PET finding (19%) had similar 5-year recurrence rate to those within the Milan criteria (6%). They also had significantly lower 5-year recurrence rate than those beyond Milan criteria with high serum AFP level and positive PET finding (53%). They suggested that FDG PET could provide additional information for making decisions regarding liver transplantation for HCC patients^[60].

The prognostic value of FDG PET has also been assessed in HCC patients treated with palliative treatments including TACE, concurrent chemoradiotherapy (CCRT), radiotherapy, transarterial radioembolization (TARE), and sorafenib (Table 4)^[40,64-76]. For patients treated with TACE, CCRT, or radiotherapy, previous studies showed longer progression-free survival and overall survival in patients with low FDG uptake of HCCs, indicating significant associations between FDG avidity of HCCs and clinical outcomes^[64-70]. For patients treated with TARE using yttrium-90 (^{90}Y), contradictory results have been shown between studies. Previous studies have revealed longer progression-free survival and overall survival in patients with low FDG uptake of HCCs^[72,74], including a recent prospective study with uniform patient cohort^[75]. In contrast, one study showed no significant association between FDG uptake of HCCs and survival^[73] and another study even showed better progression-free survival in patients with high FDG uptake^[71]. This controversy could be due to the small number of enrolled patients with heterogeneous clinical conditions among studies and further larger studies are warranted. Only two studies have evaluated the prognostic value of FDG PET in patients treated with sorafenib monotherapy^[40,76]. Both studies showed significantly better survival in patients with low FDG uptake of HCCs^[40,76]. However, only a small number of patients are enrolled in both studies and concomitant local therapies are also commonly performed in patients with BCLC stage C. These might have limited analyses in these studies.

Recently, the Korean Society of Nuclear Medicine Clinical Trial Network (KSNM

Table 2 Current literature evaluating the prognostic value of ^{18}F -fluorodeoxyglucose positron emission tomography in hepatocellular carcinoma patients with surgical resection

First author	Year	No. of patients	Study design	PET parameter	Cut-off values of PET parameter	Findings
Hatano <i>et al</i> ^[41]	2006	31	Retrospective	TLR	2.0	TLR showed significant positive association with overall survival
Ahn <i>et al</i> ^[47]	2011	93	Retrospective	SUV, TLR	4.0, 2.0	High SUV and TLR were predictors for early recurrence, but showed no statistical significance on multivariate analysis
Kitamura <i>et al</i> ^[42]	2012	63	Retrospective	TLR	2.0	TLR was an independent predictor for early recurrence
Han <i>et al</i> ^[43]	2014	298	Retrospective	SUV	3.5	SUV was an independent predictor for recurrence-free survival and overall survival
Baek <i>et al</i> ^[48]	2015	54	Retrospective	Tumor-to-muscle ratio	6.36	Tumor-to-muscle ratio was associated with recurrence-free survival, but, no statistical significance on multivariate analysis
Cho <i>et al</i> ^[44]	2017	56	Retrospective	SUV	4.9	Recurrence rate was higher in patients with high SUV, but, no significant difference of disease-free survival and overall survival according to SUV
Hwang <i>et al</i> ^[50]	2018	526	Retrospective	Visual analysis	-	Combination of ADV score and PET finding can predict risk of early recurrence and survival
Kim <i>et al</i> ^[49]	2018	226 HBV-related HCC	Retrospective	Visual analysis	-	Positive PET finding was associated with overall survival, but, not a predisposing factor for disease-free survival in HBV-related HCC patients
Lim <i>et al</i> ^[45]	2018	78	Prospective	Visual analysis	-	Positive PET finding was an independent predictor for early recurrence
Yoh <i>et al</i> ^[46]	2018	207	Retrospective	TLR	2.0	Prognostic model incorporating ALBI grade and PET finding can predict the disease-free survival and overall survival

FDG: ^{18}F -fluorodeoxyglucose; PET: Positron emission tomography; HCC: Hepatocellular carcinoma; HBV: Hepatitis B virus; TLR: Tumor-to-non-tumor liver uptake ratio; SUV: Standardized uptake value; ADV: Alpha-fetoprotein-Des-gamma-carboxy prothrombin-tumor volume; ALBI: Albumin-bilirubin.

CTN) working group has performed a retrospective multicenter study to assess clinical role of FDG PET in HCC patients^[77-80]. They retrospectively recruited 847

Table 3 Current literature evaluating the prognostic value of ^{18}F -fluorodeoxyglucose positron emission tomography in hepatocellular carcinoma patients with liver transplantation

First author	Year	No. of patients	Study design	PET parameter	Cut-off values of PET parameter	Findings
Yang <i>et al</i> ^[51]	2006	38	Retrospective	Visual analysis	-	Patients with negative PET findings had significantly higher recurrence-free survival than those with positive findings
Kornberg <i>et al</i> ^[52]	2009	42	Retrospective	Visual analysis	-	Patients with positive PET findings had significantly higher recurrence rate with lower recurrence-free survival than those with negative findings
Lee <i>et al</i> ^[39]	2009	59	Retrospective	Tmax/Lmax	1.15	Tmax/Lmax was an independent predictor for recurrence-free survival
Kornberg <i>et al</i> ^[53]	2012	91	Retrospective	Visual analysis	-	PET finding was an independent prognostic variable for recurrence-free survival, and positive PET status was the independent predictor of patient dropout from the waiting list of liver transplantation
Lee <i>et al</i> ^[54]	2013	191	Retrospective	Visual analysis	-	Positive PET status was an independent prognostic factor for disease-free survival influencing early recurrence
Detry <i>et al</i> ^[55]	2015	27	Retrospective	Tmax/Lmax	1.15	Tmax/Lmax independently predicted recurrence-free survival
Hong <i>et al</i> ^[56]	2016	123	Retrospective	TLR	1.10	Combination of serum AFP and PET finding predicted better disease-free survival than using the Milan criteria
Hsu <i>et al</i> ^[57]	2016	147	Retrospective	SUV, TLR	4.8, 2.0	Combination of UCSF criteria and PET finding can predict the risk of recurrence
Lee <i>et al</i> ^[58]	2016	280	Retrospective	Visual analysis	-	The criteria combined of FDG PET and total tumor size can predict disease-free survival and overall survival, and showed similar area under the ROC curve of the Milan and UCSF criteria

Kornberg <i>et al</i> ^[59]	2017	116	Retrospective	Visual analysis	-	Combining radiographic criteria with FDG PET finding can predict recurrence-free survival
Takada <i>et al</i> ^[60]	2017	182	Retrospective	Visual analysis	-	PET positive status was an independent risk factor for recurrence-free survival
Ye <i>et al</i> ^[61]	2017	103	Retrospective	Visual analysis	-	Patients beyond the Milan criteria with a negative PET finding had comparable recurrence-free survival in comparison with those within the Milan criteria

FDG: ¹⁸F-fluorodeoxyglucose; PET: Positron emission tomography; HCC: Hepatocellular carcinoma; Tmax/Lmax: Maximum FDG uptake of tumor-to-maximum FDG uptake of the normal liver ratio; TLR: Tumor-to-non-tumor liver uptake ratio; SUV: Standardized uptake value; AFP: Alpha-fetoprotein; UCSF: University of California San Francisco; ROC: Receiver operating characteristic.

patients with newly diagnosed HCC who underwent pretreatment FDG PET/CT from seven university hospitals at Korea and published several studies regarding the prognostic value of FDG PET^[77,78]. One of their studies included 317 patients with BCLC stage 0 or A from the cohort and evaluated the predictive value of FDG PET for recurrence-free survival and overall survival^[77]. They classified the 317 patients into two groups, a curative therapy cohort (patients who underwent surgical resection, liver transplantation, and local ablation) and a TACE cohort, and assessed the relationship between FDG PET findings and survival in each group. TLR was an independent predictor for both recurrence-free survival and overall survival in the curative therapy cohort. However, TLR failed to show association with survival in the TACE cohort. In the TACE cohort, only the Model for End-Stage Liver Disease score was an independent prognostic factor for overall survival. Considering that only patients who could not undergo curative therapy due to unsuitable HCC location or impaired liver function were included in the TACE cohort, underlying liver function rather than FDG uptake of HCC might have a significant association with survival^[77]. Another study by KSNM CTN has evaluated prognostic value of FDG PET in 291 patients with BCLC stage C^[78]. They classified patients into two groups; patients with intrahepatic metastasis and patients with extrahepatic metastasis. They showed that higher TLR was associated with extrahepatic metastasis and was an independent predictor for overall survival in both groups. Furthermore, patients with intrahepatic metastases but high TLR had a poor prognosis comparable to patients with extrahepatic metastases and low TLR, suggesting the prognostic significance of primary HCCs uptake irrespective of the extent of metastasis.

In addition to FDG uptake of primary HCC tumors, a recent study by Lee *et al*^[81] has evaluated the prognostic value of FDG uptake of portal vein tumor thrombosis. HCC cells can spread to other segments of the liver and distant organs via portal vein; therefore, portal vein tumor thrombosis has a significant impact on the prognosis of HCC patients^[81-83]. Lee *et al*^[81] have enrolled 166 HCC patients with portal vein tumor thrombosis but no extrahepatic metastasis and compared the prognostic value of FDG uptake of portal vein tumor thrombosis with FDG uptake of primary tumor. Their results revealed that only FDG uptake of portal vein tumor thrombosis was an independent predictor for both progression-free survival and overall survival. They also found that patients with high FDG uptake of portal vein tumor thrombosis had worse survival than those with low FDG uptake, irrespective of the degree of FDG uptake of primary HCCs. Based on these results, they concluded that FDG uptake of portal vein tumor thrombosis rather than FDG uptake of primary tumor should be used to predict clinical outcomes in locally advanced HCC.

VOLUMETRIC PARAMETERS OF PET AND RECURRENCE PATTERN OF HCC

Table 4 Current literature evaluating the prognostic value of ^{18}F -fluorodeoxyglucose positron emission tomography in hepatocellular carcinoma patients with treatments other than surgical resection and liver transplantation

First author	Year	No. of patients	Study design	PET parameter	Cut-off values of PET parameter	Treatment	Findings
Song <i>et al</i> ^[64]	2012	83	Retrospective	TLR	1.90	TACE	Patients with low TLR ratios had significantly longer overall survival than those with high ratios, but, no significant difference of time-to-progression was shown between them
Song <i>et al</i> ^[65]	2013	58	Retrospective	TLR	1.70	TACE	FDG PET can predict response to TACE and tumor progression
Ma <i>et al</i> ^[66]	2014	27	Retrospective	$\Delta\text{TSUVmax\%}$	0.1	TACE	$\Delta\text{TSUVmax\%}$ can predict response to TACE and overall survival
Kim <i>et al</i> ^[67]	2015	77	Retrospective	TLR	1.83	TACE	TLR was an independent predictor of overall survival and tumor progression
Kim <i>et al</i> ^[68]	2011	107	Retrospective	SUV	6.1	CCRT	SUV was significantly associated with progression-free survival and overall survival, and patients with high SUV was more likely to have extrahepatic metastasis
Huang <i>et al</i> ^[69]	2013	31	Retrospective	SUV	3.2	SABR	SUV was the significant prognostic indicator of disease control rate
Rhee <i>et al</i> ^[70]	2017	228	Retrospective	SUV, TLR	4.825, 2.355	Radiotherapy	Low FDG uptake group had better treatment response, longer median progression-free and overall survival
Kucuk <i>et al</i> ^[71]	2013	19	Retrospective	Visual analysis	-	Radioembolization	High FDG uptake lesions unexpectedly had better progression-free survival rates
Sabet <i>et al</i> ^[72]	2014	33	Retrospective	Visual analysis	-	Radioembolization	Findings on pre-therapeutic PET and relative changes of FDG uptake on post-therapeutic PET independently predict overall survival

Soydal <i>et al</i> ^[73]	2015	28	Retrospective	Visual analysis, SUV	Not specified	Radioembolization	Age, serum AFP level, and tumor size were significantly associated with survival, but, SUV showed no significant association
Abuodeh <i>et al</i> ^[74]	2016	34	Retrospective	Visual analysis	-	Radioembolization	FDG avidity independently predicts local liver control, distant liver control, and progression-free survival
Jreige <i>et al</i> ^[75]	2017	48	Prospective	SUV, TLR	5.0, 2.0	Radioembolization	Both SUV and TLR were predictive markers of overall survival
Lee <i>et al</i> ^[76]	2011	29	Retrospective	SUV	5.0	Sorafenib	SUV was an independent prognostic factor for overall survival
Sung <i>et al</i> ^[40]	2018	35	Retrospective	TLR	2.9	Sorafenib	TLR was significant predictor for progression-free survival and overall survival

FDG: ¹⁸F-fluorodeoxyglucose; PET: Positron emission tomography; HCC: Hepatocellular carcinoma; TLR: Tumor-to-non-tumor liver uptake ratio; Δ SUVmax%; Relative changes of maximum FDG uptake of tumor between pre-therapeutic and post-therapeutic FDG PET scans; SUV: Standardized uptake value; TACE: Transarterial chemoembolization; CCRT: Concurrent chemoradiotherapy; SABR: Stereotactic ablative radiotherapy; AFP: Alpha-fetoprotein.

In recent decades, volumetric PET indices such as metabolic tumor volume (MTV) and total lesion glycolysis (TLG) have been considered as promising PET parameters that can accurately reflect the metabolic burden of malignant lesion^[84-86]. SUV and TLR represent only the highest metabolic activity of cancer lesion. On the other hand, MTV is defined as tumor tissue volume that has FDG uptake beyond the intensity of FDG uptake of normal tissue; thus, it can reflect tumor extent^[85-87]. TLG is the product of MTV and mean FDG uptake of tumor, which combines both metabolic and volumetric information of the tumor^[84,86]. A number of studies have demonstrated that MTV and TLG have higher predictive values for survival than SUV in various malignant diseases during the last two decades^[84,86-89]. However, in HCC patients, clinical study that calculated MTV and assessed the prognostic value of MTV was first published in 2015^[90]. Since then, only a few studies have evaluated the clinical implication of volumetric PET parameters^[91-93].

To measure MTV of cancer lesion, two processes should be performed: delineating tumor lesion from surrounding normal tissue and determining threshold SUV to identify metabolically active tumor volume^[90]. Due to heterogeneous and diverse degrees of FDG uptake in HCC and relatively high FDG uptake in normal liver tissue, it is difficult to perform both processes in HCC, thus hindering attempts to measure volumetric PET parameters^[90]. Lee *et al*^[90] have proposed a novel method using intensity-volume histogram to measure MTV of HCCs that can surpass these limitations. They drew regions of interest over HCC lesion and normal liver tissue and prepared intensity-volume histogram (a plot of volume of a given structure as a function of the SUV) of the HCC lesion and normal liver tissue (Figure 1). Using such intensity-volume histograms of HCC and normal liver tissue, the sum of tumor voxels with higher FDG uptake than normal liver tissue could be calculated for each patient. They calculated MTV_{2SD} (defined as the sum of the tumor voxels over the SUV of the 97.5th percentile of the normal liver tissue voxels) from 59 HCC patients without extrahepatic metastasis. On survival analysis of their study, MTV_{2SD} has more significant prognostic value for predicting progression-free survival and overall survival than TLR.

After publishing the first study with MTV in HCC, authors of the study have tried

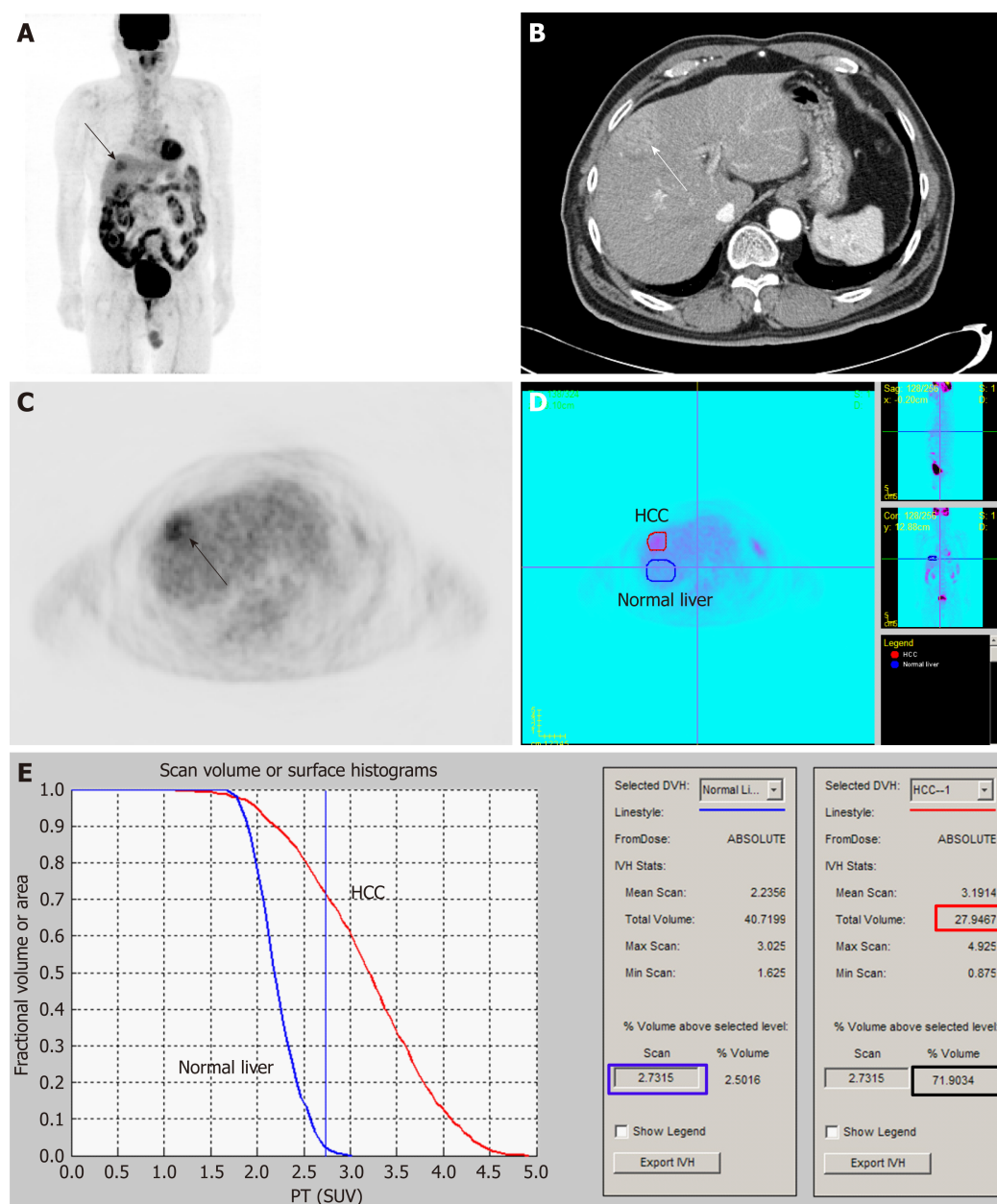


Figure 1 An example of the method for measuring metabolic tumor volume based on intensity-volume histogram from reference^[88] with permission.

Maximal intensity projection (A) and transaxial image (C) of ^{18}F -fluorodeoxyglucose (FDG) positron emission tomography (PET) and contrast-enhanced computed tomography image (B) showed a single hepatocellular carcinoma (HCC) with moderately increased FDG uptake. Regions of interest of HCC (red) and normal liver tissue (blue) are manually drawn on transaxial PET images (D). Cumulative intensity-volume histogram plots for HCC (red) and normal liver tissue (blue) are calculated from regions of interest. Standardized uptake value of the 97.5th percentile of the voxels of the normal liver tissue was 2.7 (blue box) and the fraction of the tumor volume with ≥ 2.7 was 71.9% (black box). As the total tumor volume was 27.9 cm^3 (red box), sum of the tumor voxels over the standardized uptake value of the 97.5th percentile of the normal liver tissue voxels of the patient was 20.1 cm^3 . HCC: Hepatocellular carcinoma; SUV: Standardized uptake value.

to assess the clinical value of volumetric PET parameters for predicting recurrence pattern of HCC^[92,93]. In HCC patients, extrahepatic metastasis after curative surgical resection is known to be associated with poor prognosis due to limited therapeutic option^[42,92]. Furthermore, early recurrence with an interval of less than one year after operation is also known to be a significant indicator for worse survival which is comparable to the survival of patients with extrahepatic metastasis^[47,93,94]. In previous studies, tumor factors associated with tumor aggressiveness including tumor stage, size, and grade have been found to be significant predictors for both extrahepatic and early recurrences^[47,93,95,96]. FDG uptake of HCC is also related to tumor grade and aggressiveness, therefore, SUV and TLR of HCCs have also been shown to be associated with the risk of extrahepatic and early recurrences^[42,45,47,97]. Considering that volumetric PET parameters can more precisely reflect metabolic characteristics and burden of cancer lesions than FDG uptake intensity^[86,89], volumetric PET parameters of HCC can have more significant association with recurrence patterns of HCC than

SUV or TLR. In two recent studies on the relationship between volumetric PET parameters and recurrence pattern of HCC, the authors have measured MTV and TLG of HCCs using SUV of the 97.5th percentile of the normal liver tissue as threshold SUV and demonstrated that both MTV and TLG have superior prognostic value for predicting both extrahepatic recurrence and early intrahepatic recurrence than TLR in HCC patients after curative surgical resection^[92,93]. On the other hand, late intrahepatic recurrence with an interval of more than 1 year after surgery was associated with HCV positivity and serum albumin level, while none of volumetric PET parameters could predict the risk of late intrahepatic recurrence^[93]. These results indicate that the risk of both extrahepatic and early intrahepatic recurrences is associated with metabolic tumor burden, while the risk of late intrahepatic recurrence is related to underlying liver function and multicentric tumor formation tendency^[93]. Authors of these studies have suggested that volumetric PET parameters of HCC could be used to predict the recurrence pattern and to select patients who might show poor survival after curative surgical resection^[92,93].

Kim *et al*^[91] have calculated volumetric PET indices and evaluated their prognostic values in 110 HCC patients who underwent liver transplantation. Different from the method used in the study by Lee *et al*^[90], they calculated uptake ratio between the maximum SUV of HCCs and background tissue, inferior vena cava (TBR_{IVC}) or normal liver tissue (TBR_{NL}), and used TBR_{IVC} of 2.0 and TBR_{NL} of 1.5 as threshold values for measuring MTV. MTV_{IVC} and MTV_{NL} (defined as the sum of the tumor voxels which had TBR_{IVC} of more than 2.0 and TBR_{NL} of more than 1.5) were measured. With MTV and mean value of TBR, uptake-volume product (UVP) was calculated for each background tissue. Results of their study revealed that both TBR_{IVC} and UVP_{IVC} were independent predictors for recurrence-free survival. The authors suggested that inferior vena cava might be a more reliable background tissue than the normal liver in measuring MTV. They have also suggested that volumetric parameters as well as metabolic activity of HCCs are effective predictors of recurrence after liver transplantation^[91].

USING FDG PET FOR SELECTING TREATMENT OF HCC

Increased FDG uptake in HCCs reflects aggressive biological activity of tumor and is associated with poor survival^[18,19,78]. Therefore, patients with high FDG uptake of HCCs might have poor response to treatment. Previous studies on patients treated with TACE have shown that patients with high FDG uptake have poor response to treatment^[65,98]. Furthermore, in HCC patients with high FDG uptake, major hepatectomy that can minimize the possibility of residual tumor rather than minor hepatectomy should be selected to obtain survival benefit^[99]. However, in studies on HCC patients treated with external beam radiotherapy, paradoxical relationship between FDG uptake of HCC and treatment response has been shown^[100-102]. Kim *et al*^[100] have retrospectively enrolled 35 HCC patients with TNM stage III-IV who underwent FDG PET and subsequent radiotherapy with concurrent chemotherapy or TACE. They showed that patients having HCCs of SUV ≥ 2.5 (80%; 16 out of 20 patients) had significantly higher objective response rate to radiotherapy than those with HCCs of SUV < 2.5 (40%; 6 out of 15 patients). Choi *et al*^[101] have retrospectively reviewed 45 metastatic bone lesions in 22 HCC patients treated with radiotherapy. They also revealed significantly better infield progression-free survival and infield event-free survival in tumors with SUV of ≥ 3.0 compared to those in tumors with SUV of < 3.0 (1-year progression-free survival, 88% *vs* 34%; 1-year event-free survival, 82% *vs* 52%). Another retrospective study by Jo *et al*^[102] has investigated the predictive value of FDG uptake of HCC in 36 HCC patients treated with radiotherapy. In that study, patient group with high SUV (≥ 5.1) showed significantly higher objective tumor response (63.6% *vs* 36.4%) than patient group with low SUV (< 5.1). In spite of high tumor response, patient group with high SUV had worse overall survival mainly due to the occurrence of distant metastasis. Authors of these studies have explained this paradoxical relationship by radiosensitivity of highly proliferating tumor^[100,102]. In a previous study, FDG uptake of HCCs has shown a positive association with tumor doubling time^[38]. Because rapidly proliferating tumors are radiosensitive, HCCs with high FDG uptake are considered to have better response to radiotherapy than those with low uptake^[100,102]. However, HCCs with high FDG uptake also have high risk for early recurrence and distant metastasis^[92,93]. Therefore, viable tumor cells in residual lesions after radiotherapy could spread more rapidly and more frequently to extrahepatic organs, resulting in worse overall survival^[102].

Results of these studies on radiotherapy have indicated that HCCs might show different responses to treatment according to the degree of FDG uptake of HCC. In

this respect, a recent study reported by KSNM CTN working group has demonstrated interesting results^[79]. The study retrospectively enrolled 214 intermediate-to-advanced stage patients without extrahepatic metastasis who underwent CCRT or TACE as an initial treatment from a cohort of 847 HCC patients from seven hospitals. Authors of the study have classified these enrolled patients into two patient groups according to TLR of HCCs (patient groups with TLR > 2.0 and ≤ 2.0) and compared clinical outcomes between patients treated with CCRT and TACE for each patient group. In patient group with TLR > 2.0, patients treated with CCRT demonstrated significantly longer progression-free survival and overall survival than those treated with TACE. Meanwhile, for patient group with TLR ≤ 2.0, there were no significant differences in progression-free survival or overall survival between patients treated with CCRT and those treated with TACE. The authors suggested that, for patients with high FDG uptake, multimodality treatment including radiotherapy could be more effective in tumor control while HCCs with low FDG uptake seemed to be less affected by the treatment modality. Considering that HCCs with low and high FDG uptake have different tumor characteristics, genetic disposition, and recurrence pattern^[18,19,21,93], different treatment strategy might be needed according to findings of FDG PET in HCC patients. However, as the study by KSNM CTN working group^[79] was retrospectively performed, further prospective study is needed to validate the role of FDG PET in selecting treatment modality.

RADIOMICS OF FDG PET IN HCC

Currently, the concept of radiomics has been widespread in the field of oncology^[103]. Radiomics is defined as high-throughput extraction of a large number of imaging features that can comprehensively quantify tumor phenotypes^[104,105]. Textural features of cancer tissue on medical images are associated with genomic and proteomic expression patterns of cancer cells and many studies have revealed that radiomics signature made of textural features can independently predict prognosis in diverse cancers including head and neck cancer, lung cancer, breast cancer, and esophageal cancer^[103,105,106]. However, in HCC, only a single study by Blanc-Durand *et al*^[107] has evaluated the prognostic value of textural features of HCC. In radiomics study of FDG PET, image preprocessing including the process of delineation and segmentation of tumor lesion is essential for textural analysis of PET images^[105,108]. Considering that HCC lesions have heterogeneous and variable FDG uptake, it is difficult to delineate HCC lesions from normal liver tissue accurately as shown in aforementioned section with volumetric PET parameters^[90]. This might act as the main hurdle to perform textural analysis in FDG PET images of HCC. Blanc-Durand *et al*^[107] have retrospectively enrolled 47 HCC patients who underwent pretreatment FDG PET and subsequent transarterial radioembolization using ⁹⁰Y. Using PET images of whole liver including both tumor and non-tumoral liver for textural analysis, they extracted 108 textural features from these images. They claimed that, by introducing whole-liver in the radiomics model, both hepatic function and HCC biology could be integrated into one system. With mainly using two textural features, strength (a textural feature describing pattern perceivability, its value is high when intensity pattern is easily defined and visible) and variance (a textural feature describing a deviation from the mean), predictive radiomics scoring systems for progression-free survival and overall survival were generated. On multivariate survival analysis, these radiomics scoring systems turned out to be independent negative predictors for both progression-free survival and overall survival. Moreover, prognostic values of radiomics scoring systems did not differ even after stratification by BCLC staging and tumor size. The authors suggested that whole-liver radiomics approach representing a balance between normal liver tissue and tumor burden could provide prognostic information for HCC patients. However, further studies with more patients are warranted to validate the methodology and results of their study.

CONCLUSION

FDG PET is a non-invasive imaging method that can evaluate biological activity of HCC. Although FDG PET has been considered to have low sensitivity for detecting HCCs, it can detect unexpected extrahepatic metastasis with incremental prognostic value for predicting survival. Furthermore, recent studies have demonstrated encouraging results of FDG PET for predicting recurrence pattern and aiding the selection of treatment for HCC. With development of new analytic methods of FDG PET images such as volumetric and textural analyses, clinical use of FDG PET in HCC

patients would be continuously evolving. FDG PET should be considered as an imaging biomarker that can provide information for selecting management strategies in HCC patients rather than a simple diagnostic imaging modality with a limited sensitivity.

REFERENCES

- 1 **Bray F**, Ferlay J, Soerjomataram I, Siegel RL, Torre LA, Jemal A. Global cancer statistics 2018: GLOBOCAN estimates of incidence and mortality worldwide for 36 cancers in 185 countries. *CA Cancer J Clin* 2018; **68**: 394-424 [PMID: 30207593 DOI: 10.3322/caac.21492]
- 2 **Yang JD**, Roberts LR. Hepatocellular carcinoma: A global view. *Nat Rev Gastroenterol Hepatol* 2010; **7**: 448-458 [PMID: 20628345 DOI: 10.1038/nrgastro.2010.100]
- 3 **Marengo A**, Rosso C, Bugianesi E. Liver Cancer: Connections with Obesity, Fatty Liver, and Cirrhosis. *Annu Rev Med* 2016; **67**: 103-117 [PMID: 26473416 DOI: 10.1146/annurev-med-090514-013832]
- 4 **European Association For The Study Of The Liver; European Organisation For Research And Treatment Of Cancer**. EASL-EORTC clinical practice guidelines: management of hepatocellular carcinoma. *J Hepatol* 2012; **56**: 908-943 [PMID: 22424438 DOI: 10.1016/j.jhep.2011.12.001]
- 5 **Kelloff GJ**, Hoffman JM, Johnson B, Scher HI, Siegel BA, Cheng EY, Cheson BD, O'shaughnessy J, Guyton KZ, Mankoff DA, Shankar L, Larson SM, Sigman CC, Schilsky RL, Sullivan DC. Progress and promise of FDG-PET imaging for cancer patient management and oncologic drug development. *Clin Cancer Res* 2005; **11**: 2785-2808 [PMID: 15837727 DOI: 10.1158/1078-0432.ccr-04-2626]
- 6 **Lee JW**, Lee MS, Chung IK, Son MW, Cho YS, Lee SM. Clinical implication of FDG uptake of bone marrow on PET/CT in gastric cancer patients with surgical resection. *World J Gastroenterol* 2017; **23**: 2385-2395 [PMID: 28428718 DOI: 10.3748/wjg.v23.i13.2385]
- 7 **Lee JW**, Lee SM, Chung YA. Prognostic value of CT attenuation and FDG uptake of adipose tissue in patients with pancreatic adenocarcinoma. *Clin Radiol* 2018; **73**: 1056.e1-1056.e10 [PMID: 30077337 DOI: 10.1016/j.crad.2018.07.094]
- 8 **Pourhassan Shamchi S**, Khosravi M, Taghvaei R, Zirakchian Zadeh M, Paydary K, Emamzadehfard S, Werner TJ, Høilund-Carlson PF, Alavi A. Normal patterns of regional brain ¹⁸F-FDG uptake in normal aging. *Hell J Nucl Med* 2018; **21**: 175-180 [PMID: 30411727 DOI: 10.1967/S002449910902]
- 9 **Cheng G**, Huang H. Prognostic Value of ¹⁸F-Fluorodeoxyglucose PET/Computed Tomography in Non-Small-Cell Lung Cancer. *PET Clin* 2018; **13**: 59-72 [PMID: 29157386 DOI: 10.1016/j.cpet.2017.08.006]
- 10 **Diao W**, Tian F, Jia Z. The prognostic value of SUV_{max} measuring on primary lesion and ALN by ¹⁸F-FDG PET or PET/CT in patients with breast cancer. *Eur J Radiol* 2018; **105**: 1-7 [PMID: 30017264 DOI: 10.1016/j.ejrad.2018.05.014]
- 11 **Lee Y**, Yoo IR, Boo SH, Kim H, Park HL, Hyun O J. The Role of F-18 FDG PET/CT in Intrahepatic Cholangiocarcinoma. *Nucl Med Mol Imaging* 2017; **51**: 69-78 [PMID: 28250860 DOI: 10.1007/s13139-016-0440-y]
- 12 **Khan MA**, Combs CS, Brunt EM, Lowe VJ, Wolverson MK, Solomon H, Collins BT, Di Bisceglie AM. Positron emission tomography scanning in the evaluation of hepatocellular carcinoma. *J Hepatol* 2000; **32**: 792-797 [PMID: 10845666 DOI: 10.1016/S0168-8278(00)80248-2]
- 13 **Trojan J**, Schroeder O, Raedle J, Baum RP, Herrmann G, Jacobi V, Zeuzem S. Fluorine-18 FDG positron emission tomography for imaging of hepatocellular carcinoma. *Am J Gastroenterol* 1999; **94**: 3314-3319 [PMID: 10566736 DOI: 10.1111/j.1572-0241.1999.01544.x]
- 14 **Delbeke D**, Martin WH, Sandler MP, Chapman WC, Wright JK, Pinson CW. Evaluation of benign vs malignant hepatic lesions with positron emission tomography. *Arch Surg* 1998; **133**: 510-5; discussion 515-6 [PMID: 9605913 DOI: 10.1001/archsurg.133.5.510]
- 15 **Ong LC**, Jin Y, Song IC, Yu S, Zhang K, Chow PK. 2-[¹⁸F]-2-deoxy-D-glucose (FDG) uptake in human tumor cells is related to the expression of GLUT-1 and hexokinase II. *Acta Radiol* 2008; **49**: 1145-1153 [PMID: 18979289 DOI: 10.1080/02841850802482486]
- 16 **Zhao S**, Kuge Y, Mochizuki T, Takahashi T, Nakada K, Sato M, Takei T, Tamaki N. Biologic correlates of intratumoral heterogeneity in ¹⁸F-FDG distribution with regional expression of glucose transporters and hexokinase-II in experimental tumor. *J Nucl Med* 2005; **46**: 675-682 [PMID: 15809491]
- 17 **Zimmerman RL**, Burke M, Young NA, Solomides CC, Bibbo M. Diagnostic utility of Glut-1 and CA 15-3 in discriminating adenocarcinoma from hepatocellular carcinoma in liver tumors biopsied by fine-needle aspiration. *Cancer* 2002; **96**: 53-57 [PMID: 11836704 DOI: 10.1102/cncr.10309]
- 18 **Lee JD**, Yang WI, Park YN, Kim KS, Choi JS, Yun M, Ko D, Kim TS, Cho AE, Kim HM, Han KH, Im SS, Ahn YH, Choi CW, Park JH. Different glucose uptake and glycolytic mechanisms between hepatocellular carcinoma and intrahepatic mass-forming cholangiocarcinoma with increased (18)F-FDG uptake. *J Nucl Med* 2005; **46**: 1753-1759 [PMID: 16204727]
- 19 **Torizuka T**, Tamaki N, Inokuma T, Magata Y, Sasayama S, Yonekura Y, Tanaka A, Yamaoka Y, Yamamoto K, Konishi J. In vivo assessment of glucose metabolism in hepatocellular carcinoma with FDG-PET. *J Nucl Med* 1995; **36**: 1811-1817 [PMID: 7562048]
- 20 **Ho CL**, Yu SC, Yeung DW. ¹¹C-acetate PET imaging in hepatocellular carcinoma and other liver masses. *J Nucl Med* 2003; **44**: 213-221 [PMID: 12571212]
- 21 **Lee M**, Jeon JY, Neugent ML, Kim JW, Yun M. ¹⁸F-Fluorodeoxyglucose uptake on positron emission tomography/computed tomography is associated with metastasis and epithelial-mesenchymal transition in hepatocellular carcinoma. *Clin Exp Metastasis* 2017; **34**: 251-260 [PMID: 28429188 DOI: 10.1007/s10585-017-9847-9]
- 22 **Ferda J**, Ferdová E, Baxa J, Kreuzberg B, Daum O, Třeška V, Skalický T. The role of ¹⁸F-FDG accumulation and arterial enhancement as biomarkers in the assessment of typing, grading and staging of hepatocellular carcinoma using ¹⁸F-FDG-PET/CT with integrated dual-phase CT angiography. *Anticancer Res* 2015; **35**: 2241-2246 [PMID: 25862885]
- 23 **Zeisberg M**, Neilson EG. Biomarkers for epithelial-mesenchymal transitions. *J Clin Invest* 2009; **119**: 1429-1437 [PMID: 19487819 DOI: 10.1172/JCI36183]
- 24 **Wudel LJ**, Delbeke D, Morris D, Rice M, Washington MK, Shyr Y, Pinson CW, Chapman WC. The role of [¹⁸F]fluorodeoxyglucose positron emission tomography imaging in the evaluation of hepatocellular carcinoma. *Am Surg* 2003; **69**: 117-24; discussion 124-6 [PMID: 12641351]

- 25 **Ijichi H**, Shirabe K, Taketomi A, Yoshizumi T, Ikegami T, Mano Y, Aishima S, Abe K, Honda H, Maehara Y. Clinical usefulness of (18) F-fluorodeoxyglucose positron emission tomography/computed tomography for patients with primary liver cancer with special reference to rare histological types, hepatocellular carcinoma with sarcomatous change and combined hepatocellular and cholangiocarcinoma. *Hepatol Res* 2013; **43**: 481-487 [PMID: [23145869](#) DOI: [10.1111/j.1872-034X.2012.01107.x](#)]
- 26 **Kawamura E**, Shiomi S, Kotani K, Kawabe J, Hagihara A, Fujii H, Uchida-Kobayashi S, Iwai S, Morikawa H, Enomoto M, Murakami Y, Tamori A, Kawada N. Positioning of 18F-fluorodeoxyglucose-positron emission tomography imaging in the management algorithm of hepatocellular carcinoma. *J Gastroenterol Hepatol* 2014; **29**: 1722-1727 [PMID: [24730671](#) DOI: [10.1111/jgh.12611](#)]
- 27 **Teefey SA**, Hildeboldt CC, Dehdashti F, Siegel BA, Peters MG, Heiken JP, Brown JJ, McFarland EG, Middleton WD, Balfé DM, Ritter JH. Detection of primary hepatic malignancy in liver transplant candidates: prospective comparison of CT, MR imaging, US, and PET. *Radiology* 2003; **226**: 533-542 [PMID: [12563151](#) DOI: [10.1148/radiol.2262011980](#)]
- 28 **Ho CL**, Chen S, Yeung DW, Cheng TK. Dual-tracer PET/CT imaging in evaluation of metastatic hepatocellular carcinoma. *J Nucl Med* 2007; **48**: 902-909 [PMID: [17504862](#) DOI: [10.2967/jnumed.106.036673](#)]
- 29 **Katyal S**, Oliver JH, Peterson MS, Ferris JV, Carr BS, Baron RL. Extrahepatic metastases of hepatocellular carcinoma. *Radiology* 2000; **216**: 698-703 [PMID: [10966697](#) DOI: [10.1148/radiology.216.3.r00se24698](#)]
- 30 **Uka K**, Aikata H, Takaki S, Shirakawa H, Jeong SC, Yamashina K, Hiramatsu A, Kodama H, Takahashi S, Chayama K. Clinical features and prognosis of patients with extrahepatic metastases from hepatocellular carcinoma. *World J Gastroenterol* 2007; **13**: 414-420 [PMID: [17230611](#) DOI: [10.3748/wjg.v13.i3.414](#)]
- 31 **Lee JE**, Jang JY, Jeong SW, Lee SH, Kim SG, Cha SW, Kim YS, Cho YD, Kim HS, Kim BS, Jin SY, Choi DL. Diagnostic value for extrahepatic metastases of hepatocellular carcinoma in positron emission tomography/computed tomography scan. *World J Gastroenterol* 2012; **18**: 2979-2987 [PMID: [22736922](#) DOI: [10.3748/wjg.v18.i23.2979](#)]
- 32 **Sugiyama M**, Sakahara H, Torizuka T, Kanno T, Nakamura F, Futatsubashi M, Nakamura S. 18F-FDG PET in the detection of extrahepatic metastases from hepatocellular carcinoma. *J Gastroenterol* 2004; **39**: 961-968 [PMID: [15549449](#) DOI: [10.1007/s00535-004-1427-5](#)]
- 33 **Park JW**, Kim JH, Kim SK, Kang KW, Park KW, Choi JI, Lee WJ, Kim CM, Nam BH. A prospective evaluation of 18F-FDG and 11C-acetate PET/CT for detection of primary and metastatic hepatocellular carcinoma. *J Nucl Med* 2008; **49**: 1912-1921 [PMID: [18997056](#) DOI: [10.2967/jnumed.108.055087](#)]
- 34 **Yoon KT**, Kim JK, Kim DY, Ahn SH, Lee JD, Yun M, Rha SY, Chon CY, Han KH. Role of 18F-fluorodeoxyglucose positron emission tomography in detecting extrahepatic metastasis in pretreatment staging of hepatocellular carcinoma. *Oncology* 2007; **72** Suppl 1: 104-110 [PMID: [18087190](#) DOI: [10.1159/000111715](#)]
- 35 **Cho Y**, Lee DH, Lee YB, Lee M, Yoo JJ, Choi WM, Cho YY, Paeng JC, Kang KW, Chung JK, Yu SJ, Lee JH, Yoon JH, Lee HS, Kim YJ. Does 18F-FDG positron emission tomography-computed tomography have a role in initial staging of hepatocellular carcinoma? *PLoS One* 2014; **9**: e105679 [PMID: [25153834](#) DOI: [10.1371/journal.pone.0105679](#)]
- 36 **Lee JW**, Lee SM, Lee MS, Shin HC. Role of 18F-FDG PET/CT in the prediction of gastric cancer recurrence after curative surgical resection. *Eur J Nucl Med Mol Imaging* 2012; **39**: 1425-1434 [PMID: [22673973](#) DOI: [10.1007/s00259-012-2164-2](#)]
- 37 **Lee JW**, Na JO, Kang DY, Lee SY, Lee SM. Prognostic Significance of FDG Uptake of Bone Marrow on PET/CT in Patients With Non-Small-Cell Lung Cancer After Curative Surgical Resection. *Clin Lung Cancer* 2017; **18**: 198-206 [PMID: [27495385](#) DOI: [10.1016/j.clcc.2016.07.001](#)]
- 38 **Shiomi S**, Nishiguchi S, Ishizu H, Iwata Y, Sasaki N, Tamori A, Habu D, Takeda T, Kubo S, Ochi H. Usefulness of positron emission tomography with fluorine-18-fluorodeoxyglucose for predicting outcome in patients with hepatocellular carcinoma. *Am J Gastroenterol* 2001; **96**: 1877-1880 [PMID: [11419843](#) DOI: [10.1111/j.1572-0241.2001.03888.x](#)]
- 39 **Lee JW**, Paeng JC, Kang KW, Kwon HW, Suh KS, Chung JK, Lee MC, Lee DS. Prediction of tumor recurrence by 18F-FDG PET in liver transplantation for hepatocellular carcinoma. *J Nucl Med* 2009; **50**: 682-687 [PMID: [19372474](#) DOI: [10.2967/jnumed.108.060574](#)]
- 40 **Sung PS**, Park HL, Yang K, Hwang S, Song MJ, Jang JW, Choi JY, Yoon SK, Yoo IR, Bae SH. 18F-fluorodeoxyglucose uptake of hepatocellular carcinoma as a prognostic predictor in patients with sorafenib treatment. *Eur J Nucl Med Mol Imaging* 2018; **45**: 384-391 [PMID: [29124280](#) DOI: [10.1007/s00259-017-3871-5](#)]
- 41 **Hatano E**, Ikai I, Higashi T, Teramukai S, Torizuka T, Saga T, Fujii H, Shimahara Y. Preoperative positron emission tomography with fluorine-18-fluorodeoxyglucose is predictive of prognosis in patients with hepatocellular carcinoma after resection. *World J Surg* 2006; **30**: 1736-1741 [PMID: [16850145](#) DOI: [10.1007/s00268-005-0791-5](#)]
- 42 **Kitamura K**, Hatano E, Higashi T, Seo S, Nakamoto Y, Yamanaka K, Iida T, Taura K, Yasuchika K, Uemoto S. Preoperative FDG-PET predicts recurrence patterns in hepatocellular carcinoma. *Ann Surg Oncol* 2012; **19**: 156-162 [PMID: [21850564](#) DOI: [10.1245/s10434-011-1990-y](#)]
- 43 **Han JH**, Kim DG, Na GH, Kim EY, Lee SH, Hong TH, You YK. Evaluation of prognostic factors on recurrence after curative resections for hepatocellular carcinoma. *World J Gastroenterol* 2014; **20**: 17132-17140 [PMID: [25493027](#) DOI: [10.3748/wjg.v20.i45.17132](#)]
- 44 **Cho KJ**, Choi NK, Shin MH, Chong AR. Clinical usefulness of FDG-PET in patients with hepatocellular carcinoma undergoing surgical resection. *Ann Hepatobiliary Pancreat Surg* 2017; **21**: 194-198 [PMID: [29264581](#) DOI: [10.14701/ahbps.2017.21.4.194](#)]
- 45 **Lim C**, Salloum C, Chalaye J, Lahat E, Costentin CE, Osseis M, Itti E, Feray C, Azoulay D. 18F-FDG PET/CT predicts microvascular invasion and early recurrence after liver resection for hepatocellular carcinoma: A prospective observational study. *HPB (Oxford)* 2018 [PMID: [30401520](#) DOI: [10.1016/j.hpb.2018.10.007](#)]
- 46 **Yoh T**, Seo S, Ogiso S, Kawai T, Okuda Y, Ishii T, Taura K, Higashi T, Nakamoto Y, Hatano E, Kaïdo T, Uemoto S. Proposal of a New Preoperative Prognostic Model for Solitary Hepatocellular Carcinoma Incorporating 18F-FDG-PET Imaging with the ALBI Grade. *Ann Surg Oncol* 2018; **25**: 542-549 [PMID: [29168098](#) DOI: [10.1245/s10434-017-6262-z](#)]
- 47 **Ahn SG**, Kim SH, Jeon TJ, Cho HJ, Choi SB, Yun MJ, Lee JD, Kim KS. The role of preoperative [18F]fluorodeoxyglucose positron emission tomography in predicting early recurrence after curative resection of hepatocellular carcinomas. *J Gastrointest Surg* 2011; **15**: 2044-2052 [PMID: [21904962](#) DOI: [10.1007/s12006-011-0007-1](#)]

- 10.1007/s11605-011-1660-1]
- 48 **Back YH**, Lee SW, Jeong YJ, Jeong JS, Roh YH, Han SY. Tumor-to-muscle ratio of 8F-FDG PET for predicting histologic features and recurrence of HCC. *Hepatogastroenterology* 2015; **62**: 383-388 [PMID: 25916068]
 - 49 **Kim JM**, Kwon CHD, Joh JW, Sinn DH, Choi GS, Paik SW. Prognosis of preoperative positron emission tomography uptake in hepatectomy patients. *Ann Surg Treat Res* 2018; **94**: 183-189 [PMID: 29629352 DOI: 10.4174/ast.2018.94.4.183]
 - 50 **Hwang S**, Joh JW, Wang HJ, Kim DG, Kim KS, Suh KS, Kim SH, Yu HC, Cho CK, Lee YJ, Kim KH, Kim JM, Kim BW, Lee SG. Prognostic Prediction Models for Resection of Large Hepatocellular Carcinoma: A Korean Multicenter Study. *World J Surg* 2018; **42**: 2579-2591 [PMID: 29340726 DOI: 10.1007/s00268-018-4468-2]
 - 51 **Yang SH**, Suh KS, Lee HW, Cho EH, Cho JY, Cho YB, Yi NJ, Lee KU. The role of (18)F-FDG-PET imaging for the selection of liver transplantation candidates among hepatocellular carcinoma patients. *Liver Transpl* 2006; **12**: 1655-1660 [PMID: 16964589 DOI: 10.1002/lt.20861]
 - 52 **Kornberg A**, Freesmeyer M, Bärthel E, Jandt K, Katenkamp K, Steenbeck J, Sappeler A, Habrecht O, Gottschild D, Settmacher U. 18F-FDG-uptake of hepatocellular carcinoma on PET predicts microvascular tumor invasion in liver transplant patients. *Am J Transplant* 2009; **9**: 592-600 [PMID: 19191771 DOI: 10.1111/j.1600-6143.2008.02516.x]
 - 53 **Kornberg A**, Küpper B, Tannapfel A, Büchler P, Krause B, Witt U, Gottschild D, Friess H. Patients with non-[18 F]fludeoxyglucose-avid advanced hepatocellular carcinoma on clinical staging may achieve long-term recurrence-free survival after liver transplantation. *Liver Transpl* 2012; **18**: 53-61 [PMID: 21850692 DOI: 10.1002/lt.22416]
 - 54 **Lee SD**, Kim SH, Kim YK, Kim C, Kim SK, Han SS, Park SJ. (18)F-FDG-PET/CT predicts early tumor recurrence in living donor liver transplantation for hepatocellular carcinoma. *Transpl Int* 2013; **26**: 50-60 [PMID: 23106431 DOI: 10.1111/j.1432-2277.2012.01572.x]
 - 55 **Detry O**, Govaerts L, Deroover A, Vandermeulen M, Meurisse N, Malenga S, Bletard N, Mbendi C, Lamproye A, Honoré P, Meunier P, Delwaide J, Hustinx R. Prognostic value of (18)F-FDG PET/CT in liver transplantation for hepatocarcinoma. *World J Gastroenterol* 2015; **21**: 3049-3054 [PMID: 25780305 DOI: 10.3748/wjg.v21.i10.3049]
 - 56 **Hong G**, Suh KS, Suh SW, Yoo T, Kim H, Park MS, Choi Y, Paeng JC, Yi NJ, Lee KW. Alpha-fetoprotein and (18)F-FDG positron emission tomography predict tumor recurrence better than Milan criteria in living donor liver transplantation. *J Hepatol* 2016; **64**: 852-859 [PMID: 26658686 DOI: 10.1016/j.jhep.2015.11.033]
 - 57 **Hsu CC**, Chen CL, Wang CC, Lin CC, Yong CC, Wang SH, Liu YW, Lin TL, Lee WF, Lin YH, Chan YC, Wu YJ, Eng HL, Cheng YF. Combination of FDG-PET and UCSF Criteria for Predicting HCC Recurrence After Living Donor Liver Transplantation. *Transplantation* 2016; **100**: 1925-1932 [PMID: 27306534 DOI: 10.1097/TP.0000000000001297]
 - 58 **Lee SD**, Lee B, Kim SH, Joo J, Kim SK, Kim YK, Park SJ. Proposal of new expanded selection criteria using total tumor size and (18)F-fluorodeoxyglucose - positron emission tomography/computed tomography for living donor liver transplantation in patients with hepatocellular carcinoma: The National Cancer Center Korea criteria. *World J Transplant* 2016; **6**: 411-422 [PMID: 27358787 DOI: 10.5500/wjt.v6.i2.411]
 - 59 **Kornberg A**, Witt U, Schernhammer M, Kornberg J, Ceyhan GO, Mueller K, Friess H, Thrum K. Combining ¹⁸F-FDG positron emission tomography with Up-to-seven criteria for selecting suitable liver transplant patients with advanced hepatocellular carcinoma. *Sci Rep* 2017; **7**: 14176 [PMID: 29074969 DOI: 10.1038/s41598-017-14430-9]
 - 60 **Takada Y**, Kaido T, Shirabe K, Nagano H, Egawa H, Sugawara Y, Taketomi A, Takahara T, Wakabayashi G, Nakanishi C, Kawagishi N, Kenjo A, Gotoh M, Toyoki Y, Hakamada K, Ohtsuka M, Akamatsu N, Kokudo N, Takeda K, Endo I, Takamura H, Okajima H, Wada H, Kubo S, Kuramitsu K, Ku Y, Ishiyama K, Ohdan H, Ito E, Machara Y, Honda M, Inomata Y, Furukawa H, Uemoto S, Yamaue H, Miyazaki M, Takada T; LTx-PET study group of the Japanese Society of Hepato-Biliary-Pancreatic Surgery and the Japanese Liver Transplantation Society. Significance of preoperative fluorodeoxyglucose-positron emission tomography in prediction of tumor recurrence after liver transplantation for hepatocellular carcinoma patients: a Japanese multicenter study. *J Hepatobiliary Pancreat Sci* 2017; **24**: 49-57 [PMID: 27806426 DOI: 10.1002/jhbp.412]
 - 61 **Ye YF**, Wang W, Wang T, Yu J, Geng L, Yu SF, Yan S, Zheng SS. Role of [¹⁸F] fludeoxyglucose positron emission tomography in the selection of liver transplantation candidates in patients with hepatocellular carcinoma. *Hepatobiliary Pancreat Dis Int* 2017; **16**: 257-263 [PMID: 28603093 DOI: 10.1016/S1499-3872(17)60011-0]
 - 62 **Mazzaferro V**, Regalia E, Doci R, Andreola S, Pulvirenti A, Bozzetti F, Montalto F, Ammatuna M, Morabito A, Gennari L. Liver transplantation for the treatment of small hepatocellular carcinomas in patients with cirrhosis. *N Engl J Med* 1996; **334**: 693-699 [PMID: 8594428 DOI: 10.1056/nejm199603143341104]
 - 63 **Yao FY**, Ferrell L, Bass NM, Watson JJ, Bacchetti P, Venook A, Ascher NL, Roberts JP. Liver transplantation for hepatocellular carcinoma: expansion of the tumor size limits does not adversely impact survival. *Hepatology* 2001; **33**: 1394-1403 [PMID: 11391528 DOI: 10.1053/jhep.2001.24563]
 - 64 **Song MJ**, Bae SH, Yoo IeR, Park CH, Jang JW, Chun HJ, Choi BG, Lee HG, Choi JY, Yoon SK. Predictive value of ¹⁸F-fluorodeoxyglucose PET/CT for transarterial chemolipiodolization of hepatocellular carcinoma. *World J Gastroenterol* 2012; **18**: 3215-3222 [PMID: 22783045 DOI: 10.3748/wjg.v18.i25.3215]
 - 65 **Song MJ**, Bae SH, Lee SW, Song DS, Kim HY, Yoo IeR, Choi JI, Lee YJ, Chun HJ, Lee HG, Choi JY, Yoon SK. 18F-fluorodeoxyglucose PET/CT predicts tumour progression after transarterial chemoembolization in hepatocellular carcinoma. *Eur J Nucl Med Mol Imaging* 2013; **40**: 865-873 [PMID: 23436073 DOI: 10.1007/s00259-013-2366-2]
 - 66 **Ma W**, Jia J, Wang S, Bai W, Yi J, Bai M, Quan Z, Yin Z, Fan D, Wang J, Han G. The prognostic value of 18F-FDG PET/CT for hepatocellular carcinoma treated with transarterial chemoembolization (TACE). *Theranostics* 2014; **4**: 736-744 [PMID: 24883123 DOI: 10.7150/thno.8725]
 - 67 **Kim MJ**, Kim YS, Cho YH, Jang HY, Song JY, Lee SH, Jeong SW, Kim SG, Jang JY, Kim HS, Kim BS, Lee WH, Park JM, Lee JM, Lee MH, Choi DL. Use of (18)F-FDG PET to predict tumor progression and survival in patients with intermediate hepatocellular carcinoma treated by transarterial chemoembolization. *Korean J Intern Med* 2015; **30**: 308-315 [PMID: 25995661 DOI: 10.3904/kjim.2015.30.3.308]

- 68 **Kim BK**, Kang WJ, Kim JK, Seong J, Park JY, Kim DY, Ahn SH, Lee DY, Lee KH, Lee JD, Han KH. 18F-fluorodeoxyglucose uptake on positron emission tomography as a prognostic predictor in locally advanced hepatocellular carcinoma. *Cancer* 2011; **117**: 4779-4787 [PMID: [21469082](#) DOI: [10.1002/cncr.26099](#)]
- 69 **Huang WY**, Kao CH, Huang WS, Chen CM, Chang LP, Lee MS, Chao HL, Chiu CH, Lo CH, Jen YM. 18F-FDG PET and combined 18F-FDG-contrast CT parameters as predictors of tumor control for hepatocellular carcinoma after stereotactic ablative radiotherapy. *J Nucl Med* 2013; **54**: 1710-1716 [PMID: [23970365](#) DOI: [10.2967/jnumed.112.119370](#)]
- 70 **Rhee WJ**, Hwang SH, Byun HK, Yun M, Han KH, Seong J. Risk stratification for locally advanced hepatocellular carcinoma using pretreatment alpha-fetoprotein and ¹⁸F-fluoro-2-deoxyglucose positron emission tomography. *Liver Int* 2017; **37**: 592-599 [PMID: [27804192](#) DOI: [10.1111/liv.13297](#)]
- 71 **Kucuk ON**, Soydal C, Araz M, Bilgic S, Ibis E. Prognostic importance of 18F-FDG uptake pattern of hepatocellular cancer patients who received SIRT. *Clin Nucl Med* 2013; **38**: e283-e289 [PMID: [23531737](#) DOI: [10.1097/RLU.0b013e3182867f17](#)]
- 72 **Sabet A**, Ahmadzadehfard H, Bruhman J, Sabet A, Meyer C, Wasmuth JC, Pieper CC, Biersack HJ, Ezziddin S. Survival in patients with hepatocellular carcinoma treated with 90Y-microsphere radioembolization. Prediction by 18F-FDG PET. *Nuklearmedizin* 2014; **53**: 39-45 [PMID: [24777354](#) DOI: [10.3413/Nukmed-0622-13-09](#)]
- 73 **Soydal C**, Keskin O, Kucuk ON, Ozkan E, Bilgic S, Idilman R, Kir MK. Prognostic factors for prediction of survival of hepatocellular cancer patients after selective internal radiation therapy. *Ann Nucl Med* 2015; **29**: 426-430 [PMID: [25783289](#) DOI: [10.1007/s12149-015-0962-x](#)]
- 74 **Abuodeh Y**, Naghavi AO, Ahmed KA, Venkat PS, Kim Y, Kis B, Choi J, Biebel B, Sweeney J, Anaya DA, Kim R, Malafa M, Frakes JM, Hoffe SE, El-Haddad G. Prognostic value of pre-treatment F-18-FDG PET-CT in patients with hepatocellular carcinoma undergoing radioembolization. *World J Gastroenterol* 2016; **22**: 10406-10414 [PMID: [28058021](#) DOI: [10.3748/wjg.v22.i47.10406](#)]
- 75 **Jreige M**, Mitsakis P, Van Der Gucht A, Pomoni A, Silva-Monteiro M, Gnesin S, Boubaker A, Nicod-Lalonde M, Duran R, Prior JO, Denys A, Schaefer N. ¹⁸F-FDG PET/CT predicts survival after ⁹⁰Y transarterial radioembolization in unresectable hepatocellular carcinoma. *Eur J Nucl Med Mol Imaging* 2017; **44**: 1215-1222 [PMID: [28233086](#) DOI: [10.1007/s00259-017-3653-0](#)]
- 76 **Lee JH**, Park JY, Kim DY, Ahn SH, Han KH, Seo HJ, Lee JD, Choi HJ. Prognostic value of 18F-FDG PET for hepatocellular carcinoma patients treated with sorafenib. *Liver Int* 2011; **31**: 1144-1149 [PMID: [21745288](#) DOI: [10.1111/j.1478-3231.2011.02541.x](#)]
- 77 **Hyun SH**, Eo JS, Lee JW, Choi JY, Lee KH, Na SJ, Hong IK, Oh JK, Chung YA, Song BI, Kim TS, Kim KS, Moon DH, Yun M. Prognostic value of (18)F-fluorodeoxyglucose positron emission tomography/computed tomography in patients with Barcelona Clinic Liver Cancer stages 0 and A hepatocellular carcinomas: a multicenter retrospective cohort study. *Eur J Nucl Med Mol Imaging* 2016; **43**: 1638-1645 [PMID: [26936852](#) DOI: [10.1007/s00259-016-3348-y](#)]
- 78 **Na SJ**, Oh JK, Hyun SH, Lee JW, Hong IK, Song BI, Kim TS, Eo JS, Lee SW, Yoo IR, Chung YA, Yun M. ¹⁸F-FDG PET/CT Can Predict Survival of Advanced Hepatocellular Carcinoma Patients: A Multicenter Retrospective Cohort Study. *J Nucl Med* 2017; **58**: 730-736 [PMID: [27789714](#) DOI: [10.2967/jnumed.116.182022](#)]
- 79 **Lee JW**, Oh JK, Chung YA, Na SJ, Hyun SH, Hong IK, Eo JS, Song BI, Kim TS, Kim DY, Kim SU, Moon DH, Lee JD, Yun M. Prognostic Significance of ¹⁸F-FDG Uptake in Hepatocellular Carcinoma Treated with Transarterial Chemoembolization or Concurrent Chemoradiotherapy: A Multicenter Retrospective Cohort Study. *J Nucl Med* 2016; **57**: 509-516 [PMID: [26742711](#) DOI: [10.2967/jnumed.115.167338](#)]
- 80 **Hyun SH**, Eo JS, Song BI, Lee JW, Na SJ, Hong IK, Oh JK, Chung YA, Kim TS, Yun M. Preoperative prediction of microvascular invasion of hepatocellular carcinoma using ¹⁸F-FDG PET/CT: a multicenter retrospective cohort study. *Eur J Nucl Med Mol Imaging* 2018; **45**: 720-726 [PMID: [29167923](#) DOI: [10.1007/s00259-017-3880-4](#)]
- 81 **Lee JW**, Hwang SH, Kim DY, Han KH, Yun M. Prognostic Value of FDG Uptake of Portal Vein Tumor Thrombosis in Patients With Locally Advanced Hepatocellular Carcinoma. *Clin Nucl Med* 2017; **42**: e35-e40 [PMID: [27775940](#) DOI: [10.1097/rlu.0000000000001422](#)]
- 82 **Toyosaka A**, Okamoto E, Mitsunobu M, Oriyama T, Nakao N, Miura K. Intrahepatic metastases in hepatocellular carcinoma: evidence for spread via the portal vein as an efferent vessel. *Am J Gastroenterol* 1996; **91**: 1610-1615 [PMID: [8759671](#)]
- 83 **Addario L**, Tritto G, Cavaglià E, Amodio F, Giannelli E, Di Costanzo GG. Preserved liver function, portal thrombosis and absence of oesophageal varices are risk factors for metastasis of hepatocellular carcinoma. *Dig Liver Dis* 2011; **43**: 319-324 [PMID: [20952262](#) DOI: [10.1016/j.dld.2010.09.003](#)]
- 84 **Larson SM**, Erdi Y, Akhurst T, Mazumdar M, Macapinlac HA, Finn RD, Casilla C, Fazzari M, Srivastava N, Yeung HW, Humm JL, Guillem J, Downey R, Karpeh M, Cohen AE, Ginsberg R. Tumor Treatment Response Based on Visual and Quantitative Changes in Global Tumor Glycolysis Using PET-FDG Imaging. The Visual Response Score and the Change in Total Lesion Glycolysis. *Clin Positron Imaging* 1999; **2**: 159-171 [PMID: [14516540](#)]
- 85 **Choi MY**, Lee KM, Chung JK, Lee DS, Jeong JM, Park JG, Kim JH, Lee MC. Correlation between serum CEA level and metabolic volume as determined by FDG PET in postoperative patients with recurrent colorectal cancer. *Ann Nucl Med* 2005; **19**: 123-129 [PMID: [15909492](#)]
- 86 **Lee JW**, Kang CM, Choi HJ, Lee WJ, Song SY, Lee JH, Lee JD. Prognostic Value of Metabolic Tumor Volume and Total Lesion Glycolysis on Preoperative ¹⁸F-FDG PET/CT in Patients with Pancreatic Cancer. *J Nucl Med* 2014; **55**: 898-904 [PMID: [24711649](#) DOI: [10.2967/jnumed.113.131847](#)]
- 87 **Im HJ**, Bradshaw T, Solaiyappan M, Cho SY. Current Methods to Define Metabolic Tumor Volume in Positron Emission Tomography: Which One is Better? *Nucl Med Mol Imaging* 2018; **52**: 5-15 [PMID: [29391907](#) DOI: [10.1007/s13139-017-0493-6](#)]
- 88 **Hyun SH**, Choi JY, Kim K, Kim J, Shim YM, Um SW, Kim H, Lee KH, Kim BT. Volume-based parameters of (18)F-fluorodeoxyglucose positron emission tomography/computed tomography improve outcome prediction in early-stage non-small cell lung cancer after surgical resection. *Ann Surg* 2013; **257**: 364-370 [PMID: [22968069](#) DOI: [10.1097/SLA.0b013e318262a6ec](#)]
- 89 **Ryu IS**, Kim JS, Roh JL, Lee JH, Cho KJ, Choi SH, Nam SY, Kim SY. Prognostic value of preoperative metabolic tumor volume and total lesion glycolysis measured by 18F-FDG PET/CT in salivary gland carcinomas. *J Nucl Med* 2013; **54**: 1032-1038 [PMID: [23670902](#) DOI: [10.2967/jnumed.112.116053](#)]
- 90 **Lee JW**, Yun M, Cho A, Han KH, Kim DY, Lee SM, Lee JD. The predictive value of metabolic tumor

- volume on FDG PET/CT for transarterial chemoembolization and transarterial chemotherapy infusion in hepatocellular carcinoma patients without extrahepatic metastasis. *Ann Nucl Med* 2015; **29**: 400-408 [PMID: 25652647 DOI: 10.1007/s12149-015-0956-8]
- 91 **Kim YI**, Paeng JC, Cheon GJ, Suh KS, Lee DS, Chung JK, Kang KW. Prediction of Posttransplantation Recurrence of Hepatocellular Carcinoma Using Metabolic and Volumetric Indices of 18F-FDG PET/CT. *J Nucl Med* 2016; **57**: 1045-1051 [PMID: 26985057 DOI: 10.2967/jnumed.115.170076]
 - 92 **Hwang SH**, Lee JW, Cho HJ, Kim KS, Choi GH, Yun M. Prognostic Value of Metabolic Tumor Volume and Total Lesion Glycolysis on Preoperative 18F-FDG PET/CT in Patients With Very Early and Early Hepatocellular Carcinoma. *Clin Nucl Med* 2017; **42**: 34-39 [PMID: 27775949 DOI: 10.1097/rlu.0000000000001449]
 - 93 **Lee JW**, Hwang SH, Kim HJ, Kim D, Cho A, Yun M. Volumetric parameters on FDG PET can predict early intrahepatic recurrence-free survival in patients with hepatocellular carcinoma after curative surgical resection. *Eur J Nucl Med Mol Imaging* 2017; **44**: 1984-1994 [PMID: 28695236 DOI: 10.1007/s00259-017-3764-7]
 - 94 **Shimada M**, Takenaka K, Gion T, Fujiwara Y, Kajiyama K, Maeda T, Shirabe K, Nishizaki T, Yanaga K, Sugimachi K. Prognosis of recurrent hepatocellular carcinoma: a 10-year surgical experience in Japan. *Gastroenterology* 1996; **111**: 720-726 [PMID: 8780578]
 - 95 **Poon RT**, Fan ST, Ng IO, Lo CM, Liu CL, Wong J. Different risk factors and prognosis for early and late intrahepatic recurrence after resection of hepatocellular carcinoma. *Cancer* 2000; **89**: 500-507 [PMID: 10931448]
 - 96 **Uchino K**, Tateishi R, Shiina S, Kanda M, Masuzaki R, Kondo Y, Goto T, Omata M, Yoshida H, Koike K. Hepatocellular carcinoma with extrahepatic metastasis: clinical features and prognostic factors. *Cancer* 2011; **117**: 4475-4483 [PMID: 21437884 DOI: 10.1002/cncr.25960]
 - 97 **Ochi H**, Hirooka M, Hiraoka A, Koizumi Y, Abe M, Sogabe I, Ishimaru Y, Furuya K, Miyagawa M, Kawasaki H, Michitaka K, Takada Y, Mochizuki T, Hiasa Y. ¹⁸F-FDG-PET/CT predicts the distribution of microsatellite lesions in hepatocellular carcinoma. *Mol Clin Oncol* 2014; **2**: 798-804 [PMID: 25054048 DOI: 10.3892/mco.2014.328]
 - 98 **Park S**, Kim TS, Kang SH, Kim HB, Park JW, Kim SK. 11C-acetate and 18F-fluorodeoxyglucose positron emission tomography/computed tomography dual imaging for the prediction of response and prognosis after transarterial chemoembolization. *Medicine (Baltimore)* 2018; **97**: e12311 [PMID: 30212970 DOI: 10.1097/MD.00000000000012311]
 - 99 **Ahn SG**, Jeon TJ, Lee SD, Kim SH, Cho HJ, Yun M, Park YN, Lee JD, Park SJ, Kim KS. A survival benefit of major hepatectomy for hepatocellular carcinoma identified by preoperative [18F] fluorodeoxyglucose positron emission tomography in patients with well-preserved hepatic function. *Eur J Surg Oncol* 2013; **39**: 964-973 [PMID: 23859893 DOI: 10.1016/j.ejso.2013.06.019]
 - 100 **Kim JW**, Seong J, Yun M, Lee IJ, Yoon HI, Cho HJ, Han KH. Usefulness of positron emission tomography with fluorine-18-fluorodeoxyglucose in predicting treatment response in unresectable hepatocellular carcinoma patients treated with external beam radiotherapy. *Int J Radiat Oncol Biol Phys* 2012; **82**: 1172-1178 [PMID: 21570203 DOI: 10.1016/j.ijrobp.2010.11.076]
 - 101 **Choi SH**, Chang JS, Jeong YH, Lee Y, Yun M, Seong J. FDG-PET predicts outcomes of treated bone metastasis following palliative radiotherapy in patients with hepatocellular carcinoma. *Liver Int* 2014; **34**: 1118-1125 [PMID: 24528941 DOI: 10.1111/liv.12487]
 - 102 **Jo IY**, Son SH, Kim M, Sung SY, Won YK, Kang HJ, Lee SJ, Chung YA, Oh JK, Kay CS. Prognostic value of pretreatment (18)F-FDG PET-CT in radiotherapy for patients with hepatocellular carcinoma. *Radiat Oncol J* 2015; **33**: 179-187 [PMID: 26484301 DOI: 10.3857/roj.2015.33.3.179]
 - 103 **Aerts HJ**, Velazquez ER, Leijenaar RT, Parmar C, Grossmann P, Carvalho S, Bussink J, Monshouwer R, Haibe-Kains B, Rietveld D, Hoebbers F, Rietbergen MM, Leemans CR, Dekker A, Quackenbush J, Gillies RJ, Lambin P. Decoding tumour phenotype by noninvasive imaging using a quantitative radiomics approach. *Nat Commun* 2014; **5**: 4006 [PMID: 24892406 DOI: 10.1038/ncomms5006]
 - 104 **Lambin P**, Rios-Velazquez E, Leijenaar R, Carvalho S, van Stiphout RG, Granton P, Zegers CM, Gillies R, Boellard R, Dekker A, Aerts HJ. Radiomics: extracting more information from medical images using advanced feature analysis. *Eur J Cancer* 2012; **48**: 441-446 [PMID: 22257792 DOI: 10.1016/j.ejca.2011.11.036]
 - 105 **Lee JW**, Lee SM. Radiomics in Oncological PET/CT: Clinical Applications. *Nucl Med Mol Imaging* 2018; **52**: 170-189 [PMID: 29942396 DOI: 10.1007/s13139-017-0500-y]
 - 106 **Hatt M**, Majdoub M, Vallières M, Tixier F, Le Rest CC, Groheux D, Hindié E, Martineau A, Pradier O, Hustinx R, Perdrisot R, Guillemin R, El Naqa I, Visvikis D. 18F-FDG PET uptake characterization through texture analysis: investigating the complementary nature of heterogeneity and functional tumor volume in a multi-cancer site patient cohort. *J Nucl Med* 2015; **56**: 38-44 [PMID: 25500829 DOI: 10.2967/jnumed.114.144055]
 - 107 **Blanc-Durand P**, Van Der Gucht A, Jreige M, Nicod-Lalonde M, Silva-Monteiro M, Prior JO, Denys A, Depeursinge A, Schaefer N. Signature of survival: a ¹⁸F-FDG PET based whole-liver radiomic analysis predicts survival after ⁹⁰Y-TARE for hepatocellular carcinoma. *Oncotarget* 2017; **9**: 4549-4558 [PMID: 29435123 DOI: 10.18632/oncotarget.23423]
 - 108 **Choi H**. Deep Learning in Nuclear Medicine and Molecular Imaging: Current Perspectives and Future Directions. *Nucl Med Mol Imaging* 2018; **52**: 109-118 [PMID: 29662559 DOI: 10.1007/s13139-017-0504-7]

P- Reviewer: Tsoulfas G

S- Editor: Ma RY L- Editor: A E- Editor: Huang Y





Noninvasive evaluation of nonalcoholic fatty liver disease: Current evidence and practice

Jiang-Hua Zhou, Jing-Jing Cai, Zhi-Gang She, Hong-Liang Li

ORCID number: Jiang-Hua Zhou (0000-0001-7285-9488); Jing-Jing Cai (0000-0002-7820-536X); Zhi-Gang She (0000-0001-9402-4166); Hong-Liang Li (0000-0002-9821-0297).

Author contributions: Zhou JH and Cai J performed the literature search and wrote the paper; Li H and She ZG supervised and approved the final version of the review.

Supported by the Key Project of the National Natural Science Foundation (No. 81630011, to H.L.); the National Science Fund for Distinguished Young Scholars (No. 81425005, to H.L.); the Major Research Plan of the National Natural Science Foundation of China (No. 91639304 and No. 91729303, to H.L.); the Creative Group Project of Hubei Province (No. 2016CFA010, to H.L.); the Hubei Science and Technology Support Project (No. 2018BEC473, to H.L.).

Conflict-of-interest statement: No potential conflicts of interest exist.

Open-Access: This is an open-access article that was selected by an in-house editor and fully peer-reviewed by external reviewers. It is distributed in accordance with the Creative Commons Attribution Non Commercial (CC BY-NC 4.0) license, which permits others to distribute, remix, adapt, build upon this work non-commercially, and license their derivative works on different terms, provided the original work is properly cited and the use is non-commercial. See: <http://creativecommons.org/licenses/by-nc/4.0/>

Jiang-Hua Zhou, Zhi-Gang She, Hong-Liang Li, Department of Cardiology, Renmin Hospital of Wuhan University, Institute of Model Animal of Wuhan University, Wuhan 430071, Hubei Province, China

Jing-Jing Cai, Department of Cardiology, The 3rd Xiangya Hospital of Central South University, Changsha 410013, Hunan Province, China

Corresponding author: Hong-Liang Li, MD, PhD, Professor, Department of Cardiology, Renmin Hospital of Wuhan University, Institute of Model Animal of Wuhan University, No. 115, Donghu Road, Wuchang District, Wuhan 430071, Hubei Province, China.

lihl@whu.edu.cn

Telephone: +86-27-68759302

Fax: +86-27-68759302

Abstract

With the increasing number of individuals with diabetes and obesity, nonalcoholic fatty liver disease (NAFLD) is becoming increasingly prevalent, affecting one-quarter of adults worldwide. The spectrum of NAFLD ranges from simple steatosis or nonalcoholic fatty liver (NAFL) to nonalcoholic steatohepatitis (NASH). NAFLD, especially NASH, may progress to fibrosis, leading to cirrhosis and hepatocellular carcinoma. NAFLD can impose a severe economic burden, and patients with NAFLD-related terminal or deteriorative liver diseases have become one of the main groups receiving liver transplantation. The increasing prevalence of NAFLD and the severe outcomes of NASH make it necessary to use effective methods to identify NAFLD. Although recognized as the gold standard, biopsy is limited by its sampling bias, poor acceptability, and severe complications, such as mortality, bleeding, and pain. Therefore, noninvasive methods are urgently needed to avoid biopsy for diagnosing NAFLD. This review discusses the current noninvasive methods for assessing NAFLD, including steatosis, NASH, and NAFLD-related fibrosis, and explores the advantages and disadvantages of measurement tools. In addition, we analyze potential noninvasive biomarkers for tracking disease processes and monitoring treatment effects, and explore effective algorithms consisting of imaging and nonimaging biomarkers for diagnosing advanced fibrosis and reducing unnecessary biopsies in clinical practice.

Key words: Nonalcoholic fatty liver disease; Nonalcoholic steatohepatitis; Steatosis; Fibrosis; Noninvasive evaluation

©The Author(s) 2019. Published by Baishideng Publishing Group Inc. All rights reserved.

Manuscript source: Invited manuscript

Received: January 14, 2019

Peer-review started: January 18, 2019

First decision: January 30, 2019

Revised: February 20, 2019

Accepted: February 22, 2019

Article in press: February 22, 2019

Published online: March 21, 2019

Core tip: Nonalcoholic fatty liver disease (NAFLD) is becoming a major public health issue worldwide. Currently, biopsy is the gold standard for the diagnosis of NAFLD, but it has well-known limitations including sampling errors and severe complications. Thus, noninvasive methods are best alterations to avoid the biopsy. Herein, the noninvasive methods currently available for the assessment of NAFLD in adults are discussed, and we further evaluate the advantages and disadvantages of different assessing tools. In addition, we also analyze the potential of noninvasive biomarkers and their application for tracking NAFLD progression and monitoring the treatment response.

Citation: Zhou JH, Cai JJ, She ZG, Li HL. Noninvasive evaluation of nonalcoholic fatty liver disease: Current evidence and practice. *World J Gastroenterol* 2019; 25(11): 1307-1326

URL: <https://www.wjgnet.com/1007-9327/full/v25/i11/1307.htm>

DOI: <https://dx.doi.org/10.3748/wjg.v25.i11.1307>

INTRODUCTION

With the increasing number of individuals with diabetes and obesity, nonalcoholic fatty liver disease (NAFLD) is becoming increasingly prevalent, affecting more than one-quarter of adults in the world^[1] and 60% of diabetic patients^[2] and rising to 90% in the obese people^[3,4]. In the United States, the prevalence of NAFLD in adults is 24.13%^[1], and it is forecasted to be 33.5% in 2030, and NAFLD cases will reach 100.9 million in the general population^[5]. In Asian, the prevalence of NAFLD has reached to 27.37%^[1], with 20.09% in China^[6]. In some developing countries, such as Sudan, Nigeria, and Iran, the prevalence of NAFLD is about 8.7%-20%^[7-9]. The spectrum of NAFLD covers from simple steatosis or nonalcoholic fatty liver (NAFL) to nonalcoholic steatohepatitis (NASH). NAFLD, especially NASH, may progress to fibrosis, leading to cirrhosis and hepatocellular carcinoma (HCC)^[10]. NAFLD can impose a severe economic burden^[11-13], and patients with NAFLD-related terminal or deteriorative liver diseases have become one of the main groups receiving liver transplantation, overtaking hepatitis C patients^[14,15]. Based on the double pressure of the increasing prevalence of NAFLD and severe outcomes of NASH, many effective treatments for NAFLD are under development. Lifestyle interventions combined with the loss of 10% of body weight may improve the state of steatosis, inflammation, and even fibrosis^[16]. However, the majority of people poorly adhere to long-term, effective lifestyle interventions, which leads to the rapid development of pharmacological treatment. The current therapeutic targets of medicine in clinical trials cover metabolic targets, oxidative stress and inflammation, gut health, and antifibrotics^[17-27]. During this period of clinical drug registration, histological biopsy is the key endpoint replacing the long-term main outcomes, such as mortality^[28,29]. However, liver biopsy specimens have several limitations, such as representing only approximately 1/50000 of the organ and sampling bias. On the other hand, fibrosis is not uniformly distributed^[30], and liver biopsy may cause severe complications, such as mortality, bleeding, and pain. Therefore, it is preferable to use effective noninvasive methods in clinical practice for identifying NAFLD, tracking disease processes, and monitoring treatment effects^[31].

DIAGNOSIS OF NAFLD

Normal hepatic fat content is commonly defined when steatosis in liver histology is less than 5% of hepatocytes^[32-34]. NAFLD is diagnosed by a histological phenotype of steatosis with the exclusion of other chronic liver diseases in more than 5% of cases^[35,36]. However, in clinical practice, noninvasive methods, including assessment of biomarker panels and imaging, are widely applied instead of biopsy for diagnosing NAFLD.

Serum biomarkers and biomarker panels

Fatty liver index (FLI): The FLI is a prevalent biomarker panel consisting of body mass index (BMI), waist circumference, triglycerides, and gamma-glutamyl transferase for identifying NAFLD, with a total score varying between 0 and 100^[37]. The area under the receiver operating characteristic curve (AUROC) of FLI for identifying NAFLD is 0.84^[37], a low cutoff of 30 is used to rule out NAFLD (the

negative likelihood ratio 0.2), and a high cutoff of 60 rule is used with a positive likelihood ratio of 4.3. However, the FLI poorly distinguishes moderate-to-severe steatosis from mild steatosis^[38].

Hepatic steatosis index (HSI): The HSI is a biomarker panel consisting of BMI, diabetes, and the alanine transaminase (ALT)/ aspartate transaminase (AST) ratio. It had an AUROC of 0.79 and 0.82 in the derivation and validation groups, and the two cutoffs, 30 and 36, achieved a > 90% sensitivity and specificity^[39]. However, the HSI accuracy decreases in obese children, with an AUROC of 0.67, sensitivity of 67%, and specificity of 62%^[40]. In addition, like the FLI, the HSI poorly distinguishes moderate-to-severe steatosis from mild steatosis^[38].

SteatoTest: The SteatoTest is a biomarker panel consisting of 10 biochemical tests, age, gender, and BMI. SteatoTest exhibited an AUROC of 0.8 for identifying a > 5% liver fat content in patients with chronic liver diseases^[41]. Further studies are needed to validate the SteatoTest for differentiating individuals with NAFLD from healthy people.

NAFL screening score: The NAFL screening score is an easy-to-calculate model for identifying NAFLD with age, fasting blood glucose, BMI, triglyceride, ALT/AST, and uric acid. In a study of 48,489 patients with the gold standard of ultrasound (US), the NAFL screening score had different cutoffs for males and females, with a cutoff of 32 yielding an AUROC of 0.83 for males and a cutoff of 29 yielding an AUROC of 0.86 for females^[42]. In recent years, machine learning models based on laboratory parameters have been constructed. Yip *et al.*^[42] conducted a study in 922 patients involving 264 NAFLD patients diagnosed by proton-magnetic resonance spectroscopy (¹H-MRS). Six biomarkers from 23 routine laboratory tests were included to construct the NAFLD ridge score, with an AUROC of 0.87-0.88. The low cutoff of 0.24 achieved a sensitivity of 92% and negative predictive value (NPV) of 95%, and the high cutoff of 0.44 achieved a 90% specificity with a corresponding positive predictive value (PPV) of 84%^[42]. Other biomarker panels, such as the triglyceride and glucose index (TyG) and the FLD index, had a moderate AUROC of 0.78 (0.82-0.87) for identifying NAFLD in Chinese subjects^[43-45]. In sum, most studies of biomarker panels for diagnosing NAFLD are based on suboptimal gold standards with US or ¹H-MRS, and few panels are validated in an independent group. Thus, future studies should not only focus on the gold standard of biopsy but also include a large independent validation group.

Imaging

US: US is the first-line imaging test used in clinical practice in individuals with suspected NAFLD^[35], with a typical appearance of a hyperechogenic liver. One recent meta-analysis demonstrated that compared with histology, US had a pooled sensitivity of 85% and specificity of 94% for moderate-to-severe steatosis^[46]. In contrast, US was incapable of detecting steatosis of less than 20%^[36,47] or steatosis in individuals with morbid obesity^[38]. In addition, the accuracy of US for hepatic steatosis assessment is affected by the presence of severe fibrosis^[48] and intra- and inter-observer variability. To detect NAFLD at early stage, the computed-assisted US hepatic/renal ratio (H/R) and US hepatic attenuation rate are used to assess steatosis quantitatively^[47,48]. Both measurements exhibit a slightly better performance than conventional US for assessing hepatic steatosis with an excellent performance with a sensitivity of 95% and specificity of 100%, but the NPV is still low (72% for US H/R ratio and 67% for US hepatic attenuation rate)^[48,49]. In addition, this quantitative US model could improve the reliability and reproducibility in comparison with conventional US, when it is standardized by a tissue-mimicking phantom, while these findings are needed to verify in further studies^[49]. Above all, US is still recommended for diagnosing moderate and severe steatosis in current guideline^[44].

Computed tomography (CT): Nonenhanced CT has been used in clinics to evaluate the severity of fatty liver since 1970, based on the fact that hepatic attenuation is inversely associated with the hepatic fat content. Normal liver has an attenuation value of 50-65 HU, and 8-10 HU higher than that of the spleen. However, the attenuation value of the liver may decrease to less than 40 HU when fatty infiltration occurs. Nonenhanced CT outperforms US in evaluating the severity of fatty liver, achieving a specificity of 100% and sensitivity of 82% for diagnosing higher (>30%) degrees of hepatic steatosis^[50]. Contrast-enhanced CT images are another CT model that can reduce the radiation exposure of nonenhanced CT^[51]. However, contrast-enhanced CT may be more suitable for severe hepatic steatosis using paraspinal or intercostal muscle as the standard reference^[52] because its sensitivity for mild-moderate hepatic steatosis is only 25%^[53]. CT may also be used for hepatic fat

quantification, such as dual-energy CT and hepatic attenuation measurement, but these methods for assessing fatty liver should be sufficiently validated in future clinical studies^[54]. Although CT is more effective for evaluating hepatic steatosis, it is also limited by insufficient accuracy for mild-to-moderate hepatic steatosis and radiation exposure, especially in children^[52].

Controlled attenuation parameter (CAP): CAP, a parameter based on ultrasonic signals, is measured by the FibroScan® with an M probe (3.5 MHz), with a result of 100-400 dB/m. CAP with an M probe is reported to have an AUROC of 0.82 for differentiating any degree of steatosis *vs* no steatosis^[55]. In addition, the cutoff of 248 dB/m yields a sensitivity of 69% and specificity of 82%^[55]. In addition, the study suggests deducting 10 dB/m from the optimal cutoff of the CAP value for individuals with NAFLD or NASH. However, the M probe is less accurate in differentiating hepatic steatosis in obese people^[56]. Therefore, the XL probe was devised to overcome these limitations of the M probe with a lower failure rate and low reliability for measuring liver stiffness in patients with a BMI $\geq 28\text{kg/m}^2$ ^[57]. The XL probe has a higher AUROC than the M probe for distinguishing any degree of steatosis and no steatosis^[58]. Even so, CAP is limited by a low sensitivity for mild steatosis and operator dependency. Few studies have compared CAP with ¹H-MRS for measuring steatosis, and more studies in the future are required to further explore the role of CAP for steatosis assessment.

Magnetic resonance based techniques: Magnetic resonance imaging (MRI) determines steatosis by signal intensity differences on opposed-phase or fat saturation MRI^[59]. MRI-derived proton density fat fraction (MRI-PDFF) is a robust, noninvasive MRI-based methods for assessing hepatic steatosis^[60]. It uses MRI-visible protons that combine with fat in the liver to quantify steatosis by dividing all protons in the liver. Tang *et al*^[60] found that MRI-PDFF was significantly associated with the histological steatosis grade according to the NASH-CRN grade ($\rho = 0.69$, $P < 0.001$), independent of age, sex, other NASH parameters, and NASH diagnosis. The robust correlation was confirmed in several studies^[61-63]. Tang *et al*^[60] also reported an AUROC value of 0.99 for any grade of steatosis *vs* grade 0, 0.83 for grade 2 or higher *vs* grade 1 or lower, and 0.89 for grade 3 *vs* grade 2 or lower. In addition, MRI-PDFF is superior to other imaging tools for the assessment of hepatic steatosis^[64,65], and its performance is not affected by obesity. MRI-PDFF is also regarded as a robust noninvasive method to monitor the treatment effect^[66]; this aspect will be described in detail below. ¹H-MRS is another MR-based technique that directly measures the chemical compositions of the liver^[67]. It is usually used in clinical studies of NAFLD representing biopsy for measurement of intrahepatocellular lipid (IHCL) through calculating PDFF^[6,52]. ¹H-MRS was reported to have a high correlation with biopsy in steatosis assessment^[69] and a sensitivity of 80% for diagnosis of liver fat content $\geq 5\%$ ^[70]. ¹H-MRS was reported to have a good accuracy to detect small amounts of liver fat. Nasr *et al*^[6] found that ¹H-MRS had a specificity of 100% and sensitivity of 79% with a PDFF cut-off value of 3%, a specificity of 94% and sensitivity of 87% with a PDFF cut-off value of 2%. Although recognized as the most accurate noninvasive tool to assess PDFF quantitatively, MRS is limited to its device- and operator-dependency, complexity, and potentially errors^[71]. Complex-based chemical shift imaging-based MRI (CSEMRI) is regarded as a promising method to quantify PDFF, which could quantitatively assess liver fat content with a refined pulse sequence^[72-74]. It exhibits a high correlation with MRSPDFF ($r^2 = 0.985$ for 1.5 T MR systems, $r^2 = 0.991$ for 3.0 T MR systems)^[71]. MR diffusion weighted imaging (DWI) measures motion of water protons diffusing and tissue perfusing^[75,76] and is regarded another promising tool for assessing liver fat content^[77], while it exerts poor performance for detecting steatosis in comparison with MRS and dual echo in phase and out of phase imaging^[78]. Therefore, more studies are needed to evaluate the performance of DWI in the future.

Clinical implication

US is recommended as the first-line diagnostic method in assessing steatosis, while serum biomarkers and biomarker panels are alternative tools when imaging tools are not available in larger scale screening studies (Table 1)^[35]. An increasing number of biomarker panels are used in clinical and research applications, while most are validated in studies with relatively small populations, in individuals at their health checkup, or in studies with suboptimal gold criteria. Therefore, future well-designed studies are needed to develop a more effective noninvasive biomarker panel for identifying NAFLD. MRI-PDFF not only exerts an excellent performance for diagnosing NAFLD but also accurately detects changes in fat content during disease progression^[79]; however, MRI-PDFF is costly, time-consuming, and device dependent, which makes it difficult for wide application. More effective, feasible, and easily

operated tools are needed for diagnosing NAFLD, especially for early steatosis.

DIAGNOSIS OF NASH

NASH is characterized by steatosis, ballooning, and inflammation, with/without fibrosis, which accelerates disease progression. Early detection of NASH is conducive to the prevention of NASH-related fibrosis. Noninvasive biomarkers for NASH include simple serum biomarkers, biomarker panels, and imaging.

Serum biomarkers

Cytokeratin-18 (CK18): CK18, an intermediate filament protein, is one of the most studied biomarkers for the diagnosis of NASH. It is cleaved during the period of cell death, containing CK18 M30 and CK18 M65^[80]. A meta-analysis of 25 studies reported that M30 and M65 had pooled AUROCs of 0.82 and 0.80, while the pooled sensitivity and specificity were 75% and 77%, and 71% and 77%, respectively^[81]. Therefore, CK18 is commonly used with other serum biomarkers to diagnose NASH. Anty *et al*^[82] found that combining metabolic syndrome, ALT, and CK18 in a morbidly obese population could achieve an AUROC of 0.88 compared with CK18 alone, with an AUROC of 0.74. Grigorescu *et al*^[83] reported that the triple combination of adiponectin, CK18, and interleukin (IL)-6 achieved an AUROC of 0.90, a specificity of 85.7%, and a sensitivity of 84.5%. However, the results should be further verified in future studies. In addition, some studies have examined the difference in the accuracy of CK18 in assessing NASH with different stages of fibrosis. Huang *et al*^[84] found an AUROC of 0.93 for NASH with fibrosis stages 3-4 and 0.63-0.78 for NASH with fibrosis stages 0-2, which may indicate that CK18 can predict the disease severity in NASH patients.

Inflammatory markers: CXCL10 is a proinflammatory cytokine involved in diabetes and obesity^[85]. In a previous study, CXCL10 exhibited a moderate accuracy for differentiating NASH from simple steatosis (AUROC, 0.68) and non-NASH (AUROC, 0.77)^[86]. Tumor necrosis factor- α (TNF- α) and IL-8 are common inflammatory markers, which also exhibit a moderate performance with a sensitivity and specificity of 72% and 76%, and 65% and 68%, respectively^[87]. However, when combining these two markers with pyroglutamate, the panel could achieve a sensitivity of 91% and specificity of 87%^[87].

Adipocytokines and hormones: Fibroblast growth factor 21 (FGF21) secreted by the liver is another potential biomarker for NASH. One study reported that FGF21 had an AUROC of 0.62, and the two cutoffs of 126 and 578 pg/mL had a > 90% sensitivity and specificity for diagnosing NASH, but the PPV and NPV of FGF21 were moderate (0.59-0.78) and low (0.49-0.60), respectively^[88]. To improve the PPV and NPV, FGF21 was combined with CK18, which improved the PPV to 82% and the NPV to 74%. Adiponectin was reported to be decrease in NASH patients^[89], which had an AUROC of 0.71 for diagnosing NASH^[83]. However, the AUROC could reach to 0.90 when adiponectin was combined with CK18 M65 and IL-8^[83]. Other adipocytokines, such as leptin and resistin, may be potentially markers for diagnosing NASH, while they are needed to be further validated in more groups^[29].

Other serum biomarkers: Serum iron is a common protein associated with oxygen radicals, which contribute to necroinflammation and fibrosis, two important parameters of NAFLD^[90,91]. Serum iron was higher in individuals with NASH than in those with simple steatosis^[92,93]. In a Japanese study, serum ferritin exhibited a moderate performance for diagnosing NASH (AUROC, 0.73)^[94]. Another study of 619 biopsy-proven NAFLD patients constructed a scoring system that combined serum ferritin with type IV collagen 7S and fasting insulin, which could be used to predict NASH with an AUROC of 0.78-0.85^[95].

Biomarker panel

NASHTest: The NASHTest combines 13 parameters to diagnose NASH in three categories, namely, NASH, Borderline NASH, and No-NASH, according to Kleiner's criteria^[96,97]. A study with 257 people found that the NASHTest achieved an AUROC of 0.79 for NASH, 0.69 for borderline NASH, and 0.77-0.83 for no-NASH^[98].

NASH ClinLipMet score: The NASH Clin score is a biomarker panel combining AST, fasting insulin, and the PNPLA3 genotype at rs738409, which achieved an AUROC of 0.78 for diagnosing NASH in 384 patients with a histological diagnosis^[98,99]. To improve the accuracy, Zhou *et al*^[98] added metabolic syndrome-based factors to the NASH Clin score, which was named the 'NASH ClinLipMet score'. This latter score can improve the AUROC to 0.87 and the sensitivity to 75%. However, it is more

Table 1 Imaging modalities for diagnosing nonalcoholic fatty liver disease

Test	Description	Accuracy	Advantages	Disadvantages	Guideline recommendation
Ultrasound	Hyperechoic texture or a bright liver	AUROC 0.93, Sn 85%, Sp 94% for diagnosis of steatosis ^[33]	Cheap; No radiation; Available; Easy to perform	Low sensitivity in individuals with steatosis < 20% or BMI > 40 kg/m ² ; Observer-dependency; Influenced by fibrosis or iron overload	The first-line diagnostic test for diagnosing moderate and severe steatosis ^[32]
Computed tomography	Measurement of liver steatosis with attenuation values of liver and spleen	AUROC 0.99, Sn 100%, Sp 82% for diagnosis of steatosis > 30% ^[29]	Visualize the whole liver; Higher applicability; Quantify moderate-severe steatosis	Low sensitivity for light-moderate steatosis; Radiation exposure	NA
CAP	Measurement of liver steatosis with ultrasound attenuation by Fibroscan	AUROC 0.82, Sn 69%, Sp 82% for diagnosis of any steatosis ^[44]	Immediate assessment; Can be used in ambulatory clinic setting; Measure LSM simultaneously	Operator-dependency; Limited sensitivity; High failure rates in obesity patient; Low accuracy for quantifying steatosis; Uncertain cut-off values	The role of CAP for steatosis assessment is inclusive, more future studies are needed to define the role of CAP ^[32]
Magnetic resonance based techniques	Quantitative measurement of steatosis over the entire liver by adding parameter to MRI scanners	MRI-PDFF: AUROC 0.99, Sn 96%, Sp 100% for diagnosis of any steatosis ^[49] MRS: Sn 80%, Sp 80% for diagnosing steatosis ≥ 5% ^[58]	Not affected by obesity; Quantify assess steatosis over the entire liver; Lower sampling variability	Expensive; Time consuming; Device- and operator-dependency; Not suitable for patients with implantable devices	It is excellent to quantify steatosis, but the high price limits its application ^[32]

AUROC: Area under the receiver operating characteristic curve; Sn: Sensitivity; Sp: Specificity; BMI: Body mass index; CAP: Controlled attenuation parameter; NA: Not applicable; MRI: Magnetic resonance imaging; MRI-PDFF: Magnetic resonance imaging-derived proton density fat fraction; MRS: Magnetic resonance spectroscopy; LSM: Liver stiffness measurement.

suitable for research because the measurement of fasting insulin and PNPLA3 genotype is costly and complex in clinical practice.

Other biomarker panels: Tai *et al*^[100] constructed a simple biomarker panel with the parameters of BMI, ALT, and triglycerides. It achieved an AUROC of 0.80-0.82 in the training and validation cohorts and only included 180 morbidly obese patients after bariatric surgery. Li *et al*^[101] developed a clinical score with ALT, gamma-glutamyl transpeptidase, C-reactive protein, and ApoB/ApoA1 ratios. The cutoff of 3.8 gave a sensitivity of 90% and a specificity of 87% for distinguishing NASH from NAFLD, but the panel is limited to a small sample and lacks validation in an independent group.

Imaging for NASH

NASH consists of various parameters; thus, it is difficult to use routine imaging techniques (ultrasonography, CT, or MRI) to distinguish between NASH and simple steatosis. Elastography was investigated to distinguish NASH and simple steatosis. Chen *et al*^[102] found that the cutoff of 2.74 kPa of magnetic resonance elastography (MRE) had an AUROC of 0.93, but the study had several limitations, such as a small sample and a clear histological definition. Vibration-controlled transient elastography (VCTE) was performed in South Korean patients with an AUROC of 0.75 and a sensitivity of 86% for diagnosing NASH, but the specificity was only 58%^[103]. Another biomarker, liver iron accumulation (LIC), measured by the MR signal decay values, is reported to be significantly related to NAFLD disease severity or fibrosis progression. The MRI-based technology assessing LIC was found to have an AUROC of 0.91 for assessing NASH, with a sensitivity of 83% and specificity of 80%^[103]. Multiparametric MRI technology was used to quantify hepatic steatosis, iron accumulation and fibrosis by 1H-MRS, a T2* map and a T1 relaxation time map, respectively^[104-107]. The technology is regarded as a promising imaging biomarker in small studies^[108] but awaits independent confirmation from larger trials.

New biomarkers

Many potential biomarkers involving NASH are under study^[109-114]. Circulating microRNAs are potentially regarded as attractive biomarkers for NAFLD disease severity due to their stability. A meta-analysis found that miR-34a was reported to have a moderate AUROC of 0.78^[115]. MiR-122 had a pooled AUROC of 0.64-0.70 for

differentiating NASH and simple steatosis^[116,117]. The combination of miR-122, -192, and -21 with CK18-Asp396 achieved an AUROC of 0.83 for diagnosing NASH, while the optimal cutoff gave a moderate sensitivity and specificity^[118]. Other new methods have been investigated, such as breath volatile organic compounds (VOCs). Breath VOCs are closely related to oxidative stress, inflammation, and liver diseases^[119-121]. Froukje *et al.*^[122] found that a panel consisting of three exhaled compounds, 1-propanol, 3-methyl-butanonitrile, and n-tridecane, had an AUROC of 0.77, PPV of 81%, and NPV of 82% for differentiating NASH and non-NASH. In addition, some studies have focused on omic markers. The production of lipidomic, proteomic, metabolomics, and microbiome markers was elevated in NASH patients^[123-131], but more studies with larger validation groups in the future are needed to confirm these findings.

Clinical implication

Noninvasive biomarkers for NASH are an attractive field. CK18 is regarded as a popular biomarker for NASH, but the accuracy varies in current studies. Biomarker panels perform well in diagnosing NASH, but most of them are not validated in an independent group. Although other noninvasive biomarkers, such as imaging and gene biomarkers, are reported to be relatively high in accuracy, effective methods should be available, simple, inexpensive, and accurate in the clinic. In addition, serum biomarkers (*e.g.*, CK18) are less accurate for diagnosing NASH with mild fibrosis, which could lead to higher rates of misdiagnosis. To improve the diagnosis of early NASH, biomarker panels or the combination of serum biomarkers with imaging may contribute to ruling in or ruling out NASH with early fibrosis, but this prospect should be verified in future studies.

DIAGNOSIS OF NAFLD RELATED FIBROSIS

According to the recommendation of the NASH-CRN, fibrosis is categorized into nonfibrosis or mild fibrosis (Metavir = F0-F1), significant fibrosis (SF, Metavir ≥ F2), advanced fibrosis (AF, Metavir ≥ F3), and cirrhosis (Metavir = F4)^[88]. The fibrosis stage is reported to increase the overall mortality in individuals with NAFLD, but not NASH^[127]. Furthermore, SF, AF, and cirrhosis increased the hazard ratios by 1.6-, 3.04-, and 6.53-fold for overall mortality in comparison with that of F0-F1^[127]. Therefore, it is urgent to identify early fibrosis through effective noninvasive methods.

Proprietary biomarkers of fibrosis

The proprietary biomarkers of fibrosis include the procollagen of type III collagen (PIIINP), precursor C3-protein (PRO-C3), hyaluronic acid (HA), and TIMP1. Serum PIIINP is a common fibrosis marker during fibrogenesis. It has a good performance for diagnosing SF (AUROC, 0.81)^[128]. Another PRO-C3 is a marker of the N-terminal propeptide of type III collagen. Several studies have demonstrated that PRO-C3 has an AUROC of 0.75-0.83 for diagnosing AF and 0.76 for cirrhosis^[129,130]. HA is an important element of the extracellular matrix, and it has AUROCs of 0.87, 0.89, and 0.92 for SF, AF, and cirrhosis, respectively^[131]. TIMP1 is a fibrosis biomarker reflecting tissue matrix remodeling, while TIMP1 shows a moderate performance for diagnosing SF (AUROC, 0.74)^[128]. To improve the accuracy, some models were constructed by combining several specific fibrosis biomarkers or combinations of these fibrosis biomarkers with other variables. The enhanced liver fibrosis (ELF) test is a commercial tool that combines three circulating matrix turnover components, including HA, PIIINP, and TIMP-1, with age^[128]. Using a cutoff of 9.8, the ELF test identified AF with a PPV of 72% and NPV of 97%^[132]. Another model consisting of PRO-C3, age, platelets, and the presence of diabetes can achieve an AUROC of 0.86-0.87 and an NPV of 0.97 for identifying AF^[129]. However, further studies validating these biomarkers in a large independent group are needed in the future.

Nonproprietary biomarkers of fibrosis or biomarker panels

AST-to-platelet ratio index (APRI): The APRI was originally a simpler calculation for diagnosing fibrosis severity in chronic hepatitis C^[133]. A recent meta-analysis reported that the APRI had an AUROC of 0.70 for SF, 0.75 for AF, and 0.75 for cirrhosis^[49]. Additionally, the pooled sensitivity of the APRI was relatively low, with a range of 0.33-0.73 for different cutoffs.

FIB-4: FIB-4 is a common biomarker panel used for assessing fibrosis severity and includes age, platelet count, AST, and ALT. FIB-4 was primarily devised to assess the liver fibrosis severity in hepatitis C patients who were also infected with human immunodeficiency virus^[134]. An AUROC value of 0.75 for SF, 0.80 for AF, and 0.85 for cirrhosis was reported in NAFLD patients^[49]. Two cutoffs were used for a higher PPV

and NPV. For instance, using a cutoff of 1.3 for FIB-4, the panel predicted AF with an 85% sensitivity, 65% specificity, 36% PPV, and 95% NPV. On the other hand, using a cutoff of 3.25, FIB-4 predicted AF with a 26% sensitivity, 98% specificity, 75% PPV, and 85% NPV^[135]. The two cutoffs may improve the PPV and NPV, avoiding unnecessary biopsy, while the specificity of FIB-4 was 0.35 for assessing AF in elderly individuals ≥ 65 years of age, which contributed to a high false positive rate^[136]. Therefore, this study recommended a low cutoff of 2 for elderly patients > 65 years of age, with a 77% sensitivity and 70% specificity. In addition, a recent Japanese study of 1050 biopsy-confirmed NAFLD patients recommended cutoffs of 1.88 and 2.67 for 60-69 years of age and 1.95 and 2.67 for ≥ 70 years of age^[137].

NAFLD fibrosis score (NFS): The NFS is the most common noninvasive biomarker panel for assessing fibrosis severity; the panel consists of age, BMI, hyperglycemia, AST/ALT ratio, platelets, and albumin. A multicenter study of 733 people reported a low cutoff of -1.455 for AF with a PPV of 51%-56% and NPV of 88%-93%, and a high cutoff of 0.676 yielded a PPV of 82%-90% and NPV of 80%-85%^[138]. Using this model, 75% of biopsies could be spared with 90% correct prediction. In addition, Xiao *et al*^[49] demonstrated that the NFS had an AUROC of 0.72 for SF, 0.73 for AF, and 0.83 for cirrhosis. The NFS was widely validated in different races, with a high AUROC and NPV^[135,137,138]. However, a low cutoff of 0.12 for NFS assessing fibrosis is recommended for the elderly due to a high false positive rate^[136]. The NFS and FIB-4 are recommended to identify those at low or high risk for AF or cirrhosis in clinical guidelines.

BARD score: The BARD score was an easily calculated score system for assessing fibrosis severity, containing the parameters of BMI, aldosterone renin activity ratio, and the presence of type 2 diabetes mellitus. A score of 2-4 increased the risk of AF by 17-fold, with an AUROC of 0.81 and NPV of 96%, but a low PPV of 43%^[139]. However, a subsequent study validated that the tool in the Japanese group could not achieve a similar performance with an AUROC of 0.73 and NPV of 77% for AF^[140]. In addition, a meta-analysis reported that the BARD score had a pooled AUROC of 0.64 for SF, 0.73 for AF, and 0.70 for cirrhosis in NAFLD patients^[49]. Even so, the BARD score was a valuable model for predicting SF due to its ease and lack of indeterminate results in clinical application.

Imaging

VCTE: VCTE is the first Food and Drug Administration (FDA)-approved elastographic modality performed by FibroScan employing US-based technology. This technology measures the velocity of a 50 MHz shear wave that is emitted by a probe in the intercostal space into the liver. The velocity is positively related to liver stiffness with a range of 1.5 to 75 kPa. A higher shear wave value indicates higher liver stiffness. However, technical failure was found to be a common phenomenon during the operation, ranging from 6.7% to 27.0%, and was primarily reported to be related to a high BMI^[141,142]. The “M” probe was the most prevalent probe measuring shear wave velocity, with an AUROC of 0.83 for SF, 0.87 for AF, and 0.92 for cirrhosis^[49]. Although the “XL” probe was usually used for fibrosis in obese people to reduce the failure rate, this rate was still 35% in patients with a BMI over 30 kg/m²^[143]. Even so, the FibroScan XL probe yields an AUROC of 0.82 for SF, 0.86 for AF, and 0.94 for cirrhosis. One study investigating the suitable cutoffs indicated that 5.8 and 9.0, 7.9 and 9.6, and 10.3 and 11.5 had a $> 90\%$ sensitivity and specificity for SF, AF, and cirrhosis, respectively^[141]. However, the PPV was low for diagnosing fibrosis, and transient elastography easily misclassifies AF as mild. One study comparing transient elastography with the NFS and FIB-4 found that transient elastography was better for AF and cirrhosis but less accurate for diagnosing fibrosis *vs* nonfibrosis and significant fibrosis^[70]. Therefore, some studies have used VCTE along with a serum biomarker. Thomson *et al*^[144] combined VCTE with a FibroMeter and achieved a PPV of 84% for SF and PPV of 89% for AF.

Shear wave elastography (SWE): SWE is a new method integrated into conventional US for assessing fibrosis. It can measure the shear wave velocity and provide a 2-D, real-time, color map of liver elasticity, but it should be conducted under apnea, and the region of the color map should be large vessel-free and at least 15 mm below the capsule. SWE reportedly has a high diagnostic performance for fibrosis assessment in chronic hepatitis patients^[145,146]. In NAFLD patients, SWE yielded an AUROC value of 0.86 for SF, 0.89 for AF, and 0.88 for cirrhosis, respectively^[147]. The results also demonstrated that SWE was better than FibroScan and acoustic radiation force impulse (ARFI). No specific regulations are recommended by the manufacturer for assessing the quality of measurement; thus, some studies assessed the failure rate of SWE with reliability criteria of FibroScan^[147]. In addition, as with the ARFI, the

accuracy of SWE is affected by interobserver variation and food intake^[148]. Therefore, these measurements are recommended to be performed by very experienced radiologists in patients with fasting for at least 2 h^[148].

ARFI: ARFI elastography is an alternative tool for fibrosis assessment integrated into conventional US. It uses short-term acoustic pulses to produce shear waves^[149], with the results expressed in m/s. ARFI should be operated under apnea, and the region of interest should be a vessel-free region. ARFI had an AUROC of 0.77 for SF, 0.84 for AF, and 0.84 for cirrhosis^[147]. Another meta-analysis reported that the pooled sensitivity and specificity were 80.2% and 85.2%, respectively, for detecting SF^[150]. However, its accuracy was affected by the presence of severe steatosis^[151,152]. Further studies are needed to explore the optimal cutoffs of ARFI at different levels of steatosis.

MRE: MRE is a noninvasive MRI-based method measuring liver stiffness by using a modified phase-contrast method^[153-156]. MRE can assess the entire liver with a high success rate^[157]. It is not affected by steatosis and may be applied in patients with obesity, ascites, or bowel interposition between the liver and anterior abdominal wall^[158]. The available MRE model contains 2D-MRE (shear wave frequency 60Hz) and 3D-MRE (shear wave frequency 40Hz). 2D-MRE is more frequently used for assessing liver fibrosis in NAFLD patients. A meta-analysis reported that the pooled AUROCs of 2D MRE for diagnosing SF, AF, and cirrhosis were 0.87, 0.90 and 0.91, respectively^[159]. 3D-MRE had a better performance (AUROC, 0.98) for detecting AF than 2D-MRE (AUROC, 0.92)^[160], and the NPVs of 2D-MRE and 3D-MRE were 0.98 and 1.0, respectively^[160]. Compared to other noninvasive fibrosis biomarkers, MRE was superior to FibroScan, ARFI, and common biomarker panels for discriminating dichotomized fibrosis stages in NAFLD patients^[65,161]. Xiao *et al.*^[42] found that MRE had an AUROC of 0.96, sensitivity of 0.84, and specificity of 0.90 for detecting AF, which was better than BARD score, NFS, and FibroScan. Considering the higher accuracy of MRE in diagnosing fibrosis, it is increasingly regarded as a promising surrogate biomarker for monitoring fibrosis progression and endpoints of fibrosis therapy^[60]. However, MRE has several limitations. It cannot be applied to individuals with hepatic iron overload due to the interfering signal intensity. On the other hand, the cost of MRE and its dependence on MRI facilities limit its wide application.

New biomarkers

Serum DNA methylation has been investigated as a potential biomarker for assessing fibrosis. The plasma DNA methylation of PPAR γ promoter was reported to have a good performance for diagnosing AF (AUROC, 0.91), and the cutoff of 0.81 gave a PPV of 91% and NPV of 87%^[162]. In addition, the DNA methylation at the PPAR γ promoter is superior to the NFS in diagnostic performance and avoids using two cutoffs, but it should be validated in more independent groups.

Clinical implication

Biomarker panels are cheap, feasible, reproducible, and have a good NPV for fibrosis, but they are limited by its low PPV (Table 2). MRE shows excellent accuracy for fibrosis severity but may only be used in some drug studies due to its high cost and unavailability (Table 3). Transient elastography together with biomarker panels would be widely used for assessing fibrosis, but the efficiency should be evaluated in more independent groups. Above all, it is recommended to combine serum biomarkers or clinical rules with imaging tools to diagnose fibrosis, which could reduce unnecessary diagnostic liver biopsies.

NONINVASIVE BIOMARKERS FOR DISEASE PROGRESSION AND THERAPY

Tracking disease progression

NAFLD significantly increases the risk of liver disease-related morbidity, mortality, and liver transplantation^[163,164]. Fibrosis, but not simple steatosis and NASH, increased the risk of mortality in NAFLD patients in a retrospective study with a mean follow-up period of 20 years^[119]. Singh *et al.*^[165] found that one stage of fibrosis progression takes 14.3 years and 7.1 years in individuals with simple steatosis and NASH patients, respectively. In addition, most NAFLD cases are asymptomatic until the disease has progressed to cirrhosis, and repeated biopsy is impractical. Therefore, there is a need to apply useful noninvasive biomarkers to monitor disease progression. A prospective study with a median of seven follow-ups found that the ELF test had an AUROC of 0.87 for predicting liver-related clinical outcomes, which was higher than that of

Table 2 Biomarker panels for diagnosing nonalcoholic fatty liver disease related fibrosis

Test	Description	Accuracy	Advantages	Disadvantages	Guideline recommendation
APRI	AST/platelet ratio index	AUROC 0.70 for SF, 0.75 for AF, and 0.75 for cirrhosis ^[28]	High feasibility; Cheap; Reproducible	Low specificity to diagnose AF; The application of two cut-offs could not discriminate between intermediate stages of fibrosis	NA
Fibrosis-4 index	Age, AST, ALT, and platelet count	AUROC 0.75 for SF, 0.80 for AF, and 0.85 for cirrhosis ^[28]	High feasibility; Cheap; Reproducible	The application of two cut-offs could not discriminate between intermediate stages of fibrosis; Influenced by age	FIB-4 can be used to identify those at low or high risk for AF or cirrhosis ^[32,34]
NFS	Age, BMI, impaired fasting glucose and/or diabetes, AST, ALT, platelet, Count, and albumin	AUROC 0.72 for SF, 0.73 for AF, and 0.83 for cirrhosis ^[28]	High feasibility; Cheap; Reproducible	The application of two cut-offs could not discriminate between intermediate stages of fibrosis; Influenced by age; Influenced by interpretation of BMI across different ethnic groups	NFS can be used to identify those at low or high risk for AF or cirrhosis ^[32]
BARD score	AST, ALT, BMI, and diabetes	AUROC 0.64 for SF, 0.73 for AF, and 0.70 for cirrhosis ^[28]	High feasibility; Cheap; Reproducible; No intermediate stages of fibrosis	Low specificity to diagnose SF and cirrhosis; Influenced by interpretation of BMI across different ethnic groups	NA

ALT: Alanine aminotransferase; AST: Aspartate aminotransferase; BMI: Body mass index; AUROC: Area under the receiver-operating characteristics curve; NFS: Nonalcoholic fatty liver disease fibrosis score; APRI: AST/platelet ratio index; NA: Not applicable; SF: Significant fibrosis; AF: Advanced fibrosis.

biopsy (AUROC, 0.82)^[166]. Sebastiani *et al*^[167] found that baseline liver histology, APRI, FIB-4, and NFS for predicting clinical outcomes had AUROCs of 0.85, 0.89, 0.89 and 0.79, respectively. Another study reported that FibroScan had an accuracy of 0.73 for predicting all-course mortality^[168]. Further studies are needed to determine more effective noninvasive biomarkers for the progression of NASH to NASH-related fibrosis and the progression of NASH-related fibrosis to adverse clinical outcomes.

Monitoring responses to therapies

In terms of NAFLD treatment, it is impractical to observe the primary endpoint of mortality due to long-term follow-up^[28,169,170]. Therefore, the FDA recommends that histological improvement be confirmed when the resolution of NASH is obtained without the worsening of fibrosis or when fibrosis is improved without the worsening of NASH^[171]. However, repeated biopsy hinders the development of drugs; thus, there is a need to investigate noninvasive surrogates replacing biopsy. MRI-PDFF was usually employed to evaluate the liver fat content change in clinical trials of NASH patients^[66]. A study of 113 NASH patients treated with obeticholic acid found that MRI-PDFF had an AUROC of 0.81 for reduced histological steatosis grade^[172]. In contrast, a recent phase II trial of selonsertib found that MRI-PDFF had an AUROC of 0.70 for reduced histological steatosis grade, and the optimal cutoff was 0% with a PPV of 39% and NPV of 92%^[173]. Therefore, whether the change in MRI-PDFF could be regarded as an effective surrogate endpoint for NASH treatment should be further evaluated. Liver function has been regularly regarded as a noninvasive biomarker for assessing the monitoring treatment effect, while ALT concentrations in about two-thirds of patients is normal^[174], and NASH patients usually exhibit spontaneous changes in liver function. Therefore, the ALT change is usually accompanied by a steatosis change, which is regarded as an effective noninvasive endpoint substituting the histological changes in NASH^[171]. The change in liver stiffness measurement (LSM) measured by MRE was evaluated to investigate the antifibrosis effect in NAFLD. Jayakumar *et al*^[173] showed that the MRE had an AUROC of 0.62, PPV of 39%, and NPV of 92% for fibrosis improvement. The biomarker panel has also been investigated for predicting fibrosis improvement in intervention studies of NASH patients. Vilar *et al*^[175] constructed a model consisting of three variables, glycated

Table 3 Imaging modalities for diagnosing nonalcoholic fatty liver disease related fibrosis

Test	Description	Accuracy	Advantages	Disadvantages	Guideline recommendation
VCTE	Measuring the velocity of a 50 mHz shear wave, which is positively related to liver stiffness	AUROC 0.83, 0.87, and 0.92, respectively, for AF, SF, and cirrhosis with M probe ^[28] ; AUROC 0.82, 0.86, and 0.94, respectively, for AF, SF, and cirrhosis with XL probe ^[117]	Relatively low cost; Good reproducibility; Short processing time; Can be used in ambulatory clinic setting	Fasting for 2 h; Device- and operator-dependency; Influenced by obesity, congestion, and inflammation; Uncertain cut-off values; Intermediate stages due to two cut-offs	FibroScan can be used to identify those at low or high risk for AF ^[32,34]
SWE	A method integrated into conventional ultrasound provides a 2-D, real-time, color map of liver elasticity	AUROC 0.86, 0.89, and 0.88, respectively, for AF, SF, and cirrhosis ^[123]	Good reproducibility; Not affected by obesity or ascites	Relatively high cost; Fasting for 2 h; Device- and operator-dependency; Quality criteria not well defined	NA
ARFI	A method integrated into a conventional ultrasound measures shear wave speed	AUROC 0.77, 0.84, and 0.84, respectively, for AF, SF, and cirrhosis ^[123]	Good reproducibility; Not affected by obesity or ascites; ROI smaller than transient elastography	High cost; Fasting for 2 h; Device- and operator-dependency; Quality criteria not well defined; Intermediate stages due to two cut-offs	NA
MRE	A noninvasive MRI based method measures liver stiffness by a modified phase-contrast method	AUROC 0.87, 0.90, and 0.91, respectively, for AF, SF, and cirrhosis ^[131]	Good reproducibility; Not affected by obesity or ascites	High cost; Time consuming; Fasting for 2 h; Device- and operator-dependency; Intermediate stages due to two cut-offs	MRE is clinically useful tools for identifying advanced fibrosis in patients with nonalcoholic fatty liver disease ^[34]

AUROC: Area under the receiver operating characteristic curve; MRE: Magnetic resonance elastography; VCTE: Vibration-controlled transient elastography; SWE: Shear wave elastography; TE: Transient elastography; ARFI: Acoustic radiation force impulse; NA: Not applicable; ROI: Region of interest.

hemoglobin, platelets, and ALT, which demonstrated an AUROC of 0.96 for fibrosis improvement, which is higher than the change in platelet count (AUROC, 0.80), APRI (AUROC, 0.50), FIB-4 index (AUROC, 0.63), and NFS (AUROC, 0.77). The biomarker panels may be the ideal noninvasive tools for assessing the response during the process of therapy, but they should be accurate, available, inexpensive, and simple.

CONCLUSION

The past several years have witnessed the extensive development of noninvasive methods in the NAFLD field, from serum biomarkers and imaging to omics. US and H-MRI have a relatively high accuracy for diagnosing NAFLD, and US is prevalently used in clinical practice and research due to its availability and low cost. There are currently no effective noninvasive biomarkers recommended for diagnosing NASH. Future studies are needed to investigate more efficient noninvasive biomarkers for distinguishing NASH from simple steatosis. VCTE is the FDA-approved elastographic model for assessing fibrosis severity, and it could further improve the diagnostic performance when combined with biomarker panels. Furthermore, effective algorithms consisting of imaging and nonimaging biomarkers should be applied to clinical practice to reduce unnecessary biopsies (Figure 1). In addition, there is a need to investigate the cost-effectiveness of noninvasive evaluations in diagnosing NAFLD, tracking disease progression, and monitoring responses to the therapies.

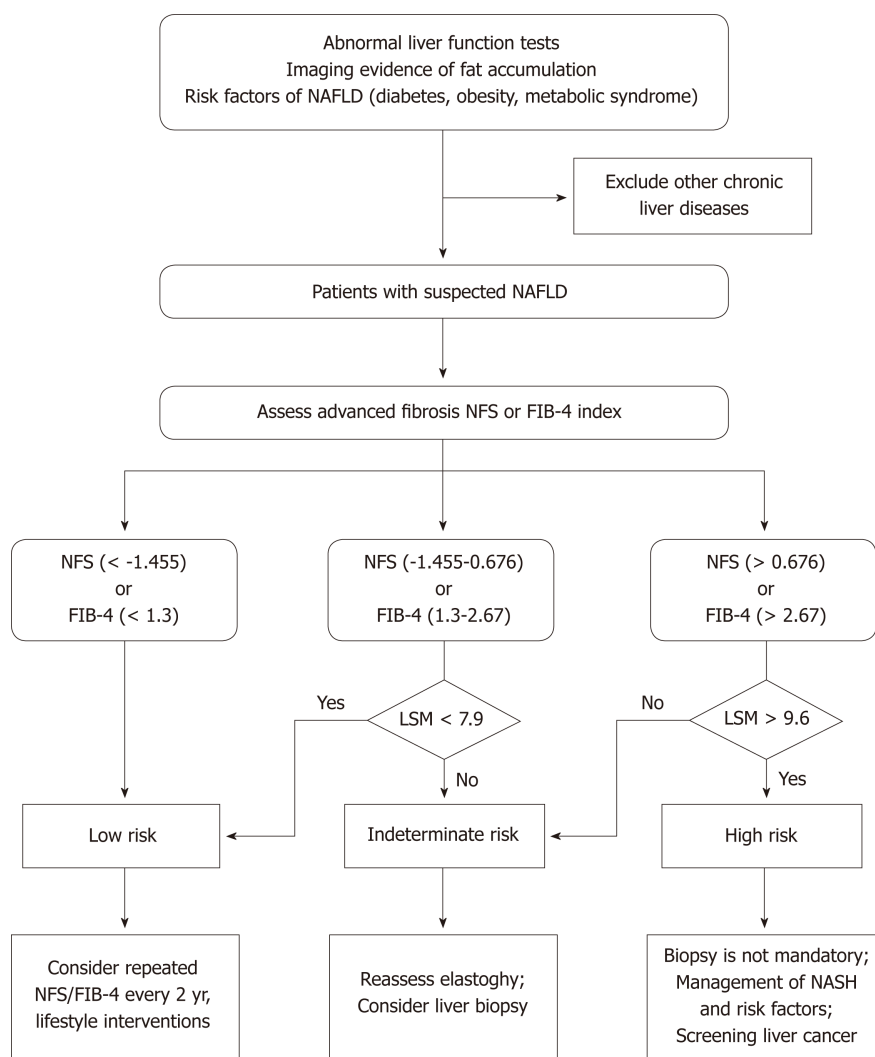


Figure 1 Clinical algorithm with noninvasive testing and liver content measurement by Fibroskan for detecting advanced fibrosis in nonalcoholic fatty liver disease patients. NFS: Nonalcoholic fatty liver disease fibrosis score; NAFLD: Nonalcoholic fatty liver disease; NASH: Nonalcoholic fatty hepatitis; LSM: Liver stiffness measurement.

ACKNOWLEDGEMENTS

The authors thank the staff at Institute of Model Animal of Wuhan University and Department of Cardiology, Renmin Hospital of Wuhan University.

REFERENCES

- 1 **Younossi ZM**, Koenig AB, Abdelatif D, Fazel Y, Henry L, Wymer M. Global epidemiology of nonalcoholic fatty liver disease-Meta-analytic assessment of prevalence, incidence, and outcomes. *Hepatology* 2016; **64**: 73-84 [PMID: 26707365 DOI: 10.1002/hep.28431]
- 2 **Dai W**, Ye L, Liu A, Wen SW, Deng J, Wu X, Lai Z. Prevalence of nonalcoholic fatty liver disease in patients with type 2 diabetes mellitus: A meta-analysis. *Medicine (Baltimore)* 2017; **96**: e8179 [PMID: 28953675 DOI: 10.1097/MD.00000000000008179]
- 3 **Machado M**, Marques-Vidal P, Cortez-Pinto H. Hepatic histology in obese patients undergoing bariatric surgery. *J Hepatol* 2006; **45**: 600-606 [PMID: 16899321 DOI: 10.1016/j.jhep.2006.06.013]
- 4 **Milić S**, Lulić D, Štimac D. Non-alcoholic fatty liver disease and obesity: biochemical, metabolic and clinical presentations. *World J Gastroenterol* 2014; **20**: 9330-9337 [PMID: 25071327 DOI: 10.3748/wjg.v20.i28.9330]
- 5 **Estes C**, Razavi H, Loomba R, Younossi Z, Sanyal AJ. Modeling the epidemic of nonalcoholic fatty liver disease demonstrates an exponential increase in burden of disease. *Hepatology* 2018; **67**: 123-133 [PMID: 28802062 DOI: 10.1002/hep.29466]
- 6 **Li Z**, Xue J, Chen P, Chen L, Yan S, Liu L. Prevalence of nonalcoholic fatty liver disease in mainland of China: a meta-analysis of published studies. *J Gastroenterol Hepatol* 2014; **29**: 42-51 [PMID: 24219010 DOI: 10.1111/jgh.12428]
- 7 **Almobarak AO**, Barakat S, Khalifa MH, Elhoweris MH, Elhassan TM, Ahmed MH. Non alcoholic fatty

- liver disease (NAFLD) in a Sudanese population: What is the prevalence and risk factors? *Arab J Gastroenterol* 2014; **15**: 12-15 [PMID: [24630507](#) DOI: [10.1016/j.ajg.2014.01.008](#)]
- 8 **Onyekwere CA**, Ogbera AO, Balogun BO. Non-alcoholic fatty liver disease and the metabolic syndrome in an urban hospital serving an African community. *Ann Hepatol* 2011; **10**: 119-124 [PMID: [21502672](#)]
- 9 **Eshraghian A**, Dabbaghmanesh MH, Eshraghian H, Fattahi MR, Omrani GR. Nonalcoholic fatty liver disease in a cluster of Iranian population: thyroid status and metabolic risk factors. *Arch Iran Med* 2013; **16**: 584-589 [PMID: [24093139](#)]
- 10 **Ji YX**, Huang Z, Yang X, Wang X, Zhao LP, Wang PX, Zhang XJ, Alves-Bezerra M, Cai L, Zhang P, Lu YX, Bai L, Gao MM, Zhao H, Tian S, Wang Y, Huang ZX, Zhu XY, Zhang Y, Gong J, She ZG, Li F, Cohen DE, Li H. The deubiquitinating enzyme cylindromatosis mitigates nonalcoholic steatohepatitis. *Nat Med* 2018; **24**: 213-223 [PMID: [29291351](#) DOI: [10.1038/nm.4461](#)]
- 11 **Younossi ZM**, Blissett D, Blissett R, Henry L, Stepanova M, Younossi Y, Racila A, Hunt S, Beckerman R. The economic and clinical burden of nonalcoholic fatty liver disease in the United States and Europe. *Hepatology* 2016; **64**: 1577-1586 [PMID: [27543837](#) DOI: [10.1002/hep.28785](#)]
- 12 **Zhang XJ**, She ZG, Li H. Time to step-up the fight against NAFLD. *Hepatology* 2018; **67**: 2068-2071 [PMID: [29451316](#) DOI: [10.1002/hep.29845](#)]
- 13 **Perumpail BJ**, Khan MA, Yoo ER, Cholankeril G, Kim D, Ahmed A. Clinical epidemiology and disease burden of nonalcoholic fatty liver disease. *World J Gastroenterol* 2017; **23**: 8263-8276 [PMID: [29307986](#) DOI: [10.3748/wjg.v23.i47.8263](#)]
- 14 **Wong RJ**, Cheung R, Ahmed A. Nonalcoholic steatohepatitis is the most rapidly growing indication for liver transplantation in patients with hepatocellular carcinoma in the U.S. *Hepatology* 2014; **59**: 2188-2195 [PMID: [24375711](#) DOI: [10.1002/hep.26986](#)]
- 15 **Mikolasevic I**, Filipec-Kanizaj T, Mijic M, Jakopcic I, Milic S, Hrstic I, Sobocan N, Stimac D, Burra P. Nonalcoholic fatty liver disease and liver transplantation - Where do we stand? *World J Gastroenterol* 2018; **24**: 1491-1506 [PMID: [29662288](#) DOI: [10.3748/wjg.v24.i14.1491](#)]
- 16 **Lassailly G**, Caiazzo R, Pattou F, Mathurin P. Perspectives on Treatment for Nonalcoholic Steatohepatitis. *Gastroenterology* 2016; **150**: 1835-1848 [PMID: [26971824](#) DOI: [10.1053/j.gastro.2016.03.004](#)]
- 17 **Rotman Y**, Sanyal AJ. Current and upcoming pharmacotherapy for non-alcoholic fatty liver disease. *Gut* 2017; **66**: 180-190 [PMID: [27646933](#) DOI: [10.1136/gutjnl-2016-312431](#)]
- 18 **Xie L**, Wang PX, Zhang P, Zhang XJ, Zhao GN, Wang A, Guo J, Zhu X, Zhang Q, Li H. DKK3 expression in hepatocytes defines susceptibility to liver steatosis and obesity. *J Hepatol* 2016; **65**: 113-124 [PMID: [27016281](#) DOI: [10.1016/j.jhep.2016.03.008](#)]
- 19 **Yan FJ**, Zhang XJ, Wang WX, Ji YX, Wang PX, Yang Y, Gong J, Shen LJ, Zhu XY, Huang Z, Li H. The E3 ligase tripartite motif 8 targets TAK1 to promote insulin resistance and steatohepatitis. *Hepatology* 2017; **65**: 1492-1511 [PMID: [27981609](#) DOI: [10.1002/hep.28971](#)]
- 20 **Gao L**, Wang PX, Zhang Y, Yu CJ, Ji Y, Wang X, Zhang P, Jiang X, Jin H, Huang Z, Zhang ZR, Li H. Tumor necrosis factor receptor-associated factor 5 (Traf5) acts as an essential negative regulator of hepatic steatosis. *J Hepatol* 2016; **65**: 125-136 [PMID: [27032381](#) DOI: [10.1016/j.jhep.2016.03.006](#)]
- 21 **Cai J**, Xu M, Zhang X, Li H. Innate Immune Signaling in Nonalcoholic Fatty Liver Disease and Cardiovascular Diseases. *Annu Rev Pathol* 2019; **14**: 153-184 [PMID: [30230967](#) DOI: [10.1146/annurev-pathmechdis-012418-013003](#)]
- 22 **Wang XA**, Zhang R, Zhang S, Deng S, Jiang D, Zhong J, Yang L, Wang T, Hong S, Guo S, She ZG, Zhang XD, Li H. Interferon regulatory factor 7 deficiency prevents diet-induced obesity and insulin resistance. *Am J Physiol Endocrinol Metab* 2013; **305**: E485-E495 [PMID: [23695216](#) DOI: [10.1152/ajpendo.00505.2012](#)]
- 23 **Wang PX**, Zhang XJ, Luo P, Jiang X, Zhang P, Guo J, Zhao GN, Zhu X, Zhang Y, Yang S, Li H. Hepatocyte TRAF3 promotes liver steatosis and systemic insulin resistance through targeting TAK1-dependent signalling. *Nat Commun* 2016; **7**: 10592 [PMID: [26882989](#) DOI: [10.1038/ncomms10592](#)]
- 24 **Xu M**, Liu PP, Li H. Innate Immune Signaling and Its Role in Metabolic and Cardiovascular Diseases. *Physiol Rev* 2019; **99**: 893-948 [PMID: [30565509](#) DOI: [10.1152/physrev.00065.2017](#)]
- 25 **Xiang M**, Wang PX, Wang AB, Zhang XJ, Zhang Y, Zhang P, Mei FH, Chen MH, Li H. Targeting hepatic TRAF1-ASK1 signaling to improve inflammation, insulin resistance, and hepatic steatosis. *J Hepatol* 2016; **64**: 1365-1377 [PMID: [26860405](#) DOI: [10.1016/j.jhep.2016.02.002](#)]
- 26 **Eshraghian A**. Current and emerging pharmacological therapy for non-alcoholic fatty liver disease. *World J Gastroenterol* 2017; **23**: 7495-7504 [PMID: [29204050](#) DOI: [10.3748/wjg.v23.i42.7495](#)]
- 27 **Kanda T**, Matsuoka S, Yamazaki M, Shibata T, Nirei K, Takahashi H, Kaneko T, Fujisawa M, Higuchi T, Nakamura H, Matsumoto N, Yamagami H, Ogawa M, Imazu H, Kuroda K, Moriyama M. Apoptosis and non-alcoholic fatty liver diseases. *World J Gastroenterol* 2018; **24**: 2661-2672 [PMID: [29991872](#) DOI: [10.3748/wjg.v24.i25.2661](#)]
- 28 **Ekstedt M**, Franzén LE, Mathiesen UL, Thorelius L, Holmqvist M, Bodemar G, Kechagias S. Long-term follow-up of patients with NAFLD and elevated liver enzymes. *Hepatology* 2006; **44**: 865-873 [PMID: [17006923](#) DOI: [10.1002/hep.21327](#)]
- 29 **Wong VW**, Adams LA, de Lédinghen V, Wong GL, Sookoian S. Noninvasive biomarkers in NAFLD and NASH - current progress and future promise. *Nat Rev Gastroenterol Hepatol* 2018; **15**: 461-478 [PMID: [29844588](#) DOI: [10.1038/s41575-018-0014-9](#)]
- 30 **Merat S**, Sotoudehmanesh R, Nouraie M, Peikan-Heirati M, Sepanlou SG, Malekzadeh R, Sotoudeh M. Sampling error in histopathology findings of nonalcoholic fatty liver disease: a post mortem liver histology study. *Arch Iran Med* 2012; **15**: 418-421 [PMID: [22724878](#)]
- 31 **Cai J**, Zhang XJ, Li H. Progress and challenges in the prevention and control of nonalcoholic fatty liver disease. *Med Res Rev* 2019; **39**: 328-348 [PMID: [29846945](#) DOI: [10.1002/med.21515](#)]
- 32 **Petäjä EM**, Yki-Järvinen H. Definitions of Normal Liver Fat and the Association of Insulin Sensitivity with Acquired and Genetic NAFLD-A Systematic Review. *Int J Mol Sci* 2016; **17** [PMID: [27128911](#) DOI: [10.3390/ijms17050633](#)]
- 33 **Roldan-Valadez E**, Favila R, Martínez-López M, Uribe M, Rios C, Méndez-Sánchez N. In vivo 3T spectroscopic quantification of liver fat content in nonalcoholic fatty liver disease: Correlation with biochemical method and morphometry. *J Hepatol* 2010; **53**: 732-737 [PMID: [20594607](#) DOI: [10.1016/j.jhep.2010.04.018](#)]
- 34 **Kottronen A**, Johansson LE, Johansson LM, Roos C, Westerbacka J, Hamsten A, Bergholm R, Arkkila P, Arola J, Kiviluoto T, Fisher RM, Ehrenborg E, Orho-Melander M, Ridderstråle M, Groop L, Yki-Järvinen H. A common variant in PNPLA3, which encodes adiponutrin, is associated with liver fat content in humans. *Diabetologia* 2009; **52**: 1056-1060 [PMID: [19224197](#) DOI: [10.1007/s00125-009-1285-z](#)]

- 35 **European Association for the Study of the Liver (EASL); European Association for the Study of Diabetes (EASD); European Association for the Study of Obesity (EASO).** EASL-EASD-EASO Clinical Practice Guidelines for the management of non-alcoholic fatty liver disease. *J Hepatol* 2016; **64**: 1388-1402 [PMID: 27062661 DOI: 10.1016/j.jhep.2015.11.004]
- 36 **Chalasani N, Younossi Z, Lavine JE, Charlton M, Cusi K, Rinella M, Harrison SA, Brunt EM, Sanyal AJ.** The diagnosis and management of nonalcoholic fatty liver disease: Practice guidance from the American Association for the Study of Liver Diseases. *Hepatology* 2018; **67**: 328-357 [PMID: 28714183 DOI: 10.1002/hep.29367]
- 37 **Bedogni G, Bellentani S, Miglioli L, Masutti F, Passalacqua M, Castiglione A, Tiribelli C.** The Fatty Liver Index: a simple and accurate predictor of hepatic steatosis in the general population. *BMC Gastroenterol* 2006; **6**: 33 [PMID: 17081293 DOI: 10.1186/1471-230x-6-33]
- 38 **Fedchuk L, Nascimbeni F, Pais R, Charlotte F, Housset C, Ratzu V; LIDO Study Group.** Performance and limitations of steatosis biomarkers in patients with nonalcoholic fatty liver disease. *Aliment Pharmacol Ther* 2014; **40**: 1209-1222 [PMID: 25267215 DOI: 10.1111/apt.12963]
- 39 **Kotronen A, Peltonen M, Hakkarainen A, Sevestianova K, Bergholm R, Johansson LM, Lundbom N, Rissanen A, Ridderstråle M, Groop L, Orho-Melander M, Yki-Järvinen H.** Prediction of non-alcoholic fatty liver disease and liver fat using metabolic and genetic factors. *Gastroenterology* 2009; **137**: 865-872 [PMID: 19524579 DOI: 10.1053/j.gastro.2009.06.005]
- 40 **Koot BG, van der Baan-Slootweg OH, Bohte AE, Nederveen AJ, van Werven JR, Tamminga-Smeulders CL, Merkus MP, Schaap FG, Jansen PL, Stoker J, Benninga MA.** Accuracy of prediction scores and novel biomarkers for predicting nonalcoholic fatty liver disease in obese children. *Obesity (Silver Spring)* 2013; **21**: 583-590 [PMID: 23592667 DOI: 10.1002/oby.20173]
- 41 **Poynard T, Ratzu V, Naveau S, Thabut D, Charlotte F, Messous D, Capron D, Abella A, Massard J, Ngo Y, Munteanu M, Mercadier A, Manns M, Albrecht J.** The diagnostic value of biomarkers (SteatoTest) for the prediction of liver steatosis. *Comp Hepatol* 2005; **4**: 10 [PMID: 16375767 DOI: 10.1186/1476-5926-4-10]
- 42 **Zhou YJ, Zhou YF, Zheng JN, Liu WY, Van Poucke S, Zou TT, Zhang DC, Shen S, Shi KQ, Wang XD, Zheng MH.** NAFL screening score: A basic score identifying ultrasound-diagnosed non-alcoholic fatty liver. *Clin Chim Acta* 2017; **475**: 44-50 [PMID: 28964832 DOI: 10.1016/j.cca.2017.09.020]
- 43 **Fuyan S, Jing L, Wenjun C, Zhijun T, Weijing M, Suzhen W, Yongyong X.** Fatty liver disease index: a simple screening tool to facilitate diagnosis of nonalcoholic fatty liver disease in the Chinese population. *Dig Dis Sci* 2013; **58**: 3326-3334 [PMID: 23900558 DOI: 10.1007/s10620-013-2774-y]
- 44 **Zhu J, He M, Zhang Y, Li T, Liu Y, Xu Z, Chen W.** Validation of simple indexes for nonalcoholic fatty liver disease in western China: a retrospective cross-sectional study. *Endocr J* 2018; **65**: 373-381 [PMID: 29434074 DOI: 10.1507/endocrj.EJ17-0466]
- 45 **Zhang S, Du T, Zhang J, Lu H, Lin X, Xie J, Yang Y, Yu X.** The triglyceride and glucose index (TyG) is an effective biomarker to identify nonalcoholic fatty liver disease. *Lipids Health Dis* 2017; **16**: 15 [PMID: 28103934 DOI: 10.1186/s12944-017-0409-6]
- 46 **Hernaez R, Lazo M, Bonekamp S, Kamel I, Brancati FL, Guallar E, Clark JM.** Diagnostic accuracy and reliability of ultrasonography for the detection of fatty liver: a meta-analysis. *Hepatology* 2011; **54**: 1082-1090 [PMID: 21618575 DOI: 10.1002/hep.24452]
- 47 **Xia MF, Yan HM, He WY, Li XM, Li CL, Yao XZ, Li RK, Zeng MS, Gao X.** Standardized ultrasound hepatic/renal ratio and hepatic attenuation rate to quantify liver fat content: an improvement method. *Obesity (Silver Spring)* 2012; **20**: 444-452 [PMID: 22016092 DOI: 10.1038/oby.2011.302]
- 48 **Zhang B, Ding F, Chen T, Xia LH, Qian J, Lv GY.** Ultrasound hepatic/renal ratio and hepatic attenuation rate for quantifying liver fat content. *World J Gastroenterol* 2014; **20**: 17985-17992 [PMID: 25548498 DOI: 10.3748/wjg.v20.i47.17985]
- 49 **Xiao G, Zhu S, Xiao X, Yan L, Yang J, Wu G.** Comparison of laboratory tests, ultrasound, or magnetic resonance elastography to detect fibrosis in patients with nonalcoholic fatty liver disease: A meta-analysis. *Hepatology* 2017; **66**: 1486-1501 [PMID: 28586172 DOI: 10.1002/hep.29302]
- 50 **Park SH, Kim PN, Kim KW, Lee SW, Yoon SE, Park SW, Ha HK, Lee MG, Hwang S, Lee SG, Yu ES, Cho EY.** Macrovesicular hepatic steatosis in living liver donors: use of CT for quantitative and qualitative assessment. *Radiology* 2006; **239**: 105-112 [PMID: 16484355 DOI: 10.1148/radiol.2391050361]
- 51 **Kodama Y, Ng CS, Wu TT, Ayers GD, Curley SA, Abdalla EK, Vauthey JN, Charnsangavej C.** Comparison of CT methods for determining the fat content of the liver. *AJR Am J Roentgenol* 2007; **188**: 1307-1312 [PMID: 17449775 DOI: 10.2214/ajr.06.0992]
- 52 **Schwenzer NF, Springer F, Schraml C, Stefan N, Machann J, Schick F.** Non-invasive assessment and quantification of liver steatosis by ultrasound, computed tomography and magnetic resonance. *J Hepatol* 2009; **51**: 433-445 [PMID: 19604596 DOI: 10.1016/j.jhep.2009.05.023]
- 53 **Panicek DM, Giess CS, Schwartz LH.** Qualitative assessment of liver for fatty infiltration on contrast-enhanced CT: is muscle a better standard of reference than spleen? *J Comput Assist Tomogr* 1997; **21**: 699-705 [PMID: 9294555]
- 54 **Ma X, Holalkere NS, Kambadakone R A, Mino-Kenudson M, Hahn PF, Sahani DV.** Imaging-based quantification of hepatic fat: methods and clinical applications. *Radiographics* 2009; **29**: 1253-1277 [PMID: 19755595 DOI: 10.1148/rg.295085186]
- 55 **Karlas T, Petroff D, Sasso M, Fan JG, Mi YQ, de Lédinghen V, Kumar M, Lupsor-Platon M, Han KH, Cardoso AC, Ferraioli G, Chan WK, Wong VW, Myers RP, Chayama K, Friedrich-Rust M, Beaugrand M, Shen F, Hiriart JB, Sarin SK, Badea R, Jung KS, Marcellin P, Filice C, Mahadeva S, Wong GL, Crotty P, Masaki K, Bojunga J, Bedossa P, Keim V, Wiegand J.** Individual patient data meta-analysis of controlled attenuation parameter (CAP) technology for assessing steatosis. *J Hepatol* 2017; **66**: 1022-1030 [PMID: 28039099 DOI: 10.1016/j.jhep.2016.12.022]
- 56 **Chan WK, Nik Mustapha NR, Mahadeva S.** Controlled attenuation parameter for the detection and quantification of hepatic steatosis in nonalcoholic fatty liver disease. *J Gastroenterol Hepatol* 2014; **29**: 1470-1476 [PMID: 24548002 DOI: 10.1111/jgh.12557]
- 57 **Myers RP, Pomier-Layrargues G, Kirsch R, Pollett A, Duarte-Rojas A, Wong D, Beaton M, Levstik M, Crotty P, Elkashab M.** Feasibility and diagnostic performance of the FibroScan XL probe for liver stiffness measurement in overweight and obese patients. *Hepatology* 2012; **55**: 199-208 [PMID: 21898479 DOI: 10.1002/hep.24624]
- 58 **Chan WK, Nik Mustapha NR, Wong GL, Wong VW, Mahadeva S.** Controlled attenuation parameter using the FibroScan® XL probe for quantification of hepatic steatosis for non-alcoholic fatty liver disease in an Asian population. *United European Gastroenterol J* 2017; **5**: 76-85 [PMID: 28405325 DOI: 10.1093/ueg/ujw001]

- 10.1177/2050640616646528]
- 59 **Springer F**, Machann J, Claussen CD, Schick F, Schweser NF. Liver fat content determined by magnetic resonance imaging and spectroscopy. *World J Gastroenterol* 2010; **16**: 1560-1566 [PMID: 20355234 DOI: 10.3748/wjg.v16.i13.1560]
 - 60 **Dulai PS**, Sirlin CB, Loomba R. MRI and MRE for non-invasive quantitative assessment of hepatic steatosis and fibrosis in NAFLD and NASH: Clinical trials to clinical practice. *J Hepatol* 2016; **65**: 1006-1016 [PMID: 27312947 DOI: 10.1016/j.jhep.2016.06.005]
 - 61 **Tang A**, Tan J, Sun M, Hamilton G, Bydder M, Wolfson T, Gamst AC, Middleton M, Brunt EM, Loomba R, Lavine JE, Schwimmer JB, Sirlin CB. Nonalcoholic fatty liver disease: MR imaging of liver proton density fat fraction to assess hepatic steatosis. *Radiology* 2013; **267**: 422-431 [PMID: 23382291 DOI: 10.1148/radiol.12120896]
 - 62 **Idilman IS**, Aniktar H, Idilman R, Kabacam G, Savas B, Elhan A, Celik A, Bahar K, Karcaaltincaba M. Hepatic steatosis: quantification by proton density fat fraction with MR imaging versus liver biopsy. *Radiology* 2013; **267**: 767-775 [PMID: 23382293 DOI: 10.1148/radiol.13121360]
 - 63 **Bannas P**, Kramer H, Hernando D, Agni R, Cunningham AM, Mandal R, Motosugi U, Sharma SD, Munoz del Rio A, Fernandez L, Reeder SB. Quantitative magnetic resonance imaging of hepatic steatosis: Validation in ex vivo human livers. *Hepatology* 2015; **62**: 1444-1455 [PMID: 26224591 DOI: 10.1002/hep.28012]
 - 64 **Reeder SB**, Cruite I, Hamilton G, Sirlin CB. Quantitative assessment of liver fat with magnetic resonance imaging and spectroscopy. *J Magn Reson Imaging* 2011; **34**: 729-749 [PMID: 21928307 DOI: 10.1002/jmri.22580]
 - 65 **Park CC**, Nguyen P, Hernandez C, Bettencourt R, Ramirez K, Fortney L, Hooker J, Sy E, Savides MT, Alquraish MH, Valasek MA, Rizo E, Richards L, Brenner D, Sirlin CB, Loomba R. Magnetic Resonance Elastography vs Transient Elastography in Detection of Fibrosis and Noninvasive Measurement of Steatosis in Patients With Biopsy-Proven Nonalcoholic Fatty Liver Disease. *Gastroenterology* 2017; **152**: 598-607.e2 [PMID: 27911262 DOI: 10.1053/j.gastro.2016.10.026]
 - 66 **Caussy C**, Reeder SB, Sirlin CB, Loomba R. Noninvasive, Quantitative Assessment of Liver Fat by MRI-PDFF as an Endpoint in NASH Trials. *Hepatology* 2018; **68**: 763-772 [PMID: 29356032 DOI: 10.1002/hep.29797]
 - 67 **Cassidy FH**, Yokoo T, Aganovic L, Hanna RF, Bydder M, Middleton MS, Hamilton G, Chavez AD, Schwimmer JB, Sirlin CB. Fatty liver disease: MR imaging techniques for the detection and quantification of liver steatosis. *Radiographics* 2009; **29**: 231-260 [PMID: 19168847 DOI: 10.1148/rg.291075123]
 - 68 **Nasr P**, Forsgren MF, Ignatova S, Dahlström N, Cedersund G, Leinhard OD, Norén B, Ekstedt M, Lundberg P, Kechagias S. Using a 3% Proton Density Fat Fraction as a Cut-Off Value Increases Sensitivity of Detection of Hepatic Steatosis, Based on Results From Histopathology Analysis. *Gastroenterology* 2017; **153**: 53-55.e7 [PMID: 28286210 DOI: 10.1053/j.gastro.2017.03.005]
 - 69 **Cowin GJ**, Jonsson JR, Bauer JD, Ash S, Ali A, Osland EJ, Purdie DM, Clouston AD, Powell EE, Galloway GJ. Magnetic resonance imaging and spectroscopy for monitoring liver steatosis. *J Magn Reson Imaging* 2008; **28**: 937-945 [PMID: 18821619 DOI: 10.1002/jmri.21542]
 - 70 **Lee SS**, Park SH, Kim HJ, Kim SY, Kim MY, Kim DY, Suh DJ, Kim KM, Bae MH, Lee JY, Lee SG, Yu ES. Non-invasive assessment of hepatic steatosis: prospective comparison of the accuracy of imaging examinations. *J Hepatol* 2010; **52**: 579-585 [PMID: 20185194 DOI: 10.1016/j.jhep.2010.01.008]
 - 71 **Kim HJ**, Cho HJ, Kim B, You MW, Lee JH, Huh J, Kim JK. Accuracy and precision of proton density fat fraction measurement across field strengths and scan intervals: A phantom and human study. *J Magn Reson Imaging* 2018 [PMID: 30430684 DOI: 10.1002/jmri.26575]
 - 72 **Liu CY**, McKenzie CA, Yu H, Brittain JH, Reeder SB. Fat quantification with IDEAL gradient echo imaging: correction of bias from T(1) and noise. *Magn Reson Med* 2007; **58**: 354-364 [PMID: 17654578 DOI: 10.1002/mrm.21301]
 - 73 **Yu H**, McKenzie CA, Shimakawa A, Vu AT, Brau AC, Beatty PJ, Pineda AR, Brittain JH, Reeder SB. Multiecho reconstruction for simultaneous water-fat decomposition and T2* estimation. *J Magn Reson Imaging* 2007; **26**: 1153-1161 [PMID: 17896369 DOI: 10.1002/jmri.21090]
 - 74 **Yu H**, Shimakawa A, McKenzie CA, Brodsky E, Brittain JH, Reeder SB. Multiecho water-fat separation and simultaneous R2* estimation with multifrequency fat spectrum modeling. *Magn Reson Med* 2008; **60**: 1122-1134 [PMID: 18956464 DOI: 10.1002/mrm.21737]
 - 75 **Lewis S**, Dyvorne H, Cui Y, Taouli B. Diffusion-weighted imaging of the liver: techniques and applications. *Magn Reson Imaging Clin N Am* 2014; **22**: 373-395 [PMID: 25086935 DOI: 10.1016/j.mric.2014.04.009]
 - 76 **Taouli B**, Koh DM. Diffusion-weighted MR imaging of the liver. *Radiology* 2010; **254**: 47-66 [PMID: 20032142 DOI: 10.1148/radiol.09090021]
 - 77 **Manning P**, Murphy P, Wang K, Hooker J, Wolfson T, Middleton MS, Newton KP, Behling C, Awai HI, Durrelle J, Paiz MN, Angeles JE, De La Pena D, McCutchan JA, Schwimmer JB, Sirlin CB. Liver histology and diffusion-weighted MRI in children with nonalcoholic fatty liver disease: A MAGNET study. *J Magn Reson Imaging* 2017; **46**: 1149-1158 [PMID: 28225568 DOI: 10.1002/jmri.25663]
 - 78 **d'Assignies G**, Ruel M, Khiat A, Lepanto L, Chagnon M, Kauffmann C, Tang A, Gaboury L, Boulanger Y. Noninvasive quantitation of human liver steatosis using magnetic resonance and bioassay methods. *Eur Radiol* 2009; **19**: 2033-2040 [PMID: 19280194 DOI: 10.1007/s00330-009-1351-4]
 - 79 **Imajo K**, Kessoku T, Honda Y, Tomeno W, Ogawa Y, Mawatari H, Fujita K, Yoneda M, Taguri M, Hyogo H, Sumida Y, Ono M, Eguchi Y, Inoue T, Yamanaka T, Wada K, Saito S, Nakajima A. Magnetic Resonance Imaging More Accurately Classifies Steatosis and Fibrosis in Patients With Nonalcoholic Fatty Liver Disease Than Transient Elastography. *Gastroenterology* 2016; **150**: 626-637.e7 [PMID: 26677985 DOI: 10.1053/j.gastro.2015.11.048]
 - 80 **Verma S**, Jensen D, Hart J, Mohanty SR. Predictive value of ALT levels for non-alcoholic steatohepatitis (NASH) and advanced fibrosis in non-alcoholic fatty liver disease (NAFLD). *Liver Int* 2013; **33**: 1398-1405 [PMID: 23763360 DOI: 10.1111/liv.12226]
 - 81 **He L**, Deng L, Zhang Q, Guo J, Zhou J, Song W, Yuan F. Diagnostic Value of CK-18, FGF-21, and Related Biomarker Panel in Nonalcoholic Fatty Liver Disease: A Systematic Review and Meta-Analysis. *Biomed Res Int* 2017; **2017**: 9729107 [PMID: 28326329 DOI: 10.1155/2017/9729107]
 - 82 **Anty R**, Iannelli A, Patouraux S, Bonnafous S, Lavallard VJ, Senni-Buratti M, Amor IB, Staccini-Myx A, Saint-Paul MC, Berthier F, Huet PM, Le Marchand-Brustel Y, Gugenheim J, Gual P, Tran A. A new composite model including metabolic syndrome, alanine aminotransferase and cytokeratin-18 for the diagnosis of non-alcoholic steatohepatitis in morbidly obese patients. *Aliment Pharmacol Ther* 2010; **32**:

- 1315-1322 [PMID: [21050233](#) DOI: [10.1111/j.1365-2036.2010.04480.x](#)]
- 83 **Grigorescu M**, Crisan D, Radu C, Grigorescu MD, Sparchez Z, Serban A. A novel pathophysiological-based panel of biomarkers for the diagnosis of nonalcoholic steatohepatitis. *J Physiol Pharmacol* 2012; **63**: 347-353 [PMID: [23070083](#)]
 - 84 **Huang JF**, Yeh ML, Huang CF, Huang CI, Tsai PC, Tai CM, Yang HL, Dai CY, Hsieh MH, Chen SC, Yu ML, Chuang WL. Cytokeratin-18 and uric acid predicts disease severity in Taiwanese nonalcoholic steatohepatitis patients. *PLoS One* 2017; **12**: e0174394 [PMID: [28472039](#) DOI: [10.1371/journal.pone.0174394](#)]
 - 85 **Schulthess FT**, Paroni F, Sauter NS, Shu L, Ribaux P, Haataja L, Strieter RM, Oberholzer J, King CC, Maedler K. CXCL10 impairs beta cell function and viability in diabetes through TLR4 signaling. *Cell Metab* 2009; **9**: 125-139 [PMID: [19187771](#) DOI: [10.1016/j.cmet.2009.01.003](#)]
 - 86 **Zhang X**, Shen J, Man K, Chu ES, Yau TO, Sung JC, Go MY, Deng J, Lu L, Wong VW, Sung JJ, Farrell G, Yu J. CXCL10 plays a key role as an inflammatory mediator and a non-invasive biomarker of non-alcoholic steatohepatitis. *J Hepatol* 2014; **61**: 1365-1375 [PMID: [25048951](#) DOI: [10.1016/j.jhep.2014.07.006](#)]
 - 87 **Qi S**, Xu D, Li Q, Xie N, Xia J, Huo Q, Li P, Chen Q, Huang S. Metabonomics screening of serum identifies pyroglutamate as a diagnostic biomarker for nonalcoholic steatohepatitis. *Clin Chim Acta* 2017; **473**: 89-95 [PMID: [28842175](#) DOI: [10.1016/j.cca.2017.08.022](#)]
 - 88 **Shen J**, Chan HL, Wong GL, Choi PC, Chan AW, Chan HY, Chim AM, Yeung DK, Chan FK, Woo J, Yu J, Chu WC, Wong VW. Non-invasive diagnosis of non-alcoholic steatohepatitis by combined serum biomarkers. *J Hepatol* 2012; **56**: 1363-1370 [PMID: [22314419](#) DOI: [10.1016/j.jhep.2011.12.025](#)]
 - 89 **Tietge UJ**, Schmidt HH, Schütz T, Dippe P, Lochs H, Pirlich M. Reduced plasma adiponectin in NASH: central obesity as an underestimated causative risk factor. *Hepatology* 2005; **41**: 401; author reply 401-401; author reply 402 [PMID: [15660429](#) DOI: [10.1002/hep.20546](#)]
 - 90 **George DK**, Goldwurm S, MacDonald GA, Cowley LL, Walker NI, Ward PJ, Jazwinska EC, Powell LW. Increased hepatic iron concentration in nonalcoholic steatohepatitis is associated with increased fibrosis. *Gastroenterology* 1998; **114**: 311-318 [PMID: [9453491](#) DOI: [10.1016/S0016-5085\(98\)70482-2](#)]
 - 91 **Kalantar-Zadeh K**, Rodriguez RA, Humphreys MH. Association between serum ferritin and measures of inflammation, nutrition and iron in haemodialysis patients. *Nephrol Dial Transplant* 2004; **19**: 141-149 [PMID: [14671049](#) DOI: [10.1093/ndt/gfg493](#)]
 - 92 **Puljiz Z**, Stimac D, Kovac D, Puljiz M, Bratanić A, Kovacic V, Kardum D, Bonacin D, Hozo I. Predictors of nonalcoholic steatohepatitis in patients with elevated alanine aminotransferase activity. *Coll Antropol* 2010; **34** Suppl 1: 33-37 [PMID: [20402293](#)]
 - 93 **Canbakan B**, Senturk H, Tahan V, Hatemi I, Balci H, Toptas T, Sonsuz A, Velet M, Aydin S, Dirican A, Ozgulle S, Ozbay G. Clinical, biochemical and histological correlations in a group of non-drinker subjects with non-alcoholic fatty liver disease. *Acta Gastroenterol Belg* 2007; **70**: 277-284 [PMID: [18074737](#)]
 - 94 **Yoneda M**, Nozaki Y, Endo H, Mawatari H, Iida H, Fujita K, Yoneda K, Takahashi H, Kirikoshi H, Inamori M, Kobayashi N, Kubota K, Saito S, Maeyama S, Hotta K, Nakajima A. Serum ferritin is a clinical biomarker in Japanese patients with nonalcoholic steatohepatitis (NASH) independent of HFE gene mutation. *Dig Dis Sci* 2010; **55**: 808-814 [PMID: [19267193](#) DOI: [10.1007/s10620-009-0771-y](#)]
 - 95 **Sumida Y**, Yoneda M, Hyogo H, Yamaguchi K, Ono M, Fujii H, Eguchi Y, Suzuki Y, Imai S, Kanemasa K, Fujita K, Chayama K, Yasui K, Saibara T, Kawada N, Fujimoto K, Kohgo Y, Okanoue T, Japan Study Group of Nonalcoholic Fatty Liver Disease (JSG-NAFLD). A simple clinical scoring system using ferritin, fasting insulin, and type IV collagen 7S for predicting steatohepatitis in nonalcoholic fatty liver disease. *J Gastroenterol* 2011; **46**: 257-268 [PMID: [20842510](#) DOI: [10.1007/s00535-010-0305-6](#)]
 - 96 **Poynard T**, Ratziu V, Charlotte F, Messous D, Munteanu M, Imbert-Bismut F, Massard J, Bonyhay L, Tahiri M, Thabut D, Cadranet JF, Le Bail B, de Ledinghen V, LIDO Study Group, CYTOL study group. Diagnostic value of biochemical markers (NashTest) for the prediction of non alcoholic steato hepatitis in patients with non-alcoholic fatty liver disease. *BMC Gastroenterol* 2006; **6**: 34 [PMID: [17096854](#) DOI: [10.1186/1471-230x-6-34](#)]
 - 97 **Kleiner DE**, Brunt EM, Van Natta M, Behling C, Contos MJ, Cummings OW, Ferrell LD, Liu YC, Torbenson MS, Unalp-Arida A, Yeh M, McCullough AJ, Sanyal AJ. Nonalcoholic Steatohepatitis Clinical Research Network. Design and validation of a histological scoring system for nonalcoholic fatty liver disease. *Hepatology* 2005; **41**: 1313-1321 [PMID: [15915461](#) DOI: [10.1002/hep.20701](#)]
 - 98 **Zhou Y**, Orešić M, Leivonen M, Gopalacharyulu P, Hyysalo J, Arola J, Verrijken A, Francque S, Van Gaal L, Hyötyläinen T, Yki-Järvinen H. Noninvasive Detection of Nonalcoholic Steatohepatitis Using Clinical Markers and Circulating Levels of Lipids and Metabolites. *Clin Gastroenterol Hepatol* 2016; **14**: 1463-1472.e6 [PMID: [27317851](#) DOI: [10.1016/j.cgh.2016.05.046](#)]
 - 99 **Hyysalo J**, Männistö VT, Zhou Y, Arola J, Kärjä V, Leivonen M, Juuti A, Jaser N, Lallukka S, Käkälä P, Venesmaa S, Simonen M, Saltevo J, Moilanen L, Korpi-Hyövalti E, Keinänen-Kiukkaanniemi S, Oksa H, Orho-Melander M, Valenti L, Fargion S, Pihlajamäki J, Peltonen M, Yki-Järvinen H. A population-based study on the prevalence of NASH using scores validated against liver histology. *J Hepatol* 2014; **60**: 839-846 [PMID: [24333862](#) DOI: [10.1016/j.jhep.2013.12.009](#)]
 - 100 **Tai CM**, Yu ML, Tu HP, Huang CK, Hwang JC, Chuang WL. Derivation and validation of a scoring system for predicting nonalcoholic steatohepatitis in Taiwanese patients with severe obesity. *Surg Obes Relat Dis* 2017; **13**: 686-692 [PMID: [28089433](#) DOI: [10.1016/j.soard.2016.11.028](#)]
 - 101 **Chunming L**, Jianhui S, Hongguang Z, Chunwu Q, Xiaoyun H, Lijun Y, Xuejun Y. The development of a clinical score for the prediction of nonalcoholic steatohepatitis in patients with nonalcoholic fatty liver disease using routine parameters. *Turk J Gastroenterol* 2015; **26**: 408-416 [PMID: [26215061](#) DOI: [10.5152/tjg.2015.6336](#)]
 - 102 **Chen J**, Talwalkar JA, Yin M, Glaser KJ, Sanderson SO, Ehman RL. Early detection of nonalcoholic steatohepatitis in patients with nonalcoholic fatty liver disease by using MR elastography. *Radiology* 2011; **259**: 749-756 [PMID: [21460032](#) DOI: [10.1148/radiol.11101942](#)]
 - 103 **Kim TH**, Jeong CW, Jun HY, Kim YR, Kim JY, Lee YH, Yoon KH. Noninvasive Differential Diagnosis of Liver Iron Contents in Nonalcoholic Steatohepatitis and Simple Steatosis Using Multiecho Dixon Magnetic Resonance Imaging. *Acad Radiol* 2018 [PMID: [30143402](#) DOI: [10.1016/j.acra.2018.06.022](#)]
 - 104 **Ferreira VM**, Piechnik SK, Dall'Armellina E, Karamitsos TD, Francis JM, Choudhury RP, Friedrich MG, Robson MD, Neubauer S. Non-contrast T1-mapping detects acute myocardial edema with high diagnostic accuracy: a comparison to T2-weighted cardiovascular magnetic resonance. *J Cardiovasc Magn Reson* 2012; **14**: 42 [PMID: [22720998](#) DOI: [10.1186/1532-429X-14-42](#)]
 - 105 **Piechnik SK**, Ferreira VM, Dall'Armellina E, Cochlin LE, Greiser A, Neubauer S, Robson MD. Shortened

- Modified Look-Locker Inversion recovery (ShMOLLI) for clinical myocardial T1-mapping at 1.5 and 3 T within a 9 heartbeat breathhold. *J Cardiovasc Magn Reson* 2010; **12**: 69 [PMID: [21092095](#) DOI: [10.1186/1532-429X-12-69](#)]
- 106 **Rial B**, Robson MD, Neubauer S, Schneider JE. Rapid quantification of myocardial lipid content in humans using single breath-hold 1H MRS at 3 Tesla. *Magn Reson Med* 2011; **66**: 619-624 [PMID: [21721038](#) DOI: [10.1002/mrm.23011](#)]
 - 107 **Banerjee R**, Pavlides M, Tunncliffe EM, Piechnik SK, Sarania N, Philips R, Collier JD, Booth JC, Schneider JE, Wang LM, Delaney DW, Fleming KA, Robson MD, Barnes E, Neubauer S. Multiparametric magnetic resonance for the non-invasive diagnosis of liver disease. *J Hepatol* 2014; **60**: 69-77 [PMID: [24036007](#) DOI: [10.1016/j.jhep.2013.09.002](#)]
 - 108 **Eddowes PJ**, McDonald N, Davies N, Semple SIK, Kendall TJ, Hodson J, Newsome PN, Flintham RB, Wesolowski R, Blake L, Duarte RV, Kelly CJ, Herlihy AH, Kelly MD, Olliff SP, Hübscher SG, Fallowfield JA, Hirschfield GM. Utility and cost evaluation of multiparametric magnetic resonance imaging for the assessment of non-alcoholic fatty liver disease. *Aliment Pharmacol Ther* 2018; **47**: 631-644 [PMID: [29271504](#) DOI: [10.1111/apt.14469](#)]
 - 109 **Zhang P**, Wang PX, Zhao LP, Zhang X, Ji YX, Zhang XJ, Fang C, Lu YX, Yang X, Gao MM, Zhang Y, Tian S, Zhu XY, Gong J, Ma XL, Li F, Wang Z, Huang Z, She ZG, Li H. The deubiquitinating enzyme TNFAIP3 mediates inactivation of hepatic ASK1 and ameliorates nonalcoholic steatohepatitis. *Nat Med* 2018; **24**: 84-94 [PMID: [29227477](#) DOI: [10.1038/nm.4453](#)]
 - 110 **Wang S**, Yan ZZ, Yang X, An S, Zhang K, Qi Y, Zheng J, Ji YX, Wang PX, Fang C, Zhu XY, Shen LJ, Yan FJ, Bao R, Tian S, She ZG, Tang YD. Hepatocyte DUSP14 maintains metabolic homeostasis and suppresses inflammation in the liver. *Hepatology* 2018; **67**: 1320-1338 [PMID: [29077210](#) DOI: [10.1002/hep.29616](#)]
 - 111 **Zhao GN**, Zhang P, Gong J, Zhang XJ, Wang PX, Yin M, Jiang Z, Shen LJ, Ji YX, Tong J, Wang Y, Wei QF, Wang Y, Zhu XY, Zhang X, Fang J, Xie Q, She ZG, Wang Z, Huang Z, Li H. Tmbim1 is a multivesicular body regulator that protects against non-alcoholic fatty liver disease in mice and monkeys by targeting the lysosomal degradation of Tlr4. *Nat Med* 2017; **23**: 742-752 [PMID: [28481357](#) DOI: [10.1038/nm.4334](#)]
 - 112 **Wang PX**, Ji YX, Zhang XJ, Zhao LP, Yan ZZ, Zhang P, Shen LJ, Yang X, Fang J, Tian S, Zhu XY, Gong J, Zhang X, Wei QF, Wang Y, Li J, Wan L, Xie Q, She ZG, Wang Z, Huang Z, Li H. Targeting CASP8 and FADD-like apoptosis regulator ameliorates nonalcoholic steatohepatitis in mice and nonhuman primates. *Nat Med* 2017; **23**: 439-449 [PMID: [28218919](#) DOI: [10.1038/nm.4290](#)]
 - 113 **Zhu LH**, Wang A, Luo P, Wang X, Jiang DS, Deng W, Zhang X, Wang T, Liu Y, Gao L, Zhang S, Zhang X, Zhang J, Li H. Mindin/Spondin 2 inhibits hepatic steatosis, insulin resistance, and obesity via interaction with peroxisome proliferator-activated receptor α in mice. *J Hepatol* 2014; **60**: 1046-1054 [PMID: [24445216](#) DOI: [10.1016/j.jhep.2014.01.011](#)]
 - 114 **Liu XL**, Pan Q, Zhang RN, Shen F, Yan SY, Sun C, Xu ZJ, Chen YW, Fan JG. Disease-specific miR-34a as diagnostic marker of non-alcoholic steatohepatitis in a Chinese population. *World J Gastroenterol* 2016; **22**: 9844-9852 [PMID: [27956809](#) DOI: [10.3748/wjg.v22.i44.9844](#)]
 - 115 **Liu CH**, Ampuero J, Gil-Gómez A, Montero-Vallejo R, Rojas Á, Muñoz-Hernández R, Gallego-Durán R, Romero-Gómez M. miRNAs in patients with non-alcoholic fatty liver disease: A systematic review and meta-analysis. *J Hepatol* 2018; **69**: 1335-1348 [PMID: [30142428](#) DOI: [10.1016/j.jhep.2018.08.008](#)]
 - 116 **Cermelli S**, Ruggieri A, Marrero JA, Ioannou GN, Beretta L. Circulating microRNAs in patients with chronic hepatitis C and non-alcoholic fatty liver disease. *PLoS One* 2011; **6**: e23937 [PMID: [21886843](#) DOI: [10.1371/journal.pone.0023937](#)]
 - 117 **Pirola CJ**, Fernández Gianotti T, Castaño GO, Mallardi P, San Martino J, Mora Gonzalez Lopez Ledesma M, Flichman D, Mirshahi F, Sanyal AJ, Sookoian S. Circulating microRNA signature in non-alcoholic fatty liver disease: from serum non-coding RNAs to liver histology and disease pathogenesis. *Gut* 2015; **64**: 800-812 [PMID: [24973316](#) DOI: [10.1136/gutjnl-2014-306996](#)]
 - 118 **Becker PP**, Rau M, Schmitt J, Malsch C, Hammer C, Bantel H, Müllhaupt B, Geier A. Performance of Serum microRNAs -122, -192 and -21 as Biomarkers in Patients with Non-Alcoholic Steatohepatitis. *PLoS One* 2015; **10**: e0142661 [PMID: [26565986](#) DOI: [10.1371/journal.pone.0142661](#)]
 - 119 **Van Berkel JJ**, Dallinga JW, Möller GM, Godschalk RW, Moonen EJ, Wouters EF, Van Schooten FJ. A profile of volatile organic compounds in breath discriminates COPD patients from controls. *Respir Med* 2010; **104**: 557-563 [PMID: [19906520](#) DOI: [10.1016/j.rmed.2009.10.018](#)]
 - 120 **Dallinga JW**, Robroeks CM, van Berkel JJ, Moonen EJ, Godschalk RW, Jöbsis Q, Dompeling E, Wouters EF, van Schooten FJ. Volatile organic compounds in exhaled breath as a diagnostic tool for asthma in children. *Clin Exp Allergy* 2010; **40**: 68-76 [PMID: [19793086](#) DOI: [10.1111/j.1365-2222.2009.03343.x](#)]
 - 121 **Lang AL**, Beier JI. Interaction of volatile organic compounds and underlying liver disease: a new paradigm for risk. *Biol Chem* 2018; **399**: 1237-1248 [PMID: [29924722](#) DOI: [10.1515/hsz-2017-0324](#)]
 - 122 **Verdam FJ**, Dallinga JW, Driessen A, de Jonge C, Moonen EJ, van Berkel JB, Luijk J, Bouvy ND, Buurman WA, Rensen SS, Greve JW, van Schooten FJ. Non-alcoholic steatohepatitis: a non-invasive diagnosis by analysis of exhaled breath. *J Hepatol* 2013; **58**: 543-548 [PMID: [23142062](#) DOI: [10.1016/j.jhep.2012.10.030](#)]
 - 123 **Duarte SMB**, Stefano JT, Miele L, Ponziani FR, Souza-Basqueira M, Okada LSRR, de Barros Costa FG, Toda K, Mazo DFC, Sabino EC, Carrilho FJ, Gasbarrini A, Oliveira CP. Gut microbiome composition in lean patients with NASH is associated with liver damage independent of caloric intake: A prospective pilot study. *Nutr Metab Cardiovasc Dis* 2018; **28**: 369-384 [PMID: [29482963](#) DOI: [10.1016/j.numecd.2017.10.014](#)]
 - 124 **Alonso C**, Fernández-Ramos D, Varela-Rey M, Martínez-Arranz I, Navasa N, Van Liempd SM, Lavín Trueba JL, Mayo R, Ilisso CP, de Juan VG, Iruarizaga-Lejarreta M, delaCruz-Villar L, Mincholé I, Robinson A, Crespo J, Martín-Duce A, Romero-Gómez M, Sann H, Platon J, Van Eyk J, Aspichueta P, Noureddin M, Falcón-Pérez JM, Anguita J, Aransay AM, Martínez-Chantar ML, Lu SC, Mato JM. Metabolomic Identification of Subtypes of Nonalcoholic Steatohepatitis. *Gastroenterology* 2017; **152**: 1449-1461.e7 [PMID: [28132890](#) DOI: [10.1053/j.gastro.2017.01.015](#)]
 - 125 **Soga T**, Sugimoto M, Honma M, Mori M, Igarashi K, Kashikura K, Ikeda S, Hirayama A, Yamamoto T, Yoshida H, Otsuka M, Tsuji S, Yatomi Y, Sakuragawa T, Watanabe H, Nihei K, Saito T, Kawata S, Suzuki H, Tomita M, Suematsu M. Serum metabolomics reveals γ -glutamyl dipeptides as biomarkers for discrimination among different forms of liver disease. *J Hepatol* 2011; **55**: 896-905 [PMID: [21334394](#) DOI: [10.1016/j.jhep.2011.01.031](#)]
 - 126 **Puri P**, Wiest MM, Cheung O, Mirshahi F, Sargeant C, Min HK, Contos MJ, Sterling RK, Fuchs M, Zhou

- H, Watkins SM, Sanyal AJ. The plasma lipidomic signature of nonalcoholic steatohepatitis. *Hepatology* 2009; **50**: 1827-1838 [PMID: [19937697](#) DOI: [10.1002/hep.23229](#)]
- 127 **Hagström H**, Nasr P, Ekstedt M, Hammar U, Stål P, Hultcrantz R, Kechagias S. Fibrosis stage but not NASH predicts mortality and time to development of severe liver disease in biopsy-proven NAFLD. *J Hepatol* 2017; **67**: 1265-1273 [PMID: [28803953](#) DOI: [10.1016/j.jhep.2017.07.027](#)]
- 128 **Polyzos SA**, Slavakis A, Koumerkeridis G, Katsinelos P, Kountouras J. Noninvasive Liver Fibrosis Tests in Patients with Nonalcoholic Fatty Liver Disease: An External Validation Cohort. *Horm Metab Res* 2019; **51**: 134-140 [PMID: [30273934](#) DOI: [10.1055/a-0713-1330](#)]
- 129 **Hansen JF**, Juul Nielsen M, Nyström K, Leeming DJ, Lagging M, Norkrans G, Brehm Christensen P, Karsdal M. PRO-C3: a new and more precise collagen marker for liver fibrosis in patients with chronic hepatitis C. *Scand J Gastroenterol* 2018; **53**: 83-87 [PMID: [29069995](#) DOI: [10.1080/00365521.2017.1392596](#)]
- 130 **Daniels SJ**, Leeming DJ, Eslam M, Hashem AM, Nielsen MJ, Krag A, Karsdal MA, Grove JJ, Guha IN, Kawaguchi T, Torimura T, McLeod D, Akiba J, Kaye P, de Boer B, Aithal GP, Adams LA, George J. ADAPT: An algorithm incorporating PRO-C3 accurately identifies patients with NAFLD and advanced fibrosis. *Hepatology* 2018 [PMID: [30014517](#) DOI: [10.1002/hep.30163](#)]
- 131 **Suzuki A**, Angulo P, Lypm J, Li D, Satomura S, Lindor K. Hyaluronic acid, an accurate serum marker for severe hepatic fibrosis in patients with non-alcoholic fatty liver disease. *Liver Int* 2005; **25**: 779-786 [PMID: [15998429](#) DOI: [10.1111/j.1478-3231.2005.01064.x](#)]
- 132 **Miele L**, De Michele T, Marrone G, Antonietta Isgrò M, Basile U, Cefalo C, Biolato M, Maria Vecchio F, Lodovico Rapaccini G, Gasbarrini A, Zuppi C, Grieco A. Enhanced liver fibrosis test as a reliable tool for assessing fibrosis in nonalcoholic fatty liver disease in a clinical setting. *Int J Biol Markers* 2017; **32**: e397-e402 [PMID: [28862712](#) DOI: [10.5301/ijbm.5000292](#)]
- 133 **Wai CT**, Greenon JK, Fontana RJ, Kalbfleisch JD, Marrero JA, Conjeevaram HS, Lok AS. A simple noninvasive index can predict both significant fibrosis and cirrhosis in patients with chronic hepatitis C. *Hepatology* 2003; **38**: 518-526 [PMID: [12883497](#) DOI: [10.1053/jhep.2003.50346](#)]
- 134 **Sterling RK**, Lissen E, Clumeck N, Sola R, Correa MC, Montaner J, Sulkowski M, Torriani FJ, Dieterich DT, Thomas DL, Messinger D, Nelson M; APRICOT Clinical Investigators. Development of a simple noninvasive index to predict significant fibrosis in patients with HIV/HCV coinfection. *Hepatology* 2006; **43**: 1317-1325 [PMID: [16729309](#) DOI: [10.1002/hep.21178](#)]
- 135 **McPherson S**, Stewart SF, Henderson E, Burt AD, Day CP. Simple non-invasive fibrosis scoring systems can reliably exclude advanced fibrosis in patients with non-alcoholic fatty liver disease. *Gut* 2010; **59**: 1265-1269 [PMID: [20801772](#) DOI: [10.1136/gut.2010.216077](#)]
- 136 **McPherson S**, Hardy T, Dufour JF, Petta S, Romero-Gomez M, Allison M, Oliveira CP, Francque S, Van Gaal L, Schattenberg JM, Tiniakos D, Burt A, Bugianesi E, Ratz V, Day CP, Anstee QM. Age as a Confounding Factor for the Accurate Non-Invasive Diagnosis of Advanced NAFLD Fibrosis. *Am J Gastroenterol* 2017; **112**: 740-751 [PMID: [27725647](#) DOI: [10.1038/ajg.2016.453](#)]
- 137 **Ishiba H**, Sumida Y, Tanaka S, Yoneda M, Hyogo H, Ono M, Fujii H, Eguchi Y, Suzuki Y, Yoneda M, Takahashi H, Nakahara T, Seko Y, Mori K, Kanemasa K, Shimada K, Imai S, Imajo K, Kawaguchi T, Nakajima A, Chayama K, Saibara T, Shima T, Fujimoto K, Okanoue T, Itoh Y; Japan Study Group of Non-Alcoholic Fatty Liver Disease (JSG-NAFLD). The novel cutoff points for the FIB4 index categorized by age increase the diagnostic accuracy in NAFLD: a multi-center study. *J Gastroenterol* 2018; **53**: 1216-1224 [PMID: [29744597](#) DOI: [10.1007/s00535-018-1474-y](#)]
- 138 **Angulo P**, Hui JM, Marchesini G, Bugianesi E, George J, Farrell GC, Enders F, Saksena S, Burt AD, Bida JP, Lindor K, Sanderson SO, Lenzi M, Adams LA, Kench J, Thorneau TM, Day CP. The NAFLD fibrosis score: a noninvasive system that identifies liver fibrosis in patients with NAFLD. *Hepatology* 2007; **45**: 846-854 [PMID: [17393509](#) DOI: [10.1002/hep.21496](#)]
- 139 **Harrison SA**, Oliver D, Arnold HL, Gogia S, Neuschwander-Tetri BA. Development and validation of a simple NAFLD clinical scoring system for identifying patients without advanced disease. *Gut* 2008; **57**: 1441-1447 [PMID: [18390575](#) DOI: [10.1136/gut.2007.146019](#)]
- 140 **Fujii H**, Enomoto M, Fukushima W, Tamori A, Sakaguchi H, Kawada N. Applicability of BARD score to Japanese patients with NAFLD. *Gut* 2009; **58**: 1566-7; author reply 1567 [PMID: [19834122](#) DOI: [10.1136/gut.2009.182758](#)]
- 141 **Wong VW**, Vergniol J, Wong GL, Foucher J, Chan HL, Le Bail B, Choi PC, Kow M, Chan AW, Merrouche W, Sung JJ, de Lédinghen V. Diagnosis of fibrosis and cirrhosis using liver stiffness measurement in nonalcoholic fatty liver disease. *Hepatology* 2010; **51**: 454-462 [PMID: [20101745](#) DOI: [10.1002/hep.23312](#)]
- 142 **de Lédinghen V**, Vergniol J. Transient elastography (FibroScan). *Gastroenterol Clin Biol* 2008; **32**: 58-67 [PMID: [18973847](#) DOI: [10.1016/S0399-8320\(08\)73994-0](#)]
- 143 **Wong VW**, Vergniol J, Wong GL, Foucher J, Chan AW, Chermak F, Choi PC, Merrouche W, Chu SH, Pesque S, Chan HL, de Lédinghen V. Liver stiffness measurement using XL probe in patients with nonalcoholic fatty liver disease. *Am J Gastroenterol* 2012; **107**: 1862-1871 [PMID: [23032979](#) DOI: [10.1038/ajg.2012.331](#)]
- 144 **Loong TC**, Wei JL, Leung JC, Wong GL, Shu SS, Chim AM, Chan AW, Choi PC, Tse YK, Chan HL, Wong VW. Application of the combined FibroMeter vibration-controlled transient elastography algorithm in Chinese patients with non-alcoholic fatty liver disease. *J Gastroenterol Hepatol* 2017; **32**: 1363-1369 [PMID: [27936280](#) DOI: [10.1111/jgh.13671](#)]
- 145 **Leung VY**, Shen J, Wong VW, Abrigo J, Wong GL, Chim AM, Chu SH, Chan AW, Choi PC, Ahuja AT, Chan HL, Chu WC. Quantitative elastography of liver fibrosis and spleen stiffness in chronic hepatitis B carriers: comparison of shear-wave elastography and transient elastography with liver biopsy correlation. *Radiology* 2013; **269**: 910-918 [PMID: [23912619](#) DOI: [10.1148/radiol.13130128](#)]
- 146 **Ferraioli G**, Tinelli C, Dal Bello B, Zicchetti M, Filice G, Filice C; Liver Fibrosis Study Group. Accuracy of real-time shear wave elastography for assessing liver fibrosis in chronic hepatitis C: a pilot study. *Hepatology* 2012; **56**: 2125-2133 [PMID: [22767302](#) DOI: [10.1002/hep.25936](#)]
- 147 **Cassinotto C**, Boursier J, de Lédinghen V, Lebigot J, Lapuyade B, Cales P, Hiriart JB, Michalak S, Bail BL, Cartier V, Mouries A, Oberti F, Fouchard-Hubert I, Vergniol J, Aubé C. Liver stiffness in nonalcoholic fatty liver disease: A comparison of supersonic shear imaging, FibroScan, and ARFI with liver biopsy. *Hepatology* 2016; **63**: 1817-1827 [PMID: [26659452](#) DOI: [10.1002/hep.28394](#)]
- 148 **Karagoz E**, Ozturker C, Sonmez G. Noninvasive Evaluation of Liver Fibrosis: Supersonic Shear Imaging or Acoustic Radiation Force Impulse Imaging? *Radiology* 2016; **279**: 979-980 [PMID: [27183412](#) DOI: [10.1148/radiol.2016152532](#)]

- 149 **Friedrich-Rust M**, Romen D, Vermehren J, Kriener S, Sadet D, Herrmann E, Zeuzem S, Bojunga J. Acoustic radiation force impulse-imaging and transient elastography for non-invasive assessment of liver fibrosis and steatosis in NAFLD. *Eur J Radiol* 2012; **81**: e325-e331 [PMID: [22119555](#) DOI: [10.1016/j.ejrad.2011.10.029](#)]
- 150 **Liu H**, Fu J, Hong R, Liu L, Li F. Acoustic Radiation Force Impulse Elastography for the Non-Invasive Evaluation of Hepatic Fibrosis in Non-Alcoholic Fatty Liver Disease Patients: A Systematic Review & Meta-Analysis. *PLoS One* 2015; **10**: e0127782 [PMID: [26131717](#) DOI: [10.1371/journal.pone.0127782](#)]
- 151 **Joo SK**, Kim W, Kim D, Kim JH, Oh S, Lee KL, Chang MS, Jung YJ, So YH, Lee MS, Bae JM, Kim BG. Steatosis severity affects the diagnostic performances of noninvasive fibrosis tests in nonalcoholic fatty liver disease. *Liver Int* 2018; **38**: 331-341 [PMID: [28796410](#) DOI: [10.1111/liv.13549](#)]
- 152 **Yanrong Guo**. Haoming Lin, Xinyu Zhang, Huiying Wen, Siping Chen, Xin Chen. The influence of hepatic steatosis on the evaluation of fibrosis with non-alcoholic fatty liver disease by acoustic radiation force impulse. *Conf Proc IEEE Eng Med Biol Soc* 2017; **2017**: 2988-2991 [PMID: [29060526](#) DOI: [10.1109/EMBC.2017.8037485](#)]
- 153 **Wang QB**, Zhu H, Liu HL, Zhang B. Performance of magnetic resonance elastography and diffusion-weighted imaging for the staging of hepatic fibrosis: A meta-analysis. *Hepatology* 2012; **56**: 239-247 [PMID: [22278368](#) DOI: [10.1002/hep.25610](#)]
- 154 **Loomba R**. Role of imaging-based biomarkers in NAFLD: Recent advances in clinical application and future research directions. *J Hepatol* 2018; **68**: 296-304 [PMID: [29203392](#) DOI: [10.1016/j.jhep.2017.11.028](#)]
- 155 **Doycheva I**, Cui J, Nguyen P, Costa EA, Hooker J, Hofflich H, Bettencourt R, Brouha S, Sirlin CB, Loomba R. Non-invasive screening of diabetics in primary care for NAFLD and advanced fibrosis by MRI and MRE. *Aliment Pharmacol Ther* 2016; **43**: 83-95 [PMID: [26369383](#) DOI: [10.1111/apt.13405](#)]
- 156 **Cui J**, Ang B, Haufe W, Hernandez C, Verna EC, Sirlin CB, Loomba R. Comparative diagnostic accuracy of magnetic resonance elastography vs. eight clinical prediction rules for non-invasive diagnosis of advanced fibrosis in biopsy-proven non-alcoholic fatty liver disease: a prospective study. *Aliment Pharmacol Ther* 2015; **41**: 1271-1280 [PMID: [25873207](#) DOI: [10.1111/apt.13196](#)]
- 157 **Yin M**, Talwalkar JA, Glaser KJ, Manduca A, Grimm RC, Rossman PJ, Fidler JL, Ehman RL. Assessment of hepatic fibrosis with magnetic resonance elastography. *Clin Gastroenterol Hepatol* 2007; **5**: 1207-1213.e2 [PMID: [17916548](#) DOI: [10.1016/j.cgh.2007.06.012](#)]
- 158 **Venkatesh SK**, Yin M, Ehman RL. Magnetic resonance elastography of liver: technique, analysis, and clinical applications. *J Magn Reson Imaging* 2013; **37**: 544-555 [PMID: [23423795](#) DOI: [10.1002/jmri.23731](#)]
- 159 **Singh S**, Venkatesh SK, Loomba R, Wang Z, Sirlin C, Chen J, Yin M, Miller FH, Low RN, Hassanein T, Godfrey EM, Asbach P, Murad MH, Lomas DJ, Talwalkar JA, Ehman RL. Magnetic resonance elastography for staging liver fibrosis in non-alcoholic fatty liver disease: a diagnostic accuracy systematic review and individual participant data pooled analysis. *Eur Radiol* 2016; **26**: 1431-1440 [PMID: [26314479](#) DOI: [10.1007/s00330-015-3949-z](#)]
- 160 **Loomba R**, Cui J, Wolfson T, Haufe W, Hooker J, Szeverenyi N, Ang B, Bhatt A, Wang K, Aryafar H, Behling C, Valasek MA, Lin GY, Gamst A, Brenner DA, Yin M, Glaser KJ, Ehman RL, Sirlin CB. Novel 3D Magnetic Resonance Elastography for the Noninvasive Diagnosis of Advanced Fibrosis in NAFLD: A Prospective Study. *Am J Gastroenterol* 2016; **111**: 986-994 [PMID: [27002798](#) DOI: [10.1038/ajg.2016.65](#)]
- 161 **Cui J**, Heba E, Hernandez C, Haufe W, Hooker J, Andre MP, Valasek MA, Aryafar H, Sirlin CB, Loomba R. Magnetic resonance elastography is superior to acoustic radiation force impulse for the Diagnosis of fibrosis in patients with biopsy-proven nonalcoholic fatty liver disease: A prospective study. *Hepatology* 2016; **63**: 453-461 [PMID: [26560734](#) DOI: [10.1002/hep.28337](#)]
- 162 **Hardy T**, Zeybel M, Day CP, Dipper C, Masson S, McPherson S, Henderson E, Tiniakos D, White S, French J, Mann DA, Anstee QM, Mann J. Plasma DNA methylation: a potential biomarker for stratification of liver fibrosis in non-alcoholic fatty liver disease. *Gut* 2017; **66**: 1321-1328 [PMID: [27002005](#) DOI: [10.1136/gutjnl-2016-311526](#)]
- 163 **Pais R**, Barritt AS 4th, Calmus Y, Scatton O, Runge T, Lebray P, Poynard T, Ratzliff V, Conti F. NAFLD and liver transplantation: Current burden and expected challenges. *J Hepatol* 2016; **65**: 1245-1257 [PMID: [27486010](#) DOI: [10.1016/j.jhep.2016.07.033](#)]
- 164 **Ray K**. NAFLD-the next global epidemic. *Nat Rev Gastroenterol Hepatol* 2013; **10**: 621 [PMID: [24185985](#) DOI: [10.1038/nrgastro.2013.197](#)]
- 165 **Singh S**, Allen AM, Wang Z, Prokop LJ, Murad MH, Loomba R. Fibrosis progression in nonalcoholic fatty liver vs nonalcoholic steatohepatitis: a systematic review and meta-analysis of paired-biopsy studies. *Clin Gastroenterol Hepatol* 2015; **13**: 643-654.e1-9; quiz e39-40 [PMID: [24768810](#) DOI: [10.1016/j.cgh.2014.04.014](#)]
- 166 **Parkes J**, Roderick P, Harris S, Day C, Mutimer D, Collier J, Lombard M, Alexander G, Ramage J, Dusheiko G, Wheatley M, Gough C, Burt A, Rosenberg W. Enhanced liver fibrosis test can predict clinical outcomes in patients with chronic liver disease. *Gut* 2010; **59**: 1245-1251 [PMID: [20675693](#) DOI: [10.1136/gut.2009.203166](#)]
- 167 **Sebastiani G**, Alshaalan R, Wong P, Rubino M, Salman A, Metrakos P, Deschenes M, Ghali P. Prognostic Value of Non-Invasive Fibrosis and Steatosis Tools, Hepatic Venous Pressure Gradient (HVPG) and Histology in Nonalcoholic Steatohepatitis. *PLoS One* 2015; **10**: e0128774 [PMID: [26083565](#) DOI: [10.1371/journal.pone.0128774](#)]
- 168 **Boursier J**, Vergniol J, Guillet A, Hiriart JB, Lannes A, Le Bail B, Michalak S, Chermak F, Bertrais S, Foucher J, Oberti F, Charbonnier M, Fouchard-Hubert I, Rousselet MC, Calès P, de Ledinghen V. Diagnostic accuracy and prognostic significance of blood fibrosis tests and liver stiffness measurement by FibroScan in non-alcoholic fatty liver disease. *J Hepatol* 2016; **65**: 570-578 [PMID: [27151181](#) DOI: [10.1016/j.jhep.2016.04.023](#)]
- 169 **Buckley AJ**, Thomas EL, Lessan N, Trovato FM, Trovato GM, Taylor-Robinson SD. Non-alcoholic fatty liver disease: Relationship with cardiovascular risk markers and clinical endpoints. *Diabetes Res Clin Pract* 2018; **144**: 144-152 [PMID: [30170074](#) DOI: [10.1016/j.diabetes.2018.08.011](#)]
- 170 **Trovato FM**, Tognarelli JM, Crossey MM, Catalano D, Taylor-Robinson SD, Trovato GM. Challenges of liver cancer: Future emerging tools in imaging and urinary biomarkers. *World J Hepatol* 2015; **7**: 2664-2675 [PMID: [26609343](#) DOI: [10.4254/wjh.v7.i26.2664](#)]
- 171 **Sanyal AJ**, Brunt EM, Kleiner DE, Kowdley KV, Chalasani N, Lavine JE, Ratzliff V, McCullough A. Endpoints and clinical trial design for nonalcoholic steatohepatitis. *Hepatology* 2011; **54**: 344-353 [PMID: [21486010](#) DOI: [10.1002/hep.24111](#)]

- 21520200 DOI: [10.1002/hep.24376](https://doi.org/10.1002/hep.24376)]
- 172 **Middleton MS**, Heba ER, Hooker CA, Bashir MR, Fowler KJ, Sandrasegaran K, Brunt EM, Kleiner DE, Doo E, Van Natta ML, Lavine JE, Neuschwander-Tetri BA, Sanyal A, Loomba R, Sirlin CB; NASH Clinical Research Network. Agreement Between Magnetic Resonance Imaging Proton Density Fat Fraction Measurements and Pathologist-Assigned Steatosis Grades of Liver Biopsies From Adults With Nonalcoholic Steatohepatitis. *Gastroenterology* 2017; **153**: 753-761 [PMID: [28624576](https://pubmed.ncbi.nlm.nih.gov/28624576/) DOI: [10.1053/j.gastro.2017.06.005](https://doi.org/10.1053/j.gastro.2017.06.005)]
 - 173 **Jayakumar S**, Middleton MS, Lawitz EJ, Mantry PS, Caldwell SH, Arnold H, Mae Diehl A, Ghalib R, Elkhatab M, Abdelmalek MF, Kowdley KV, Stephen Djedjos C, Xu R, Han L, Mani Subramanian G, Myers RP, Goodman ZD, Afdhal NH, Charlton MR, Sirlin CB, Loomba R. Longitudinal correlations between MRE, MRI-PDFF, and liver histology in patients with non-alcoholic steatohepatitis: Analysis of data from a phase II trial of selonsertib. *J Hepatol* 2019; **70**: 133-141 [PMID: [30291868](https://pubmed.ncbi.nlm.nih.gov/30291868/) DOI: [10.1016/j.jhep.2018.09.024](https://doi.org/10.1016/j.jhep.2018.09.024)]
 - 174 **Wieckowska A**, Feldstein AE. Diagnosis of nonalcoholic fatty liver disease: invasive versus noninvasive. *Semin Liver Dis* 2008; **28**: 386-395 [PMID: [18956295](https://pubmed.ncbi.nlm.nih.gov/18956295/) DOI: [10.1055/s-0028-1091983](https://doi.org/10.1055/s-0028-1091983)]
 - 175 **Vilar-Gomez E**, Calzadilla-Bertot L, Friedman SL, Gra-Oramas B, Gonzalez-Fabian L, Lazo-Del Vallin S, Diago M, Adams LA. Serum biomarkers can predict a change in liver fibrosis 1 year after lifestyle intervention for biopsy-proven NASH. *Liver Int* 2017; **37**: 1887-1896 [PMID: [28544769](https://pubmed.ncbi.nlm.nih.gov/28544769/) DOI: [10.1111/liv.13480](https://doi.org/10.1111/liv.13480)]

P- Reviewer: Arslan N, Senturk H, Sijens PE, Tiribelli C, Toriguchi K, Trovato GM

S- Editor: Ma RY **L- Editor:** Wang TQ **E- Editor:** Huang Y





Basic Study

Economic evaluation of the hepatitis C elimination strategy in Greece in the era of affordable direct-acting antivirals

Ilias Gountas, Vana Sypsa, George Papatheodoridis, Kyriakos Souliotis, Kostas Athanasakis, Homie Razavi, Angelos Hatzakis

ORCID number: Ilias Gountas (0000-0002-6584-0313); Vana Sypsa (0000-0002-9430-7614); George Papatheodoridis (0000-0002-3518-4060); Kyriakos Souliotis (0000-0003-1624-9444); Kostas Athanasakis (0000-0002-1024-3802); Homie Razavi (0000-0002-2658-6930); Angelos Hatzakis (0000-0001-8420-3830).

Author contributions: Gountas I and Hatzakis A conceived the study; Gountas I performed the modelling and drafted the manuscript; Hatzakis A coordinated the study; Sypsa V, Papatheodoridis G, Souliotis K, Athanasakis K and Razavi H provided essential inputs and contributed extensively to writing the manuscript; All authors contributed to model interpretation and approved the final version.

Conflict-of-interest statement: No conflicts of interest.

Data sharing statement: No additional data are available.

Open-Access: This is an open-access article that was selected by an in-house editor and fully peer-reviewed by external reviewers. It is distributed in accordance with the Creative Commons Attribution Non Commercial (CC BY-NC 4.0) license, which permits others to distribute, remix, adapt, build upon this work non-commercially, and license their derivative works on different terms, provided the original work is properly cited and the use is non-commercial. See:

Ilias Gountas, Vana Sypsa, Angelos Hatzakis, Department of Hygiene, Epidemiology and Medical Statistics, Medical School, National and Kapodistrian University of Athens, Athens 11527, Greece

Ilias Gountas, Angelos Hatzakis, Hellenic Scientific Society for the Study of AIDS and Sexually Transmitted Diseases, Athens 11527, Greece

George Papatheodoridis, Department of Gastroenterology, Medical School, National and Kapodistrian University of Athens, Laiko General Hospital, Athens 11527, Greece

Kyriakos Souliotis, Faculty of Social and Political Sciences, University of Peloponnese, Korinthos 20100, Greece

Kostas Athanasakis, Department of Health Economics, National School of Public Health, Athens 11521, Greece

Homie Razavi, Center for Disease Analysis, Lafayette, CO 80026, United States

Corresponding author: Angelos Hatzakis, PhD, Doctor, Senior Researcher, Senior Scientist, Department of Hygiene, Epidemiology and Medical Statistics, Medical School, National and Kapodistrian University of Athens, 22 Mikras Asias Str., Athens 11527, Greece.

ahatzak@med.uoa.gr

Telephone: +30-210-7474058

Fax: +30-210-7474058

Abstract

BACKGROUND

Hepatitis C virus (HCV) is a leading cause of worldwide liver-related morbidity and mortality. The World Health Organization released an integrated strategy targeting HCV-elimination by 2030. This study aims to estimate the required interventions to achieve elimination using updated information for direct-acting antiviral (DAA) treatment coverage, to compute the total costs (including indirect/societal costs) of the strategy and to identify whether the elimination strategy is cost-effective/cost-saving in Greece.

AIM

To estimate the required interventions and subsequent costs to achieve HCV elimination in Greece.

METHODS

<http://creativecommons.org/licenses/by-nc/4.0/>

Manuscript source: Invited manuscript

Received: October 16, 2018

Peer-review started: October 16, 2018

First decision: December 5, 2018

Revised: February 20, 2019

Accepted: February 22, 2019

Article in press: February 22, 2019

Published online: March 21, 2019

A previously validated mathematical model was adapted to the Greek HCV-infected population to compare the outcomes of DAA treatment without the additional implementation of awareness or screening campaigns versus an HCV elimination strategy, which includes a sufficient number of treated patients. We estimated the total costs (direct and indirect costs), the disability-adjusted life years and the incremental cost-effectiveness ratio using two different price scenarios.

RESULTS

Without the implementation of awareness or screening campaigns, approximately 20000 patients would be diagnosed and treated with DAAs by 2030. This strategy would result in a 19.6% increase in HCV-related mortality in 2030 compared to 2015. To achieve the elimination goal, 90000 patients need to be treated by 2030. Under the elimination scenario, viremic cases would decrease by 78.8% in 2030 compared to 2015. The cumulative direct costs to eliminate the disease would range from 2.1-2.3 billion euros (€) by 2030, while the indirect costs would be €1.1 billion. The total elimination cost in Greece would range from €3.2-3.4 billion by 2030. The cost per averted disability-adjusted life year is estimated between €10100 and €13380, indicating that the elimination strategy is very cost-effective. Furthermore, HCV elimination strategy would save €560-895 million by 2035.

CONCLUSION

Without large screening programs, elimination of HCV cannot be achieved. The HCV elimination strategy is feasible and cost-saving despite the uncertainty of the future cost of DAAs in Greece.

Key words: Hepatitis C elimination; Cost effectiveness; Cost of elimination; Indirect costs; Projections; Mathematical modelling; Awareness and screening programs; World Health Organization targets

©The Author(s) 2019. Published by Baishideng Publishing Group Inc. All rights reserved.

Core tip: Elimination of hepatitis C virus (commonly known as HCV) cannot be achieved in Greece without the implementation of large awareness and screening programs, as treatment coverage will be suboptimal. To achieve the elimination goals, 90000 patients need to be treated by 2030. The overall cumulative cost of elimination would range from 3.2-3.4 billion euros by 2030. The HCV elimination strategy in Greece is feasible and cost-saving despite the uncertainty of the future cost of the direct-acting antivirals.

Citation: Gountas I, Sypsa V, Papatheodoridis G, Souliotis K, Athanasakis K, Razavi H, Hatzakis A. Economic evaluation of the hepatitis C elimination strategy in Greece in the era of affordable direct-acting antivirals. *World J Gastroenterol* 2019; 25(11): 1327-1340

URL: <https://www.wjgnet.com/1007-9327/full/v25/i11/1327.htm>

DOI: <https://dx.doi.org/10.3748/wjg.v25.i11.1327>

INTRODUCTION

Hepatitis C virus (HCV) infection is a major public health problem; it affects 1% of the world population^[1] and is one of the main causes of chronic liver disease-related death in the developed world^[1,2]. It has been estimated that approximately 50%-85% of HCV cases developed chronic hepatitis. Many patients with chronic HCV (CHC) infection do not result in clinically apparent liver disease because it is generally a slow progressive infection. Five percent to 30% of chronically infected individuals developed cirrhosis over a span of 20 to 30 yr^[3,4]. The recent introduction of direct-acting antivirals (DAAs) has the potential to change the future disease burden, as they achieve higher sustained virological response (SVR) rates, have fewer side effects and are simpler regimens compared to interferon (IFN)-based therapies^[5,6]. Due to recent developments of antiviral treatments, the target of eliminating HCV by 2030 has become achievable^[7]. Although the cost of providing DAAs has been extensively

debated since their introduction, the cost and cost-effectiveness of implementing an HCV elimination strategy has recently been put on the agenda^[8-12].

Greece has one of the highest prevalence rates of CHC infection in Europe, with approximately 33% of chronically infected patients in the advanced fibrosis stages (\geq F3)^[13,14]. Additionally, it has an older infected population compared to other countries, meaning that the mean fibrosis progression is relatively rapid and the probability of HCV-related mortality or morbidity is high^[15-17]. Therefore, although HCV prevalence in Greece has been decreasing since its peak in 2005, morbidity and mortality are forecasted to increase in the next years^[14,18]. Moreover, the diagnostic rate is low (approximately 20%). Except for the significant HCV epidemic, Greece has faced a substantial financial crisis since 2008. Since then, the Greek economy has substantially shrunk; the gross domestic product (GDP) fell by 22%, about one-fifth of the aggregate production was lost and the public pharmaceutical expenditure was reduced by more than 50%^[19].

Recently, a modeling study quantified the impact of IFN-free DAAs on HCV-related morbidity and mortality in Greece under the World Health Organization (WHO) Global Hepatitis Strategy^[14]. This study showed that improved prevention strategies, large and effective screening programs and increased treatment coverage with DAAs were necessary to reach the goal of HCV elimination in Greece by 2030. To implement this strategy, it is vital to consider the cost of the proposed strategy, which poses significant financial challenges for the healthcare system.

The aims of this study are (1) to estimate the required interventions to achieve elimination using updated information for DAA treatment coverage, (2) to compute the total costs (including the indirect costs) of the strategy and to (3) identify whether the elimination strategy is cost-effective for Greece.

MATERIALS AND METHODS

Disease burden model

To estimate the current number of patients in the various disease stages and to project the future disease burden and the associated costs, we used an Excel-based disease progression model, which represents the natural history of CHC according to the METAVIR scoring system constructed by the Center for Disease Analysis (CO, United States)^[20]. It has been used in several countries with country-specific data as input^[18]. Appropriate input for Greece was obtained from the literature. Further details about the description of the model and Greek-specific epidemiological inputs have been previously published^[14,18].

To examine the epidemiological and economic impact of the WHO Global Hepatitis Strategy, we created a scenario according to WHO recommendations and compared it with the current HCV management strategy in Greece, where patients are treated with INF-free DAA regimens with limited population coverage due to the low diagnostic rate and the lack of awareness or screening campaigns.

Examined epidemiological scenarios

Base case: In the baseline scenario, patients are treated with IFN-free DAA regimens without the additional implementation of awareness or screening campaigns. This would lead to a gradual decrease in the available patients for treatment. Treatment is limited to fibrosis stage ≥ 2 , which represents the 2017 national treatment guideline. Approximately 2,000 cases were treated in Greece in 2017. We assumed that this figure would be the same in 2018 but would gradually decrease to 1000 cases by 2020 and would then remain at this number. SVR rates were assumed to be 90% for genotype 1, 3 and 95% for genotype 2, 4^[15] (Table 1).

WHO Global Hepatitis Strategy: The WHO Global Hepatitis Strategy integrates both prevention and disease burden targets^[7]. More specifically, the prevention target aims to reduce new infections by 90%, while the mortality target aims to reduce HCV mortality to 65% by 2030 compared to 2015. To achieve the WHO goals in Greece, the number of diagnosed and treated patients should gradually increase up to 7000 and 6800 patients per year, respectively. Initially, through 2018, patients with fibrosis stage \geq F2 will be treated. After 2019, treatment coverage should be expanded to all patients (Table 1).

Economic portion of the model

Regarding the economic portion of the model, we have computed the direct and the indirect/societal costs of HCV infection.

Direct and indirect/societal costs: Direct costs include the cost of antiviral treatment

Table 1 Evaluated scenarios for projections of the future burden of hepatitis C infection in Greece

Scenario	Year	SVR	Treatment coverage/yr	Fibrosis stage	Diagnosed patients/yr
Base case	2015-2016	90%-95%	~1000	≥ F3	4000
	2017-2019	95%	~2000	≥ F2	3200
	2020-2021	95%	~1300	≥ F2	2000
	2022-2023	95%	~1000	≥ F2	1400
	2024-2035	95%	~1000	≥ F2	1000
WHO Global Hepatitis Strategy	2015-2016	90%-95%	~1000	≥ F3	4000
	2017-2019	95%	~4700	≥ F2	4800
	2020-2021	95%	~6800	≥ F0	6820
	2022-2023	95%	~6800	≥ F0	6130
	2024-2035	95%	~7000	≥ F0	6130

SVR: Sustained virologic response rates; WHO: World Health Organization.

per treated patient per year, annual health care costs per patient, screening/diagnostic costs per patient, as well as laboratory costs per treated patient (Table 2)^[21].

Data for healthcare costs were obtained through a database from Greek liver clinics. The annual cost for F0-F3 patients, for the third-party payer in Greece, without antiviral treatment, is 230 €. The costs of compensated cirrhosis (F4), decompensated cirrhosis and hepatocellular carcinoma (HCC) without the cost of antiviral treatments are 1340 €, 4460 €, and 33000 € per year, respectively. Liver transplant patients have a cost of 134630 € in the first year and 4640 € in subsequent years^[22]. Lab costs (*e.g.*, anti-HCV, RNA test, genotyping exam and liver biopsy/elastography) are 350 €, while the cost per anti-HCV screening is 10 €.

The average treatment cost per DAA-treated patient in Greece in 2016 was 42000 €^[23]. Recently, price negotiations concerning the cost of DAAs were implemented, resulting in reduced treatment costs. The price per DAA regimen is confidential. However, the average cost per treatment can be calculated. According to the official press release of the Ministry of Health, a closed pharmaceutical budget of about 67.6 million has been committed to treat 5500 patients in the next 14 mo^[24,25]. Dividing the budgeted money by the expected treated patients equates to a cost of treatment of about 12300 €. Furthermore, the Minister for Health stated^[26,27] that the negotiation achieved a savings of 68% compared to the average pre-negotiated price (42000 € × 32% = 13400 €). Combining the above estimations, we assumed that the average cost of DAAs after negotiation can be estimated at 13000 € per treated patient.

Due to the considerable uncertainty of the future price evolution for DAAs, we considered two cost-scenarios. In the first scenario (conservative scenario), we assumed that the price of DAAs would remain constant through our study (until 2035), while in the second scenario (optimistic scenario), we assumed a further 35% price reduction after 2024. Under the base case, we assumed no price reduction of DAAs due to the limited number of treated patients (Table 2).

The indirect or societal cost was used to approximate loss of productivity due to HCV related disabilities and loss of life. The disability-adjusted life year (DALY) metric^[28] was used to estimate the indirect costs of the disease. One DALY can be thought of as one lost year of "healthy" life. DALYs are computed by combining years of life lost (YLLs) and years lost due to disability (YLDs) and weighted by the severity of the disease^[29]. Future direct and indirect costs were discounted at rate of 3%. The cost per DALY was estimated to be equal to the gross national income (GNI) per capita in 2016 (19000 €).

The cost-effectiveness of the elimination strategy was estimated using the incremental cost-effectiveness ratio (ICER), which have been compared to the GNI per capita of Greece in 2016. If ICER is lower than 1 GNI per capita, then the intervention is considered "highly cost effective"^[30].

$ICER = (\text{Cost of examine strategy} - \text{cost of the base strategy}) / |\text{DALYs of examine strategy} - \text{DALYs of the base strategy}|$

We considered a strategy as "cost-saving" when the difference between all direct and indirect costs of the elimination scenario up to 2035 from those of the base case was positive.

$$\text{Incremental total costs}_{\text{Scenario}} = \sum_{t=2014}^{2035} \text{Total costs of Scenario}_t - \sum_{t=2014}^{2035} \text{Total costs of base case}_t$$

Table 2 Annual direct costs per patients in Euros

	Annual costs, €
Lab costs for anti-HCV, RNA test, genotyping exam and liver biopsy/elastography	350
Screening cost per screen	10 ¹
Cost per diagnosed patient without antiviral treatment	
F0-F3	230
Compensated cirrhosis, F4	1340
Decompensated cirrhosis	4460
Hepatocellular carcinoma	33000
Liver transplantation	134600 ²
Liver transplant - subsequent years	4600
Antiviral treatment costs of DAAs	
2015-2016	42000
2017-2023	13000
2024-2035	13000/8500 ³

¹Cost per screen;²Cost per patient for one time (includes all pre-transplantation, transplantation and post-transplantation courses);³Under optimistic price reduction scenario. DAAs: Direct-acting antivirals; HCV: Hepatitis C virus.

RESULTS

Epidemiological projections

Under the base case scenario, the model predicted a continuous decline in the number of viremic cases in Greece through 2035 (Table 3, Figure 1A-E). The viremic population would decrease by 8.3% and 11.1% in 2030 and 2035 compared to 2015, respectively. However, unlike viremic cases, HCV complications are anticipated to increase over the same time period.

The number of patients with compensated cirrhosis is anticipated to be 21100 cases by 2030 (19.2% higher than 2015). In 2035, the number of compensated cirrhosis cases is expected to be 21280 (20.2% higher than 2015). Similarly, the number of decompensated cirrhosis cases would increased to 2160 (18.3% higher than 2015) and 2200 (20.2% higher than 2015) cases in 2030 and 2035, respectively. Regarding HCC cases, the model projected an increase of 19.4% (705 cases) and 20.3% (710 cases) in 2030 and 2035 compared to 2015, respectively. Concerning liver related deaths, the model projects an increase to 790 (19.6% higher than 2015) and 805 (21.9% higher than 2015) in 2030 and 2035, respectively (Table 3, Figure 1A-E). Under the base case, the model estimates that about 20000 patients would be diagnosed and treated with DAAs by 2030.

Under the Global Hepatitis Strategy, significant declines would be observed in HCV morbidity and mortality. More specifically, individuals with compensated and decompensated cirrhosis are expected to decrease by 63.3%, 66.7% in 2030 and 93.9%, 91.2% in 2035, respectively, compared to the corresponding number of cases of compensated and decompensated cirrhosis in 2015. Similarly, HCC cases are anticipated to decrease by 66.9% (195 cases) and 94.9% (30 cases) in 2030 and 2035 compared to 2015, respectively. Liver related deaths are projected to decrease by 65.7% (226 deaths) in 2030 and 91.4% (57 deaths) in 2035 compared to 2015, respectively. Finally, the number of viremic cases would decrease by 78.8% (28000 cases) and 98.4% (2100 cases) in 2030 and 2035 compared to the number of viremic cases in 2015, respectively (Table 3, Figure 1A-E). To achieve the elimination goals, 90000 patients need to be treated by 2030.

Economic projections

Annual direct costs: Under the base case scenario, the annual direct costs of HCV in 2016 are €105 million. Without the additional implementation of awareness or screening campaigns, the number of available patients for treatment would drop, leading to a corresponding decrease in the cost attributed to antiviral therapies. Specifically, the annual direct costs would decline from €105 to €83 million by 2019 and remain at this level through 2035 (Figures 2 and 3).

Regarding the WHO Global Hepatitis Strategy, the model predicts a steep upward trend in direct costs until 2023 and 2028 for the optimistic and the conservative price

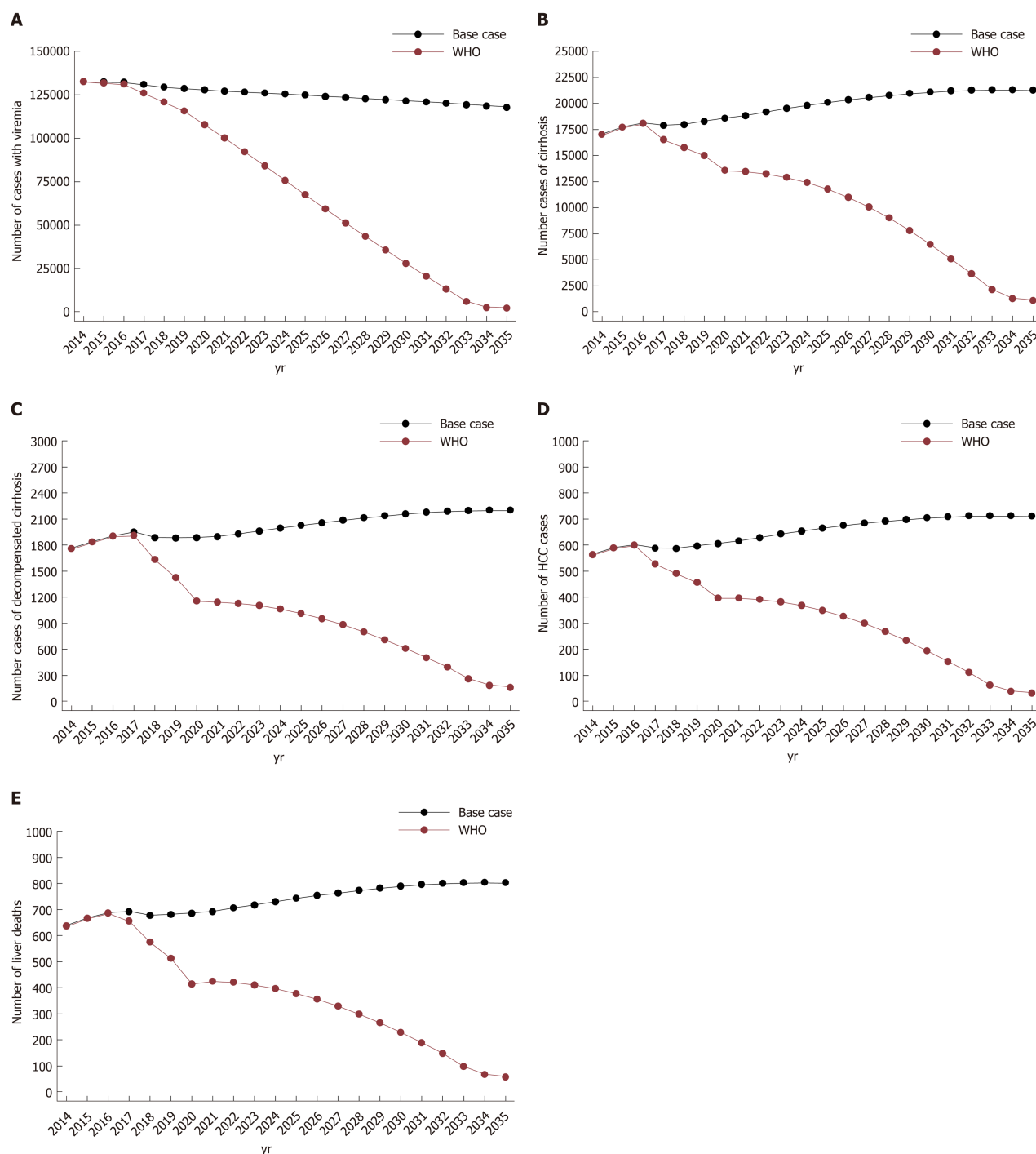


Figure 1 Projections of future chronic hepatitis C virus infection and complications under different treatment strategies. A: Total number of viremic cases; B: Cirrhosis; C: Decompensated cirrhosis; D: Hepatocellular carcinoma; E: Liver deaths. WHO: World Health Organization.

reduction scenario, respectively, followed by a significant decline through 2035. Compared to the base case, the annual direct cost of the elimination scenario would be higher until 2032 and 2034 under the optimistic and the conservative price reduction scenario, respectively (Figures 2 and 3).

The cost distribution is significantly different between the two strategies. In the base case, where treatment coverage is relatively low, the majority of the cost is attributed to healthcare costs. In contrast, under the HCV elimination scenario, the dominant costs would be for antiviral treatments and laboratory costs. Under the HCV elimination strategy (irrespective of price reduction scenarios), screening costs would represent a significant share of direct costs between 2026 and 2029 due to the fact that it would become more difficult to diagnose HCV infections due to the low prevalence (Figure 3).

Annual indirect/societal costs: Concerning indirect/societal costs, the WHO strategy

Table 3 Estimated number of total hepatitis C virus infected (viremic cases), compensated cirrhosis, decompensated cirrhosis and hepatocellular carcinoma cases in 2030 and 2035 under base and hepatitis C virus elimination scenarios

	2015, Base <i>n</i>	2020, <i>n</i> (% change compared to 2015)	2030, <i>n</i> (% change compared to 2015)	2035, <i>n</i> (% change compared to base case in 2015)
Base case				
Total infected	132500	127940 (-3.4)	121460 (-8.3)	117750 (-11.1)
Compensated cirrhosis	17700	18584 (+4.9)	21100 (+19.2)	21280 (+20.2)
Decompensated cirrhosis	1830	1885 (+3.0)	2160 (+18.3)	2200 (+20.2)
HCC	590	605 (+2.5)	705 (+19.4)	710 (+20.3)
Liver related deaths	660	686 (+3.9)	790 (+19.6)	805 (+21.9)
WHO Global Hepatitis Strategy				
Total infected		107910 (-18.5)	28000 (-78.8)	2100 (-98.4)
Compensated cirrhosis		13584 (-23.2)	6480 (-63.3)	1084 (-93.9)
Compensated cirrhosis		1155 (-36.9)	610 (-66.7)	160 (-91.2)
HCC		395 (-33.0)	195 (-66.9)	30 (-94.9)
Liver related deaths		415 (-37.2)	226 (-65.7)	57 (-91.4)

HCC: Hepatocellular carcinoma; WHO: World Health Organization.

is expected to result in substantial savings throughout the length of the study compared to the base case. More specifically, the indirect costs of WHO strategy would be €16, €89, and €95 million lower compared to the base case in 2016, 2030 and 2035, respectively. The above results arise from the significant reduction of HCV related end-stage liver disease, as well as the subsequent aversion of disability and premature deaths (Figure 2).

Overall annual cost (total direct and indirect costs): The annual overall cost of base case would have a slight decrease by 2035 due to the limited cost of antiviral treatment (limited available patients for treatment). Compared to the base case, the elimination strategy would be more expensive in the first phase, but it would become less costly by 2024 and 2028 under the optimistic or the conservative price reduction scenario, respectively.

Cost-effectiveness

It was estimated that to achieve elimination, an investment (direct costs) of €2.12 or 2.33 billion should be made by 2030 under the optimistic or the conservative price reduction scenario, respectively. It is also important that at the same time, about €1.1 billion would be lost (indirect costs). Summing up the above, the overall cumulative cost of HCV elimination would be range between €3.2 and 3.4 billion by 2030. The corresponding costs by 2035 would vary between €3.5 and 3.8 billion (Figure 4).

The ICER computes that the cost per averted DALY by 2030 would be €10100 and €13380 under the optimistic or the conservative price reduction scenario, respectively. Similarly, the cost per averted DALYs by 2035 would be €5100 and €8300. In all scenarios, the elimination strategy was always a very cost-effective strategy (Table 4).

The HCV elimination strategy appears to be a cost-saving strategy, as €895 million and €560 million would be saved by 2035 under the optimistic or the conservative price reduction scenario, respectively (Figures 2D and 4).

DISCUSSION

The analysis shows that while overall HCV prevalence in Greece will decline, disease burden related to HCV and associated costs will continue to grow in the era of DAAs due to failure to diagnose and treat sufficient numbers of patients. Similar patterns have been observed in the IFN era^[13,16,31-33].

Our analysis highlights that HCV management without effective awareness and screening campaigns would be an expensive and ineffective health policy strategy. The reason is that few patients would be diagnosed and treated, leaving a significant proportion of patients to progress to more advanced stages of the disease. Thus, the additional budget gained from lower HCV awareness campaigns or low treatment coverage would be paid in the next years in healthcare costs to treat the new cases of

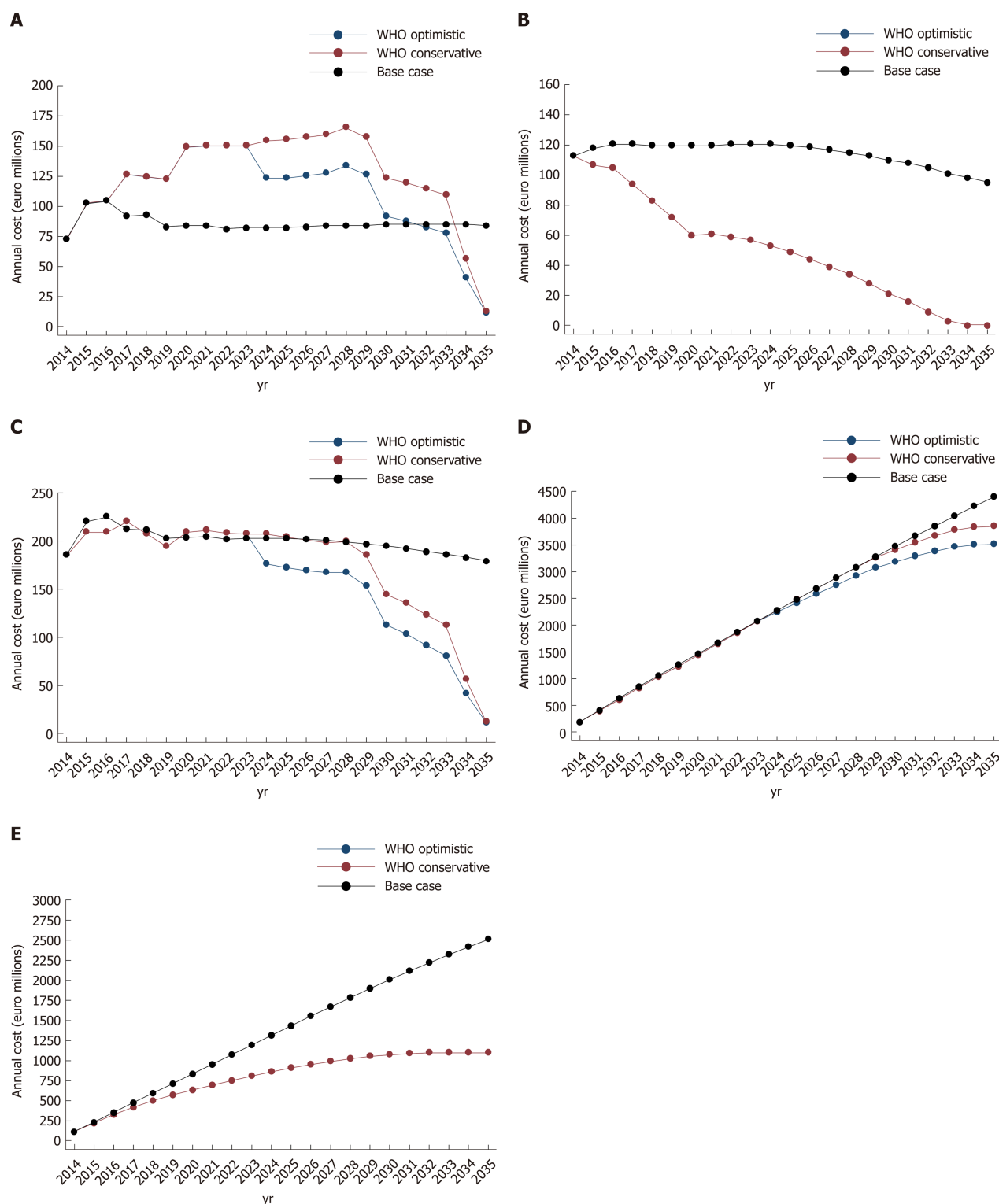


Figure 2 Projections of future costs of hepatitis C virus infection under different treatment strategies. A: Direct costs; B: Indirect costs; C: Annual total direct and indirect costs; D: Total cumulative direct and indirect costs; E: Total cumulative direct and indirect costs. WHO: World Health Organization.

compensated or decompensated cirrhosis and HCC. On the contrary, the HCV elimination strategy is a cost saving intervention (savings by 2035 varies from €560-890 million), as it eliminates the high cost of HCV attributed to related end-stage liver disease or premature death. It is important to note that the HCV elimination strategy is an upfront investment, as a significant amount of money should be spent in the beginning in order to save money later. For example, in Greece, the direct costs need to be increased by 142% in 2020 compared to 2016.

Although the cumulative direct costs of the elimination strategy are costlier than the base scenario (Table 4), when we take also into account the indirect costs caused

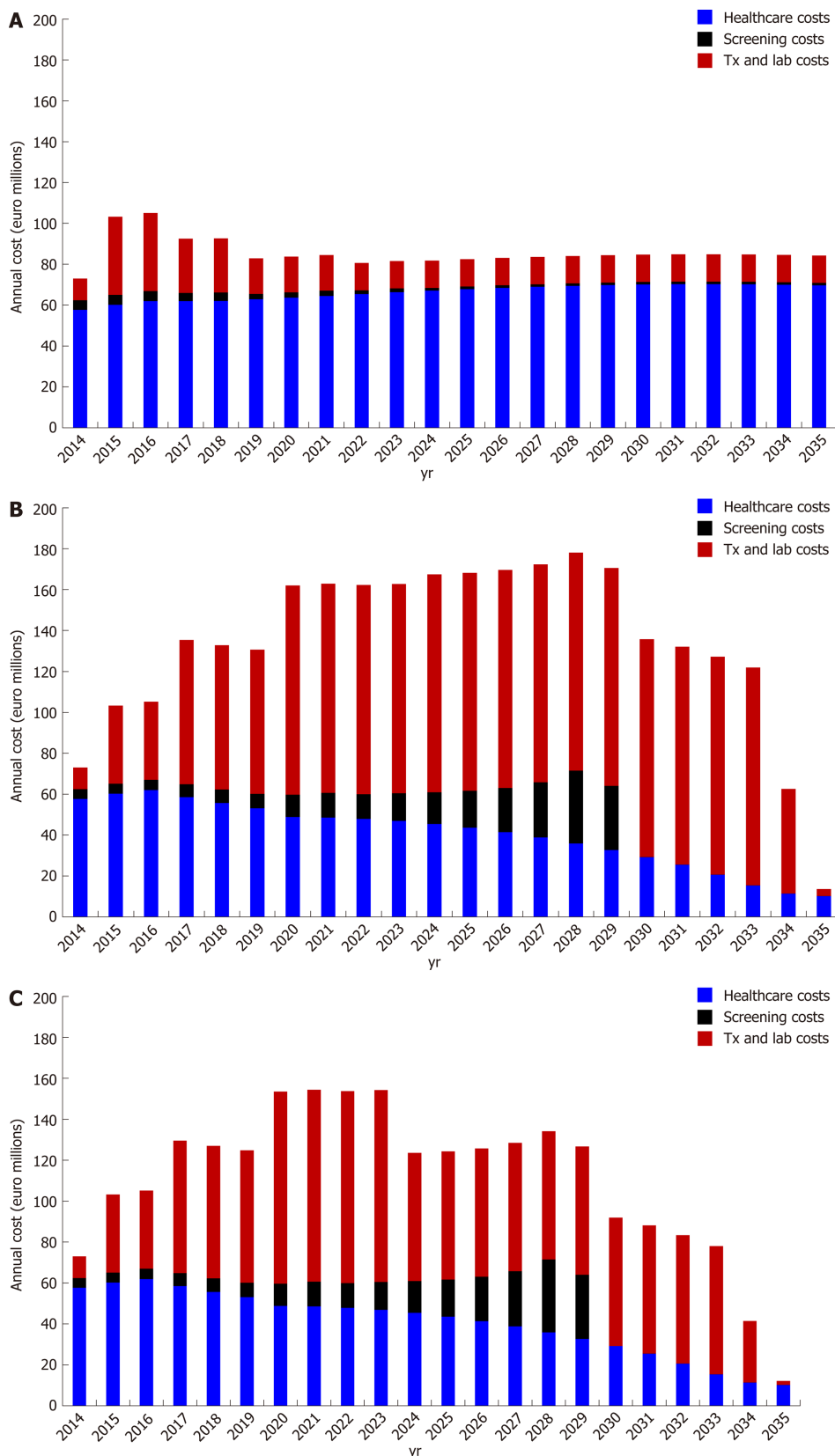


Figure 3 Distribution of direct costs by direct-acting antiviral price scenario (conservative or optimistic). A: Base case scenario; B: Hepatitis C virus (HCV) elimination conservative scenario; C: HCV elimination optimistic scenario.

by the disease, this relation changes and the elimination scenario become cheaper, as HCV is a disease with high indirect costs (Figure 2D). In line with other studies, our results have shown that the indirect cost of HCV is a significant component of the elimination strategy, almost comparable to the corresponding direct cost of the disease^[9,10,20,33,34], as the vast majority of HCV-infected persons are of working age and

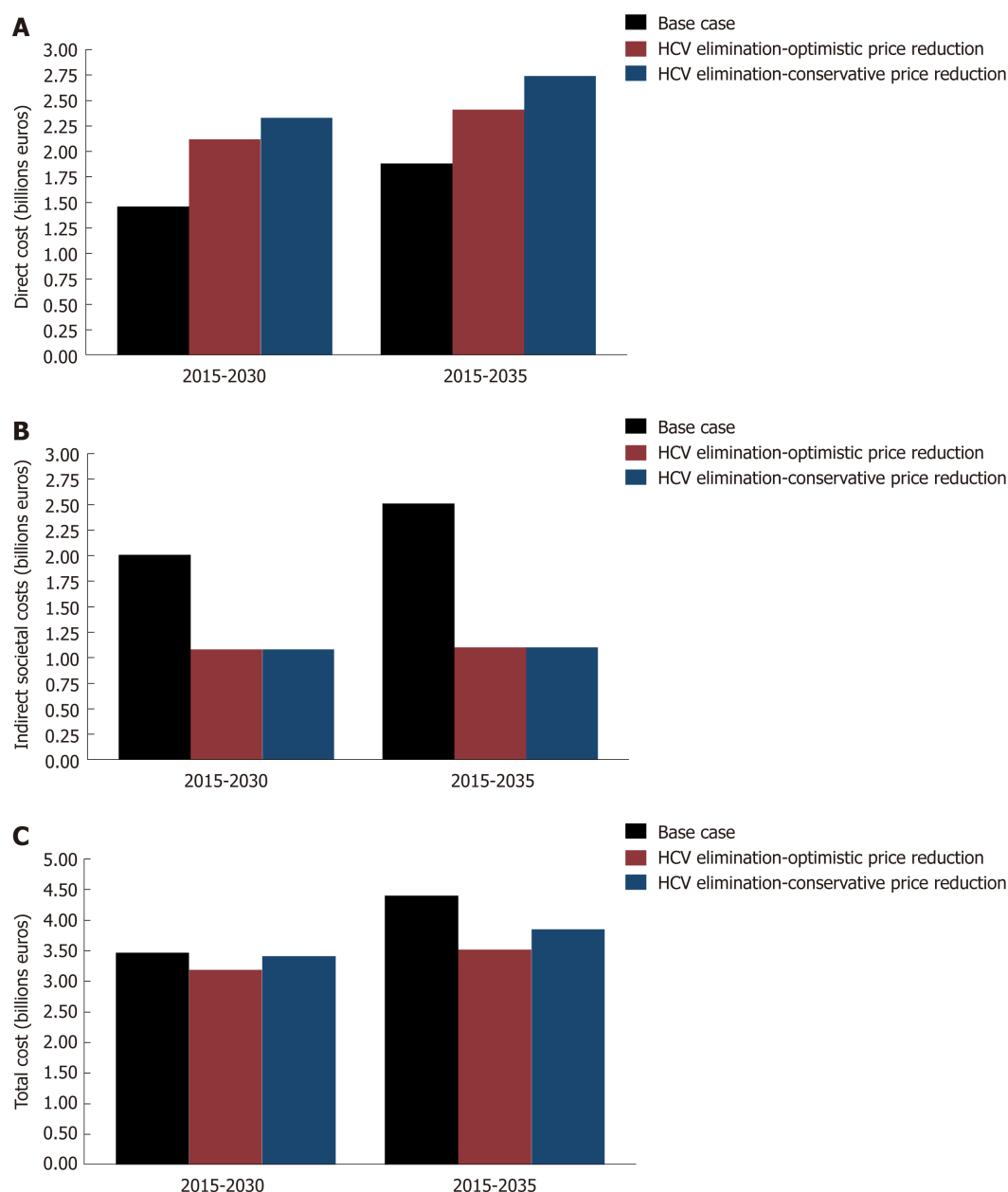


Figure 4 Estimated cumulative costs of base case and hepatitis C virus elimination scenarios in 2030 and 2035. A: Direct costs; B: Indirect/societal costs; C: Total costs. HCV: Hepatitis C virus.

HCV-infected patients are more likely to incur absenteeism (lost hours of work) and presenteeism (decreased productivity while at work)^[35,36].

The HCV elimination strategy is a cost-saving investment in the case of Greece (*i.e.*, improved life expectancy and reduced costs at the same time). More specifically, this investment would save €560-895 million by 2035, making it a very rewarding public health investment.

There are a number of limitations that could impact the outcomes of the study. First, patients who achieved SVR were not tracked, so all reinfection cases in the model were managed as naïve ones. Second, there is an assumption that new infections would remain stable at the 2015 levels. Thus, the model does not account for treatment as prevention, and its predictions would be more conservative. However, the strategy was cost effective despite the use of conservative assumptions, since the probability of reaching cost-effectiveness would be increased in the dynamic approach from the inclusion of the prevention of secondary cases. Third, the model assumed that new therapies, guidelines or treatment strategies are adopted immediately - a fact that may not be the case in real life settings. Fourth, although extrahepatic manifestations of HCV represent a significant part of direct cost^[37,38], they were not considered in this analysis. Fifth, possible reductions in the future cost of screening tests were not considered.

Table 4 Direct costs by price reduction scenario in billions of euros, disability-adjusted life years and incremental cost-effectiveness ratios

Base case			HCV elimination strategy					
			Optimistic			Conservative		
Years	Direct cost (billion euros)	DALYS	Direct cost (billion euros)	DALYS	ICER (compared to base case)	Direct cost (billion euros)	DALYS	ICER (compared to base case)
2015-2030	1.46	145.920	2.12	80.920	10.100 €	2.33	80.920	13.400 €
2015-2035	1.88	187.470	2.41	84.250	5.100 €	2.74	84.250	8.300 €

HCV: Hepatitis C virus; DALYs: Disability-adjusted life years; ICER: Incremental cost-effectiveness ratio.

In conclusion, our results support that elimination of HCV cannot be achieved without the implementation of large awareness and screening programs, as treatment coverage will be suboptimal. Nevertheless, HCV elimination is a cost-saving strategy, irrespective the uncertainty of the future cost of DAAs in Greece.

ARTICLE HIGHLIGHTS

Research background

Hepatitis C virus (HCV) infection is a major global public health problem. Greece has one of the highest rates of chronic HCV (CHC) infection in Europe, and approximately 33% of the chronically infected patients are at advanced fibrosis stages (\geq F3).

Research motivation

Greece faces a substantial economic crisis, which has resulted in more than 50% cut off in the public pharmaceutical expenditure. Therefore, it is important that every proposed healthcare intervention be accompanied by a cost-effectiveness analysis.

Research objectives

The main objectives of the study are (1) to estimate the required interventions to achieve elimination using updated information for direct-acting antiviral treatment coverage, (2) to compute the total costs (including the indirect/societal costs) of the strategy, and (3) to identify whether the elimination strategy is cost-effective/cost-saving in Greece.

Research methods

To project the future burden of disease and to estimate subsequent future costs, we used a previously validated, Excel-based disease progression model constructed by the Center for Disease Analysis. This model simulates the progression of HCV-infected persons through the various stages of the disease, according to the METAVIR scoring system, with appropriate transition probabilities between stages.

Progression was simulated by multiplying the total number of cases at a particular stage of disease by the appropriate progression rate to the next stage. Newly infected patients can enter the model at any year, progress through the disease stages based on progression rates, and exit the model on: (1) spontaneous clearance of HCV; (2) achieving sustained virological response rates; and (3) death (all-cause or HCV-related). Thirty-six cohorts every 5 yr of age and gender were used through 84 yr of age. Individuals older than 85 were treated as one cohort. Each year, one-fifth of the population in each age group, except for 85 and older, was moved to the next age cohort to simulate aging after taking into consideration mortality. Treated patients with sustained virological response rates were considered cured, and they had the same risk of hepatocellular carcinoma and similar mortality as the general population.

Research results

The analysis showed that while overall HCV prevalence in Greece would decline, disease burden related to HCV and associated costs would continue to grow. To achieve the elimination targets, 90000 patients need to be treated between 2015-2030. It was estimated that the investment (direct costs) of the intervention would range from €2.1-2.3 billion by 2030, while about €1.1 billion would be lost due to premature deaths or decreased productivity (indirect costs). The overall cumulative cost of HCV elimination in Greece would range from €3.2 and 3.4 billion by 2030. The model showed that the cost per averted disability-adjusted life years by 2030 would be between €8330-€13380. Furthermore, the HCV elimination strategy is cost-saving, as €560-€895 million would be saved by 2035.

Research conclusions

Our study highlighted that without the implementation of large awareness or screening programs, HCV elimination cannot be achieved, due to suboptimal treatment coverage. To eliminate the disease, significant public health reforms should be implemented (*e.g.*, enhance

harm reduction programs, implement case-finding, linkage to care interventions). Although the elimination of HCV is a costly investment, our analysis showed that it is also a cost-saving intervention, irrespective of the uncertainty of the future direct-acting antiviral cost in Greece, as the proposed strategy reduces the disease morbidity and mortality and restores productivity of the HCV-infected population.

Research perspectives

Elimination of HCV is a demanding public health intervention, which poses significant challenges in the Greek health care system. Nevertheless, our analysis highlighted that HCV elimination is a cost-saving intervention.

ACKNOWLEDGEMENTS

Angelos Hatzakis was supported by unrestricted grants from Gilead and MSD.

REFERENCES

- 1 **Polaris Observatory HCV Collaborators.** Global prevalence and genotype distribution of hepatitis C virus infection in 2015: a modelling study. *Lancet Gastroenterol Hepatol* 2017; **2**: 161-176 [PMID: 28404132 DOI: 10.1016/S2468-1253(16)30181-9]
- 2 **Lozano R,** Naghavi M, Foreman K, Lim S, Shibuya K, Aboyans V, Abraham J, Adair T, Aggarwal R, Ahn SY, Alvarado M, Anderson HR, Anderson LM, Andrews KG, Atkinson C, Baddour LM, Barker-Collo S, Bartels DH, Bell ML, Benjamin EJ, Bennett D, Bhalla K, Bikbov B, Bin Abdulhak A, Birbeck G, Blyth F, Bolliger I, Boufous S, Bucello C, Burch M, Burney P, Carapetis J, Chen H, Chou D, Chugh SS, Coffeng LE, Colan SD, Colquhoun S, Colson KE, Condon J, Connor MD, Cooper LT, Corriere M, Cortinovis M, de Vaccaro KC, Couser W, Cowie BC, Criqui MH, Cross M, Dabhadkar KC, Dahodwala N, De Leo D, Degenhardt L, Delossantos A, Denenberg J, Des Jarlais DC, Dharmaratne SD, Dorsey ER, Driscoll T, Duber H, Ebel B, Erwin PJ, Espindola P, Ezzati M, Feigin V, Flaxman AD, Forouzanfar MH, Fowkes FG, Franklin R, Fransen M, Freeman MK, Gabriel SE, Gakidou E, Gaspari F, Gillum RF, Gonzalez-Medina D, Halasa YA, Haring D, Harrison JE, Havmoeller R, Hay RJ, Hoen B, Hotez PJ, Hoy D, Jacobsen KH, James SL, Jasrasaria R, Jayaraman S, Johns N, Karthikeyan G, Kassebaum N, Keren A, Khoo JP, Knowlton LM, Kobusingye O, Koranteng A, Krishnamurthi R, Lipnick M, Lipshultz SE, Ohno SL, Mabweijano J, MacIntyre MF, Mallinger L, March L, Marks GB, Marks R, Matsumori A, Matzopoulos R, Mayosi BM, McAnulty JH, McDermott MM, McGrath J, Mensah GA, Merriman TR, Michaud C, Miller M, Miller TR, Mock C, Mocumbi AO, Mokdad AA, Moran A, Mulholland K, Nair MN, Naldi L, Narayan KM, Nasseri K, Norman P, O'Donnell M, Omer SB, Ortblad K, Osborne R, Ozgediz D, Pahari B, Pandian JD, Rivero AP, Padilla RP, Perez-Ruiz F, Perico N, Phillips D, Pierce K, Pope CA 3rd, Porrini E, Pourmalek F, Raju M, Ranganathan D, Rehm JT, Rein DB, Remuzzi G, Rivara FP, Roberts T, De León FR, Rosenfeld LC, Rushton L, Sacco RL, Salomon JA, Sampson U, Sanman E, Schwebel DC, Segui-Gomez M, Shepard DS, Singh D, Singleton J, Sliwa K, Smith E, Steer A, Taylor JA, Thomas B, Tleyjeh IM, Towbin JA, Truelsen T, Undurraga EA, Venketasubramanian N, Vijayakumar L, Vos T, Wagner GR, Wang M, Wang W, Watt K, Weinstock MA, Weintraub R, Wilkinson JD, Woolf AD, Wulf S, Yeh PH, Yip P, Zabetian A, Zheng ZJ, Lopez AD, Murray CJ, AlMazroa MA, Memish ZA. Global and regional mortality from 235 causes of death for 20 age groups in 1990 and 2010: a systematic analysis for the Global Burden of Disease Study 2010. *Lancet* 2012; **380**: 2095-2128 [PMID: 23245604 DOI: 10.1016/S0140-6736(12)61728-0]
- 3 **Davis GL,** Alter MJ, El-Serag H, Poynard T, Jennings LW. Aging of hepatitis C virus (HCV)-infected persons in the United States: a multiple cohort model of HCV prevalence and disease progression. *Gastroenterology* 2010; **138**: 513-521, 521.e1-521.e6 [PMID: 19861128 DOI: 10.1053/j.gastro.2009.09.067]
- 4 **Thein HH,** Yi Q, Dore GJ, Krahn MD. Estimation of stage-specific fibrosis progression rates in chronic hepatitis C virus infection: a meta-analysis and meta-regression. *Hepatology* 2008; **48**: 418-431 [PMID: 18563841 DOI: 10.1002/hep.22375]
- 5 **Feld JJ,** Kowdley KV, Coakley E, Sigal S, Nelson DR, Crawford D, Weiland O, Aguilar H, Xiong J, Pilot-Matias T, DaSilva-Tillmann B, Larsen L, Podsadecki T, Bernstein B. Treatment of HCV with ABT-450/r-ombitasvir and dasabuvir with ribavirin. *N Engl J Med* 2014; **370**: 1594-1603 [PMID: 24720703 DOI: 10.1056/NEJMoa1315722]
- 6 **Sulkowski MS,** Gardiner DF, Rodriguez-Torres M, Reddy KR, Hassanein T, Jacobson I, Lawitz E, Lok AS, Hineostroza F, Thuluvath PJ, Schwartz H, Nelson DR, Everson GT, Eley T, Wind-Rotolo M, Huang SP, Gao M, Hernandez D, McPhee F, Sherman D, Hindes R, Symonds W, Pasquinelli C, Grasela DM; A1444040 Study Group. Daclatasvir plus sofosbuvir for previously treated or untreated chronic HCV infection. *N Engl J Med* 2014; **370**: 211-221 [PMID: 24428467 DOI: 10.1056/NEJMoa1306218]
- 7 **WHO.** Global Health Sector Strategy on viral hepatitis, 2016-2021. 2015; <https://www.who.int/hepatitis/strategy2016-2021/ghss-hep/en/>
- 8 **Aggarwal R,** Chen Q, Goel A, Seguy N, Pendse R, Ayer T, Chhatwal J. Cost-effectiveness of hepatitis C treatment using generic direct-acting antivirals available in India. *PLoS One* 2017; **12**: e0176503 [PMID: 28520728 DOI: 10.1371/journal.pone.0176503]
- 9 **Chahal HS,** Marseille EA, Tice JA, Pearson SD, Ollendorf DA, Fox RK, Kahn JG. Cost-effectiveness of Early Treatment of Hepatitis C Virus Genotype 1 by Stage of Liver Fibrosis in a US Treatment-Naive Population. *JAMA Intern Med* 2016; **176**: 65-73 [PMID: 26595724 DOI: 10.1001/jamainternmed.2015.6011]
- 10 **Younossi ZM,** Tanaka A, Eguchi Y, Henry L, Beckerman R, Mizokami M. Treatment of hepatitis C virus leads to economic gains related to reduction in cases of hepatocellular carcinoma and decompensated cirrhosis in Japan. *J Viral Hepat* 2018; **25**: 945-951 [PMID: 29478258 DOI: 10.1111/jvh.12886]
- 11 **He T,** Lopez-Olivo MA, Hur C, Chhatwal J. Systematic review: cost-effectiveness of direct-acting antivirals for treatment of hepatitis C genotypes 2-6. *Aliment Pharmacol Ther* 2017; **46**: 711-721 [PMID: 28520728 DOI: 10.1371/journal.pone.0176503]

- 28836278 DOI: [10.1111/apt.14271](https://doi.org/10.1111/apt.14271)]
- 12 **Samur S**, Kues B, Ayer T, Roberts MS, Kanwal F, Hur C, Donnell DMS, Chung RT, Chhatwal J. Cost Effectiveness of Pre- vs Post-Liver Transplant Hepatitis C Treatment With Direct-Acting Antivirals. *Clin Gastroenterol Hepatol* 2018; **16**: 115-122.e10 [PMID: [28634131](https://pubmed.ncbi.nlm.nih.gov/28634131/)] DOI: [10.1016/j.cgh.2017.06.024](https://doi.org/10.1016/j.cgh.2017.06.024)]
 - 13 **Saraswat V**, Norris S, de Knecht RJ, Sanchez Avila JF, Sonderup M, Zuckerman E, Arkkila P, Stedman C, Acharya S, Aho I, Anand AC, Andersson MI, Arendt V, Baatarkhuu O, Barclay K, Ben-Ari Z, Bergin C, Bessone F, Blach S, Blokhina N, Brunton CR, Choudhuri G, Chulanov V, Cisneros L, Croes EA, Dahgwhadorj YA, Dalgard O, Daruich JR, Dashdorj NR, Davaadorj D, de Vree M, Estes C, Flisiak R, Gadano AC, Gane E, Halota W, Hatzakis A, Henderson C, Hoffmann P, Hornell J, Houlihan D, Hrusovsky S, Jarčuška P, Kershenobich D, Kostrzewska K, Kristian P, Leshno M, Lurie Y, Mahomed A, Mamonova N, Mendez-Sanchez N, Mossong J, Nurmukhametova E, Nymadawa P, Oltman M, Oyunbileg J, Oyunsuren Ts, Papatheodoridis G, Pimenov N, Prabdial-Sing N, Prins M, Puri P, Radke S, Rakhmanova A, Razavi H, Razavi-Shearer K, Reesink HW, Ridruejo E, Safadi R, Sagalova O, Sanduijav R, Schréter I, Seguin-Devaux C, Shah SR, Shestakova I, Shevaldin A, Shibolet O, Sokolov S, Souliotis K, Spearman CW, Staub T, Strebkova EA, Struck D, Tomasiewicz K, Undram L, van der Meer AJ, van Santen D, Veldhuijzen I, Villamil FG, Willemse S, Zuure FR, Silva MO, Sypsa V, Gower E. Historical epidemiology of hepatitis C virus (HCV) in select countries - volume 2. *J Viral Hepat* 2015; **22** Suppl 1: 6-25 [PMID: [25560839](https://pubmed.ncbi.nlm.nih.gov/25560839/)] DOI: [10.1111/jvh.12350](https://doi.org/10.1111/jvh.12350)]
 - 14 **Gountas I**, Sypsa V, Papatheodoridis G, Souliotis G, Razavi H, Hatzakis A. Is elimination of HCV possible in a country with low diagnostic rate and moderate HCV prevalence?: The case of Greece. *J Gastroenterol Hepatol* 2017; **32**: 466-472 [PMID: [27403912](https://pubmed.ncbi.nlm.nih.gov/27403912/)] DOI: [10.1111/jgh.13485](https://doi.org/10.1111/jgh.13485)]
 - 15 **Gane E**, Kershenobich D, Seguin-Devaux C, Kristian P, Aho I, Dalgard O, Shestakova I, Nymadawa P, Blach S, Acharya S, Anand AC, Andersson MI, Arendt V, Arkkila P, Baatarkhuu O, Barclay K, Ben-Ari Z, Bergin C, Bessone F, Blokhina N, Brunton CR, Choudhuri G, Chulanov V, Cisneros L, Croes EA, Dahgwhadorj YA, Daruich JR, Dashdorj NR, Davaadorj D, de Knecht RJ, de Vree M, Gadano AC, Gower E, Halota W, Hatzakis A, Henderson C, Hoffmann P, Hornell J, Houlihan D, Hrusovsky S, Jarčuška P, Kostrzewska K, Leshno M, Lurie Y, Mahomed A, Mamonova N, Mendez-Sanchez N, Mossong J, Norris S, Nurmukhametova E, Oltman M, Oyunbileg J, Oyunsuren Ts, Papatheodoridis G, Pimenov N, Prins M, Puri P, Radke S, Rakhmanova A, Razavi H, Razavi-Shearer K, Reesink HW, Ridruejo E, Safadi R, Sagalova O, Sanchez Avila JF, Sanduijav R, Saraswat V, Schréter I, Shah SR, Shevaldin A, Shibolet O, Silva MO, Sokolov S, Sonderup M, Souliotis K, Spearman CW, Staub T, Stedman C, Strebkova EA, Struck D, Sypsa V, Tomasiewicz K, Undram L, van der Meer AJ, van Santen D, Veldhuijzen I, Villamil FG, Willemse S, Zuckerman E, Zuure FR, Prabdial-Sing N, Flisiak R, Estes C. Strategies to manage hepatitis C virus (HCV) infection disease burden - volume 2. *J Viral Hepat* 2015; **22** Suppl 1: 46-73 [PMID: [25560841](https://pubmed.ncbi.nlm.nih.gov/25560841/)] DOI: [10.1111/jvh.12352](https://doi.org/10.1111/jvh.12352)]
 - 16 **Wedemeyer H**, Duberg AS, Buti M, Rosenberg WM, Frankova S, Esmat G, Örmeci N, Van Vlierberghe H, Gschwantler M, Akarca U, Aleman S, Balik I, Berg T, Bihl F, Bilodeau M, Blasco AJ, Brandão Mello CE, Bruggmann P, Calinas F, Calleja JL, Cheinquer H, Christensen PB, Clausen M, Coelho HS, Cornberg M, Cramp ME, Dore GJ, Doss W, El-Sayed MH, Ergör G, Estes C, Falconer K, Félix J, Ferraz ML, Ferreira PR, García-Samaniego J, Gerstoft J, Gíria JA, Gonçalves FL Jr, Guimarães Pessoa M, Hézode C, Hindman SJ, Hofer H, Husa P, Idilman R, Kåberg M, Kaita KD, Kautz A, Kaymakoglu S, Krajden M, Krarup H, Laleman W, Lavanchy D, Lázaro P, Marinho RT, Marotta P, Mauss S, Mendes Correa MC, Moreno C, Müllhaupt B, Myers RP, Nemecek V, Øvrehus AL, Parkes J, Peltekian KM, Ramji A, Razavi H, Reis N, Roberts SK, Roudot-Thoraval F, Ryder SD, Sarmiento-Castro R, Sarrazin C, Semela D, Sherman M, Shiha GE, Sperl J, Stärkel P, Stauber RE, Thompson AJ, Urbanek P, Van Damme P, van Thiel I, Vandijck D, Vogel W, Waked I, Weis N, Wiegand J, Yosry A, Zekry A, Negro F, Sievert F, Gower E. Strategies to manage hepatitis C virus (HCV) disease burden. *J Viral Hepat* 2014; **21** Suppl 1: 60-89 [PMID: [24713006](https://pubmed.ncbi.nlm.nih.gov/24713006/)] DOI: [10.1111/jvh.12249](https://doi.org/10.1111/jvh.12249)]
 - 17 **Gountas I**, Sypsa V, Delladetsima I, Tassopoulos N, Papatheodoridis G, Hatzakis A. The Impact of Age on Fibrosis Progression in Chronic Hepatitis C Patients. *EASL Barcelona* 2016; **64**: S459-S460 [DOI: [10.1016/S0168-8278\(16\)00769-8](https://doi.org/10.1016/S0168-8278(16)00769-8)]
 - 18 **Hatzakis A**, Chulanov V, Gadano AC, Bergin C, Ben-Ari Z, Mossong J, Schréter I, Baatarkhuu O, Acharya S, Aho I, Anand AC, Andersson MI, Arendt V, Arkkila P, Barclay K, Bessone F, Blach S, Blokhina N, Brunton CR, Choudhuri G, Cisneros L, Croes EA, Dahgwhadorj YA, Dalgard O, Daruich JR, Dashdorj NR, Davaadorj D, de Knecht RJ, de Vree M, Estes C, Flisiak R, Gane E, Gower E, Halota W, Henderson C, Hoffmann P, Hornell J, Houlihan D, Hrusovsky S, Jarčuška P, Kershenobich D, Kostrzewska K, Kristian P, Leshno M, Lurie Y, Mahomed A, Mamonova N, Mendez-Sanchez N, Norris S, Nurmukhametova E, Nymadawa P, Oltman M, Oyunbileg J, Oyunsuren Ts, Papatheodoridis G, Pimenov N, Prabdial-Sing N, Prins M, Radke S, Rakhmanova A, Razavi-Shearer K, Reesink HW, Ridruejo E, Safadi R, Sagalova O, Sanchez Avila JF, Sanduijav R, Saraswat V, Seguin-Devaux C, Shah SR, Shestakova I, Shevaldin A, Shibolet O, Silva MO, Sokolov S, Sonderup M, Souliotis K, Spearman CW, Staub T, Stedman C, Strebkova EA, Struck D, Sypsa V, Tomasiewicz K, Undram L, van der Meer AJ, van Santen D, Veldhuijzen I, Villamil FG, Willemse S, Zuckerman E, Zuure FR, Puri P, Razavi H. The present and future disease burden of hepatitis C virus (HCV) infections with today's treatment paradigm - volume 2. *J Viral Hepat* 2015; **22** Suppl 1: 26-45 [PMID: [25560840](https://pubmed.ncbi.nlm.nih.gov/25560840/)] DOI: [10.1111/jvh.12351](https://doi.org/10.1111/jvh.12351)]
 - 19 **Souliotis K**, Papageorgiou M, Politi A, Frangos N, Tountas Y. Estimating the Fiscal Effects of Public Pharmaceutical Expenditure Reduction in Greece. *Front Public Health* 2015; **3**: 203 [PMID: [26380249](https://pubmed.ncbi.nlm.nih.gov/26380249/)] DOI: [10.3389/fpubh.2015.00203](https://doi.org/10.3389/fpubh.2015.00203)]
 - 20 **Razavi H**, Elkhoury AC, Elbasha E, Estes C, Pasini K, Poynard T, Kumar R. Chronic hepatitis C virus (HCV) disease burden and cost in the United States. *Hepatology* 2013; **57**: 2164-2170 [PMID: [23280550](https://pubmed.ncbi.nlm.nih.gov/23280550/)] DOI: [10.1002/hep.26218](https://doi.org/10.1002/hep.26218)]
 - 21 **Athanasakis K**, Arzoumanidou D, Petrakis I, Karampli E, Theodoropoulou T, Retsa MP, Kyriopoulos J. A Cost-Of-Illness Analysis of Hepatitis C in Greece. *Value in Health* 2013; **16**: A496 [DOI: [10.1016/j.jval.2013.08.1108](https://doi.org/10.1016/j.jval.2013.08.1108)]
 - 22 **Chounta A**, Ellinas C, Tzanetakou V, Pliarhopoulou F, Mplani V, Oikonomou A, Leventogiannis K, Giamarellos-Bourboulis EJ. Serum soluble urokinase plasminogen activator receptor as a screening test for the early diagnosis of hepatocellular carcinoma. *Liver Int* 2015; **35**: 601-607 [PMID: [25348952](https://pubmed.ncbi.nlm.nih.gov/25348952/)] DOI: [10.1111/liv.12705](https://doi.org/10.1111/liv.12705)]
 - 23 **Papatheodoridis G**. *The use of the new antivirals for hepatitis C in the Greek clinical practice - Cost of the therapeutic intervention* 2016
 - 24 **Newspaper of the government of the hellenic republic (in Greek)**. In: Health Mo 2017.

- 25 Available from:
<http://healthmag.gr/>. Συμφωνία - σταθμός για την πρόσβαση των ασθενών με ηπατίτιδα C σε καινοτόμες 0
εραπείες υψηλού κόστους
- 26 Available from:
<http://healthmag.gr/>. Έκπτωση 68% για την ηπατίτιδα C - Καλύπτονται πενταπλάσιοι ασθενείς
- 27 Available from: <https://virus.com.gr/>. Ο κλειστός προϋπολογισμός της Ηπατίτιδας
- 28 Murray CJ, Lopez AD. Evidence-based health policy--lessons from the Global Burden of Disease Study. *Science* 1996; **274**: 740-743 [PMID: 8966556]
- 29 WHO. Health statistics and information systems, 2016. Available from:
<https://www.who.int/healthinfo/en/>
- 30 Marseille E, Larson B, Kazi DS, Kahn JG, Rosen S. Thresholds for the cost-effectiveness of interventions: alternative approaches. *Bull World Health Organ* 2015; **93**: 118-124 [PMID: 25883405 DOI: 10.2471/BLT.14.138206]
- 31 Razavi H, Waked I, Sarrazin C, Myers RP, Idilman R, Calinas F, Vogel W, Mendes Correa MC, Hézode C, Lázaro P, Akarca U, Aleman S, Balik I, Berg T, Bihl F, Bilodeau M, Blasco AJ, Brandão Mello CE, Bruggmann P, Buti M, Calleja JL, Cheinquer H, Christensen PB, Clausen M, Coelho HS, Cramp ME, Dore GJ, Doss W, Duberg AS, El-Sayed MH, Ergör G, Esmat G, Falconer K, Félix J, Ferraz ML, Ferreira PR, Frankova S, Garcia-Samaniego J, Gerstoft J, Gíria JA, Gonçalves FL Jr, Gower E, Gschwandler M, Guimaraes Pessoa M, Hindman SJ, Hofer H, Husa P, Kåberg M, Kaita KD, Kautz A, Kaymakoglu S, Krajden M, Krarup H, Laleman W, Lavanchy D, Marinho RT, Marotta P, Mauss S, Moreno C, Murphy K, Negro F, Nemecek V, Örmeci N, Øvrehus AL, Parkes J, Pasini K, Peltekian KM, Ramji A, Reis N, Roberts SK, Rosenberg WM, Roudot-Thoraval F, Ryder SD, Sarmento-Castro R, Semela D, Sherman M, Shiha GE, Sievert W, Sperl J, Stärkel P, Stauber RE, Thompson AJ, Urbanek P, Van Damme P, van Thiel I, Van Vlierberghe H, Vandijck D, Wedemeyer H, Weis N, Wiegand J, Yosry A, Zekry A, Cornberg M, Müllhaupt B, Estes C. The present and future disease burden of hepatitis C virus (HCV) infection with today's treatment paradigm. *J Viral Hepat* 2014; **21** Suppl 1: 34-59 [PMID: 24713005 DOI: 10.1111/jvh.12248]
- 32 El Khoury AC, Klimack WK, Wallace C, Razavi H. Economic burden of hepatitis C-associated diseases in the United States. *J Viral Hepat* 2012; **19**: 153-160 [PMID: 22329369 DOI: 10.1111/j.1365-2893.2011.01563.x]
- 33 Estes C, Abdel-Kareem M, Abdel-Razek W, Abdel-Sameea E, Abuzeid M, Gomaa A, Osman W, Razavi H, Zaghlal H, Waked I. Economic burden of hepatitis C in Egypt: the future impact of highly effective therapies. *Aliment Pharmacol Ther* 2015; **42**: 696-706 [PMID: 26202593 DOI: 10.1111/apt.13316]
- 34 Younossi ZM, Park H, Dieterich D, Saab S, Ahmed A, Gordon SC. Assessment of cost of innovation versus the value of health gains associated with treatment of chronic hepatitis C in the United States: The quality-adjusted cost of care. *Medicine (Baltimore)* 2016; **95**: e5048 [PMID: 27741116 DOI: 10.1097/MD.0000000000005048]
- 35 Younossi ZM, Stepanova M, Henry L, Younossi I, Weinstein A, Nader F, Hunt S. Association of work productivity with clinical and patient-reported factors in patients infected with hepatitis C virus. *J Viral Hepat* 2016; **23**: 623-630 [PMID: 26988765 DOI: 10.1111/jvh.12528]
- 36 Younossi I, Weinstein A, Stepanova M, Hunt S, Younossi ZM. Mental and Emotional Impairment in Patients With Hepatitis C is Related to Lower Work Productivity. *Psychosomatics* 2016; **57**: 82-88 [PMID: 26791515 DOI: 10.1016/j.psych.2015.10.005]
- 37 Cacoub P, Vautier M, Desbois AC, Saadoun D, Younossi Z. Direct medical costs associated with the extrahepatic manifestations of hepatitis C virus infection in France. *Aliment Pharmacol Ther* 2018; **47**: 123-128 [PMID: 29044584 DOI: 10.1111/apt.14382]
- 38 Younossi Z, Park H, Henry L, Adeyemi A, Stepanova M. Extrahepatic Manifestations of Hepatitis C: A Meta-analysis of Prevalence, Quality of Life, and Economic Burden. *Gastroenterology* 2016; **150**: 1599-1608 [PMID: 26924097 DOI: 10.1053/j.gastro.2016.02.039]

P- Reviewer: El-Shabrawi MHF, Gencdal G

S- Editor: Ma RY L- Editor: Filipodia E- Editor: Huang Y





Basic Study

Clinical assessment and identification of immuno-oncology markers concerning the 19-gene based risk classifier in stage IV colorectal cancer

Jong Lyul Lee, Seon Ae Roh, Chan Wook Kim, Yi Hong Kwon, Ye Jin Ha, Seon-Kyu Kim, Seon-Young Kim, Dong-Hyung Cho, Yong Sung Kim, Jin Cheon Kim

ORCID number: Jong Lyul Lee (0000-0002-5878-8000); Seon Ae Roh (0000-0002-6371-4778); Chan Wook Kim (0000-0002-2382-0939); Yi Hong Kwon (0000-0001-8422-4324); Ye Jin Ha (0000-0003-2001-7435); Seon-Kyu Kim (0000-0002-4176-5187); Seon-Young Kim (0000-0002-1030-7730); Dong-Hyung Cho (0000-0002-8859-0310); Yong Sung Kim (0000-0001-7113-272X); Jin Cheon Kim (0000-0003-4823-8619).

Author contributions: Lee JL, Roh SA and Kim JC made substantial contributions to the study conception and design, data acquisition, analysis, and interpretation, drafting a critical revision of the manuscript, and approving the final version of the text. Lee JL and Roh SA contributed equally. Kim CW made contributions to the study design, provided data from his patients, and approved the final version of the text. Kwon YH performed research, helped to write parts of the manuscript related to method, and approved the final version of the text. Ha YJ performed research and approved the final version of the text. Kim SK made contributions to the study design and helped to analyze data. Kim SY made contributions to the study design and helped to analyze data. Cho DH made substantial contributions to the study conception and interpretation. Kim YS made substantial contributions to the study conception and design, drafting a revision of the

Jong Lyul Lee, Chan Wook Kim, Jin Cheon Kim, Department of Surgery, University of Ulsan College of Medicine, Seoul 05505, South Korea

Jong Lyul Lee, Seon Ae Roh, Chan Wook Kim, Yi Hong Kwon, Ye Jin Ha, Jin Cheon Kim, Institute of Innovative Cancer Research, Asan Medical Center, Seoul 05505, South Korea

Seon-Kyu Kim, Seon-Young Kim, Yong Sung Kim, Medical Genomics Research Center, Korea Research Institute of Bioscience and Biotechnology, Daejeon 34141, South Korea

Dong-Hyung Cho, School of Life Sciences, Kyungpook National University 80 Daehak-ro, Daegu 41566, South Korea

Corresponding author: Jin Cheon Kim, MD, PhD, Doctor, Professor, Surgeon, Department of Surgery, University of Ulsan College of Medicine, Asan Medical Center, 88 Olympic-ro 43-gil, Songpa-gu, Seoul 05505, South Korea. jckim@amc.seoul.kr
Telephone: +82-2-30103489
Fax: +82-2-4749027

Abstract

BACKGROUND

Genomic profiling of tumors has contributed to the understanding of colorectal cancer (CRC), facilitating diagnosis, prognosis and selection of treatments, including targeted regimens. A report suggested that a 19-gene-based risk classifier (TCA19) was a prognostic tool for patients with stage III CRC. The survival outcomes in patients with stage IV CRC are still poor and appropriate selection of targeted therapies and immunotherapies is challenging.

AIM

To assess clinical implication of TCA19 in patients with stage IV CRC, and to identify TCA19 with involvement in immune-oncology.

METHODS

A retrospective review of the medical records of 60 patients with stage IV CRC was conducted, assessing clinicopathological variables and progression-free survival (PFS). TCA19 gene expression was determined by quantitative polymerase chain reaction (qPCR) in matched normal and tumor tissues taken from the study cohort. Expression of potential immune-oncology regulatory

manuscript.

Supported by Korea Research Foundation, No. 2016R1E1A1A02919844 to Kim JC and No. 2017R1A2B1009062 to Roh SA; Ministry of Science, ICT, and Future Planning, Republic of Korea and the Asan Institute for Life Sciences, No. 2016-710 to Lee JL.

Institutional review board

statement: The study protocol was approved by the Institutional Review Board of Asan Medical Center (registration No. 2015-0581), in accord with the Declaration of Helsinki.

Conflict-of-interest statement: The authors declare that they have no conflict of interest.

Data sharing statement: No additional data are available.

ARRIVE guidelines statement: The ARRIVE Guidelines have been adopted.

Open-Access: This is an open-access article that was selected by an in-house editor and fully peer-reviewed by external reviewers. It is distributed in accordance with the Creative Commons Attribution Non Commercial (CC BY-NC 4.0) license, which permits others to distribute, remix, adapt, build upon this work non-commercially, and license their derivative works on different terms, provided the original work is properly cited and the use is non-commercial. See: <http://creativecommons.org/licenses/by-nc/4.0/>

Manuscript source: Unsolicited manuscript

Received: November 20, 2018

Peer-review started: November 20, 2018

First decision: January 30, 2019

Revised: February 19, 2019

Accepted: February 22, 2019

Article in press: February 22, 2019

Published online: March 21, 2019

proteins and targets was examined by immunohistochemistry (IHC), western blot, immunofluorescence staining in tissues from a validation cohort of 10 patients, and in CRC cell lines co-cultured with monocyte *in vitro*.

RESULTS

In the patients with TCA19 score higher than the median, the PFS rates of eight patients who received the targeted regimens were significantly higher than the PFS rates of four patients who received 5-fluorouracil-based regimen ($P = 0.041$). In multivariate analysis, expression of signaling lymphocytic activation molecule family, member 7 (SLAMF7) and triggering receptor expressed on myeloid cells 1 (TREM1) was associated with PFS in the 60-patient cohort. After checking another 10 validate set, the expression of the IHC, the level of real-time qPCR, and the level of western blot were lower for SLAMF7 and higher for TREM1 in primary and metastatic tumors than in normal tissues. In CRC cells expressing SLAMF7 that were co-cultured with a monocytic cell line, levels of CD 68 and CD 73 were significantly lower at day 5 of co-culture than at day 0.

CONCLUSION

The TCA19 score might be prognostic for target-regimen-specific PFS in stage IV CRC. Down-regulation of SLAMF7 and up-regulation of TREM1 occur in primary and metastatic tumor tissues.

Key words: Colorectal cancer; Prognosis; Immunotherapy; Signaling lymphocytic activation molecule family, member 7; Triggering receptor expressed on myeloid cells 1

©The Author(s) 2019. Published by Baishideng Publishing Group Inc. All rights reserved.

Core tip: The current study showed that in the patients with stage IV colorectal cancer (CRC) and a higher 19-gene based risk classifier score, the target-regimen-specific progression-free survival (PFS) was significantly increased compared with the 5-fluorouracil-regimen-specific PFS. Using another 10 validate set, down-regulation of signaling lymphocytic activation molecule family, member 7 (SLAMF7) and up-regulation of triggering receptor expressed on myeloid cells 1 were identified in primary and metastatic tumors compared with normal tissue. In CRC cells expressing SLAMF7 that were co-cultured with a monocytic cell line, levels of CD68 and CD73 were significantly lower at day 5 of co-culture than at day 0.

Citation: Lee JL, Roh SA, Kim CW, Kwon YH, Ha YJ, Kim SK, Kim SY, Cho DH, Kim YS, Kim JC. Clinical assessment and identification of immuno-oncology markers concerning the 19-gene based risk classifier in stage IV colorectal cancer. *World J Gastroenterol* 2019; 25(11): 1341-1354

URL: <https://www.wjgnet.com/1007-9327/full/v25/i11/1341.htm>

DOI: <https://dx.doi.org/10.3748/wjg.v25.i11.1341>

INTRODUCTION

According to the Korean National Cancer Information Center, colorectal cancer (CRC) is the third leading cause of cancer death in South Korea^[1]. The survival rate for CRC in Korea has increased over the past two or three decades, with screening programs, new chemotherapy regimens (including targeted agents) and advances in surgical techniques all contributing to survival improvements^[2-4]. Further improvements could be obtained by optimizing selection of treatment regimens for different patients. Pathological staging according to tumor burden (T), presence of cancer cells in lymph nodes (N) and evidence for metastasis (M) is a well-known standard for prognosis^[5], and along with other clinicopathological characteristics is used for selection of patients for adjuvant chemotherapy. However, the response to chemotherapy varies because of heterogeneity among these patients^[6-9].

Genomic profiling of tumors has contributed to our understanding of CRC, facilitating diagnosis, prognosis and selection of treatments, including targeted regimens^[10]. Multi-gene prognostic classifiers developed in the past decade on the basis of next-generation sequencing have been used clinically to identify patients at

risk of recurrence, or to select targeted therapies^[11,12]. Previously, we developed a risk-score system based on 19 genes (TCA19) regulated by activation of triggering receptor expressed on myeloid cells 1 (TREM1) or connective tissue growth factor (CTGF)^[8]. The genes were selected by their involvement in tumorigenesis and progression, and in providing benefit from adjuvant chemotherapy for stage III CRC^[8]. Because survival outcomes in patients with stage IV CRC are poor, and appropriate selection of targeted therapies is challenging, we attempted in the present study to identify whether TCA19 scores predicted survival outcomes in patients with stage IV CRC undergoing different chemotherapy regimens.

The immune-checkpoint inhibitor, pembrolizumab has been shown to have a greater effect on disease-free survival in CRC with microsatellite instability than microsatellite-stable CRC^[13]. The effects of pembrolizumab on survival in patients with stage IV CRC also depends on patterns of metastasis^[14]. Tumor-associated macrophages (TAMs) of the M2 phenotype are present in the stroma of many tumors, and frequently associated with the progression of several types of cancer and CD68 acts as macrophage marker and TAMs marker^[15]. TAMs infiltration at the invasive hotspot is associated with improvement in both hepatic metastasis and overall survival in CRC^[16]. The function of CD73 in tumor is to facilitate escape from immune surveillance and to orchestrate the tumor-stroma interaction to promote cancer growth and metastasis^[15]. High expression of CD73 was poor prognostic factor in CRC^[17].

Here, we aim to determine whether the TCA19 system could be used as a prognostic indicator for stage IV CRC. We also attempt to identify possible target or marker genes associated with immune functions among the 19 genes, and examined the biologic behavior of the selected genes in association with immune function.

MATERIALS AND METHODS

Patients

The study included matched tissues from 60 patients with stage IV CRC that were histologically identified as adenocarcinoma and normal colonic tissue (> 5 cm from the tumor border), as well as blood. Another 10 patients were also enrolled for investigation of candidate gene (Supplementary Figure 1). All patients received surgery at the Asan Medical Center between December 2008 and October 2014, and CRC tissue and blood samples were acquired at the time of surgery under the patient consent for tissue and blood sample donation and examination. The metastatic tissue samples were acquired during the resection of metastatic disease and if the resection was unavailable, tissue biopsy of metastatic disease during work-up or surgery was also accepted. The serum was used for extraction of DNA from the centrifuged blood sample. The study protocol was approved by the Institutional Review Board of Asan Medical Center (registration No. 2015-0581), in accord with the Declaration of Helsinki. Clinical and pathologic data were extracted from the medical records. Patients were staged according to the 8th American Joint Committee on Cancer (AJCC) staging system.

Reverse transcription-quantitative polymerase chain reaction

Total RNA was extracted from the matched normal and tumor tissues of the patients using TRIzol reagent (Invitrogen, Carlsbad, CA, United States) according to the manufacturer's protocol. The cDNA was synthesized from total RNA by amplification using random primers and SuperScript II RT (Invitrogen). Quantitative real-time reverse transcription-quantitative polymerase chain reaction (RT-qPCR) was performed on a LightCycler 96 using the SYBR Green I Master Mix (Roche, Mannheim, Germany), in a total volume of 20 μ L with the following amplification steps: initial denaturation at 95 °C for 10 min, which was followed by 45 cycles of amplification (95 °C for 10 s, T_m for 10 s, and 72 °C for 20 s). Gene expression determined by RT-qPCR was normalized to human glyceraldehyde 3-phosphate dehydrogenase (GAPDH). Primers for TCA19 genes are listed in Supplementary Table 1. Relative levels of gene expression were determined using the $\Delta\Delta$ Ct method in which Δ Ct values between one of the TCA19 genes and the GAPDH control [Δ Ct = (Ct)_{TCA19 genes} - (Ct)_{GAPDH}]^[18]. $\Delta\Delta$ Ct was defined as a difference in the Δ Ct values between a normal tissue and a tumor tissue of the same patient [$\Delta\Delta$ Ct = (Δ Ct)_{normal} - (Δ Ct)_{tumor}] as previously reported.¹⁸ A 2^{- $\Delta\Delta$ Ct} value over 1-fold indicates upregulation of the tested TCA19 gene in a tumor tissue compared with a normal counterpart of the same patient.

TCA19 risk score

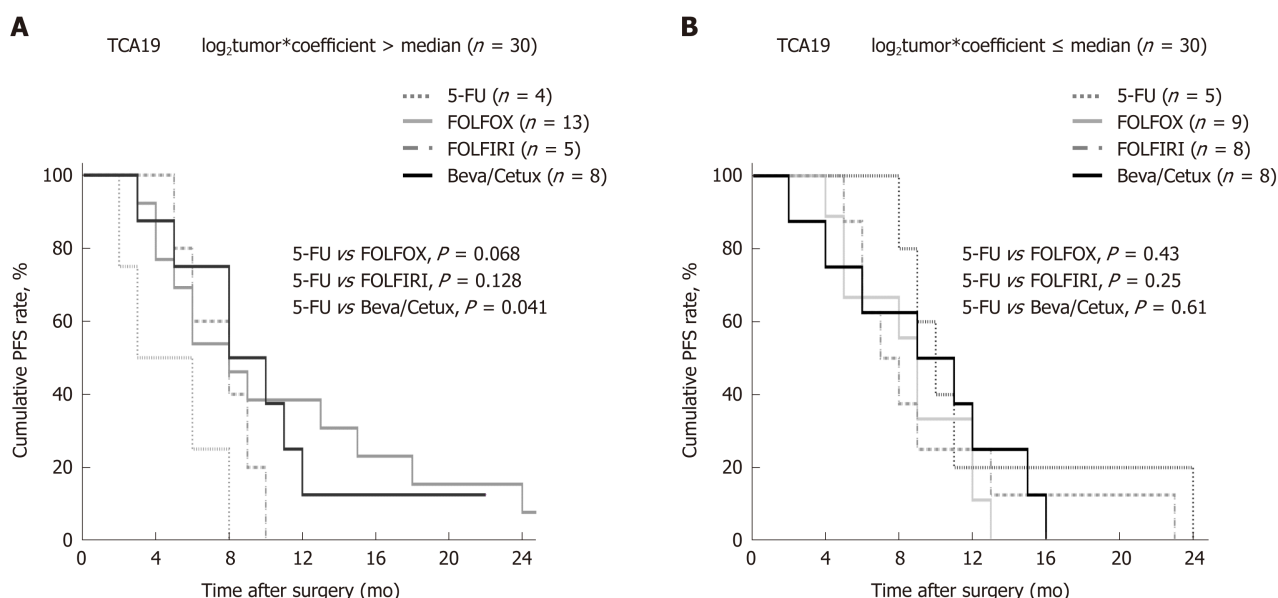


Figure 1 Progression-free survival in 60 patients with colorectal cancer, classified according to the 19-gene based risk score and chemotherapy regimens.

A: Progression-free (PFS) survival graph in the patients with higher 19-gene based risk (TCA19) score. B: PFS survival graph in the patients with lower TCA19 score. PFS: Progression-free survival; 5-FU: Fluorouracil-based regimen; FOLFOX: Combined regimen of fluorouracil, leucovorin, and oxaliplatin; FOLFIRI: Combined regimen of fluorouracil, leucovorin, and irinotecan; Beva/Cetux: Target-regimen including bevacizumab and cetuximab.

A risk score was developed via a previously reported strategy using the Cox regression coefficient for the TCA19 genes^[8,19,20]. The risk score for each patient was calculated as the sum of each gene's score, which was derived by multiplying the expression level of a gene by its corresponding coefficient using previously reported values (Supplementary Table 2)^[8]. The patients were then divided into two groups, for high or low expression of TCA19 genes using the median of the risk score as the threshold.

Immunohistochemistry and western blotting

Normal tissue, and primary and metastatic tumor tissues of 10 patients with metastatic CRC (separate from the initial study cohort of 60 patients), were used for immunohistochemistry (IHC) studies of the expression of signaling lymphocytic activation molecule family, member 7 (SLAMF7), TREM1, CD73 and CD68. Formalin fixed, paraffin-embedded tissue sections were immunohistochemically stained for protein expression of SLAMF7, TREM1, CD68, and CD73 with a BenchMark XT automatic immunostaining device (Ventana Medical Systems, Tucson, AZ, United States) with an OptiView DAB IHC Detection Kit (Ventana Medical Systems) according to the manufacturer's instructions.

Proteins were extracted from cultured cells using lysis buffer (Cells Signaling Technology, Danvers, MA, United States). Equal amounts of proteins were separated by sodium dodecyl sulfate polyacrylamide gel electrophoresis and transferred to polyvinylidene difluoride membranes (Milipore, Billerica, MA, United States). The membranes were blocked with 5% nonfat milk diluted in Tris-buffer saline containing of Tween-20 (TBST) for 1h at room temperature before the addition of the appropriate primary antibody. The membranes were then washed with TBST and incubated with the appropriate HRP-conjugated secondary antibody (1:10000; Abcam, Cambridge, United Kingdom) for 1h at room temperature. Protein-antibody complexes were visualized using a chemiluminescence reagent (New England Nuclear, Boston, MA, United States). Antibodies used in IHC and western blotting were listed in Supplementary Table 3.

CRC cell lines, cloning and THP-1 cells

The 10 CRC cell lines (DLD-1, HCT116, HCT15, HT29, LoVo, LS174T, RKO, SW480, SW620 and WIDR) and two normal colonic cell lines (CCD-18Co and CCD841) were purchased from the American Type Tissue Culture Collection (ATCC, Manassas, VA, United States) and maintained in RPMI-1640 medium supplemented with 10% fetal bovine serum (FBS). CRC cell lines (DLD-1, RKO, HCT116 and HT29) with minimal protein expression for SLAMF7 and TREM1 were selected for gene transfection (Supplementary Figure 2). SLAMF7 and TREM1 cDNA tagged with the peptide epitope Myc-DDK were purchased from OriGene (Rockville, MD, United States).

Table 1 Association between differential regulation of 19-gene-based risk classifier genes and clinicopathological factors in 60 patients with stage IV colorectal cancer

Variables (No. of patients)	Percentage of tumors with a log ₂ 2 ^{ΔΔ} CT value > 1 compared with matched normal tissue (P value)																			
	GAD D45B 1	S1P R3	CDK N2B	EGR 2	CTG F	SER PINE 1	RGS 16	RHO U	TIMP 1	PHL DA1	IL36 RN	SLA MF7	E2F7	DTL	CFB	CDK 1	CXC L1	CXC L3	CKS 2	TRE M1
Mean ± SEM of 2 ^{ΔΔ} CT	0.78 ± 0.74	1.45 ± 4.23	1.64 ± 6.03	3.24 ± 10.88	1.23 ± 1.66	8.19 ± 22.49	10.39 ± 35.49	1.01 ± 1.59	2.90 ± 2.79	5.49 ± 14.95	4.40 ± 15.22	1.17 ± 5.10	9.84 ± 34.23	2.46 ± 4.68	3.29 ± 5.62	2.94 ± 6.51	22.76 ± 75.79	30.55 ± 76.03	2.65 ± 4.14	14.14 ± 71.65
Sex	25.9/24.2	25.9/27.3	22.2/15.2	33.3/39.4	37.0/36.4	74.1/81.8	81.5/69.7	33.3/24.2	74.1/75.8	63.0/66.7	33.3/42.4	3.7/18.2	85.2/84.8	44.4/60.6	70.4/69.7	51.9/60.6	92.6/78.8	96.3/84.8	55.6/75.8	29.6/42.4
Female/male (27/33)	0.56	0.57	0.35	0.42	0.58	0.34	0.23	0.31	0.56	0.49	0.33	0.89	0.63	0.16	0.59	0.34	0.13	0.15	0.08	0.23
Age	23.2/50.0	26.8/25.0	17.9/25.0	37.5/25.0	35.7/50.0	76.8/100	75.0/75.0	28.6/25.0	73.2/100	64.3/75.0	39.3/25.0	10.7/25.0	83.9/100	55.4/25.0	71.4/50.0	58.9/25.0	83.9/100	89.3/100	66.1/75.0	35.7/50.0
≤ 75 vs > 75 (56/4)	0.26	0.71	0.57	0.53	0.47	0.37	0.69	0.68	0.31	0.56	0.5	0.4	0.51	0.26	0.35	0.21	0.51	0.65	0.59	0.47
Comorbidity	20.0/32.0	31.4/20.0	20.0/16.0	42.9/28.0	37.1/36.0	74.3/84.0	80.0/68.0	34.3/20.0	68.6/84.0	62.9/68.0	45.7/28.0	8.6/16.0	80.0/92.0	60.0/44.0	71.4/68.0	68.6/40.0	82.9/88.0	88.6/92.0	68.6/64.0	37.1/36.0
No/Yes (35/25)	0.22	0.25	0.48	0.18	0.57	0.28	0.22	0.18	0.14	0.45	0.13	0.31	0.18	0.17	0.5	0.03	0.43	0.51	0.46	0.57
Family history	24.0/30.0	28.0/20.0	18.0/20.0	38.0/30.0	36.0/40.0	78.0/80.0	72.0/90.0	28.0/30.0	74.0/80.0	64.0/70.0	42.0/20.0	12.0/10.0	88.0/70.0	56.0/40.0	70.0/70.0	60.0/40.0	88.0/70.0	94.0/70.0	72.0/40.0	36.0/40.0
No/Yes (50/10)	0.48	0.46	0.59	0.46	0.54	0.63	0.22	0.59	0.52	0.51	0.17	0.67	0.16	0.28	0.63	0.21	0.16	0.05	0.06	0.54
Synchronous Lm	33.3/21.4	33.3/23.8	22.2/16.7	33.3/38.1	33.3/38.1	72.2/81.0	83.3/71.4	44.4/21.4	77.8/73.8	66.7/64.3	44.4/35.7	22.2/7.1	72.2/90.5	55.6/52.4	83.3/64.3	72.2/50.0	100/78.6	100/85.7	83.3/59.5	38.9/35.7
No/Yes (18/42)	0.25	0.32	0.43	0.48	0.48	0.33	0.26	0.07	0.51	0.55	0.36	0.11	0.08	0.52	0.12	0.09	0.03	0.1	0.06	0.52
Synchronous Pm	28.9/13.3	26.7/26.7	17.8/20.0	37.8/33.3	35.6/40.0	77.8/80.0	77.8/66.7	31.1/20.0	77.8/66.7	66.7/60.0	40.0/33.3	13.3/6.7	86.7/80.0	57.8/40.0	71.1/66.7	62.2/40.0	88.9/73.3	91.1/86.7	66.7/66.7	40.0/26.7
No/Yes (45/15)	0.2	0.64	0.56	0.51	0.49	0.58	0.3	0.32	0.3	0.43	0.44	0.43	0.4	0.18	0.49	0.11	0.15	0.47	0.62	0.27
AJC stage	0/25.9	0/27.6	0/11	0/37.9	50/36.2	50/79.3	100/74.1	50/27.6	0/77.6	50/65.5	50/37.9	0/12.1	100/84.5	100/51.7	100/69.0	100/55.2	100/84.5	100/89.7	100/65.5	0/37.9
III/IV (2/58)	0.56	0.53	0.66	0.4	0.6	0.39	0.56	0.49	0.06	0.58	0.62	0.78	0.72	0.28	0.49	0.32	0.72	0.81	0.44	0.4

LVI	10.0/ 32.5	20.0/ 30.0	15.0/ 20.0	25.0/ 42.5	25.0/ 42.5	65.0/ 85.0	65.0/ 80.0	30.0/ 27.5	75.0/ 75.0	45.0/ 75.0	25.0/ 45.0	0/17. 5	70.0/ 92.5	35.0/ 62.5	60.0/ 75.0	45.0/ 62.5	75.0/ 90.0	85.0/ 92.5	55.0/ 72.5	30.0/ 40.0
No/ Yes (20/ 40)	0.05	0.31	0.47	0.15	0.15	0.08	0.17	0.53	0.63	0.02	0.11	0.05	0.03	0.04	0.18	0.16	0.13	0.31	0.14	0.32
PNI	12.0/ 34.3	32.0/ 22.9	16.0/ 20.0	40.0/ 34.3	32.0/ 40.0	76.0/ 80.0	60.0/ 85.7	36.0/ 22.9	72.0/ 77.1	56.0/ 71.4	40.0/ 37.1	8.0/1 4.3	76.0/ 91.4	52.0/ 54.3	68.0/ 71.4	56.0/ 57.1	76.0/ 91.4	84.0/ 94.3	64.0/ 68.6	24.0/ 45.7
No/ Yes (25/ 35)	0.04	0.31	0.48	0.43	0.36	0.47	0.02	0.2	0.44	0.17	0.52	0.37	0.1	0.53	0.5	0.57	0.1	0.19	0.46	0.07
CR M invo lve men t	22.4/ 36.4	26.5/ 27.3	18.4/ 18.2	34.7/ 45.5	38.8/ 27.3	79.6/ 72.7	73.5/ 81.8	30.6/ 18.2	73.5/ 81.8	63.3/ 72.7	36.7/ 45.5	6.1/3 6.4	83.7/ 90.9	51.0/ 63.6	69.4/ 72.7	53.1/ 72.7	85.7/ 81.8	89.8/ 90.9	61.2/ 90.9	30.6/ 63.6
No/ Yes (49/ 11)	0.27	0.61	0.68	0.37	0.36	0.44	0.44	0.34	0.44	0.41	0.42	0.02	0.47	0.34	0.57	0.2	0.52	0.7	0.05	0.04

¹GADD45B, control gene. Rt: Right; Lt: Left; Re: Rectum; Lm: Hepatic metastasis; Pm: Pulmonary metastasis; AJCC: American Joint Committee on Cancer; LVI: Lymphovascular invasion; PNI: Perineural invasion; CRM: Circumferential resection margin; IHC: Immunohistochemistry.

Transient transfection was performed to establish each cell mixture using Lipofectamine 2000 (Invitrogen). Stable clones were selected by culturing with aminoglycoside antibiotic G418 for 10 d, and at least two different clones were generated for each cell line. Human monocytic THP-1 cells were purchased from ATCC and maintained in RPMI-1640 medium supplemented with 10% FBS. M2-polarized THP-1 cells were generated by treatment 50 ng/mL phorbol myristate acetate (PMA, Sigma-Aldrich, St. Louis, MO, United States) for 24 h followed by incubation with 25 ng/mL interleukin (IL)-4 and 25 ng/mL IL-13 for 18 h. For lipopolysaccharide (LPS)-mediated THP-1 activation, cells were plated at a concentration of 1×10^4 cells/ well in the presence of 1 µg/mL LPS for 18 h.

Co-culturing of THP-1 cells and CRC cells

DLD-1, RKO, HCT116 and HT29 cells were co-cultured with THP-1 cells using Transwell inserts (Becton Dickinson, Franklin Lakes, NJ, United States) with a 0.4 µm porous membrane to create separate upper and lower chambers. CRC cells were cultured in the lower chamber at 1×10^4 cells/mL, and THP-1 cells were cultured in the upper chamber. CRC cells and THP-1 cells were collected 5 d after co-culture (Supplementary Figure 3).

Immunofluorescence staining

Adherent CRC cells collected after 5 d of co-culture were seeded on 96-well plates coated with collagen type I (Greiner Bio-One #655956, Frickenhausen, Germany). Cells were fixed for 30 min with 4% paraformaldehyde in ice-cold phosphate-buffered saline (PBS), quenched for 5 min with 50 mmol/L NH_4Cl , and incubated overnight at 4 °C with primary antibody diluted 1:100 in 5% normal goat serum (NGS) in PBS. Cells were washed three times with PBS and incubated for 1 h with secondary antibody at 1:500 dilution. Primary and secondary antibodies used in immunofluorescence staining (IFS) were listed in Supplementary Table 3. Cells were then washed three times with PBS, followed by nuclear counterstaining with 2 µg/mL DAPI for 1 min.

High-throughput imaging

Stained 96-well plates were imaged with a high-content wide-field fluorescence imaging system coupled to Harmony software version 3.5 (Operetta: PerkinElmer, Waltham, MA, United States). Wells were imaged with a $\times 40$ objective lens in a single focal plane across each plate. Twelve fields of views (each $510 \mu\text{m} \times 675 \mu\text{m}$) were imaged per well, with an identical pattern of fields used in every well.

Statistical analysis

Differential expression of individual TCA19 genes was compared with levels of clinico-pathological variables by the χ -square test, and the unpaired Student's *t*-test or Mann-Whitney *U*-test, as appropriate. The Kaplan-Meier method was used to

Table 2 Multivariate analyses of prognostic factors associated with progression-free survival using Cox-regression

	<i>P</i> value	Hazard ratio	CI lower	CI upper
N-category	0.02	0.569	0.349	0.927
LVI	0.004	2.559	1.347	4.862
PNI	0.538	0.837	0.476	1.473
CRM	0.004	2.931	1.398	6.143
Bormann type	0.3	0.731	0.402	1.327
SLAMF7	0.003	0.206	0.072	0.589
CKS2	0.018	0.484	0.266	0.883
TREM1	0.017	0.471	0.254	0.875

CI: Confidence interval; CKS-2: Cyclin-dependent kinases regulatory subunit 2; CRM: Circumferential resection margin; LVI: Lymphovascular invasion; PNI: Perineural invasion; SLAMF7: Signaling lymphocytic activation molecule family, member 7; TREM1: Triggering receptor expressed on myeloid cells 1.

calculate the survival outcomes, and the difference in survival between two groups was assessed using log-rank tests. The prognostic association between the signature and potential risk factors was assessed using multivariate Cox proportional hazard regression models. Statistical significance was expressed as $P < 0.05$, and the analyses were performed using SPSS software version 21 (IBM Corporation, Armonk, NY, United States).

RESULTS

Characteristics of the patients

Of the study cohort, 33 were male and 27 were female, with a median age of 61 years (interquartile range 52-69 years). The cancer was located in the right colon (cecum-splenic flexure of transverse colon) in 16 patients, the left colon (splenic flexure of transverse colon-distal sigmoid colon) in 28 patients, and in the rectum in 16 patients. Curative surgery (R0 resection) was performed in 14 patients. All patients received chemotherapy after the surgery consisting of single-agent treatment with 5-fluorouracil (5-FU) or capecitabine ($n = 9$), a combination of 5-FU and oxaliplatin ($n = 22$), 5-FU and irinotecan ($n = 13$), or targeted agents ($n = 16$), whether the choice of all chemotherapy was according to the oncologist's opinion. Nine patients received postoperative concurrent chemoradiotherapy (50.4 Gy in 28 fractions with concurrent 5-FU). The median follow-up period was 16 mo with an interquartile range (IQR) of 9-24 mo (Supplementary Table 4).

Association of progression-free survival with TCA19 scores and chemotherapy regimens

The study cohort was dichotomized on the basis of TCA19 risk scores. Progression-free survival (PFS) was not significantly different in the high (8 mo, IQR 6-10 mo) and low (9 months, IQR 8-10 mo) TCA19-score groups ($P = 0.42$). Among 30 patients with high TCA19 scores, the PFS rates were significantly different ($P = 0.041$) between four patients who received 5-FU regimen and eight patients who received the targeted regimens (bevacizumab or cetuximab). PFS rates among patients with low TCA19 scores did not differ significantly according to the chemotherapy regimens ($P = 0.61$) (Figure 1).

Expression of individual TCA19 genes is associated with clinicopathological variables and PFS

For each clinicopathological variable, the proportion of patients in each different condition with qPCR $\log_2 2^{-\Delta\Delta C_t}$ values greater than one (indicating a greater than one-fold increase in gene expression in the tumor relative to normal tissue) were compared (Table 1). For lymphovascular invasion (LVI), the proportions of patients with relative expression ($\log_2 2^{-\Delta\Delta C_t}$ greater than one) were significantly higher in the presence of invasion than in its absence for PHLDA1, E2F7, and DTL, and SLAMF7 ($P = 0.02, 0.05, 0.03, 0.04$, respectively). Similarly, for perineural invasion, the proportion of patients with relative expression was significantly higher in the presence of invasion than in its absence for RGS16 ($P = 0.02$). A lower proportion of patients had CXCL1 $\log_2 2^{-\Delta\Delta C_t}$ values greater than one in the presence of synchronous hepatic

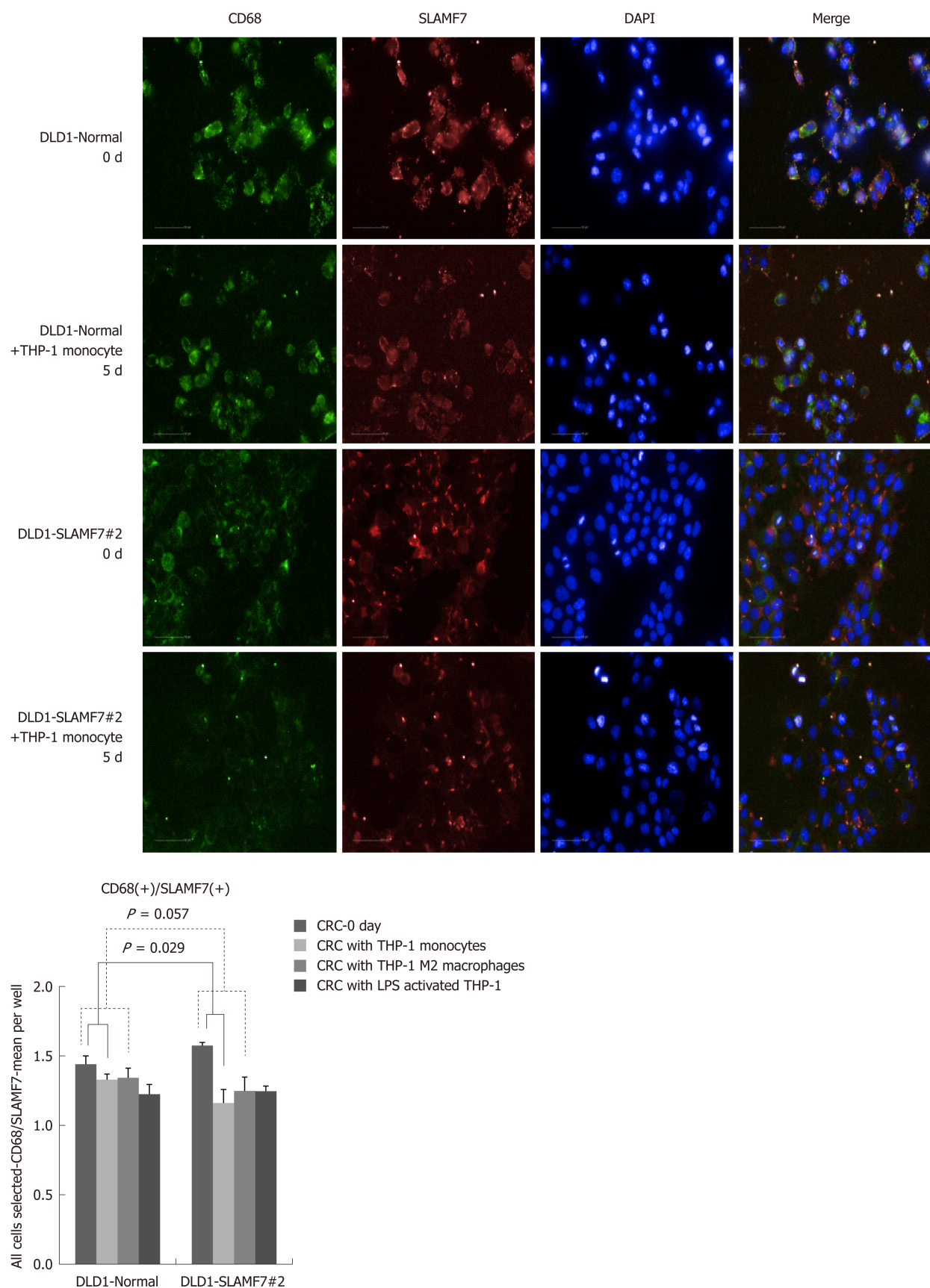


Figure 2 Expression of CD68 in a signaling lymphocytic activation molecule family, member 7-expression colorectal cancer cell line. High-through imaging and results of CD68(+)/signaling lymphocytic activation molecule family, member 7 (SLAMF7)(+) at day 0 and day 5 of co-culture with THP-1 monocytes, THP-1 M2 macrophages, and lipopolysaccharide activated THP-1. On day 5, expression of CD68 was significantly lower than day 0 in the SLAMF7-expressing region. SLAMF7: Signaling lymphocytic activation molecule family, member 7; LPS: Lipopolysaccharide; CRC: Colorectal cancer.

metastasis than its absence ($P = 0.03$). The proportion of patients with $\log_2 2^{-\Delta\Delta C_t}$ values

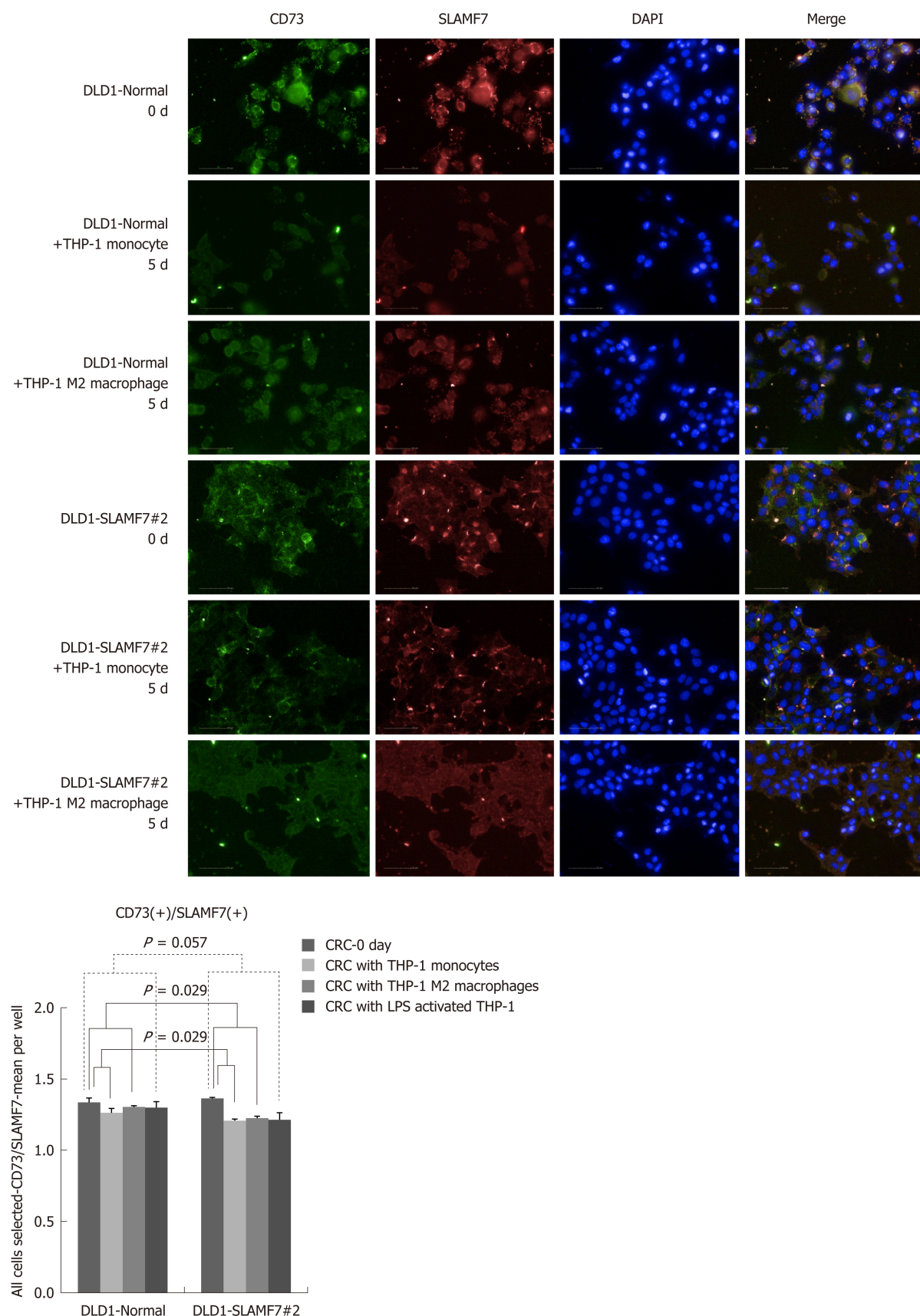


Figure 3 Expression of CD73 in a signaling lymphocytic activation molecule family, member 7-expression colorectal cancer cell line. High-through imaging and results of CD73(+)/signaling lymphocytic activation molecule family, member 7 (SLAMF7)(+) at day 0 and day 5 of co-culture with THP-1 monocytes, THP-1 M2 macrophages, and lipopolysaccharide activated THP-1. On day 5, expression of CD73 was significantly lower than day 0 in the SLAMF7-expressing region. SLAMF7: Signaling lymphocytic activation molecule family, member 7; LPS: Lipopolysaccharide; CRC: Colorectal cancer.

greater than one was significantly higher in the presence than in the absence of

involvement of circumferential resection margin (CRM) for SLAMF7, CKS2 and TREM1 ($P = 0.02, 0.05, 0.04$, respectively). These associations, as well as associations with the presence of comorbidity, family history, tumor location and the pattern of carcinoembryonic antigen, are shown in Table 1.

PFS was positively associated with relatively higher expression in tumor of SLAMF7, CXCL1, and CXCL3 and negatively associated with relatively higher expression of TREM1 (Supplementary Figure 4). Additionally, a multivariate Cox proportional hazard regression model was used to analyze the associations of PFS with expression of individual TCA19 genes and with clinicopathological variables. This analysis showed that LVI, CRM involvement, and expression of SLAMF7, CKS2 and TREM1 were significantly associated with PFS (Table 2).

SLAMF7 and TREM1 were differentially expressed in the 60 CRC patients with CRC

The association of expression of SLAMF7 and TREM1 with clinicopathological variables and PFS, as well as their immune-related gene functions, suggested that they were possible candidate genes. The relative mRNA expression of the SLAMF7 and TREM1 genes was assessed in the 60 CRC patients of the primary study group. In 53 patients, SLAMF7 expression was lower in tumor tissue than in normal tissue, giving a mean $2^{-\Delta\Delta Ct}$ value of 0.2, compared with a mean $2^{-\Delta\Delta Ct}$ value of 1.17 in 7 patients. In 22 patients, TREM1 expression was higher in tumor tissue than in normal tissue, giving a mean $2^{-\Delta\Delta Ct}$ value of 37.95, compared with a mean $2^{-\Delta\Delta Ct}$ value of 14.14 in 38 patients.

Expression of SLAMF7 and TREM1 in CRC was validated in a further 10 patients

Additional validation for the pattern of mRNA expression of SLAMF7 and TREM1 was obtained through RT-qPCR, western blotting and IHC of normal and tumor tissue samples of 10 additional patients with stage IV CRC. The results showed similar pattern to those with the initial 60-patient cohort, with lower expression of SLAMF7 and higher expression of TREM1 mRNA and protein in tumor tissue than normal tissue (Supplementary Figure 5). In additional analysis of 27 patients (separate from the 60 study cohort and the 10 validation set), SLAMF7 expression in 7 patients was lower in tumor tissue than in normal tissue (mean $2^{-\Delta\Delta Ct}$ value: 20.21) and TREM1 expression in 18 was higher in tumor tissue than in normal tissue (mean $2^{-\Delta\Delta Ct}$ value: 37.21) (Supplementary Table 5).

The results of western blotting were consistent with those of the mRNA expression study, with lower expression of SLAMF7 and higher expression of TREM1 in primary or metastatic tumor tissues than in normal colonic tissue (Supplementary Figure 6). However, in IHC, both SLAMF7 and TREM1 were expressed at significantly higher levels in primary or metastatic tumor tissues than in normal colonic tissue (Supplementary Table 6).

Results from high-throughput imaging

SLAMF7 and TREM1 have functions in immune responses, so their relationships with CD68 and CD73 were assessed by high-throughput imaging. Baseline IHC for these proteins was performed with tissues from the validation cohort of 10 patients with stage IV CRC, and showed TREM1 staining in plasma membrane, extracellular regions and intracellular regions, and SLAMF7 staining in plasma membranes and integral components of membranes (Supplementary Figure 7). CD68 was expressed in stroma (especially membranes), and CD73 was expressed in tumor stroma (Supplementary Figure 8).

CRC cells lines over-expressing SLAMF7 or TREM1 were co-cultured with THP-1 cells, and protein expression in the CRC cells before and after 5 d of co-culturing was compared by high-throughput immunofluorescence imaging. Specifically, expression of CD68 or CD73 was determined in regions expressing SLAMF7 or TREM1. At day 5, co-expression of both CD68 and CD73 with SLAMF7 was significantly lower than at day 0 (both $P = 0.029$) (Figures 2 and 3). Co-expression of CD68 or CD73 with TREM1 was not significantly different at day 5 from that at day 0 (Supplementary Figure 9).

DISCUSSION

Our results indicated that TCA19 might be useful for prediction of sensitivity of patients with stage IV CRC to targeted chemotherapy, as demonstrated previously for stage III CRC^[8]. Specifically, a high score with the TCA19 classifier suggests that a patient is a possible responder to a targeted regimen. In our cohort of 60 patients with stage IV CRC, a high TCA19 score was associated with a 4-mo survival benefit for targeted regimens compared with the 5-FU regimen. Few efficient biomarkers have been discovered for prediction of responses to targeted regimens (existing marker

include the products of *KRAS*, *NRAS*, *BRAF* and *PIK3CA* genes), although attempts to identify such markers have used laboratory and clinical approaches^[11,21-24]. A high TCA19 score might now be considered as a biomarker of the response to targeted chemotherapy in metastatic CRC.

In terms of survival outcomes, our results with multivariate analysis showed that expression levels of SLAMF7, TREM1, and CKS2 were independent risk factors of PFS. Expression of these genes was also significantly related to lympho-vascular invasion, perineural invasion, and involvement of circumferential resection margin. In our validation cohort of 10 additional patients, mRNA and protein levels were significantly different from primary tumor and metastatic tumor tissues, compared with normal tissues in SLAMF7 and TREM1. These results might suggest that expression of SLAMF7 and TREM1 was related to progression and metastasis of CRC. A previous report showed that inflammation was a critical component of tumor progression^[25] and in this specific view, both SLAMF7 and TREM1 might be associated with the link between inflammation and cancer.

SLAM-family receptors are expressed on hematopoietic cells, and SLAMF7 has an inhibitory role in human monocytes to control pro-inflammatory immune responses^[26,27]. A relationship between SLAMF7 and multiple myeloma has previously been demonstrated^[28,29], but no report have been published describing correlation between SLAMF7 and CRC. Here, we determined that SLAMF7 was under-expressed in CRC tissue compared with normal tissue, and that SLAMF7 might have an inhibitory role in expression of CD68 and CD73. Immune responses in lymphocytes and mast cells are associated with pathological responses to chemotherapy, and with PFS in metastatic CRC^[30]. Although further studies including mechanistic study to investigate the relationships between immune-check point and SLAMF7 or between MHC class and SLAMF7 or clinical studies to be use elotuzumab (SLAMF7-directed immunostimulatory antibody)^[29] in CRC are required, SLAMF7 might have potential as an immunotherapeutic target or as a marker for metastatic CRC.

TREM1 enhances degranulation and secretion of pro-inflammatory mediators, and is a potent amplifier of pro-inflammatory innate immune responses^[31]. Here, we showed that TREM1 had, overall, higher level of expression in tumor tissue than in normal tissue in RT-qPCR and IHC stain, and TREM1 gave a tendency of enhanced expression of CD68 and CD73. In results derived from experimental colitis and tissue from inflammatory bowel disease, TREM1 inhibition was shown to attenuate inflammation and tumor growth with the colon^[32]. High TREM1 expression in tumors is associated with an abundance of neutrophils and high expression of several innate pro-inflammatory genes that might be associated with tumorigenesis in CRC^[33]. Our results did not demonstrate a significant difference between day 0 and day 5 in terms of expression of CD68 and CD73 in TREM1-expressing CRC cells, possibly because expression of TREM1 was generally absent in the macrophages of normal colon mucosa, whereas TREM1-expressing macrophages showed significant up-regulation in the diseased colon tissue^[34].

To improve the survival rate in metastatic CRC, immunotherapy has been proposed as a treatment option in CRC with microsatellite instability^[35], which is associated with immune responses, including up-regulation of immune checkpoint inhibitory molecules such as PD-1, PD-L1 and CTLA4^[36,37]. Patients with CRC with microsatellite instability have more mutations and are more responsive to immunotherapy with PD-L1/PD-1 blockade than patients with microsatellite-stable CRC^[13,35]. As the number of the patients with CRC with microsatellite instability is limited and therapeutic targeting of microsatellite-stable CRC is difficult, additional immune checkpoints and immunomodulatory molecules still need to be investigated to provide adequate therapeutic coverage for all patients with CRC.

Our study had some limitations, including the small number of patients with the limited use of targeted regimens to assess a clinical implication of the TCA19 risk score and to validate SLAMF7 and TREM1 as suitable candidate. Also, our investigation was limited to assessment of relationship between SLAMF7/TREM1 and CD68/CD73. Further evaluation of other pro-inflammatory mediators with a large study cohort is required and ongoing, to identify any relationship between the expression of SLAMF7/TREM1 and immune-system regulation, and to find possible roles for the targeting of SLAMF7 and TREM1 in new treatment regimens for CRC.

In conclusion, TCA19 may provide prognostic information in patients with metastatic CRC, helping to identify those who will respond to targeted chemotherapy. Expression of SLAMF7 is down-regulated (whereas TREM1 is up-regulated) in primary or metastatic CRC tumors compared with normal colon tissue. SLAMF7 might have an inhibitory role in the immune response in CRC, whereas TREM1, if anything, has a tendency to enhance the immune response. Further mechanistic and functional studies with large cohorts are now required to confirm these relationships.

ARTICLE HIGHLIGHTS

Research background

Our team previously developed a risk score system based a 19 gene-based scoring system (TCA19), worked as a prognostic factor in stage II-III colorectal cancer (CRC). Stage IV CRC is still challenging in the treatment including target-regimen and immunotherapy.

Research motivation

It is needed to identify whether the TCA19 scores predict survival outcomes in patients with stage IV CRC undergoing different chemotherapy regimens including target-regimen and 19 genes are related to immuno-oncology.

Research objectives

The current study aims to determine whether the TCA19 system can be used as a prognostic indicator for stage IV CRC and to identify possible target or marker genes associated with immune functions from 19 genes.

Research methods

A retrospective review of the medical records of 60 patients with stage IV CRC was conducted, assessing clinico-pathologic variables, and progression-free survival (PFS). TCA19 gene expressions were determined by real-time quantitative polymerase chain reaction (RT-qPCR) in matched normal, primary tumor, and metastatic tumor tissues taken from the 60 study cohort. After selection of genes, related to immuno-oncology, expression of potential target or marker genes were examined by RT-qPCR, immunohistochemistry, western blot, and immunofluorescence staining using tissues from 10 validate set and in CRC cell lines co-cultured with monocytes *in vitro*.

Research results

In the patients with higher TCA19 score, the PFS rates of the patients with target-regimen were significantly higher than the patients with 5-fluorouracil-based regimen. In multivariable analysis, expression of signaling lymphocytic activation molecule family, member 7 (SLAMF7) and triggering receptor expressed on myeloid cells 1 (TREM1) was associated with PFS. From the results of the 10 validate set, down-regulation of SLAMF7 and up-regulation of TREM1 were observed in primary tumor and metastatic tumor tissues compared with normal tissue. In CRC cells expressing SLAMF7 that co-cultured with a monocytic cell line, levels of CD68 and CD73 in IFS imaging were significantly lower at day 5 of co-culture than at day 0. This result suggests that SLAMF7 may have an inhibitory role in the immune response.

Research conclusions

TCA19 system may be used as a prognostic indicator for stage IV CRC in terms of use of target-regimen. SLAMF7 and TREM1 may be related to tumorigenesis and progression according to down-regulation of SLAMF7 and up-regulation of TREM1 in tumor tissue.

Research perspectives

The current study found an inhibitory role of the SLAMF7 in the immune response. Recently, it is known that the patients with microsatellite-high CRC may respond the immune therapy. In this concept, the direction of the future research is the role of SLAMF7 in the patients with stage IV CRC in terms of the immune therapy.

REFERENCES

- 1 Jung KW, Won YJ, Oh CM, Kong HJ, Lee DH, Lee KH. Prediction of Cancer Incidence and Mortality in Korea, 2017. *Cancer Res Treat* 2017; **49**: 306-312 [PMID: 28301926 DOI: 10.4143/crt.2017.130]
- 2 Chang KH, Smith MJ, McAnena OJ, Aprjanto AS, Dowdall JF. Increased use of multidisciplinary treatment modalities adds little to the outcome of rectal cancer treated by optimal total mesorectal excision. *Int J Colorectal Dis* 2012; **27**: 1275-1283 [PMID: 22395659 DOI: 10.1007/s00384-012-1440-8]
- 3 Gennari L, Russo A, Rossetti C. Colorectal cancer: what has changed in diagnosis and treatment over the last 50 years? *Tumori* 2007; **93**: 235-241 [PMID: 17679456]
- 4 Allemani C, Weir HK, Carreira H, Harewood R, Spika D, Wang XS, Bannon F, Ahn JV, Johnson CJ, Bonaventure A, Marcos-Gragera R, Stiller C, Azevedo e Silva G, Chen WQ, Ogunbiyi OJ, Rachet B, Soeberg MJ, You H, Matsuda T, Bielska-Lasota M, Storm H, Tucker TC, Coleman MP; CONCORD Working Group. Global surveillance of cancer survival 1995-2009: analysis of individual data for 25,676,887 patients from 279 population-based registries in 67 countries (CONCORD-2). *Lancet* 2015; **385**: 977-1010 [PMID: 25467588 DOI: 10.1016/S0140-6736(14)62038-9]
- 5 Amin MB, Greene FL, Edge SB, Compton CC, Gershenwald JE, Brookland RK, Meyer L, Gress DM, Byrd DR, Winchester DP. The Eighth Edition AJCC Cancer Staging Manual: Continuing to build a bridge from a population-based to a more "personalized" approach to cancer staging. *CA Cancer J Clin* 2017; **67**: 93-99 [PMID: 28094848 DOI: 10.3322/caac.21388]
- 6 Sung SY, Jang HS, Kim SH, Jeong JU, Jeong S, Song JH, Chung MJ, Cho HM, Kim HJ, Kim JG, Lee IK, Lee JH. Oncologic Outcome and Morbidity in the Elderly Rectal Cancer Patients After Preoperative Chemoradiotherapy and Total Mesorectal Excision: A Multi-institutional and Case-matched Control Study. *Ann Surg* 2019; **269**: 108-113 [PMID: 28742692 DOI: 10.1097/SLA.0000000000002443]
- 7 Benson AB 3rd, Venook AP, Cederquist L, Chan E, Chen YJ, Cooper HS, Deming D, Engstrom PF, Enzinger PC, Fichera A, Grem JL, Grothey A, Hochster HS, Hoffe S, Hunt S, Kamel A, Kirilcuk N,

- Krishnamurthi S, Messersmith WA, Mulcahy MF, Murphy JD, Nurkin S, Saltz L, Sharma S, Shibata D, Skibber JM, Sofocleous CT, Stoffel EM, Stotsky-Himelfarb E, Willett CG, Wu CS, Gregory KM, Freedman-Cass D. Colon Cancer, Version 1.2017, NCCN Clinical Practice Guidelines in Oncology. *J Natl Compr Canc Netw* 2017; **15**: 370-398 [PMID: [28275037](#)]
- 8 **Kim SK**, Kim SY, Kim JH, Roh SA, Cho DH, Kim YS, Kim JC. A nineteen gene-based risk score classifier predicts prognosis of colorectal cancer patients. *Mol Oncol* 2014; **8**: 1653-1666 [PMID: [25049118](#) DOI: [10.1016/j.molonc.2014.06.016](#)]
- 9 **Provenzale D**, Gupta S, Ahnen DJ, Bray T, Cannon JA, Cooper G, David DS, Early DS, Erwin D, Ford JM, Giardiello FM, Grady W, Halverson AL, Hamilton SR, Hampel H, Ismail MK, Klapman JB, Larson DW, Lazenby AJ, Lynch PM, Mayer RJ, Ness RM, Regimbosen SE, Samadder NJ, Shike M, Steinbach G, Weinberg D, Dwyer M, Darlow S. Genetic/Familial High-Risk Assessment: Colorectal Version 1.2016, NCCN Clinical Practice Guidelines in Oncology. *J Natl Compr Canc Netw* 2016; **14**: 1010-1030 [PMID: [27496117](#)]
- 10 **Garcia EP**, Minkovsky A, Jia Y, Ducar MD, Shivdasani P, Gong X, Ligon AH, Sholl LM, Kuo FC, MacConaill LE, Lindeman NI, Dong F. Validation of OncoPanel: A Targeted Next-Generation Sequencing Assay for the Detection of Somatic Variants in Cancer. *Arch Pathol Lab Med* 2017; **141**: 751-758 [PMID: [28557599](#) DOI: [10.5858/arpa.2016-0527-OA](#)]
- 11 **De Roock W**, Claes B, Bernasconi D, De Schutter J, Biesmans B, Fountzilas G, Kalogeras KT, Kotoula V, Papamichael D, Laurent-Puig P, Penault-Llorca F, Rougier P, Vincenzi B, Santini D, Tonini G, Cappuzzo F, Frattini M, Molinari F, Saletti P, De Dosso S, Martini M, Bardelli A, Siena S, Sartore-Bianchi A, Tabernero J, Macarulla T, Di Fiore F, Gangloff AO, Ciardiello F, Pfeiffer P, Qvortrup C, Hansen TP, Van Cutsem E, Piessevaux H, Lambrechts D, Delorenzi M, Tejpar S. Effects of KRAS, BRAF, NRAS, and PIK3CA mutations on the efficacy of cetuximab plus chemotherapy in chemotherapy-refractory metastatic colorectal cancer: a retrospective consortium analysis. *Lancet Oncol* 2010; **11**: 753-762 [PMID: [20619739](#) DOI: [10.1016/S1470-2045\(10\)70130-3](#)]
- 12 **Espenschied CR**, LaDuca H, Li S, McFarland R, Gau CL, Hampel H. Multigene Panel Testing Provides a New Perspective on Lynch Syndrome. *J Clin Oncol* 2017; **35**: 2568-2575 [PMID: [28514183](#) DOI: [10.1200/JCO.2016.71.9260](#)]
- 13 **Le DT**, Uram JN, Wang H, Bartlett BR, Kemberling H, Eyring AD, Skora AD, Luber BS, Azad NS, Laheru D, Biedrzycki B, Donehower RC, Zaheer A, Fisher GA, Crocenzi TS, Lee JJ, Duffy SM, Goldberg RM, de la Chapelle A, Koshiji M, Bhajee F, Huebner T, Hruban RH, Wood LD, Cuka N, Pardoll DM, Papadopoulos N, Kinzler KW, Zhou S, Cornish TC, Taube JM, Anders RA, Eshleman JR, Vogelstein B, Diaz LA. PD-1 Blockade in Tumors with Mismatch-Repair Deficiency. *N Engl J Med* 2015; **372**: 2509-2520 [PMID: [26028255](#) DOI: [10.1056/NEJMoa1500596](#)]
- 14 **Fujiyoshi K**, Yamamoto G, Takenoya T, Takahashi A, Arai Y, Yamada M, Kakuta M, Yamaguchi K, Akagi Y, Nishimura Y, Sakamoto H, Akagi K. Metastatic Pattern of Stage IV Colorectal Cancer with High-Frequency Microsatellite Instability as a Prognostic Factor. *Anticancer Res* 2017; **37**: 239-247 [PMID: [28011498](#)]
- 15 **Pancione M**, Giordano G, Remo A, Febraro A, Sabatino L, Manfrin E, Ceccarelli M, Colantuoni V. Immune escape mechanisms in colorectal cancer pathogenesis and liver metastasis. *J Immunol Res* 2014; **2014**: 686879 [PMID: [24741617](#) DOI: [10.1155/2014/686879](#)]
- 16 **Zhou Q**, Peng RQ, Wu XJ, Xia Q, Hou JH, Ding Y, Zhou QM, Zhang X, Pang ZZ, Wan DS, Zeng YX, Zhang XS. The density of macrophages in the invasive front is inversely correlated to liver metastasis in colon cancer. *J Transl Med* 2010; **8**: 13 [PMID: [20141634](#) DOI: [10.1186/1479-5876-8-13](#)]
- 17 **Wu XR**, He XS, Chen YF, Yuan RX, Zeng Y, Lian L, Zou YF, Lan N, Wu XJ, Lan P. High expression of CD73 as a poor prognostic biomarker in human colorectal cancer. *J Surg Oncol* 2012; **106**: 130-137 [PMID: [22287455](#) DOI: [10.1002/jso.23056](#)]
- 18 **Kim Y**, Roh S, Park JY, Kim Y, Cho DH, Kim JC. Differential expression of the LOX family genes in human colorectal adenocarcinomas. *Oncol Rep* 2009; **22**: 799-804 [PMID: [19724858](#)]
- 19 **Kim YS**, Kim SH, Kang JG, Ko JH. Expression level and glycan dynamics determine the net effects of TIMP-1 on cancer progression. *BMB Rep* 2012; **45**: 623-628 [PMID: [23187000](#)]
- 20 **Paik S**, Shak S, Tang G, Kim C, Baker J, Cronin M, Baehner FL, Walker MG, Watson D, Park T, Hiller W, Fisher ER, Wickerham DL, Bryant J, Wolmark N. A multigene assay to predict recurrence of tamoxifen-treated, node-negative breast cancer. *N Engl J Med* 2004; **351**: 2817-2826 [PMID: [15591335](#) DOI: [10.1056/NEJMoa041588](#)]
- 21 **Khambata-Ford S**, Garrett CR, Meropol NJ, Basik M, Harbison CT, Wu S, Wong TW, Huang X, Takimoto CH, Godwin AK, Tan BR, Krishnamurthi SS, Burris HA, Poplin EA, Hidalgo M, Baselga J, Clark EA, Mauro DJ. Expression of epiregulin and amphiregulin and K-ras mutation status predict disease control in metastatic colorectal cancer patients treated with cetuximab. *J Clin Oncol* 2007; **25**: 3230-3237 [PMID: [17664471](#) DOI: [10.1200/JCO.2006.10.5437](#)]
- 22 **Normanno N**, Tejpar S, Morgillo F, De Luca A, Van Cutsem E, Ciardiello F. Implications for KRAS status and EGFR-targeted therapies in metastatic CRC. *Nat Rev Clin Oncol* 2009; **6**: 519-527 [PMID: [19636327](#) DOI: [10.1038/nrclinonc.2009.111](#)]
- 23 **To KK**, Tong CW, Wu M, Cho WC. MicroRNAs in the prognosis and therapy of colorectal cancer: From bench to bedside. *World J Gastroenterol* 2018; **24**: 2949-2973 [PMID: [30038463](#) DOI: [10.3748/wjg.v24.i27.2949](#)]
- 24 **Berger MD**, Stintzing S, Heinemann V, Yang D, Cao S, Sunakawa Y, Ning Y, Matsusaka S, Okazaki S, Miyamoto Y, Suenaga M, Schirripa M, Soni S, Zhang W, Falcone A, Loupakis F, Lenz HJ. Impact of genetic variations in the MAPK signaling pathway on outcome in metastatic colorectal cancer patients treated with first-line FOLFIRI and bevacizumab: data from FIRE-3 and TRIBE trials. *Ann Oncol* 2017; **28**: 2780-2785 [PMID: [29045529](#) DOI: [10.1093/annonc/mdx412](#)]
- 25 **Coussens LM**, Werb Z. Inflammation and cancer. *Nature* 2002; **420**: 860-867 [PMID: [12490959](#) DOI: [10.1038/nature01322](#)]
- 26 **Veillette A**. Immune regulation by SLAM family receptors and SAP-related adaptors. *Nat Rev Immunol* 2006; **6**: 56-66 [PMID: [16493427](#) DOI: [10.1038/nri1761](#)]
- 27 **Cannons JL**, Tangye SG, Schwartzberg PL. SLAM family receptors and SAP adaptors in immunity. *Annu Rev Immunol* 2011; **29**: 665-705 [PMID: [21219180](#) DOI: [10.1146/annurev-immunol-030409-101302](#)]
- 28 **Tai YT**, Dillon M, Song W, Leiba M, Li XF, Burger P, Lee AI, Podar K, Hideshima T, Rice AG, van Abbema A, Jesaitis L, Caras I, Law D, Weller E, Xie W, Richardson P, Munshi NC, Mathiot C, Avet-Loiseau H, Afar DE, Anderson KC. Anti-CS1 humanized monoclonal antibody HuLuc63 inhibits myeloma cell adhesion and induces antibody-dependent cellular cytotoxicity in the bone marrow milieu.

- Blood* 2008; **112**: 1329-1337 [PMID: [17906076](#) DOI: [10.1182/blood-2007-08-107292](#)]
- 29 **Lonial S**, Kaufman J, Laubach J, Richardson P. Elotuzumab: a novel anti-CS1 monoclonal antibody for the treatment of multiple myeloma. *Expert Opin Biol Ther* 2013; **13**: 1731-1740 [PMID: [24151843](#) DOI: [10.1517/14712598.2013.847919](#)]
- 30 **Tanis E**, Julié C, Emile JF, Mauer M, Nordlinger B, Aust D, Roth A, Lutz MP, Gruenberger T, Wrba F, Sorbye H, Bechstein W, Schlag P, Fisseler A, Ruers T. Prognostic impact of immune response in resectable colorectal liver metastases treated by surgery alone or surgery with perioperative FOLFOX in the randomised EORTC study 40983. *Eur J Cancer* 2015; **51**: 2708-2717 [PMID: [26342674](#) DOI: [10.1016/j.ejca.2015.08.014](#)]
- 31 **Tessaraz AS**, Cerwenka A. The TREM-1/DAP12 pathway. *Immunol Lett* 2008; **116**: 111-116 [PMID: [18192027](#) DOI: [10.1016/j.imlet.2007.11.021](#)]
- 32 **Zhou J**, Chai F, Lu G, Hang G, Chen C, Chen X, Shi J. TREM-1 inhibition attenuates inflammation and tumor within the colon. *Int Immunopharmacol* 2013; **17**: 155-161 [PMID: [23810411](#) DOI: [10.1016/j.intimp.2013.06.009](#)]
- 33 **Saurer L**, Zysset D, Rihs S, Mager L, Gusberti M, Simillion C, Lugli A, Zlobec I, Krebs P, Mueller C. TREM-1 promotes intestinal tumorigenesis. *Sci Rep* 2017; **7**: 14870 [PMID: [29093489](#) DOI: [10.1038/s41598-017-14516-4](#)]
- 34 **Schenk M**, Bouchon A, Seibold F, Mueller C. TREM-1--expressing intestinal macrophages crucially amplify chronic inflammation in experimental colitis and inflammatory bowel diseases. *J Clin Invest* 2007; **117**: 3097-3106 [PMID: [17853946](#) DOI: [10.1172/JCI30602](#)]
- 35 **Boland PM**, Ma WW. Immunotherapy for Colorectal Cancer. *Cancers (Basel)* 2017; **9** [PMID: [28492495](#) DOI: [10.3390/cancers9050050](#)]
- 36 **Watanabe T**, Wu TT, Catalano PJ, Ueki T, Satriano R, Haller DG, Benson AB, Hamilton SR. Molecular predictors of survival after adjuvant chemotherapy for colon cancer. *N Engl J Med* 2001; **344**: 1196-1206 [PMID: [11309634](#) DOI: [10.1056/NEJM200104193441603](#)]
- 37 **Llosa NJ**, Cruise M, Tam A, Wicks EC, Hechenbleikner EM, Taube JM, Blosser RL, Fan H, Wang H, Luber BS, Zhang M, Papadopoulos N, Kinzler KW, Vogelstein B, Sears CL, Anders RA, Pardoll DM, Housseau F. The vigorous immune microenvironment of microsatellite instable colon cancer is balanced by multiple counter-inhibitory checkpoints. *Cancer Discov* 2015; **5**: 43-51 [PMID: [25358689](#) DOI: [10.1158/2159-8290.CD-14-0863](#)]

P- Reviewer: Li Y, Maffei F, Wang DR

S- Editor: Ma RY **L- Editor:** A **E- Editor:** Huang Y





Basic Study

Hemodynamic changes in hepatic sinusoids of hepatic steatosis mice

Jing Fan, Chong-Jiu Chen, Yu-Chen Wang, Wei Quan, Jian-Wei Wang, Wei-Guang Zhang

ORCID number: Jing Fan (0000-0003-4604-401X); Chong-Jiu Chen (0000-0002-9512-457X); Yu-Chen Wang (0000-0002-9807-5662); Wei Quan (0000-0001-7121-707X); Jian-Wei Wang (0000-0002-7349-0325); Wei-Guang Zhang (0000-0001-5055-4907).

Author contributions: Fan J and Chen CJ performed the majority of experiments and analyzed the data; Wang YC and Quan W performed the hemorheological investigation; Fan J, Chen CJ, and Wang JW participated equally in treatment of animals; Fan J and Chen CJ designed and coordinated the research; Chen CJ wrote the paper.

Supported by Beijing Municipal Natural Science Foundation, No. 7162098.

Institutional animal care and use committee statement: All procedures involving animals were reviewed and approved by the Institutional Animal Care and Use Committee of the Peking University (IACUC protocol number: SCXK 2016-0010).

Conflict-of-interest statement: There is no conflict of interest in this study.

Data sharing statement: No additional data are available.

ARRIVE guidelines statement: The authors have read the ARRIVE guidelines, and the manuscript was prepared and revised according to the ARRIVE guidelines.

Jing Fan, Chong-Jiu Chen, Yu-Chen Wang, Wei Quan, Jian-Wei Wang, Wei-Guang Zhang, Department of Anatomy, Histology and Embryology, School of Basic Medical Sciences, Peking University Health Science Center, Beijing 100191, China

Corresponding author: Wei-Guang Zhang, MD, PhD, Professor, Department of Anatomy and Histology and Embryology, School of Basic Medical Sciences, Peking University Health Science Center, No. 38, Xueyuan Road, Haidian District, Beijing 100191, China.

zhangwg@bjmu.edu.cn

Telephone: +86-10-82802969

Fax: +86-10-82802969

Abstract

BACKGROUND

Fatty liver (FL) is now a worldwide disease. For decades, researchers have been kept trying to elucidate the mechanism of FL at the molecular level, but rarely involve the study of morphology and medical physics. Traditionally, it was believed that hemodynamic changes occur only when fibrosis occurs, but it has been proved that these changes already show in steatosis stage, which may help to reveal the pathogenesis and its progress. Because the pseudolobules are not formed during the steatosis stage, this phenomenon may be caused by the compression of the liver microcirculation and changes in the hemodynamics.

AIM

To understand the pathogenesis of hepatic steatosis and to study the hemodynamic changes associated with hepatic steatosis.

METHODS

Eight-week-old male C57BL/6 mice were divided into three groups randomly (control group, 2-wk group, and 4-wk group), with 16 mice per group. A hepatic steatosis model was established by subcutaneous injection of carbon tetrachloride in mice. After establishing the model, liver tissue from mice was stained with hematoxylin and eosin (HE), and oil red O stains. Blood was collected from the angular vein, and hemorheological parameters were estimated. A two-photon fluorescence microscope was used to examine the flow properties of red blood cells in the hepatic sinusoids.

RESULTS

Oil red O staining indicated lipid accumulation in the liver after CCl₄ treatment. HE staining indicated narrowing of the hepatic sinusoidal vessels. No significant difference was observed between the 2-wk and 4-wk groups of mice on

Open-Access: This is an open-access article that was selected by an in-house editor and fully peer-reviewed by external reviewers. It is distributed in accordance with the Creative Commons Attribution Non Commercial (CC BY-NC 4.0) license, which permits others to distribute, remix, adapt, build upon this work non-commercially, and license their derivative works on different terms, provided the original work is properly cited and the use is non-commercial. See: <http://creativecommons.org/licenses/by-nc/4.0/>

Manuscript source: Unsolicited manuscript

Received: December 19, 2018

Peer-review started: December 21, 2018

First decision: January 23, 2019

Revised: January 31, 2019

Accepted: February 22, 2019

Article in press: February 22, 2019

Published online: March 21, 2019

morphological examination. Hemorheological tests included whole blood viscosity (mPas, $\gamma = 10 \text{ s}^{-1} / \gamma = 100 \text{ s}^{-1}$) ($8.83 \pm 2.22 / 4.69 \pm 1.16$, $7.73 \pm 2.46 / 4.22 \pm 1.32$, and $8.06 \pm 2.88 / 4.22 \pm 1.50$), red blood cell volume (%) (51.00 ± 4.00 , 42.00 ± 5.00 , and 40.00 ± 3.00), the content of plasma fibrinase (g/L) (3.80 ± 0.50 , 2.90 ± 0.80 , and 2.30 ± 0.70), erythrocyte deformation index (%) (44.49 ± 5.81 , 48.00 ± 15.29 , and 44.36 ± 15.01), erythrocyte electrophoresis rate (mm/s per V/m) (0.55 ± 0.11 , 0.50 ± 0.11 , and 0.60 ± 0.20), revealing pathological changes in plasma components and red blood cells of hepatic steatosis. Assessment of blood flow velocity in the hepatic sinusoids with a laser Doppler flowmeter (mL/min per 100 g) (94.43 ± 14.64 , 80.00 ± 12.12 , and 67.26 ± 5.92) and two-photon laser scanning microscope ($\mu\text{m/s}$) (325.68 ± 112.66 , 213.53 ± 65.33 , and 173.26 ± 44.02) revealed that as the modeling time increased, the blood flow velocity in the hepatic sinusoids decreased gradually, and the diameter of the hepatic sinusoids became smaller (μm) (10.28 ± 1.40 , 6.84 ± 0.93 , and 5.82 ± 0.79).

CONCLUSION

The inner diameter of the hepatic sinusoids decreases along with the decrease in the blood flow velocity within the sinusoids and the changes in the systemic hemorheology.

Key words: Hepatic steatosis; Hemodynamics; Hepatic sinusoids; Two-photon fluorescence microscopy; Carbon tetrachloride

©The Author(s) 2019. Published by Baishideng Publishing Group Inc. All rights reserved.

Core tip: We evaluated the situation of blood flow in the hepatic sinusoids in hepatic steatosis mice, and found that both the velocity of the blood flow in the sinusoid and the diameter of the sinusoid decreased when the mice got fatty liver. Furthermore, we established the 3D imaging of the hepatic sinusoids to observe the sinusoids directly.

Citation: Fan J, Chen CJ, Wang YC, Quan W, Wang JW, Zhang WG. Hemodynamic changes in hepatic sinusoids of hepatic steatosis mice. *World J Gastroenterol* 2019; 25(11): 1355-1365

URL: <https://www.wjgnet.com/1007-9327/full/v25/i11/1355.htm>

DOI: <https://dx.doi.org/10.3748/wjg.v25.i11.1355>

INTRODUCTION

Fatty liver (FL) is a reversible condition in which large vacuoles of triglyceride fat accumulate in the liver cells by the process of steatosis, including hepatic steatosis and steatohepatitis. It is a disease related to heredity, environment, and metabolic stress and is a chronic disease that impairs multiple systems^[1]. Recent studies have reported that the pathogenesis of fatty liver is always accompanied by hepatic hemodynamic changes that induce abnormal fluid flow in the Disse space. The receptors or water channels on the surface of hepatocytes receive the signals of flow and then affect lipid metabolism in the liver cells, increasing hepatic lipid absorption and synthesis, thus resulting in the condition of hepatic steatosis^[2]. However, there has been little research on the relationship between hemodynamic changes in hepatic sinusoids and the development of hepatic steatosis.

Carbon tetrachloride-induced hepatic steatosis is a classical experimental mouse model often used to study the molecular mechanisms of liver injury and the effects of drugs^[3]. The CCl₄-induced hepatic steatosis model can accurately demonstrate the changes in the morphology and the function of hepatocytes, and it is highly stable and cost-effective. The mechanism underlying CCl₄-induced damage to the hepatocytes has been largely researched. The current consensus in the academic community is that the hepatotoxicity of CCl₄ is multifaceted, including production of CCl₄-derived reactive oxygen species (ROS), lipid peroxidation, covalent bonding of macromolecules, imbalance in calcium homeostasis, nucleic acid hypomethylation, inflammatory cytokines production and so on^[4].

The two-photon laser scanning microscope (TPLSM) was developed by Webb and his colleagues in 1990 works by using a pulsed laser that emits light in the infrared

spectrum^[5]. With the progress of two-photon fluorescence microscopy technique^[6], many studies were conducted to assess the characteristics of blood flow in the microcirculation of other organs using two-photon laser scanning microscopy^[7]. However, there has been no particular study examining the characteristics of blood flow in the hepatic sinusoids.

The hemodynamic characteristics of the liver are closely related to the anatomical structure of the liver. The liver has dual blood supply systems, which are composed of the hepatic artery and portal vein. The blood flowing in the microcirculation of the liver is different from that in other organs. In general, one-third of the liver blood is supplied by the hepatic artery and approximately two-thirds is supplied by the portal vein. Although the proportion of blood supplied by the hepatic artery is relatively small, it supplies most of the oxygenated blood needed by the liver. As the blood in the portal vein is derived from intestinal venous blood, it is rich in nutrients, which are used by the body after being metabolized in the liver. Most previous studies have focused on the hemodynamic changes in the great vessels of the liver, such as the changes in the blood pressure of the hepatic portal vein and the changes in the blood flow of the hepatic portal vein, but they have rarely focused on the hemodynamic changes in hepatic sinusoidal microcirculation^[8,9]. Therefore, we intended to use the two-photon fluorescence microscopy to study the morphological structure of the hepatic sinusoids and to assess the characteristics of blood flow in the sinusoids using the CCl₄ hepatic steatosis mouse model. This study aimed to explore the changes in blood flow in the hepatic sinusoids under the condition of hepatic steatosis, thus providing support for the prevention and treatment of hepatic steatosis.

MATERIALS AND METHODS

Animal experiments and drug treatment

All experiments were approved by the Local Ethics Committee for Animal Research Studies at the Peking University Health Science Center. Eight-week-old male C57BL/6 mice, weighting 20–25 g, kept on standard laboratory chow and with free access to drinking water, were used in this study. They were housed in a restricted access room with controlled temperature (23 °C) and a light/dark (12 h/12 h) cycle. Forty-eight male mice were divided into three groups: control group, 2-wk treatment group, and 4-wk treatment group. In the control group, the mice received injections of olive oil every three days up to 4 wk. The 2-wk group was treated with olive oil injections during the first two weeks and with CCl₄ injections (40% CCl₄ in olive oil was injected subcutaneously on the back; dose calculated as 30 µL/g body weight) during last two weeks. The 4-wk group was treated with injections of 40% CCl₄ in olive oil for 4 wk. After treatment with CCl₄ or olive oil, eight mice of each group were anaesthetized for examining the velocity of blood flow in the superficial vessels of the liver by using a laser Doppler detector. Subsequently, these mice were sacrificed; their livers were collected and fixed in 10% neutral buffered formalin (NBF) for histological examination; the blood was collected in an anticoagulant tube for hemorheological investigation. Another eight mice were prepared for hemodynamic assessment by using a TPLSM to examine hepatic sinusoidal blood flow.

Estimation of blood flow velocity in superficial hepatic vessels

The mice were anaesthetized with 1% sodium pentobarbital (50 µg/g body weight, intraperitoneally [i.p.]). The abdomen was opened, and the liver was exposed; the left lobe was selected for estimation of blood flow velocity using a laser Doppler flowmeter (Advanced Laser Flowmeter ALF2, Japan). Ten positions of the liver were explored, and the average value was calculated after estimating for 3 times per position. Finally, all ten positions were explored and the results were analyzed.

Histology assay

For the best fixation effect, the liver sample tissue of about 10 mm × 5 mm × 5 mm was used. We used 10% NBF as the fixative. Hematoxylin and eosin (HE) and oil red O staining were performed using standard procedures. The oil red O positive areas were quantified as described previously.

Hemorheological investigation

The mice were anesthetized with 1% pentobarbital sodium (50 µg/g body weight, i.p.); the blood from the angular vein was collected with a 0.5-mm capillary tube into the anticoagulant tube. For the red blood cell-specific volume [hematocrit (HCT)], we used the capillary tube. Hemorheological parameters, such as the erythrocyte deformation index (STEELLEX LGB-190, Beijing), fibrinogen level, erythrocyte electrophoresis rate (LIANG-100 Red cell electrophoresis apparatus, Beijing), and

whole blood viscosity (R80B Viscometer), were assessed.

Blood flow velocity in the hepatic sinusoids

After anesthetizing the mice, 200 μ L of fluorescein isothiocyanate -dextran (wt 70000, Sigma, America) was injected intravenously (25 mg in 1 mL saline, intravenous injection *via* the tail vein)^[10]. After 10 min when the fluorescent dye entered into the blood, it could not be taken up by blood cells due to the presence of blood cell membranes, therefore, under the laser excitation of the TPLSM, the dye in the blood fluoresced, while no such effect was seen in the cell due to no uptake of the dye. The inner side of the sinusoids often allows the pass-through of a single red blood cell when the red blood cells flow with the plasma. Therefore, the speed of red blood cells was used to represent the blood flow velocity within the sinusoids. The left lobe of the liver was surgically exposed with a small opening under the sternum. Keeping the lobe wet with saline, scanning of the lobe was performed under the TPLSM (inversion, Leica TCS SP8 MP) for estimating the velocity of blood in the sinusoids situated at 100-200 μ m from the central vein^[11]. In each mouse, ten blood vessels in different parts of the same lobe of the liver were selected for the estimation; meanwhile, the diameter of the sinusoids was measured.

Statistical analysis

All values are presented on graphs as the mean \pm SEM. The comparison between multiple groups was performed by one-way ANOVA followed by Dunnett's multiple comparison test. *P*-values < 0.05 were considered statistically significant.

RESULTS

Weight

Before injection of CCl₄ into the mice, their weights were recorded and monitored to maintain their healthy status (Figure 1). It was reported that the weights of the mice in the 2-wk group decreased during the third week, especially after injection of CCl₄, which might have resulted from the toxic effect of CCl₄. Thus, the mice experienced a weight loss in response to the stress induced by the injected drug.

Histological staining

After four weeks of treatment with CCl₄ or olive oil, the livers of the two CCl₄-treated groups were larger, harder, and had more rough surfaces than those of the control group. HE staining of paraffin sections of the liver tissue (Figure 2A) in the control group revealed that the liver morphology was normal, the cytoplasmic staining was homogeneous, and the cell nuclei were distinct. The internal diameter of the hepatic sinusoid was larger near the central vein of the hepatic lobule. The liver morphology was also normal in the 2-wk group, and no obvious lipid molecules were observed. In the 4-wk group, there were vacuolar structures of different sizes in the liver cells. The internal diameters of sinusoids were difficult to be accurately estimated by HE staining. Oil red O staining (Figure 2B) of the frozen section of the liver tissue in the control group showed no positive region, indicating that no significant lipid accumulation in the liver. After the injections of CCl₄ for two weeks, the mouse liver showed obvious orange-red lipid molecules after oil red O staining, and there were more positive areas around the central vein. Meanwhile, after CCl₄ injection for four weeks, a large number of lipid vacuoles were seen in the internal hepatic regions, as well as in regions around the central vein, indicating that as the duration of CCl₄ treatment increased, hepatic steatosis became more severe.

Hemorheology characteristics

The changes in the viscosity of the blood are shown in Figure 3A, under the shear rates of $\gamma = 10 \text{ s}^{-1}$ and $\gamma = 100 \text{ s}^{-1}$. With the extension of time after CCl₄ injection, the blood viscosity increased with a different shear rate; however, there was no statistical difference (*P* > 0.05). HCT decreased with the extension of time after CCl₄ injection (Figure 3B). The HCT value was significantly decreased in the 4-wk group compared to that in the control group (*P* = 0.029). With the extension of time after CCl₄ injection, the amount of fibrinogen in the blood decreased (Figure 3C), and the blood fibrinogen level in the 4-wk group was lower than that in the control group (*P* = 0.061). The results (Figure 3D) of estimating the erythrocyte deformation coefficient after CCl₄ injection showed a downward trend, according to which, the erythrocyte deformation index of the 4-wk group was not statistically significant as compared to that of the control group (*P* = 0.121). The results (Figure 3E) of this study showed that with the extension of time after CCl₄ injection, the erythrocyte electrophoresis rate in the mice showed an upward trend but without much statistical significance (*P* = 0.882).

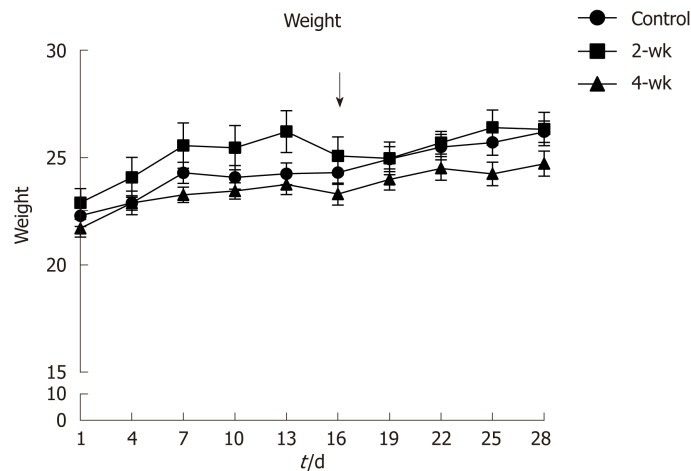


Figure 1 Change curves of mouse weights. The 2-wk group was treated with CCl_4 injection after the second week of injecting olive oil. The results show that the weights of the mice decreased after CCl_4 treatment.

Blood flow velocity and diameters of the sinusoids

Under the microscope, the bright regions represented the location of the sinusoids (Figure 4A), whereas the dark spots in the bright regions represented the red blood cells (Figure 4B). A TPLSM could selectively scan the sinusoids located along a straight line and thus one-dimensional image changes along a straight line could be visualized. As the red blood cells appeared as dark spots in the field of vision, the black line in Figure 4C indicates the trajectory of red blood cells. In the graph, the time is plotted on the vertical axis to show the time-related changes in the image of the sinusoids scanned along the straight line by the TPLSM. If the figure shows that one erythrocyte moves $107.43 \mu\text{m}$ within 302 ms , the blood velocity in the sinusoid can be calculated as $354.4 \mu\text{m/s}$. In this manner, the blood flow velocity in the left hepatic lobe of the control group, the 2-wk group, and the 4-wk group was measured (Figure 4D). It can be elucidated from the figure that, the blood flow velocity in hepatic sinusoids in 2-wk group ($P < 0.05$) and 4-wk group ($P < 0.01$) were less than that in the control group. This suggested that the rate of exchange of a single red blood cell in the sinusoids decreased significantly after hepatic steatosis in mice. At the same time, it was concluded that after measuring the hepatic sinusoidal diameters, the intravascular diameters of the hepatic sinusoids of the 2-wk ($P < 0.05$) and 4-wk ($P < 0.01$) groups were significantly lower than those of the control group (Figure 4E). Using a laser Doppler flow meter to measure the blood flow velocity of the superficial blood vessels of the mouse liver (Figure 4F), the blood flow velocity in the liver of mice decreased as a whole after CCl_4 injection. There was a statistical difference in the blood flow velocity between the control group and the 4-wk group ($P < 0.05$); however, no significant difference was noted between the control group and the 2-wk group. The morphology of the hepatic sinusoids was directly observed under a two-photon fluorescence microscope. It was found that the mice in the control group had regular and uniform hepatic sinusoids, whereas the sinusoidal falsifications in the 2-wk and 4-wk groups were obvious, and the mean hepatic sinusoidal diameters in the respective groups were reduced. Fluorescent dye was exudated from the sinusoids, which resulted in decreased brightness, suggesting a change in vascular permeability (Figure 4G). Finally, using the high penetration of the TPLSM, XYZ scanning was performed to construct a 3D image of the hepatic sinusoids (Figure 4H).

DISCUSSION

In this study, a two-photon fluorescence microscope was used to detect changes in blood flow in hepatic sinusoids in the CCl_4 -induced hepatic steatosis mouse model. The experimental results showed that in the presence of hepatic steatosis, the blood flow velocity in the hepatic sinusoids decreased along with the decrease in the internal diameter of the hepatic sinusoids. At the same time, blood flow velocity in the relatively large superficial hepatic vessels also decreased. Movement of red blood cells in the hepatic sinusoids was visually observed for the first time, to our knowledge, using a two-photon fluorescence microscope, and a 3D fluorescence image of the hepatic sinusoids was constructed.

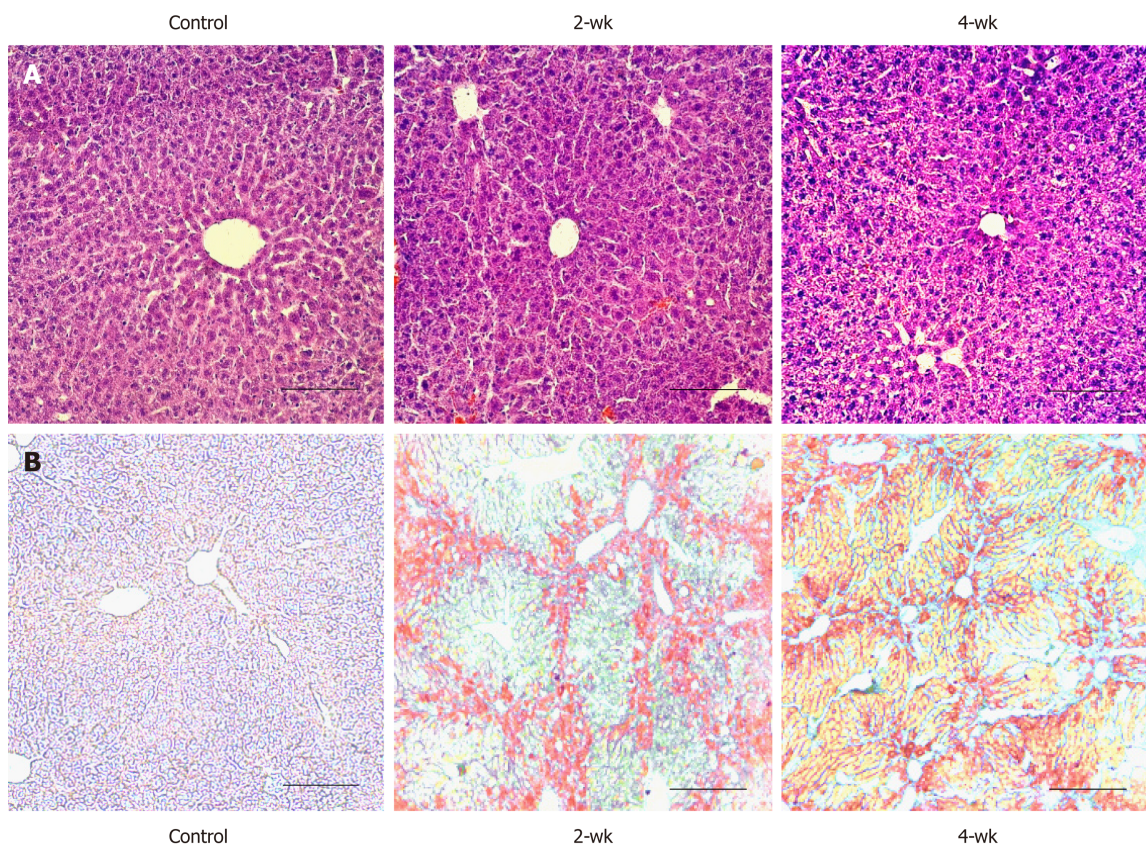


Figure 2 Lipid deposition occurring in the liver after CCl_4 treatment. A: Hematoxylin and eosin staining of paraffin section of liver tissue. The scale bar refers to 100 μm . B: Oil red O staining of frozen section of liver tissue. There was no lipid deposition in the control group; while in the 2-wk and 4-wk groups, a large amount of lipid deposition occurred after CCl_4 injection. The scale bar refers to 100 μm .

At present, the common methods for modeling of hepatic steatosis in animals include induction with a high-fat diet, with a methionine- and choline-deficient diet, and with carbon tetrachloride^[12]. Under normal circumstances of using carbon tetrachloride model, hepatic steatosis can be observed within two to four weeks^[13]. Therefore, carbon tetrachloride has become a classical method of fast and stable modeling^[14]. The mechanism of carbon tetrachloride-induced hepatic steatosis model can be explained as follows: carbon tetrachloride produces peroxidative stress in hepatocytes, which leads to changes in the lipid metabolism within hepatocytes and results in hepatic steatosis^[15]. In our study of hepatic hemodynamics, it was needed to consider the changes in liver morphology only and explore the impact of these changes on liver and systemic blood flow. There was no need to consider the metabolic processes of the liver itself, hence CCl_4 -induced hepatic steatosis model was used.

Blood viscosity is the most intuitive and direct indicator of blood rheology^[16]. Changes in blood viscosity can cause hemodynamic changes. It was found from the experimental results that the blood viscosity in mice did not change with the occurrence of fatty changes in the liver; however, an upward trend was observed among the changes in the blood viscosity. This indicated that during the early stage of hepatic steatosis, there was no significant difference in the blood viscosity. HCT is the most important factor affecting blood viscosity, and blood viscosity increases with increasing HCT^[17]. In this experiment, after the injection of CCl_4 into mice, HCT decreased to the level which was not enough to cause a significant decrease in blood viscosity. Plasma fibrinogen is an important factor affecting plasma viscosity, and plasma viscosity is an important component of overall blood viscosity^[18]. The results of this experiment revealed that plasma fibrinogen levels decreased after hepatic steatosis, which may led to the decrease in plasma viscosity, as well as to the decrease in blood viscosity. Red blood cell deformability is also an important indicator of blood rheology, which explains the morphological structure of red blood cells^[19]. The results of this study showed that after hepatic steatosis, the deformability of red blood cells decreased, while blood viscosity increased. The red blood cell electrophoresis rate is an index that affects the aggregation of red blood cells. Besides, the rate of red blood cell aggregation is closely related to blood viscosity. The experimental results showed

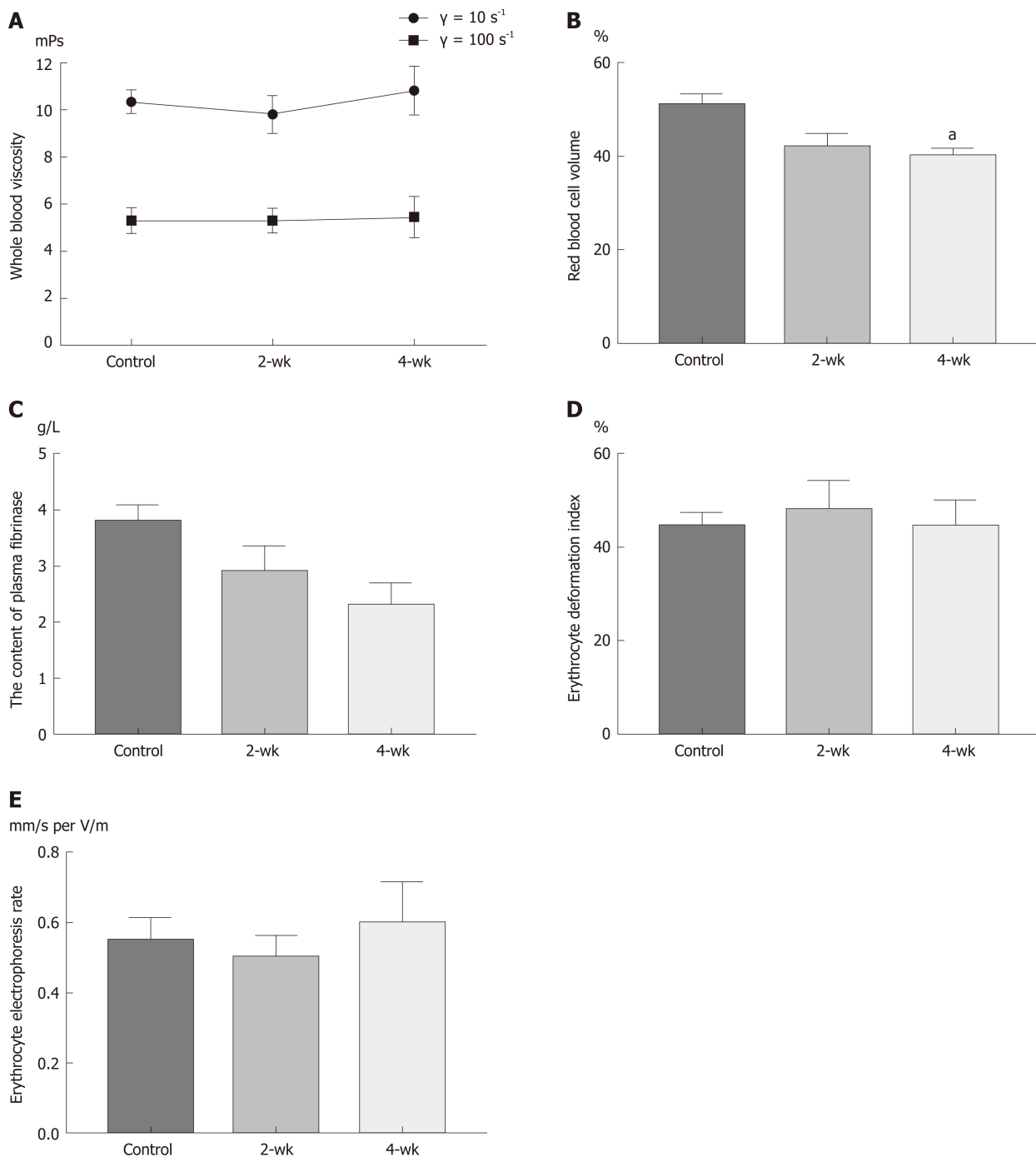


Figure 3 Changes of hemorheological parameters after CCl_4 treatment. A: There was an upward trend in total blood viscosity, but there was no statistical difference. B: The hematocrit value decreased after CCl_4 treatment. C: The fibrinogen levels decreased after CCl_4 treatment. D: Erythrocyte deformation index decreased after CCl_4 treatment. E: Erythrocyte electrophoresis rate showed an upward trend after CCl_4 treatment. ^a $P < 0.05$ vs control.

that there was no significant change in the surface charge of red blood cells after hepatic steatosis, which might be explained by the fact that during the early stage of hepatic steatosis, the physiological structure and function of red blood cell membrane might not have changed.

Being the largest digestive organ and the center of all metabolic processes in the human body, the hemodynamic characteristics of the liver have always been the focus of research. Many clinical studies have found that early hepatic steatosis occurs in the center of hepatic lobules, and with the aggravation of the disease, the steatosis spreads to the whole hepatic lobule^[20]. At the same time, experimental studies have observed that the enzymes of lipid *de novo* generation (such as FAS, SREBP1c, and SCD) in hepatocytes are overactive in the early fatty liver and lipid accumulating increased^[21]. Lipids in hepatocytes are metabolized into various metabolic products, resulting in lipid toxicity, which in turn affects the transcription of hepatocyte genes,

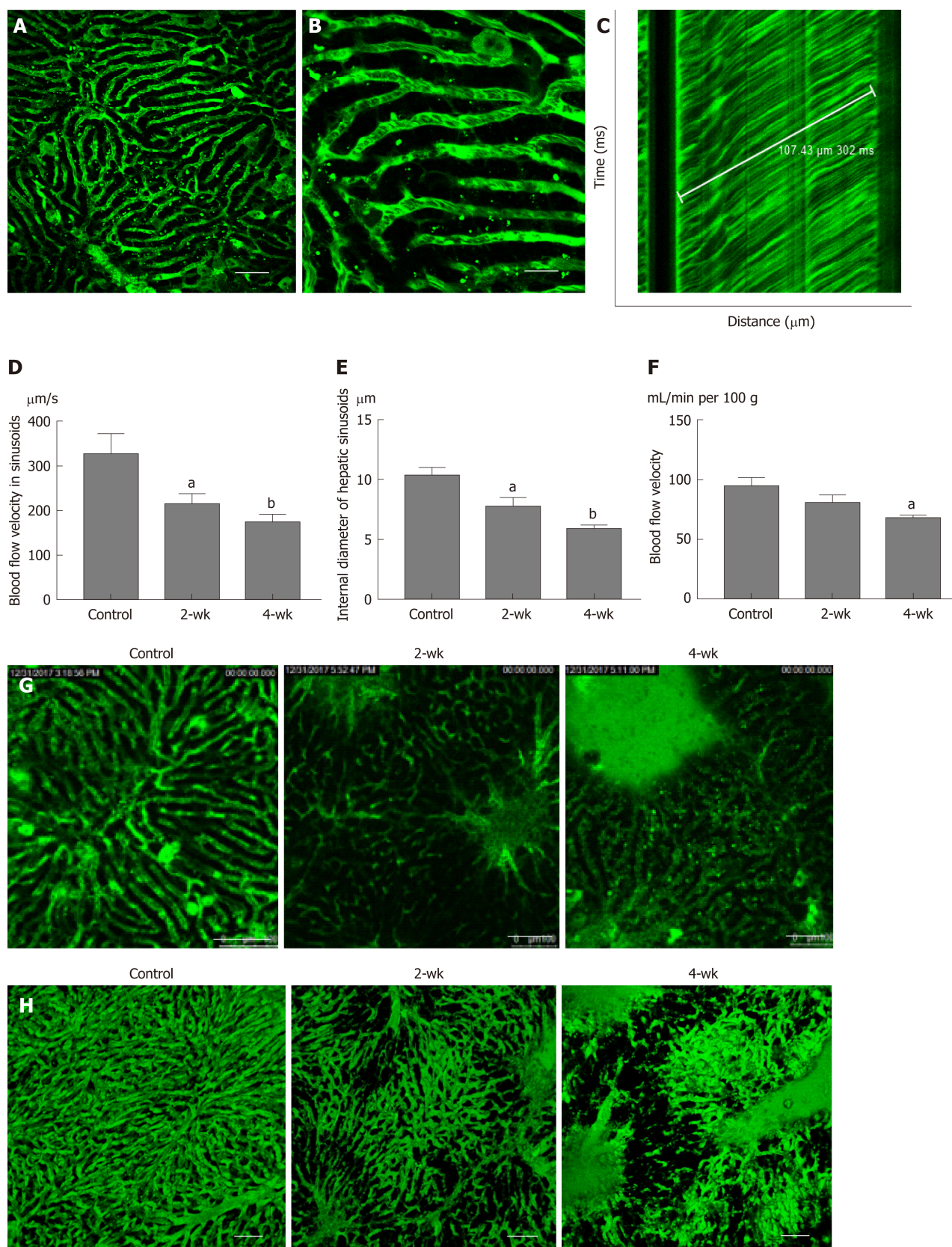


Figure 4 Changes of blood flow in the sinusoid after CCl_4 treatment. A: After the injection of fluorescent dye, the mouse liver tissue structure was observed under a two-photon fluorescence microscope. The green luminescent area represents the liver sinusoid. Scale bar refers to 100 μm . B: On enlarging the image of the sinusoid, the darker dots appeared in the sinusoids, which represent red blood cells. Scale bar refers to 30 μm . C: The distance-time image was obtained by scanning with the two-photon laser scanning microscope, and the blood flow velocity of the liver was calculated based on the image. D-F: The blood flow velocity in the hepatic sinusoid, the internal sinusoidal diameter, and the velocity of blood flow in the superficial blood vessels of the liver were estimated in all three groups. After treatment with CCl_4 , the blood flow velocity both in the sinusoid and superficial blood vessels decreased significantly. The internal sinusoidal diameter also decreased. G: In the control group, hepatic sinusoid morphology was uniform, while in the 2-wk and the 4-wk groups, the shapes of the sinusoids were significantly zigzag and the internal diameters were significantly less than the average diameter. Scale bar refers to 100 μm . H: The 3D image of the hepatic sinusoids. ^a $P < 0.05$ vs control, ^b $P < 0.01$ vs control.

intracellular signaling pathways, production of reactive oxygen, and endoplasmic reticulum stress^[22], and then induces liver fibrosis and even liver cirrhosis. The lipids in the cells gather to form large fat drops, and the hepatocytes expand, resulting in ballooning degeneration^[23], which then squeeze the surrounding blood sinusoid, making the inner diameter of the blood sinus narrow and causing increased vascular resistance in the liver.

Most of previous studies of hepatic hemodynamics have focused on the portal vein and other large hepatic vessels, and much attention has been paid to the impact of the portal vein hypertension on the whole body under various pathological conditions. However, little research has been conducted on the characteristics of blood flow in the hepatic sinusoids. This study, through direct observation of the hepatic sinusoid, found that in the fatty liver state of mice, the hepatocytes swell in a larger volume and squeeze the hepatic sinusoid, making the diameter of the hepatic sinus smaller and making it more difficult for the blood cells to pass through the sinusoid. Meanwhile, the sinusoid is obviously tortuouse, which makes the blood flow through the sinus more difficult. In addition, the permeability of the hepatic sinusoid also changes, making the components in the sinus more likely to leak out, thus affecting the blood flow of the liver. Under the influence of the above factors, hepatic hemodynamics changes. According to the Hagen-Poiseuille law, the blood pressure is related to both vascular resistance and the blood flow. In the fatty liver state, vascular resistance is increased, which is likely to cause non-cirrhotic portal hypertension^[24], and then lead to serious consequences such as varicose veins, which is harmful to health.

Under normal circumstances, microcirculations play an important role in afterload, and decide the end diastolic blood flow status in organs. However, clinical imaging examinations cannot detect these microvessels^[25,26]. Two-photon fluorescence microscopy provides us with another way to observe microcirculation in addition to electron microscopy. This observation method can link microscopic morphology with hemodynamics and complement laboratory imaging to fill gaps in clinical imaging. However, this method has limitations. For example, the test requires laparotomy *in vivo* and needs to inject fluorescent dyes *via* the vein, which directly limit its use on human specimens. Two-photon fluorescence microscopy can be used to display stereoscopic blood vessel morphology through 3D reconstruction. In the future, it can be combined with magnetic resonance imaging, ultrasound, and other fine imaging techniques to completely reconstruct the liver circulation through 3D printing, which will be a major breakthrough in the development of liver hemodynamics.

ARTICLE HIGHLIGHTS

Research background

Despite the high incidence of fatty liver, there was no specific diagnosis and treatment. And the study of morphological and medical physics changes in fatty liver have been ignored for many years. It has been reported that hemodynamic changes occur in steatosis stage, which might be caused by the compression of the liver microcirculation and changes in the hemorheology characteristics.

Research motivation

Re-examining steatosis from a new perspective - hemodynamics - may enhance our understanding of fatty liver and provide a new idea of treatment.

Research objectives

We mainly focused on the microcirculation of the liver in steatosis stage, which cannot be detected by clinical imaging technique. By the two-photon fluorescence microscopy imaging technique, we observed the structure and hemodynamic characteristics of the liver sinusoids, which linked microscopic morphology with hemodynamics and complemented laboratory imaging to fill gaps in clinical imaging.

Research methods

A hepatic steatosis model was established by subcutaneous injection of carbon tetrachloride in mice. After establishing the model, liver tissue from mice was stained with hematoxylin and eosin (HE) and oil red O stains. Blood was collected from the angular vein, and hemorheological parameters were estimated. A two-photon fluorescence microscope was used to examine the flow properties of red blood cells in the hepatic sinusoids. All result values are presented on graphs as the mean \pm SEM. The comparison between multiple groups was performed by one-way ANOVA followed by Dunnett's multiple comparison Test. *P*-values < 0.05 were considered statistically significant.

Research results

Oil red O staining indicated lipid accumulation in the liver after CCl₄ treatment. HE staining indicated narrowing of the hepatic sinusoidal vessels. No significant difference was observed

between the 2-wk and 4-wk groups of mice on morphological examination. Hemorheological tests revealed pathological changes in plasma components and red blood cells of hepatic steatosis. Assessment of blood flow velocity in the hepatic sinusoids revealed that as the modeling time increased, the blood flow velocity in the hepatic sinusoids decreased gradually; meanwhile, the diameter of the hepatic sinusoids became smaller.

These results revealed that hemodynamic changes occurring during steatosis stage (at least in the early stage) were more likely caused by sinusoidal deformation, but the mechanism of these phenomena remains to be solved.

Research conclusions

We used two-photon fluorescence microscopy imaging technique to study hemodynamic changes in fatty liver. And we observed that hemorheological change occurred in hepatic steatosis stage, and manifested as changes in blood flow velocity. We found that this change may be mainly caused by sinusoidal deformation, although it is related to hemorheology characteristics, but there was no statistical difference.

Research perspectives

Two-photon fluorescence microscopy imaging technique provides us with another way to observe microcirculation in addition to electron microscopy, and can be used to display stereoscopic blood vessel morphology through 3D reconstruction. In the future, it can be combined with magnetic resonance imaging and other fine imaging techniques to completely reconstruct the liver circulation through 3D printing, which will be a major breakthrough in the development of liver hemodynamics.

REFERENCES

- 1 **Byrne CD**, Targher G. NAFLD: a multisystem disease. *J Hepatol* 2015; **62**: S47-S64 [PMID: 25920090 DOI: 10.1016/j.jhep.2014.12.012]
- 2 **Poonkhum R**, Showpittapornchai U, Pradidarcheep W. Collagen arrangement in space of Disse correlates with fluid flow in normal and cirrhotic rat livers. *Microsc Res Tech* 2015; **78**: 187-193 [PMID: 25536906 DOI: 10.1002/jemt.22460]
- 3 **Donthamsetty S**, Bhavé VS, Mitra MS, Latendresse JR, Mehendale HM. Nonalcoholic fatty liver sensitizes rats to carbon tetrachloride hepatotoxicity. *Hepatology* 2007; **45**: 391-403 [PMID: 17256749 DOI: 10.1002/hep.21530]
- 4 **Weber LW**, Boll M, Stampfl A. Hepatotoxicity and mechanism of action of haloalkanes: carbon tetrachloride as a toxicological model. *Crit Rev Toxicol* 2003; **33**: 105-136 [PMID: 12708612 DOI: 10.1080/713611034]
- 5 **Huiskens J**, Swoger J, Del Bene F, Wittbrodt J, Stelzer EH. Optical sectioning deep inside live embryos by selective plane illumination microscopy. *Science* 2004; **305**: 1007-1009 [PMID: 15310904 DOI: 10.1126/science.1100035]
- 6 **Schenke-Layland K**, Riemann I, Damour O, Stock UA, König K. Two-photon microscopes and in vivo multiphoton tomographs--powerful diagnostic tools for tissue engineering and drug delivery. *Adv Drug Deliv Rev* 2006; **58**: 878-896 [PMID: 17011064 DOI: 10.1016/j.addr.2006.07.004]
- 7 **Katona G**, Szalay G, Maák P, Kaszás A, Veress M, Hillier D, Chiovini B, Vizi ES, Roska B, Rózsa B. Fast two-photon in vivo imaging with three-dimensional random-access scanning in large tissue volumes. *Nat Methods* 2012; **9**: 201-208 [PMID: 22231641 DOI: 10.1038/nmeth.1851]
- 8 **Solhjoo E**, Mansour-Ghanaei F, Moulaei-Langorudi R, Joukar F. Comparison of portal vein doppler indices and hepatic vein doppler waveform in patients with nonalcoholic fatty liver disease with healthy control. *Hepat Mon* 2011; **11**: 740-744 [PMID: 22235218 DOI: 10.5812/kowsar.1735143X.729]
- 9 **Mohammadinia AR**, Bakhtavar K, Ebrahimi-Daryani N, Habibollahi P, Keramati MR, Fereshtehnejad SM, Abdollahzade S. Correlation of hepatic vein Doppler waveform and hepatic artery resistance index with the severity of nonalcoholic fatty liver disease. *J Clin Ultrasound* 2010; **38**: 346-352 [PMID: 20572063 DOI: 10.1002/jcu.20696]
- 10 **Kang JJ**, Toma I, Sipos A, McCulloch F, Peti-Peterdi J. Quantitative imaging of basic functions in renal (patho)physiology. *Am J Physiol Renal Physiol* 2006; **291**: F495-F502 [PMID: 16609147 DOI: 10.1152/ajprenal.00521.2005]
- 11 **Zipfel WR**, Williams RM, Webb WW. Nonlinear magic: multiphoton microscopy in the biosciences. *Nat Biotechnol* 2003; **21**: 1369-1377 [PMID: 14595365 DOI: 10.1038/nbt899]
- 12 **Etienne-Mesmin L**, Vijay-Kumar M, Gewirtz AT, Chassaing B. Hepatocyte Toll-Like Receptor 5 Promotes Bacterial Clearance and Protects Mice Against High-Fat Diet-Induced Liver Disease. *Cell Mol Gastroenterol Hepatol* 2016; **2**: 584-604 [PMID: 28090564 DOI: 10.1016/j.jcmgh.2016.04.007]
- 13 **Seifert WF**, Bosma A, Brouwer A, Hendriks HF, Roholl PJ, van Leeuwen RE, van Thiel-de Ruiter GC, Seifert-Bock I, Knook DL. Vitamin A deficiency potentiates carbon tetrachloride-induced liver fibrosis in rats. *Hepatology* 1994; **19**: 193-201 [PMID: 8276355 DOI: 10.1002/hep.1840190129]
- 14 **Cunnane SC**. Hepatic triacylglycerol accumulation induced by ethanol and carbon tetrachloride: interactions with essential fatty acids and prostaglandins. *Alcohol Clin Exp Res* 1987; **11**: 25-31 [PMID: 3032013 DOI: 10.1111/j.1530-0277.1987.tb01255.x]
- 15 **Drasdo D**, Hoehme S, Hengstler JG. How predictive quantitative modelling of tissue organisation can inform liver disease pathogenesis. *J Hepatol* 2014; **61**: 951-956 [PMID: 24950483 DOI: 10.1016/j.jhep.2014.06.013]
- 16 **Késmárky G**, Kenyeres P, Rábai M, Tóth K. Plasma viscosity: a forgotten variable. *Clin Hemorheol Microcirc* 2008; **39**: 243-246 [PMID: 18503132 DOI: 10.3233/CH-2008-1088]
- 17 **Yokoyama N**, Sakota D, Nagaoka E, Takatani S. Alterations in red blood cell volume and hemoglobin concentration, viscoelastic properties, and mechanical fragility caused by continuous flow pumping in calves. *Artif Organs* 2011; **35**: 791-799 [PMID: 21843294 DOI: 10.1111/j.1525-1594.2011.01317.x]
- 18 **Weisel JW**, Litvinov RI. Fibrin Formation, Structure and Properties. *Subcell Biochem* 2017; **82**: 405-456 [PMID: 28101869 DOI: 10.1007/978-3-319-49674-0_13]

- 19 **Mohandas N**, Chasis JA. Red blood cell deformability, membrane material properties and shape: regulation by transmembrane, skeletal and cytosolic proteins and lipids. *Semin Hematol* 1993; **30**: 171-192 [PMID: [8211222](#)]
- 20 **Chalasani N**, Wilson L, Kleiner DE, Cummings OW, Brunt EM, Unalp A; NASH Clinical Research Network. Relationship of steatosis grade and zonal location to histological features of steatohepatitis in adult patients with non-alcoholic fatty liver disease. *J Hepatol* 2008; **48**: 829-834 [PMID: [18321606](#) DOI: [10.1016/j.jhep.2008.01.016](#)]
- 21 **Hijmans BS**, Grefhorst A, Oosterveer MH, Groen AK. Zonation of glucose and fatty acid metabolism in the liver: mechanism and metabolic consequences. *Biochimie* 2014; **96**: 121-129 [PMID: [23792151](#) DOI: [10.1016/j.biochi.2013.06.007](#)]
- 22 **Duwaerts CC**, Maher JJ. Mechanisms of Liver Injury in Non-Alcoholic Steatohepatitis. *Curr Hepatol Rep* 2014; **13**: 119-129 [PMID: [25045618](#) DOI: [10.1007/s11901-014-0224-8](#)]
- 23 **Rangwala F**, Guy CD, Lu J, Suzuki A, Burchette JL, Abdelmalek MF, Chen W, Diehl AM. Increased production of sonic hedgehog by ballooned hepatocytes. *J Pathol* 2011; **224**: 401-410 [PMID: [21547909](#) DOI: [10.1002/path.2888](#)]
- 24 **Sarin SK**, Kapoor D. Non-cirrhotic portal fibrosis: current concepts and management. *J Gastroenterol Hepatol* 2002; **17**: 526-534 [PMID: [12084024](#) DOI: [10.1046/j.1440-1746.2002.02764.x](#)]
- 25 **Topal NB**, Orcan S, Sıgırlı D, Orcan G, Eritmen Ü. Effects of fat accumulation in the liver on hemodynamic variables assessed by Doppler ultrasonography. *J Clin Ultrasound* 2015; **43**: 26-33 [PMID: [24867781](#) DOI: [10.1002/jcu.22157](#)]
- 26 **Elias J**, Altun E, Zacks S, Armao DM, Woosley JT, Semelka RC. MRI findings in nonalcoholic steatohepatitis: correlation with histopathology and clinical staging. *Magn Reson Imaging* 2009; **27**: 976-987 [PMID: [19356874](#) DOI: [10.1016/j.mri.2009.02.002](#)]

P- Reviewer: Saner F, Sijens PE

S- Editor: Ma RY **L- Editor:** Wang TQ **E- Editor:** Huang Y





Case Control Study

Diffusion-weighted magnetic resonance imaging and micro-RNA in the diagnosis of hepatic fibrosis in chronic hepatitis C virus

Tarek Besheer, Hatem Elalfy, Mohamed Abd El-Maksoud, Ahmed Abd El-Razek, Saher Taman, Khaled Zalata, Wagdy Elkashef, Hossam Zaghloul, Heba Elshahawy, Doaa Raafat, Wafaa Elemshaty, Eman Elsayed, Abdel-Hady El-Gilany, Mahmoud El-Bendary

ORCID number: Tarek Besheer (0000-0002-0583-8860); Hatem Elalfy (0000-0002-5602-0989); Mohamed Abd El-Maksoud (0000-0002-7766-3684); Ahmed Abd El-Razek (0000-0002-9613-5932); Saher Taman (0002-5721-8508); Khaled Zalata (0000-0002-6678-7438); Wagdy Elkashef (0000-0003-2600-8003); Hossam Zaghloul (0000-0002-7201-1812); Heba Elshahawy (0000-0001-8521-876x); Doaa Raafat (0000-0001-6761-9826); Wafaa Elemshaty (0000-0002-2128-5901); Eman Elsayed (0000-0001-8924-3217); Abdel-Hady El-Gilany (0000-0001-9376-6985); Mahmoud El-Bendary (0000-0002-3751-5927).

Author contributions: Besheer T, Elalfy H, and El-Bendary M were involved in study conception and design; Abd El-Razek A and Taman S performed radiological imaging; Zaghloul H, Elshahawy H, Raafat D, Elemshaty W, and Elsayed E performed laboratory techniques; Zalata K and Elkashef W performed pathological diagnosis of the liver biopsies; El-Gilany AH and Abd El-Maksoud M acquired the data and performed analysis and interpretation of data; all authors were involved in the drafting and critical revision of the manuscript; all authors approved the final version of the manuscript.

Supported by Science and Technology Development

Tarek Besheer, Hatem Elalfy, Mohamed Abd El-Maksoud, Mahmoud El-Bendary, Department of Tropical Medicine and Hepatology, Mansoura Faculty of Medicine - Mansoura University, Mansoura 35111, Egypt

Ahmed Abd El-Razek, Saher Taman, Department of Diagnostic Radiology, Mansoura Faculty of Medicine - Mansoura University, Mansoura 35111, Egypt

Khaled Zalata, Wagdy Elkashef, Department of Pathology, Mansoura Faculty of Medicine - Mansoura University, Mansoura 35111, Egypt

Hossam Zaghloul, Heba Elshahawy, Doaa Raafat, Wafaa Elemshaty, Eman Elsayed, Department of Clinical Pathology, Mansoura Faculty of Medicine - Mansoura University, Mansoura 35111, Egypt

Abdel-Hady El-Gilany, Department of Public Health and Preventive Medicine, Mansoura Faculty of Medicine - Mansoura University, Mansoura 35111, Egypt

Corresponding author: Mahmoud El-Bendary, MD, Professor, Department of Tropical Medicine and Hepatology, Mansoura Faculty of Medicine - Mansoura University, Elgomhoria Street, Mansoura 35111, Dakahlia, Egypt. mm_elbendary@mans.edu.eg

Telephone: +20-1002592205

Fax: +20-502267016

Abstract

BACKGROUND

Diffusion-weighted magnetic resonance imaging has shown promise in the detection and quantification of hepatic fibrosis. In addition, the liver has numerous endogenous micro-RNAs (miRs) that play important roles in the regulation of biological processes such as cell proliferation and hepatic fibrosis.

AIM

To assess diffusion-weighted magnetic resonance imaging and miRs in diagnosing and staging hepatic fibrosis in patients with chronic hepatitis C.

METHODS

This prospective study included 208 patients and 82 age- and sex-matched controls who underwent diffusion-weighted magnetic resonance imaging of the abdomen, miR profiling, and liver biopsy. Pathological scoring was classified according to the METAVIR scoring system. The apparent diffusion coefficient

Foundation (STDF), Project NO. 3457 (TC/4/Health/2010/hep-1.6).

Institutional review board

statement: The study protocol was reviewed and approved by the institutional ethics committee of the Mansoura Faculty of Medicine. (R.18.04.139.R1-2018/04/17).

Informed consent statement:

Written informed consent was obtained from all eligible patients who were included in the study.

Conflict-of-interest statement: No conflict of interest.

Open-Access:

This article is an open-access article that was selected by an in-house editor and fully peer-reviewed by external reviewers. It is distributed in accordance with the Creative Commons Attribution Non Commercial (CC BY-NC 4.0) license, which permits others to distribute, remix, adapt, build upon this work non-commercially, and license their derivative works on different terms, provided the original work is properly cited and the use is non-commercial. See: <http://creativecommons.org/licenses/by-nc/4.0/>

Manuscript source: Invited manuscript

Received: November 12, 2018

Peer-review started: November 12, 2018

First decision: December 28, 2018

Revised: January 30, 2019

Accepted: February 15, 2019

Article in press: February 15, 2019

Published online: March 21, 2019

(ADC) and miR were calculated and correlated with pathological scoring.

RESULTS

The ADC value decreased significantly with the progression of fibrosis, from controls (F0) to patients with early fibrosis (F1 and F2) to those with late fibrosis (F3 and F4) (median 1.92, 1.53, and 1.25×10^{-3} mm²/s, respectively) ($P = 0.001$). The cut-off ADC value used to differentiate patients from controls was 1.83×10^{-3} mm²/s with an area under the curve (AUC) of 0.992. Combining ADC and miR-200b revealed the highest AUC (0.995) for differentiating patients from controls with an accuracy of 96.9%. The cut-off ADC used to differentiate early fibrosis from late fibrosis was 1.54×10^{-3} mm²/s with an AUC of 0.866. The combination of ADC and miR-200b revealed the best AUC (0.925) for differentiating early fibrosis from late fibrosis with an accuracy of 80.2%. The ADC correlated with miR-200b ($r = -0.61$, $P = 0.001$), miR-21 ($r = -0.62$, $P = 0.001$), and miR-29 ($r = 0.52$, $P = 0.001$).

CONCLUSION

Combining ADC and miRs offers an alternative surrogate non-invasive diagnostic tool for diagnosing and staging hepatic fibrosis in patients with chronic hepatitis C.

Key words: Diffusion; Magnetic resonance imaging; Fibrosis; Liver; Hepatitis C virus; Micro-RNA

©The Author(s) 2019. Published by Baishideng Publishing Group Inc. All rights reserved.

Core tip: We aimed to assess diffusion-weighted magnetic resonance imaging and micro-RNAs in diagnosis and staging of hepatic fibrosis. Patients underwent DWI of the abdomen, micro-RNA profiling, and liver biopsy. The apparent diffusion coefficient (ADC) and miR were calculated and correlated with METAVIR score. We found that ADC value was decreased from controls (F0) to patients with early fibrosis and those with late fibrosis. Combined ADC and miR-200b revealed the best result for differentiating early from late fibrosis and offer an alternative surrogate non-invasive diagnostic tool for diagnosis and staging of hepatic fibrosis in patients with chronic hepatitis C.

Citation: Besheer T, Elalfy H, Abd El-Maksoud M, Abd El-Razek A, Taman S, Zalata K, Elkashef W, Zaghloul H, Elshahawy H, Raafat D, Elemshaty W, Elsayed E, El-Gilany AH, El-Bendary M. Diffusion-weighted magnetic resonance imaging and micro-RNA in the diagnosis of hepatic fibrosis in chronic hepatitis C virus. *World J Gastroenterol* 2019; 25(11): 1366-1377

URL: <https://www.wjgnet.com/1007-9327/full/v25/i11/1366.htm>

DOI: <https://dx.doi.org/10.3748/wjg.v25.i11.1366>

INTRODUCTION

Hepatitis C virus (HCV) is responsible for chronic hepatic infection in 150-200 million people. Chronic liver disease results in the formation of fibrous tissue that impairs normal liver function, resulting in hepatic fibrosis, cirrhosis, portal hypertension, and hepatocellular carcinoma. Early detection of hepatic fibrosis has important therapeutic and prognostic implications for HCV-infected patients, since antiviral treatment can reduce hepatic decompensation and increase patient survival^[1-5]. Liver biopsy is currently the gold standard for pathological assessment of hepatic fibrosis. However, it is an invasive maneuver with risks of complications such as hemorrhage, penetration to abdominal viscera, and pneumothorax and may result in death in 0.018% of patients; furthermore, the procedure is also prone to sampling error and observer variability^[4-6]. Non-invasive diagnosis and staging of hepatic fibrosis is important for evaluating disease progression in patients with chronic liver diseases. Serum markers of liver fibrosis are widely available, but their results are variable^[7-10]. Ultrasound elastography is used for grading hepatic fibrosis, but it is operator dependent^[11-13]. Several magnetic resonance (MR) imaging sequences, such as

perfusion-weighted MR imaging, MR spectroscopy, MR elastography, and dynamic contrast-enhanced MR have the potential to provide quantitative information with variable diagnostic accuracy in the staging of liver fibrosis^[13-15].

Micro-RNAs (miRs) are small noncoding RNA molecules that regulate gene expression at post-translational steps. The liver has numerous endogenous miRs that play important roles in the regulation of biological processes, such as cell proliferation and liver fibrosis. MiRs circulate in a cell-free form in body fluids including serum and are found mostly in exosomes and protein-RNA complexes. Several miRs were identified to be upregulated in serum in patients with chronic liver disease and liver fibrosis compared to those in healthy controls, and many of these were also correlated with the degree of liver fibrosis^[16-19]. MiRNA-21 is upregulated at the onset of fibrosis in the human liver and may promote fibrogenic activation of fibroblasts. A considerable amount of evidence has shown that the miR-200 family participates in fibrosis. Moreover, a downregulation of circulating miR-29 is seen in patients with chronic liver injury and liver fibrosis. The level of miR-29 is correlated with the stage of liver fibrosis^[18-21].

Diffusion represents the random Brownian motion of molecules, and MR imaging can detect signal changes caused by positional changes in molecules at this microscopic scale. The apparent diffusion coefficient (ADC) of the molecules measures the freedom of water proton diffusion in tissues and change according to the degree of cellularity of the lesion^[22-26]. Diffusion-weighted MR imaging (DWI) is used for the assessment of liver fibrosis in adults and children^[27-31]. The aim of the current study was to assess DWI and miRs in the diagnosis and staging of hepatic fibrosis in patients with chronic hepatitis virus C (CHC).

MATERIALS AND METHODS

Patients

The institutional review board approved this interventional study, and patients and controls provided written informed consent. The study assessed 215 consecutive patients with biopsy-proven CHC; patients were included if they had a histological diagnosis of CHC on a liver biopsy. HCV was defined by the presence of serum anti-HCV and HCV-RNA. Seven patients were excluded from our study due to the presence of hepatocellular carcinoma ($n = 3$), cardiac cirrhosis ($n = 2$), and hepatic metastasis ($n = 2$). The final number of patients was 208 (129 male and 79 female), and the median age was 36.3 ± 9.3 years. Eighty-two age- and sex-matched volunteers (47 male and 35 female) underwent MR imaging for reasons other than abdominal abnormalities; the median age was 38.3 ± 10.2 years. The patients and controls included in the study underwent DWI of the abdomen, miR tests, and liver biopsy from October 2012 to December 2015.

Routine magnetic resonance imaging

MR examinations were performed for all patients and controls using a T1.5 Tesla MR unit (Ingenia, Philips Best, Netherlands) using a bipolar diffusion encoding gradient. A 16-channel anterior phased array torso surface coil (dStream Torso coil) with a posterior body coil embedded in the table (dStream Total Spine coil) was applied. Routine axial T1-weighted images (TR/TE = 500/20 ms) and T2-weighted images (TR/TE = 6000/80 ms) were obtained.

Diffusion-weighted magnetic resonance imaging

Axial diffusion-weighted MR imaging of the liver was performed using free breathing spin echo planar sequence of echo planar imaging (EPI) readout. Automatic multi-angle projection shim and the chemical shift selective fat-suppression technique were applied. The motion probing gradient was applied before and after the 180 pulse with EPI readout. The b values applied were 0, 400, and 800 s/mm². The applied parameters were TR of 2800 ms, TE of 74 ms, EPI factor of 102, FOV of 25 cm × 25 cm, section thickness of 7 mm, interslice gap of 20%, acquisition matrix of 192 × 154, and number of excitations of six. After acquisition of the diffusion-weighted sequence, we obtained a set of images corresponding to each b -value applied. The ADC map was automatically calculated from the data set obtained at three b -values by commercially available software. The data acquisition time for the diffusion-weighted MR images was 1 min.

Image analysis

Image analysis was performed by a radiology expert in MR imaging with 25 years of experience (AA). Quantitative analysis of the ADCs of hepatic parenchyma was performed. A circular region of interest measuring 3-4 cm² was placed on the ADC

map at three different regions of hepatic parenchyma, on three consecutive slices away from the biliary and vascular structures, and more than 2 cm from the surface of the liver (Figure 1). The ADC value was calculated according to the following formula: $ADC = -(\ln Sb2 - \ln Sb1) / (b2 - b1)$, where \ln is the natural log, and $Sb1$ and $Sb2$ are the signal intensities in the region of interest placed on sections corresponding to the two different b -values ($b1$ and $b2$)^[26]. The ADC value was automatically calculated in $\times 10^{-3} \text{ mm}^2/\text{s}$. The mean of these nine values was calculated and represents the final ADC value per subject used for statistical analysis.

Serum micro-RNAs assay

Blood samples were collected for the serum miRs assay just prior biopsy, and miR-200b, miR-21, and miR-29b were measured for all patients and control groups. Total RNA was extracted using a miRNeasy serum/plasma extraction kit (Qiagen, Valencia, CA, United States) using QIAzol lysis reagent according to the manufacturer's instructions. RNA quality was determined using a NanoDrop 2000 (Thermo Scientific, Waltham, MA, United States). Reverse transcription (RT) was carried out on 100 ng of total RNA in RT reactions in a final volume of 20 μL (incubated for 60 min at 37 °C and 5 min at 95 °C) using a miScript II RT Kit (Qiagen) according to the manufacturer's instructions. Serum expression levels of mature miRNAs, miR-200b, miR-29b, and miR-21, were evaluated using miScript miRNA PCR primer assays and a miScript SYBER green PCR kit (Qiagen) according to the manufacturer's protocol. The housekeeping miRNA SNORD68 was used as the internal control.

Liver biopsy

Percutaneous liver biopsy was performed by a hepatology expert in liver biopsy with 20 years of experience (BT). The biopsy was conducted at least 60 d before imaging to avoid misinterpretation attributed to early post-biopsy changes. The length of the specimen was not less than 1.2 cm (contained at least 10 portal tracts) that was fixed in formalin, put in paraffin, and stained with special stain according to the international criteria for pathological analysis. According to METAVIR score, hepatic fibrosis staging were classified as F0, no fibrosis; F1, portal fibrosis without septa; F2, portal fibrosis with few septa; F3, numerous septa without cirrhosis; and F4, cirrhosis^[32].

Statistical analysis

Statistical analysis of the data was performed by Statistical Package for Social Science version 20 (SPSS Inc., Armonk, NY, United States). The data were presented as the mean and standard deviation (SD). The Kolmogorov-Smirnov test was performed to assess the normality of the data distribution. All data were revealed to be non-parametric. To compare two groups, Student's t -test was used. To compare more than two groups, one-way analysis of variance was used. Receiver operating characteristic (ROC) curves were used to determine the cut-off points of ADC, miR that were used to differentiate patients from controls, and early from late fibrosis with calculation of the area under the curve (AUC), accuracy, sensitivity, and specificity. The P value was considered significant if ≤ 0.05 at the 95% confidence interval. A multivariate logistic regression model was performed to determine the combination of parameters with the highest accuracy for differentiating controls from patients and early from late fibrosis. The Spearman correlation test was used to correlate the ADC with miRs.

RESULTS

Table 1 reveals the characteristics of patients and controls. The patients were divided into an early fibrosis group (F1 and F2) ($n = 112$, 38.6%) and a late fibrosis group (F3 and F4) ($n = 96$, 33.1%) along with a control group (F0) ($n = 82$, 28.3%). No significant differences in age and sex were found between patients and controls or between patients with early versus late fibrosis.

Table 2 shows the median ADC and miR values of patients versus controls. The median ADC values of patients ($1.43 \pm 0.22 \times 10^{-3} \text{ mm}^2/\text{s}$) were significantly different ($P = 0.001$) compared with those of controls ($1.92 \pm 0.08 \times 10^{-3} \text{ mm}^2/\text{s}$). The median miRNA values of patients were significantly different ($P = 0.001$) compared with those of controls.

Table 3 shows the ROC curve results with cut-off values of ADC and serum markers of patients and controls. The cut-off point of ADC values for differentiating patients from controls (Figure 2A) was $1.83 \times 10^{-3} \text{ mm}^2/\text{s}$ with an AUC of 0.992, accuracy of 97.1%, sensitivity of 98.6%, and specificity of 97%. The cut-off points of miR-200b, miR-21, and miR-29b used to differentiate patients from controls were 1.65, 1.35, and 0.91 with AUCs of 0.925, 0.865, and 0.937, respectively. The combination of

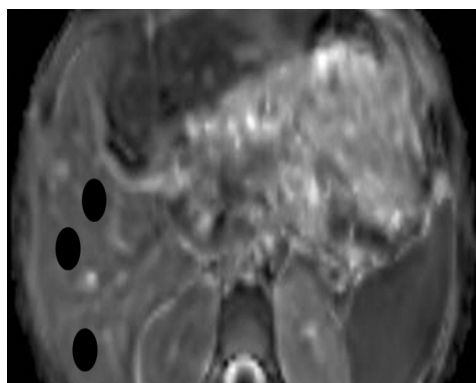


Figure 1 Regions of interest. Apparent diffusion coefficient map of the liver with locations of the regions of interest within the liver parenchyma.

ADC and miR-200 (Figure 2B) revealed an AUC of 0.995, accuracy of 96.9%, sensitivity of 100%, and specificity of 96%. ADC and miR-21 combined revealed an AUC of 0.992, accuracy of 96.2%, sensitivity of 100%, and specificity of 95%. The combination of ADC and miR-29b revealed an AUC of 0.992, accuracy of 95.9%, sensitivity of 100%, and specificity of 96%.

Table 4 shows the median, minimum, and maximum of ADC and serum markers of patients with early and late fibrosis. In differentiating the early fibrosis group from the late fibrosis, the median ADC value of early fibrosis ($1.5 \pm 0.2 \times 10^{-3} \text{ mm}^2/\text{s}$) was significantly ($P = 0.001$) different than that of late fibrosis ($1.25 \pm 0.17 \times 10^{-3} \text{ mm}^2/\text{s}$). The median values of miRNA-200b, miRNA-21, and miRNA-29b of early fibrosis were 3.4 ± 1.7 , 1.9 ± 0.7 , and 0.7 ± 0.2 , respectively, and those of late fibrosis were 10.2 ± 4.8 , 3.6 ± 1.2 , and 0.4 ± 0.2 , respectively; these values were significantly different ($P = 0.001$) between the groups.

Table 5 shows the cut-off values of ADC and miRs used to differentiate early from late fibrosis with the areas under the ROC curves, specificity, sensitivity, and accuracy. The ADC cut-off point used to differentiate early from late fibrosis was $1.54 \times 10^{-3} \text{ mm}^2/\text{sec}$ (Figure 3A) with an AUC of 0.866, accuracy of 81.7%, sensitivity of 99%, and specificity of 67%. The cut-off points of miRNA-200b, miRNA-21, and miRNA-29b used to differentiate early from late fibrosis were 3.55, 2.39, and 0.71 with AUCs of 0.888, 0.877, and 0.832 and accuracy of 73.5%, 80.2%, and 73.0%, respectively. The combined ADC and miR values used for differentiating early from late fibrosis were as follows: First, ADC and miR-200b (Figure 3B) showed an AUC of 0.925, accuracy of 80.2%, sensitivity of 71.7%, and specificity of 97.2%. Combining ADC and miR-21 revealed an AUC of 0.88, accuracy of 83.2%, sensitivity of 72.3%, and specificity of 97.5%. The combination of ADC and miRNA-29b revealed an AUC of 0.879, accuracy of 85.1%, sensitivity of 74.0%, and specificity of 96.5% (Table 5).

The values for miR-200b and miR-21 in controls were significantly increased ($P = 0.001$) compared with those in patients with early fibrosis and patients with late fibrosis. The median values of miR-200b and miR-21 increased as fibrosis decreased, and the median values of miRNA-29b decreased significantly with increased fibrosis. The ADC values were highly correlated with serum expression of miR-200b ($r = -0.61$, $P = 0.001$), miR-21 ($r = -0.62$, $P = 0.001$), and miR-29b ($r = 0.52$, $P = 0.001$).

DISCUSSION

In this study, the ADC values of patients were significantly lower than those of controls. This observation may be attributed to fibrogenesis engaging a range of cell types and mediators with progressive deposition of extracellular matrix proteins, reducing the interstitial spaces and distorting normal hepatic architecture^[2,3,5]. These changes are responsible for restricted diffusion with reduction in the ADC values in patients with hepatic fibrosis. However, the staging of liver fibrosis with diffusion-weighted MR imaging is still controversial^[33-35].

In this work, the ADC values of patients with late fibrosis are lower than those with early fibrosis. Previous studies reported that the values of the ADC are significantly different at the different stages of liver fibrosis/cirrhosis^[33,34]. On the other hand, other studies did not find an association between grading of fibrosis and the ADC values^[35,36]. The results in our study may be explained by the increase of hepatic connective tissue with accumulation of collagen, fatty tissue, and inflammatory cells,

Table 1 Comparison of demographic and laboratory data in F0, early fibrosis, and late fibrosis groups

Parameter	Control, n = 82	Early fibrosis, n = 112	Late fibrosis, n = 96	P value
Age	38.3 ± 10.2	34.1 ± 8.9	41.4 ± 7.8 ²³	0.001
Gender (M:F)	47:35	69:43	60:36	0.8
ALT	36.29 ± 17.24	52.00 ± 36.07 ¹	57.17 ± 36.88 ²³	0.001
AST	35.00 ± 15.71	49.00 ± 25.12 ¹	58.00 ± 35.12 ²³	0.001
Albumin	4.10 ± 0.45	4.20 ± 0.44	3.80 ± 0.69 ²³	0.001
Bilirubin	0.88 ± 0.48	0.81 ± 0.26	1.02 ± 0.46 ²	0.001
PCR	95746 ± 10111	391000 ± 213876 ¹	254500 ± 129314 ²³	0.001
AFP	7.50 ± 1.57	5.01 ± 2.95 ¹	10.47 ± 6.78 ²³	0.001

¹Significance between control and early;²Significance between control and late;³Significance between late and early. Data expressed as mean and standard deviation, F one way analysis of variance test was used for comparison between the three groups. Student's *t*-test was used to compare between each two groups. ALT: Alanine transaminase; AST: Aspartate transaminase; PCR: Polymerase chain reaction; AFP: Alpha-fetoprotein.

which may lead to restricted diffusion with low ADC values in patients with late fibrosis^[4,5,37].

In recent decades, miRs have emerged as key regulators of gene expression^[38]. Evidence is accumulating that miRs participate in the progression of liver fibrosis and regulation of hepatic stellate cell (HSC) proliferation/apoptosis^[39]; in addition, they have been reported as biomarkers of liver cirrhosis by some previous studies^[40]. In this study, the levels of the miRs (miR-200b, miR-21, miR-29b) used to differentiate between controls and patients and between patients with early fibrosis and those with late fibrosis (Tables 2 and 4) were significantly different, and strong positive correlations were found between ADC and levels of miR-200b and miR-21. In patients with hepatic fibrosis, several miRs were identified to be upregulated in serum when compared to those in controls, and many of these miRs were also correlated with the degree of liver fibrosis. Several studies have discussed the role of miRs in fibrogenesis, but its value is still controversial^[41,42]. Previously, miR-21 has been suggested to be upregulated at the onset of fibrosis in the human liver, and it may promote fibrogenic activation of fibroblasts.

A possible explanation for elevated miR-21 levels in advanced fibrosis is that miR-21 may regulate transforming growth factor (TGF) β 2^[41] and has been shown to activate HSCs through PTEN/AKT or ERK1 signaling pathways^[41,42]. Moreover, induction of maturation of primary miR-21 precursor into mature miR-21 occurs *via* TGF- β . Another study added that a significant increase in hepatic miR-21 expression is associated with mitogen-activated protein kinase 3 signaling and epithelial-mesenchymal transition in liver fibrosis^[42,43].

A considerable amount of evidence has demonstrated that the miR-200 family participates in fibrosis^[16-20]. Previous studies reported that these miRs were upregulated and that circulating miR-29 was downregulated in patients with chronic liver injury and liver fibrosis. Levels of miR-29 correlated with the stage of liver fibrosis^[17-21]. In the current study, the levels of miR-29 used to differentiate between controls and patients with fibrosis and between patients with early and those with late fibrosis were significantly different, and the level of miR-29 was negatively correlated with the fibrosis score. MiR-29b interferes with the process of fibrogenesis *via* inhibition of HSC activation, production of type I collagen^[44], and expression of extracellular matrix genes in HSCs through the TGF- β /SMAD-CTGF signaling network^[19,45,46]. Overexpression of miR-29 weakens collagen and matrix deposition in HSCs through interfering with genes of fibrogenesis^[46].

Few studies discuss the role of combining imaging parameters, such as ultrasound elastography, with laboratory biomarkers in the detection and staging of hepatic fibrosis, but the results of such assessments overlap^[12,13]. In the current study, combining ADC and miRs (200b, 21 and 29b) increased the sensitivity, specificity, and accuracy for differentiating controls from patients with fibrosis. The combination of ADC with miR-200 increased the AUC for detection of hepatic fibrosis and differentiation of patients with early fibrosis from those with late fibrosis.

Regarding limitations of the current work: First, the small sample size limited the statistical power. Therefore, further studies are needed at a larger scale to confirm the results of this work. Second, the use of diffusion-weighted MR imaging may have

Table 2 The median apparent diffusion coefficient and micro-RNAs values of patients versus controls

Parameter	Fibrosis, <i>n</i> = 208	Control, <i>n</i> = 82	<i>P</i> value
ADC	1.43 ± 0.22	1.92 ± 0.08	0.001
miR-200b	4.61 ± 1.21	1.20 ± 0.81	0.001
miR-21	2.70 ± 1.30	1.29 ± 0.40	0.001
miR-29b	0.58 ± 0.26	0.98 ± 0.16	0.001

Data expressed as mean and standard deviation. Student's *t*-test was used. miR: Micro-RNAs; ADC: Apparent diffusion coefficient.

limited the conclusions of our findings. Further studies using recent diffusion modules such as diffusion kurtosis imaging and diffusion tensor imaging at 3-tesla will improve the quality of the results. Third, this study used regions of interest for localization, and further studies should be performed using advanced post-processing methods, such as machine learning and histogram analysis^[47-50].

In conclusion, we demonstrated that combining ADC and miRs offers a new non-invasive method for diagnosis and staging of hepatic fibrosis in patients with chronic hepatitis C.

Table 3 The receiver operating characteristic curve results with cut-off values of apparent diffusion coefficient and serum markers for patients and controls

Parameter	AUC	Cut-off point	Sensitivity	Specificity	Accuracy
ADC	0.992	1.825	98.6%	97.0%	97.1%
miR-200b	0.925	1.65	92.3%	82.2%	91.2%
miR-21	0.865	1.35	82.2%	76.0%	84.2%
miR-29b	0.937	0.91	92.3%	81.7%	91.0%
ADC and miR-200b	0.995	-	100%	96.0%	96.9%
ADC and miR-21	0.992	-	100%	95.0%	96.2%
ADC and miR-29b	0.992	-	100%	95.9%	95.9%

ROC: Receiver operating characteristic curve; AUC: Area under the curve; miR: Micro-RNAs; ADC: Apparent diffusion coefficient.

Table 4 The median, minimum, and maximum values of apparent diffusion coefficient and serum markers of patients with early and late fibrosis

Variables	Early fibrosis, <i>n</i> = 112	Late fibrosis, <i>n</i> = 96	<i>P</i> value
ADC	1.5 ± 0.2 (1-1.9)	1.25 ± 0.17 (0.9-1.5)	0.001
miR-200b	3.43 ± 1.71 (1.0-1.4)	10.17 ± 4.81 (1-28.4)	0.001
miR-21	1.9 ± 0.7 (1.0-4.2)	3.6 ± 1.17 (1.0-6.34)	0.001
miR-29b	0.7 ± 0.12 (0.12-1.00)	0.4 ± 0.2 (0.07-1.00)	0.001

The data expressed as median and range. Mann-Whitney *u* test was used. ADC: Apparent diffusion coefficient; miR: Micro-RNAs.

Table 5 The cut-off values of apparent diffusion coefficient and micro-RNAs used to differentiate early from late fibrosis with areas under the receiver operating characteristic curves, sensitivity, specificity and accuracy

Parameter	AUC	Cut-off point	Sensitivity	Specificity	Accuracy
ADC	0.866	1.53	99.0%	67.0%	81.7%
miR-200b	0.888	3.55	90.6%	59.5%	73.5%
miR-21	0.877	2.38	91.7%	70.3%	80.2%
miR-29b	0.832	0.70	87.5%	60.7%	73%
ADC and miR-200b	0.925	-	71.7%	97.2%	80.2%
ADC and miR-21	0.88	-	72.3%	97.5%	83.2%
ADC and miR-29b	0.879	-	74%	96.5%	85.1%

AUC: Area under the curve; miR: Micro-RNAs; ADC: Apparent diffusion coefficient.

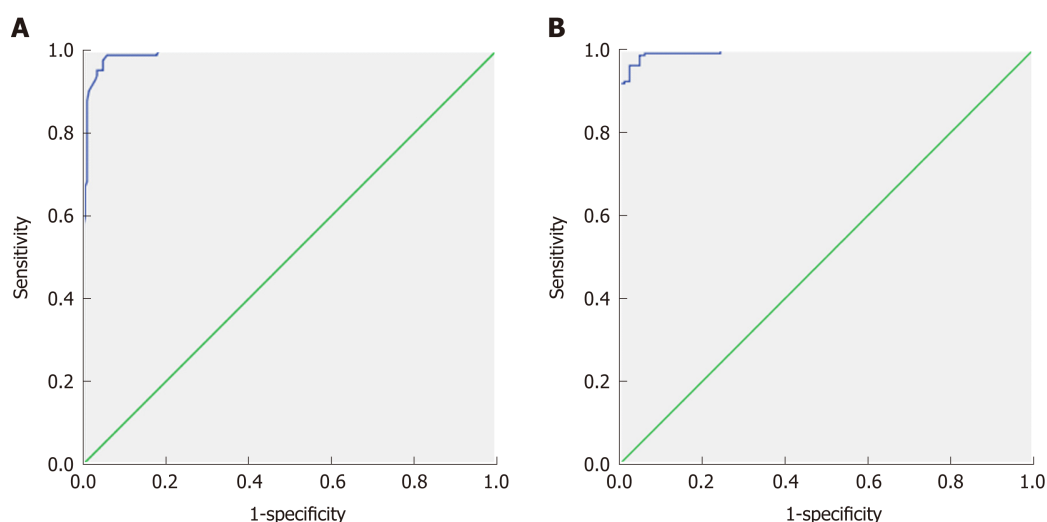


Figure 2 Receiver operating characteristic curve of patients vs controls. A: The cut-off apparent diffusion coefficient value used for differentiating patients from controls is $1.83 \times 10^{-3} \text{ mm}^2/\text{s}$ with an area under the curve of 0.992, sensitivity of 98.6%, and accuracy of 97.1%; B: The combination of apparent diffusion coefficient and miR-200b used for differentiating patients from controls shows an area under the curve of 0.995, sensitivity of 100%, and specificity of 96.9%.

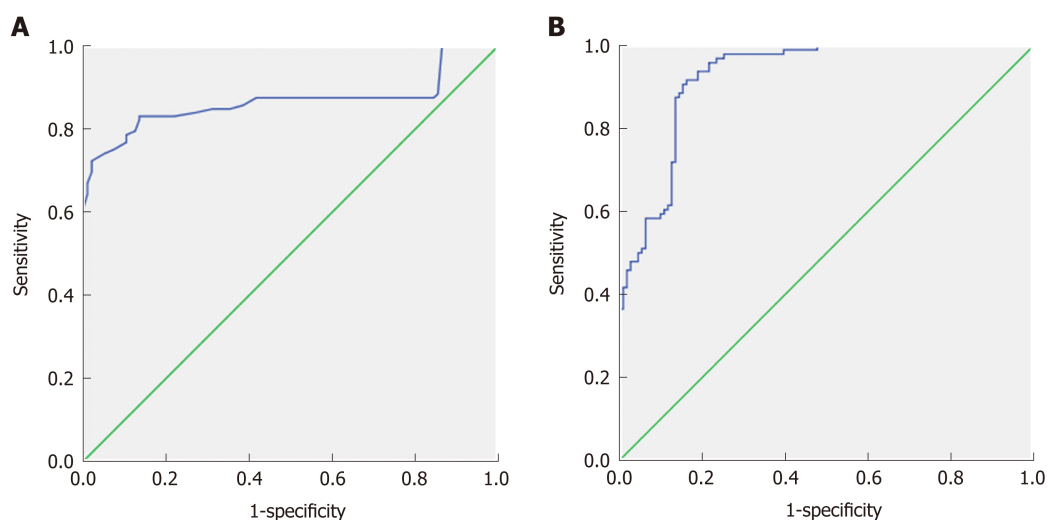


Figure 3 Receiver operating characteristic curve of early and late fibrosis. A: The cut-off apparent diffusion coefficient value for differentiating early from late fibrosis is $1.54 \times 10^{-3} \text{ mm}^2/\text{s}$ with an area under the curve of 0.866, sensitivity of 99.0% and accuracy of 81.7%; B: Combining apparent diffusion coefficient and miR-200b to differentiate early and late fibrosis patients shows an area under the curve of 0.925, sensitivity of 71.7% and accuracy of 80.2%.

ARTICLE HIGHLIGHTS

Research background

Hepatitis C virus infection is considered one of the most widespread causes of chronic liver disease that results in cirrhosis, fibrosis together with portal hypertension, and hepatocellular carcinoma. When it is possible to diagnose early hepatic fibrosis, the therapy will be more effective in the reduction of hepatic decompensation and improvement of patient survival. Liver biopsy is considered the gold standard for early detection of hepatic fibrosis, but it is invasive and has many side effects. Multiple non-invasive laboratory and imaging modalities could be used in detection and quantification of hepatic fibrosis but have variable accuracy. The liver contains multiple micro-RNAs (miR) (21, 200b and 29b) that have been correlated to the presence and degree of hepatic fibrosis. Magnetic resonance imaging (MRI) with diffusion-weighted imaging and apparent diffusion coefficient (ADC) can also detect and are correlated with hepatic fibrosis.

Research motivation

Early detection and staging of hepatic fibrosis are of great value in treatment of chronic liver disease caused by hepatitis C virus. The available methods to detect and stage fibrosis are either invasive (like biopsy) or non-invasive (like laboratory and imaging), which is not accurate. The combination of serum markers of hepatic fibrosis (miR 21, 200b and 29b) together with MRI with

diffusion-weighted imaging is a potential new dependable and non-invasive method to help in early detection and staging of hepatic fibrosis and cirrhosis.

Research objectives

In this prospective study, we evaluated the role of combining ADC and miR (21, 200b and 29b) as an alternative non-invasive tool for detection and staging of hepatic fibrosis in patients with chronic hepatitis C viral infection.

Research methods

From October 2012 to December 2015, 215 consecutive patients with histopathological evidence of chronic hepatitis C virus cirrhosis were included in our study. Seven cases were excluded, so the final number of the study patients was 208. Diffusion-weighted MRI (DWI) together with hepatitis C serum markers and serum miR (21, 200b and 29b) were performed for all patients. The MRI and laboratory results were compared with that of the control group containing 82 normal volunteers and with the results of liver biopsy histopathological examination.

Research results

In the current study, it was found that there was a significant decrease in ADC values in patients with early hepatic fibrosis and late fibrosis when compared to controls. Combining ADC results and miR data (200b, 21 and 29b) provided a highly sensitive, specific, and accurate tool to differentiate patients with hepatic fibrosis from normal control patients. This tool was best at differentiating patients from controls, with an accuracy of 96.9% and had an accuracy of 80.2% for differentiating early from late fibrosis.

Research conclusions

Combination of ADC and miR (21, 200b and 29b) is considered a safe, easy, and non-invasive tool in the detection and staging of hepatic fibrosis resulting from chronic hepatitis C viral infection.

Research perspectives

Combining imaging and laboratory results in detection and staging of hepatic fibrosis resulting from chronic hepatitis C virus infection is a valuable method because it is easy and non-invasive. However, a study with more patients will generate more accurate results. Also, use of advanced MRI machines with advanced post processing technology like diffusion tensor and diffusion kurtosis will improve the effectiveness and power of our findings.

REFERENCES

1. Aydın MM, Akçalı KC. Liver fibrosis. *Turk J Gastroenterol* 2018; **29**: 14-21 [PMID: 29391303 DOI: 10.5152/tjg.2018.17330]
2. Hézode C. Treatment of hepatitis C: Results in real life. *Liver Int* 2018; **38** Suppl 1: 21-27 [PMID: 29427481 DOI: 10.1111/liv.13638]
3. Dolman GE, Koffas A, Mason WS, Kennedy PT. Why, who and when to start treatment for chronic hepatitis B infection. *Curr Opin Virol* 2018; **30**: 39-47 [PMID: 29655092 DOI: 10.1016/j.coviro.2018.03.006]
4. Besheer T, El-Bendary M, Elalfy H, Abd El-Maksoud M, Salah M, Zalata K, Elkashef W, Elshahawy H, Raafat D, Elemshaty W, Almashad N, Zaghloul H, El-Gilany AH, Abdel Razek AA, Abd Elwahab M. Prediction of Fibrosis Progression Rate in Patients with Chronic Hepatitis C Genotype 4: Role of Cirrhosis Risk Score and Host Factors. *J Interferon Cytokine Res* 2017; **37**: 97-102 [PMID: 28068153 DOI: 10.1089/jir.2016.0111]
5. Tapper EB, Lok ASF. Use of Liver Imaging and Biopsy in Clinical Practice. *N Engl J Med* 2017; **377**: 2296-2297 [PMID: 29211669 DOI: 10.1056/NEJMc1712445]
6. Gill US, Pallett LJ, Kennedy PTF, Maini MK. Liver sampling: A vital window into HBV pathogenesis on the path to functional cure. *Gut* 2018; **67**: 767-775 [PMID: 29331944 DOI: 10.1136/gutjnl-2017-314873]
7. Yang XZ, Gen AW, Xian JC, Xiao L. Diagnostic value of various noninvasive indexes in the diagnosis of chronic hepatic fibrosis. *Eur Rev Med Pharmacol Sci* 2018; **22**: 479-485 [PMID: 29424906 DOI: 10.26355/eurrev_201801_14198]
8. Trivedi HD, Lin SC, T Y Lau D. Noninvasive Assessment of Fibrosis Regression in Hepatitis C Virus Sustained Virologic Responders. *Gastroenterol Hepatol (N Y)* 2017; **13**: 587-595 [PMID: 29391861]
9. Attallah AM, Abdallah SO, El Sayed AS, Omran MM, El-Bendary M, Farid K, Kadry M. Non-invasive predictive score of fibrosis stages in chronic hepatitis C patients based on epithelial membrane antigen in the blood in combination with routine laboratory markers. *Hepatol Res* 2011; **41**: 1075-1084 [PMID: 22035384 DOI: 10.1111/j.1872-034X.2011.00862.x]
10. Attallah AM, Omran MM, Farid K, El-Bendary M, Emran TM, Albannan MS, El-Dosoky I. Development of a novel score for liver fibrosis staging and comparison with eight simple laboratory scores in large numbers of HCV-monoinfected patients. *Clin Chim Acta* 2012; **413**: 1725-1730 [PMID: 22759976 DOI: 10.1016/j.cca.2012.06.031]
11. Horowitz JM, Venkatesh SK, Ehman RL, Jhaveri K, Kamath P, Ohliger MA, Samir AE, Silva AC, Taouli B, Torbenson MS, Wells ML, Yeh B, Miller FH. Evaluation of hepatic fibrosis: A review from the society of abdominal radiology disease focus panel. *Abdom Radiol (NY)* 2017; **42**: 2037-2053 [PMID: 28624924 DOI: 10.1007/s00261-017-1211-7]
12. Barr RG. Shear wave liver elastography. *Abdom Radiol (NY)* 2018; **43**: 800-807 [PMID: 29116341 DOI: 10.1007/s00261-017-1375-1]
13. Kennedy P, Wagner M, Castéra L, Hong CW, Johnson CL, Sirlin CB, Taouli B. Quantitative Elastography Methods in Liver Disease: Current Evidence and Future Directions. *Radiology* 2018; **286**: 738-763 [PMID: 29461949 DOI: 10.1148/radiol.2018170601]

- 14 **Petitclerc L**, Sebastiani G, Gilbert G, Cloutier G, Tang A. Liver fibrosis: Review of current imaging and MRI quantification techniques. *J Magn Reson Imaging* 2017; **45**: 1276-1295 [PMID: [27981751](#) DOI: [10.1002/jmri.25550](#)]
- 15 **Berzigotti A**, França M, Martí-Aguado D, Martí-Bonmati L. Imaging biomarkers in liver fibrosis. *Radiologia* 2018; **60**: 74-84 [PMID: [29108657](#) DOI: [10.1016/j.rx.2017.09.003](#)]
- 16 **Almas I**, Afzal S, Idrees M, Ashraf MU, Amin I, Shahid M, Zahid K, Zahid S. Role of circulatory microRNAs in the pathogenesis of hepatitis C virus. *Virusdisease* 2017; **28**: 360-367 [PMID: [29291226](#) DOI: [10.1007/s13337-017-0407-3](#)]
- 17 **Schueller F**, Roy S, Vucur M, Trautwein C, Luedde T, Roderburg C. The Role of miRNAs in the Pathophysiology of Liver Diseases and Toxicity. *Int J Mol Sci* 2018; **19**: pii: E261 [PMID: [29337905](#) DOI: [10.3390/ijms19010261](#)]
- 18 **Piedade D**, Azevedo-Pereira JM. MicroRNAs, HIV and HCV: a complex relation towards pathology. *Rev Med Virol* 2016; **26**: 197-215 [PMID: [27059433](#) DOI: [10.1002/rmv.1881](#)]
- 19 **Li Q**, Lowey B, Sodroski C, Krishnamurthy S, Alao H, Cha H, Chiu S, El-Diwany R, Ghany MG, Liang TJ. Cellular microRNA networks regulate host dependency of hepatitis C virus infection. *Nat Commun* 2017; **8**: 1789 [PMID: [29176620](#) DOI: [10.1038/s41467-017-01954-x](#)]
- 20 **Shaker OG**, Senousy MA. Serum microRNAs as predictors for liver fibrosis staging in hepatitis C virus-associated chronic liver disease patients. *J Viral Hepat* 2017; **24**: 636-644 [PMID: [28211229](#) DOI: [10.1111/jvh.12696](#)]
- 21 **Nakamura M**, Kanda T, Sasaki R, Haga Y, Jiang X, Wu S, Nakamoto S, Yokosuka O. MicroRNA-122 Inhibits the Production of Inflammatory Cytokines by Targeting the PKR Activator PACT in Human Hepatic Stellate Cells. *PLoS One* 2015; **10**: e0144295 [PMID: [26636761](#) DOI: [10.1371/journal.pone.0144295](#)]
- 22 **Shenoy-Bhangle A**, Baliyan V, Kordbacheh H, Guimaraes AR, Kambadakone A. Diffusion weighted magnetic resonance imaging of liver: Principles, clinical applications and recent updates. *World J Hepatol* 2017; **9**: 1081-1091 [PMID: [28989564](#) DOI: [10.4254/wjh.v9.i26.1081](#)]
- 23 **Culverwell AD**, Sheridan MB, Guthrie JA, Scarsbrook AF. Diffusion-weighted MRI of the liver- Interpretative pearls and pitfalls. *Clin Radiol* 2013; **68**: 406-414 [PMID: [22981728](#) DOI: [10.1016/j.crad.2012.08.008](#)]
- 24 **Kanematsu M**, Goshima S, Watanabe H, Kondo H, Kawada H, Noda Y, Moriyama N. Diffusion/perfusion MR imaging of the liver: Practice, challenges, and future. *Magn Reson Med Sci* 2012; **11**: 151-161 [PMID: [23037559](#) DOI: [10.2463/mrms.11.151](#)]
- 25 **Razek AA**. Diffusion magnetic resonance imaging of chest tumors. *Cancer Imaging* 2012; **12**: 452-463 [PMID: [23108223](#) DOI: [10.1102/1470-7330.2012.0041](#)]
- 26 **Chandarana H**, Taouli B. Diffusion-weighted MRI and liver metastases. *Magn Reson Imaging Clin N Am* 2010; **18**: 451-464, x [PMID: [21094449](#) DOI: [10.1016/j.mric.2010.07.001](#)]
- 27 **Razek AA**, Abdalla A, Omran E, Fathy A, Zalata K. Diagnosis and quantification of hepatic fibrosis in children with diffusion weighted MR imaging. *Eur J Radiol* 2011; **78**: 129-134 [PMID: [19926420](#) DOI: [10.1016/j.ejrad.2009.10.012](#)]
- 28 **Hu XR**, Cui XN, Hu QT, Chen J. Value of MR diffusion imaging in hepatic fibrosis and its correlations with serum indices. *World J Gastroenterol* 2014; **20**: 7964-7970 [PMID: [24976733](#) DOI: [10.3748/wjg.v20.i24.7964](#)]
- 29 **Razek AA**, Massoud SM, Azziz MR, El-Bendary MM, Zalata K, Motawea EM. Prediction of esophageal varices in cirrhotic patients with apparent diffusion coefficient of the spleen. *Abdom Imaging* 2015; **40**: 1465-1469 [PMID: [25732406](#) DOI: [10.1007/s00261-015-0391-2](#)]
- 30 **Pasquinielli F**, Belli G, Mazzoni LN, Regini F, Nardi C, Grazioli L, Zignego AL, Colagrande S. MR-diffusion imaging in assessing chronic liver diseases: Does a clinical role exist? *Radiol Med* 2012; **117**: 242-253 [PMID: [22020423](#) DOI: [10.1007/s11547-011-0730-5](#)]
- 31 **Leitão HS**, Doblas S, Garteiser P, d'Assignies G, Paradis V, Mouri F, Gerales CF, Ronot M, Van Beers BE. Hepatic Fibrosis, Inflammation, and Steatosis: Influence on the MR Viscoelastic and Diffusion Parameters in Patients with Chronic Liver Disease. *Radiology* 2017; **283**: 98-107 [PMID: [27788034](#) DOI: [10.1148/radiol.2016151570](#)]
- 32 **Bedossa P**, Poynard T. An algorithm for the grading of activity in chronic hepatitis C. The METAVIR Cooperative Study Group. *Hepatology* 1996; **24**: 289-293 [PMID: [8690394](#) DOI: [10.1002/hep.510240201](#)]
- 33 **Bakan AA**, Inci E, Bakan S, Gokturk S, Cimilli T. Utility of diffusion-weighted imaging in the evaluation of liver fibrosis. *Eur Radiol* 2012; **22**: 682-687 [PMID: [21984447](#) DOI: [10.1007/s00330-011-2295-z](#)]
- 34 **Sandrasegaran K**, Akisik FM, Lin C, Tahir B, Rajan J, Saxena R, Aisen AM. Value of diffusion-weighted MRI for assessing liver fibrosis and cirrhosis. *AJR Am J Roentgenol* 2009; **193**: 1556-1560 [PMID: [19933647](#) DOI: [10.2214/AJR.09.2436](#)]
- 35 **Soylu A**, Kiliçkesmez O, Poturoğlu S, Dolapçıoğlu C, Serez K, Sevindir I, Yaşar N, Akyildiz M, Kumbasar B. Utility of diffusion-weighted MRI for assessing liver fibrosis in patients with chronic active hepatitis. *Diagn Interv Radiol* 2010; **16**: 204-208 [PMID: [20658448](#) DOI: [10.4261/1305-3825.DIR.2810-09.1](#)]
- 36 **Boulanger Y**, Amara M, Lepanto L, Beaudoin G, Nguyen BN, Allaire G, Poliquin M, Nicolet V. Diffusion-weighted MR imaging of the liver of hepatitis C patients. *NMR Biomed* 2003; **16**: 132-136 [PMID: [12884356](#) DOI: [10.1002/nbm.818](#)]
- 37 **Do RK**, Chandarana H, Felker E, Hajdu CH, Babb JS, Kim D, Taouli B. Diagnosis of liver fibrosis and cirrhosis with diffusion-weighted imaging: Value of normalized apparent diffusion coefficient using the spleen as reference organ. *AJR Am J Roentgenol* 2010; **195**: 671-676 [PMID: [20729445](#) DOI: [10.2214/AJR.09.3448](#)]
- 38 **Lambrech J**, Mannaerts I, van Grunsven LA. The role of miRNAs in stress-responsive hepatic stellate cells during liver fibrosis. *Front Physiol* 2015; **6**: 209 [PMID: [26283969](#) DOI: [10.3389/fphys.2015.00209](#)]
- 39 **Coll M**, El Taghdouini A, Perea L, Mannaerts I, Vila-Casadesús M, Blaya D, Rodrigo-Torres D, Affò S, Morales-Ibanez O, Graupera I, Lozano JJ, Najimi M, Sokal E, Lambrecht J, Ginès P, van Grunsven LA, Sancho-Bru P. Integrative miRNA and Gene Expression Profiling Analysis of Human Quiescent Hepatic Stellate Cells. *Sci Rep* 2015; **5**: 11549 [PMID: [26096707](#) DOI: [10.1038/srep11549](#)]
- 40 **Krauskopf J**, de Kok TM, Schomaker SJ, Gosink M, Burt DA, Chandler P, Warner RL, Johnson KJ, Caiment F, Kleinjans JC, Aubrecht J. Serum microRNA signatures as "liquid biopsies" for interrogating hepatotoxic mechanisms and liver pathogenesis in human. *PLoS One* 2017; **12**: e0177928 [PMID: [28545106](#) DOI: [10.1371/journal.pone.0177928](#)]
- 41 **Gabriely G**, Wurdinger T, Kesari S, Esau CC, Burchard J, Linsley PS, Krichevsky AM. MicroRNA 21

- promotes glioma invasion by targeting matrix metalloproteinase regulators. *Mol Cell Biol* 2008; **28**: 5369-5380 [PMID: 18591254 DOI: 10.1128/MCB.00479-08]
- 42 **Zhao J**, Tang N, Wu K, Dai W, Ye C, Shi J, Zhang J, Ning B, Zeng X, Lin Y. MiR-21 simultaneously regulates ERK1 signaling in HSC activation and hepatocyte EMT in hepatic fibrosis. *PLoS One* 2014; **9**: e108005 [PMID: 25303175 DOI: 10.1371/journal.pone.0108005]
- 43 **Wei J**, Feng L, Li Z, Xu G, Fan X. MicroRNA-21 activates hepatic stellate cells via PTEN/Akt signaling. *Biomed Pharmacother* 2013; **67**: 387-392 [PMID: 23643356 DOI: 10.1016/j.biopha.2013.03.014]
- 44 **Huang YH**, Tiao MM, Huang LT, Chuang JH, Kuo KC, Yang YL, Wang FS. Activation of Mir-29a in Activated Hepatic Stellate Cells Modulates Its Profibrogenic Phenotype through Inhibition of Histone Deacetylases 4. *PLoS One* 2015; **10**: e0136453 [PMID: 26305546 DOI: 10.1371/journal.pone.0136453]
- 45 **Huang C**, Zheng JM, Cheng Q, Yu KK, Ling QX, Chen MQ, Li N. Serum microRNA-29 levels correlate with disease progression in patients with chronic hepatitis B virus infection. *J Dig Dis* 2014; **15**: 614-621 [PMID: 25138057 DOI: 10.1111/1751-2980.12185]
- 46 **Bandyopadhyay S**, Friedman RC, Marquez RT, Keck K, Kong B, Icardi MS, Brown KE, Burge CB, Schmidt WN, Wang Y, McCaffrey AP. Hepatitis C virus infection and hepatic stellate cell activation downregulate miR-29: MiR-29 overexpression reduces hepatitis C viral abundance in culture. *J Infect Dis* 2011; **203**: 1753-1762 [PMID: 21606534 DOI: 10.1093/infdis/jir186]
- 47 **França M**, Martí-Bonmati L, Alberich-Bayarri Á, Oliveira P, Guimaraes S, Oliveira J, Amorim J, Gonzalez JS, Vizcaino JR, Miranda HP. Evaluation of fibrosis and inflammation in diffuse liver diseases using intravoxel incoherent motion diffusion-weighted MR imaging. *Abdom Radiol (NY)* 2017; **42**: 468-477 [PMID: 27638516 DOI: 10.1007/s00261-016-0899-0]
- 48 **Razek AAKA**, Al-Adlany MAAA, Alhadidy AM, Atwa MA, Abdou NEA. Diffusion tensor imaging of the renal cortex in diabetic patients: Correlation with urinary and serum biomarkers. *Abdom Radiol (NY)* 2017; **42**: 1493-1500 [PMID: 28044190 DOI: 10.1007/s00261-016-1021-3]
- 49 **Seo N**, Chung YE, Park YN, Kim E, Hwang J, Kim MJ. Liver fibrosis: Stretched exponential model outperforms mono-exponential and bi-exponential models of diffusion-weighted MRI. *Eur Radiol* 2018; **28**: 2812-2822 [PMID: 29404771 DOI: 10.1007/s00330-017-5292-z]
- 50 **Razek AAKA**, Khashaba M, Abdalla A, Bayomy M, Barakat T. Apparent diffusion coefficient value of hepatic fibrosis and inflammation in children with chronic hepatitis. *Radiol Med* 2014; **119**: 903-909 [PMID: 24846081 DOI: 10.1007/s11547-014-0408-x]

P- Reviewer: El-Shabrawi MHF, Facciorusso A, McMillin MA, Wu C

S- Editor: Yan JP **L- Editor:** Filipodia **E- Editor:** Huang Y





Retrospective Study

Early gastric cancer diagnostic ability of ultrathin endoscope loaded with laser light source

Takuto Suzuki, Yoshiyasu Kitagawa, Rino Nankinzan, Taketo Yamaguchi

ORCID number: Takuto Suzuki (0000-0002-2706-6734); Yoshiyasu Kitagawa (0000-0003-1374-2292); Rino Nankinzan (0000-0003-1775-7811); Taketo Yamaguchi (0000-0003-0232-2508).

Author contributions: Suzuki T designed the research; Suzuki T, Kitagawa Y, Nankinzan R and Yamaguchi T performed the research; Suzuki T, Kitagawa Y and Nankinzan R analyzed the data; Suzuki T wrote the paper.

Institutional review board statement: The study was reviewed and approved by the Chiba Cancer Center Institutional Review Board.

Informed consent statement: All study participants provided informed written consent prior to study enrollment.

Conflict-of-interest statement: The authors have no conflicts of interest to declare.

Open-Access: This is an open-access article that was selected by an in-house editor and fully peer-reviewed by external reviewers. It is distributed in accordance with the Creative Commons Attribution Non Commercial (CC BY-NC 4.0) license, which permits others to distribute, remix, adapt, build upon this work non-commercially, and license their derivative works on different terms, provided the original work is properly cited and the use is non-commercial. See: <http://creativecommons.org/licenses/by-nc/4.0/>

Manuscript source: Unsolicited

Takuto Suzuki, Yoshiyasu Kitagawa, Rino Nankinzan, Department of Endoscopy, Chiba Cancer Center, Chiba 260-8717, Japan

Taketo Yamaguchi, Department of Gastroenterology, Chiba Cancer Center, Chiba 260-8717, Japan

Corresponding author: Takuto Suzuki, MD, PhD, Doctor, Department of Endoscopy, Chiba Cancer Center, 666-2 Nitonachou, Chuo-ku, Chiba 260-8717, Japan. taksuzuki@chiba-cc.jp
Telephone: +81-43-2645431
Fax: +81-43-2628680

Abstract

BACKGROUND

Conventionally, the low luminous intensity, low image resolution, and difficulty in operation have been reported with the ultrathin endoscope. However, it has markedly advanced recently. The improvement of the diagnostic ability is expected.

AIM

To compare the early gastric cancer diagnostic ability of an ultrathin endoscope loaded with a laser light source and that of the conventional endoscope.

METHODS

The target subjects were 375 consecutive patients who underwent endoscopy at our hospital for post-endoscopic submucosal dissection follow-up of gastric cancer from January to August 2018. During endoscopy, the ultrathin endoscope was used in 140 patients (37.3%), and the conventional endoscope was used in 235 patients (62.7%). Patient background was adjusted using the propensity score matching method, and gastric cancer detection ability was evaluated in the two groups.

RESULTS

The gastric cancer detection rate was 7.8% in the ultrathin endoscope group and 7.0% in the conventional endoscope group, and the mean intragastric observation time was 4.1 ± 1.7 min in the ultrathin endoscope group and 4.1 ± 1.9 min in the conventional endoscope group, showing no significant differences between the groups. Moreover, the biopsy implementation rate was 31.8% in the ultrathin endoscope group and 41.1% in the conventional endoscope group, and the biopsy prediction rate was 17.9% and 13.2%, respectively, showing no significant differences between the groups.

manuscript

Received: December 3, 2018**Peer-review started:** December 3, 2018**First decision:** January 30, 2019**Revised:** February 13, 2019**Accepted:** February 22, 2019**Article in press:** February 22, 2019**Published online:** March 21, 2019

CONCLUSION

The gastric cancer diagnostic ability of the ultrathin endoscope loaded with a laser light source was comparable to that of the conventional endoscope. The observation time was also comparable. Thus, endoscopy using the ultrathin endoscope loaded with the laser light source would be the first option in screening examinations of gastric cancer due to its low invasion.

Key words: Conventional endoscope; Gastric cancer; Laser light source; Screening; Ultrathin endoscope

©The Author(s) 2019. Published by Baishideng Publishing Group Inc. All rights reserved.

Core tip: The gastric cancer diagnostic ability of the ultrathin endoscope loaded with a laser light source is comparable to that of the conventional endoscope. From the view of low invasion, the ultrathin endoscope is superior to the conventional endoscope. Thus, endoscopy using the ultrathin endoscope loaded with the laser light source would be the first option in screening examinations of gastric cancer.

Citation: Suzuki T, Kitagawa Y, Nankinzan R, Yamaguchi T. Early gastric cancer diagnostic ability of ultrathin endoscope loaded with laser light source. *World J Gastroenterol* 2019; 25(11): 1378-1386

URL: <https://www.wjgnet.com/1007-9327/full/v25/i11/1378.htm>

DOI: <https://dx.doi.org/10.3748/wjg.v25.i11.1378>

INTRODUCTION

Barium x-ray with photofluorography has been widely used in screening examinations including health checkups because it has the effect of decreasing gastric cancer fatality rate^[1-3]. However, the sensitivity of this examination method was reportedly limited to 39% in the case of early gastric cancer^[4]. In order to overcome this drawback, esophagogastroduodenoscopy (EGD) has adopted instead. Since the marked effect of EGD to suppress gastric cancer fatality rate was demonstrated recently, EGD has been widely used in gastric cancer diagnosis^[5,6]. However, for the patients EGD is an unpleasant examination accompanied by afflictions such as nausea, gag reflex, and choking, and there are also cardiovascular loads^[7-9]. Thus, diameter thinning has advanced in the evolution of endoscope, and even an examination using an ultrathin endoscope such as transnasal endoscopy has been promoted^[10].

It was reported that less problems, higher patient acceptability, and lower loads would accompany an ultrathin endoscope to the heart and lung than those with the conventional endoscope^[11-15]. In disseminating endoscopy, an ultrathin endoscope is highly needed. In contrast, the low luminous intensity, low image resolution, and difficulty in operation were reported with the ultrathin endoscope in comparison with the conventional endoscope, and it was also pointed out that the examination time would be longer with the ultrathin endoscope due to the dark field of vision and lower absorption capacity (small channel diameter)^[16]. At present, an endoscope using a laser light source has been developed. In comparison with the conventional endoscope using the xenon light source, the field of vision is bright and broad, and high image quality has been achieved with a laser light source. Furthermore, operation has also been improved by expansion of the channel diameter (forceps diameter).

Some studies reported that the early gastric cancer diagnostic ability is comparable between the ultrathin and conventional endoscopes, but in other reports the inferiority of the ultrathin endoscope to the conventional endoscope was reported^[17-21]. In such reports, the low diagnostic capacity of the ultrathin endoscope was pointed out, particularly in the case of small early gastric cancer or gastric cancer in the U region^[22]. At this time, the aim was to compare the early gastric cancer diagnostic ability between the ultrathin endoscope and the conventional endoscope loaded with the laser light source.

MATERIALS AND METHODS

Study design

This retrospective analysis of database on EGD was conducted at the Chiba Cancer Center, Japan. This was approved by the ethics committee of Chiba Cancer Center, and the contents were displayed on the notice board for in- and outpatients. The study was conducted in accordance with the World Medical Association's Declaration of Helsinki. All patients provided informed consent to undergo EGD. All authors had access to the study data and approved the final manuscript.

Patients

The target patients were those who underwent endoscopic submucosal dissection (ESD) for gastric cancer at this hospital and were periodically undergoing endoscopy thereafter. At this hospital, post-ESD endoscopy is performed initially at 3 mo after ESD, at 1 yr after ESD, and thereafter once a year. Because gastric cancer develops metachronously, patients with a history of ESD have a high risk for gastric cancer. In this study, such patients were targeted. In addition, patients infected with *Helicobacter pylori* (*H. pylori*) must receive eradication therapy. There were 375 consecutive patients who underwent endoscopy at this hospital from January to August 2018 and were enrolled in this study. Patients with postoperative gastric remnant were excluded. At this hospital, the ultrathin endoscope was being used in the same manner as the conventional endoscope, and in the patients who prefer transnasal endoscopy, the ultrathin endoscope was used. In this study, the ultrathin endoscope was used in 140 patients (37.3%), and the conventional endoscope was used in 235 patients (62.7%). The endoscopists in charge were five specialists authorized by the Japan Gastroenterological Endoscopy Society and four non-specialists.

In order to investigate the diagnostic ability of the ultrathin endoscope, the backgrounds were adjusted with the group using the conventional endoscope by the propensity score (PS) matching method to compare gastric cancer detection rate as the primary evaluation item and intragastric observation time, biopsy implementation rate, biopsy prediction rate, and details of detected gastric cancers as the secondary evaluation items.

Ultrathin endoscope using laser light source

An endoscopic system using a laser light source (LASEREO, Fujifilm, Japan) was used. This system has two lasers with different wavelengths. One is a white light laser (wavelength 450 ± 10 nm) providing wide-spectrum white light illumination suitable for general observation. The other is a blue laser imaging mode laser (wavelength 410 ± 10 nm) with characteristics of short wavelength and narrowband. Therefore, in comparison with the endoscope system using the conventional xenon light source, it is feasible to visualize a brighter and higher-resolution image. The ultrathin endoscope (EG-L580NW) used in this system is 5.8 mm in scope outside diameter, 2.4 mm in forceps diameter, and 140° in viewing angle showing markedly improved performance as compared with the previous ultrathin endoscope. It can be used in not only the transoral but also transnasal route. As the conventional endoscope, EG-L590WR, EG-L590ZW, or EG-L600ZW was used.

Propensity score matching

We created a PS-matched cohort by attempting to match a patient who underwent the examination with an ultrathin endoscope with a patient who underwent the examination with a conventional endoscope (1:1 match) using a greedy nearest neighbor-matching technique. A caliper width of 0.05 of the standard deviation for the logit of the PS was used for the developed PS. After matching, crude comparisons of the matched cohorts were made. Upon matching, four covariates that could possibly influence the detection of gastric cancer were used, namely age, sex, degree of gastric mucosa atrophy, and endoscopist.

Statistical analysis

The clinical data were calculated as mean value with standard deviation, median value with range, and rate with 95% confidence interval (CI). In comparison between the two groups, Student's *t*-test was used to analyze numerical values. Chi-square and Fisher's exact tests were used to analyze rate values. A *P*-value < 0.05 was considered to indicate statistical significance. Statistical analyses were performed using SPSS version 23.0 for Windows (IBM Japan, Ltd., Japan).

RESULTS

The ultrathin endoscope was used via the transnasal route in 41 patients (29.3%) and transoral route in 99 patients (70.7%). In the conventional endoscope group, a sedative agent was used in 74 patients (31.5%). Due to being post-ESD, the patients were supposed to have undergone *H. pylori* eradication therapy. *H. pylori*-positive patients accounted for only 3.7% of the whole. Table 1 shows the patient backgrounds and results of the two groups before matching. After matching 140 patients of the ultrathin endoscope group and 235 patients of the conventional endoscope group, 129 patients in each group were adopted for analysis. The C-statistic of PS score was 0.557. Table 2 shows the matching results and balances. Table 3 shows the patient backgrounds of the two groups after matching. Gastric cancer was detected in 10 patients (7.8%, 95%CI 3.1%-12.4%) of the ultrathin endoscope group and 9 patients (7.0%, 95%CI 2.6%-11.4%) of the conventional endoscope group, showing no significant difference between the two groups ($P = 0.81$). All detected gastric cancers were in the early stage, and the median tumor size (range) was 7.5 mm (3-30 mm) in the ultrathin endoscope group and 6.0 mm (3-15 mm) in the conventional endoscope group, showing no significant difference between the two groups ($P = 0.42$). The region (U/M+L) of detected gastric cancer was 4/6 in the ultrathin endoscope group and 2/7 in the conventional endoscope group, showing no significant difference ($P = 0.41$) (Table 4). In addition, the mean intragastric observation time was 4.1 ± 1.7 min in the ultrathin endoscope group and 4.1 ± 1.9 min in the conventional endoscope group, showing no significant difference ($P = 0.96$). The biopsy implementation rate was 31.8% (95%CI 23.8%-39.8%) in the ultrathin endoscope group and 41.1% (95%CI 32.6%-49.6%) in the conventional endoscope group, showing no significant difference ($P = 0.12$) but a tendency to be lower in the former. The biopsy prediction rate was 17.9% (95%CI 7.9%-27.9%) and 13.2% (95%CI 5.2%-21.2%) in the ultrathin and conventional endoscope groups, respectively, showing no significant difference ($P = 0.48$) but a tendency to be lower also in the latter (Table 5). Figures 1 and 2 show the patients in whom gastric cancer was actually detected.

DISCUSSION

In this study it was shown that the ultrathin endoscope loaded with a laser light source can detect gastric cancer at the same rate as the conventional endoscope. Until recently, the problems with the ultrathin endoscope were dark images, low image quality, and weak absorption power. The inferiority of the ultrathin endoscope to the conventional endoscope in gastric cancer detection rate has been reported^[17-21]. However, the ultrathin endoscope loaded with the laser light source is markedly different from the conventional endoscope system using the xenon light source, and the image quality and brightness have been remarkably improved. In this study, patients with a history of ESD for gastric cancer were enrolled. Gastric cancer tends to multiply metachronously. In addition, according to the World Health Organization, *H. pylori* is the definite carcinogen of gastric cancer, and the majority of patients targeted in this study received *H. pylori* eradication therapy. The onset rate of gastric cancer is reduced by *H. pylori* eradication therapy, but a certain risk of gastric cancer remains even after eradication. Therefore, such patients have a higher risk of gastric cancer than the general population^[23]. The ultrathin endoscope showed a diagnostic ability that was not inferior to that in the conventional endoscope even in such patients.

It was thus far unavoidable to extend the examination time due to the poor absorption capacity, dark image, and narrow viewing angle, but in the case of the ultrathin endoscope loaded with the laser light source, the examination time was comparable to the conventional endoscope, due to the improvement of absorption capacity brought about by expansion of the forceps diameter and the expansion of observation range brought about by the improvement of viewing angle and brightness. As one of the factors, it is estimated that the amount of highly viscous gastric mucosa was small after the aforementioned *H. pylori* eradication therapy and the time required for mucosa washing and accompanying absorption could be shortened. However, because the number of *H. pylori*-negative patients is expected to increase hereafter, the situation was considered to reflect the current status.

Detected gastric cancers were not different between the two groups in lesion site and size. The lower diagnostic ability of the ultrathin endoscope was pointed out in the previous studies in the diagnosis of small gastric cancers < 20 mm in the U region, but such tendency was not seen in this study^[21,22]. Furthermore, the biopsy implementation and prediction rates were not significantly different between the two groups. There was rather a tendency of the biopsy implementation rate to be lower and the biopsy prediction rate to be higher in the ultrathin endoscope group. The

Table 1 Clinical background, gastric cancer detection rates, and the details of the two groups before matching

	Ultrathin endoscope	Conventional endoscope	<i>P</i> value
Number of screened subjects	140	235	
Transnasal	41 (29.3%)	0 (0%)	-
Sedation	16 (11.4%)	74 (31.5%)	< 0.001
Age in yr, median (range)	74 (43-89)	73 (43-93)	0.49
Gender, male	99 (70.7%)	187 (79.6%)	0.05
<i>Helicobacter pylori</i> positive	6 (4.3%)	9 (3.8%)	0.83
Atrophy, open type	108 (77.1%)	197 (83.8%)	0.11
Operator (expert/nonexpert)	99/41	178/57	0.28
Number of gastric cancer	12	20	
Number of subjects with gastric cancer/detection rate	12 (8.6%)	18 (7.7%)	0.75
Location (U/M, L)	4/4, 4	3/11, 6	0.22
Size in mm, median (range)	5 (3-30)	6.5 (3-18)	0.37
Morphological type (I, IIa/IIb, IIc)	0, 6/0, 6	2, 6/0, 12	0.09
Depth of invasion (m/sm)	10/2	20/0	0.06

reason for such tendency was not clear, but it was suggested that the ultrathin endoscope would be able to provide appropriate findings.

There are limitations in this study. First, this was a retrospective study, but the bias could be minimized in the investigation by matching the backgrounds using the PS matching method. Next, the ultrathin endoscope was used via not only the transnasal but also the transoral route in this study for pooled analysis, and a sedative agent was frequently used in the conventional endoscope group. Therefore, the influence of these factors on the analysis cannot be negated. Lastly, this study was performed in a limited number of patients at a single medical institution. It is therefore desired to perform a prospective multicenter study hereafter.

As EGD becomes widely known as a gastric cancer diagnostic procedure, the ultrathin endoscope may become the first-choice screening examination in gastric cancer diagnosis due to its low invasion.

Table 2 Confirmation of propensity score matching results and balances

	Full cohort			Propensity score-matched cohort		
	Conventional	Ultrathin	ASD, %	Conventional	Ultrathin	ASD, %
<i>n</i>	235	140		129	129	
Age in yr	73.1 ± 7.6	73.2 ± 7.6	1.9	73.2 ± 7.6	73.4 ± 7.1	2.7
Male	187, 79.6	99, 70.7	20.6	98, 76.0	97, 75.2	1.8
Specialist	178, 75.7	99, 70.7	11.4	95, 73.6	92, 71.3	5.2
Atrophy	198, 84.3	108, 77.1	18.1	103, 79.8	107, 82.9	8.0

Data: mean ± SD or *n*, %. ASD: Absolute standardized difference.**Table 3 Clinical background of the two groups after matching**

	Ultrathin endoscope	Conventional endoscope	<i>P</i> value
Number of screened subjects	129	129	
Age in yr, median (range)	74 (52-89)	74 (47-87)	0.46
Gender, males	108 (77.1%)	99 (76.7%)	0.16
<i>Helicobacter pylori</i> positive	5 (3.9%)	4 (3.1%)	0.73
Atrophy, open type	107 (82.9%)	103 (79.8%)	0.52
Operator, expert/nonexpert	92/37	95/34	0.68

Table 4 Gastric cancer detection rates and details of detected gastric cancers in the two groups after matching

	Ultrathin endoscope	Conventional endoscope	<i>P</i> value
Number of gastric cancer	10	9	
Number of subjects with gastric cancer/detection rate	10 (7.8%)	9 (7.0%)	0.81
Location (U/M + L)	4/4 + 2	2/6 + 1	0.41
Size in mm, median (range)	7.5 (3-30)	6.0 (3-15)	0.42
Morphological type (I, IIa/IIb, IIc)	0, 6/0, 4	0, 2/0, 7	0.10
Depth of invasion (m/sm)	8/2	9/0	0.16

Table 5 Comparison of intragastric observation time, biopsy implementation rate, and biopsy prediction rate between the two groups

	Ultrathin endoscope	Conventional endoscope	<i>P</i> value
Observation time of stomach in min	4.1 ± 1.7	4.1 ± 1.9	0.96
Biopsy implementation rate	31.8% (41/129) (95%CI 23.8-39.8)	41.1% (53/129) (95%CI 32.6-49.6)	0.12
Biopsy prediction rate	17.9% (10/56) (95%CI 7.9-27.9)	13.2% (9/68) (95%CI 5.2-21.2)	0.48

CI: Confidence interval.

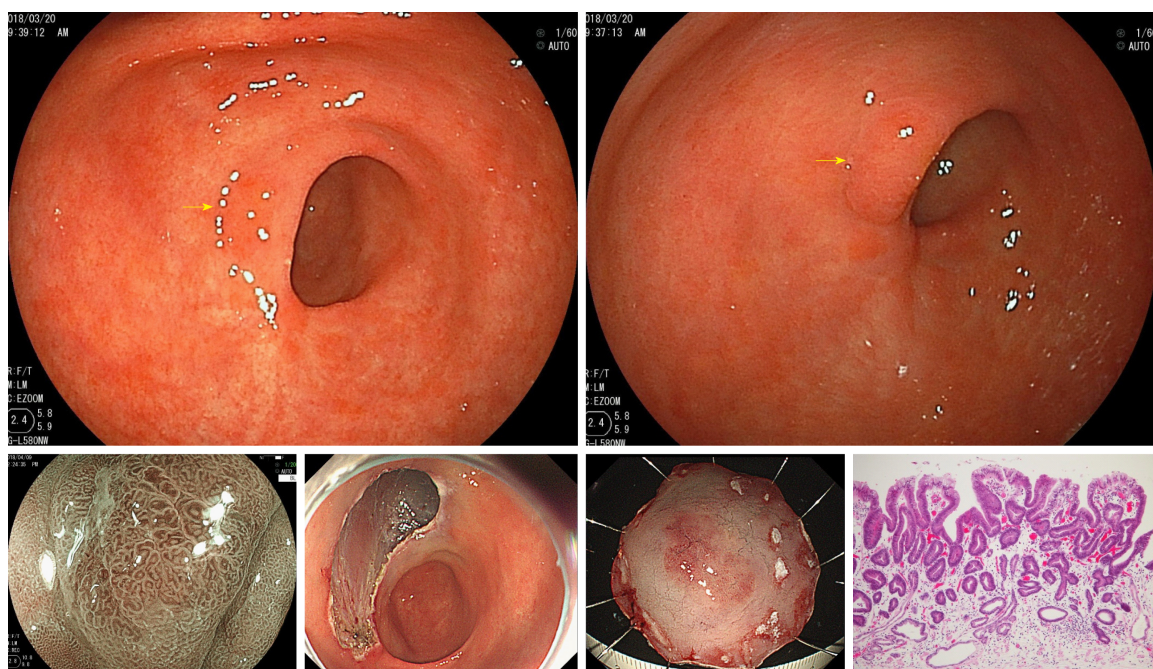


Figure 1 A patient with gastric cancer detected through the ultrathin endoscope. Ila lesion in the vicinity of previous endoscopic submucosal dissection scar on the anterior wall of the antrum. Results of endoscopic submucosal dissection: 10 mm × 10 mm, tubular adenocarcinoma, well-differentiated type, pT1a (M).

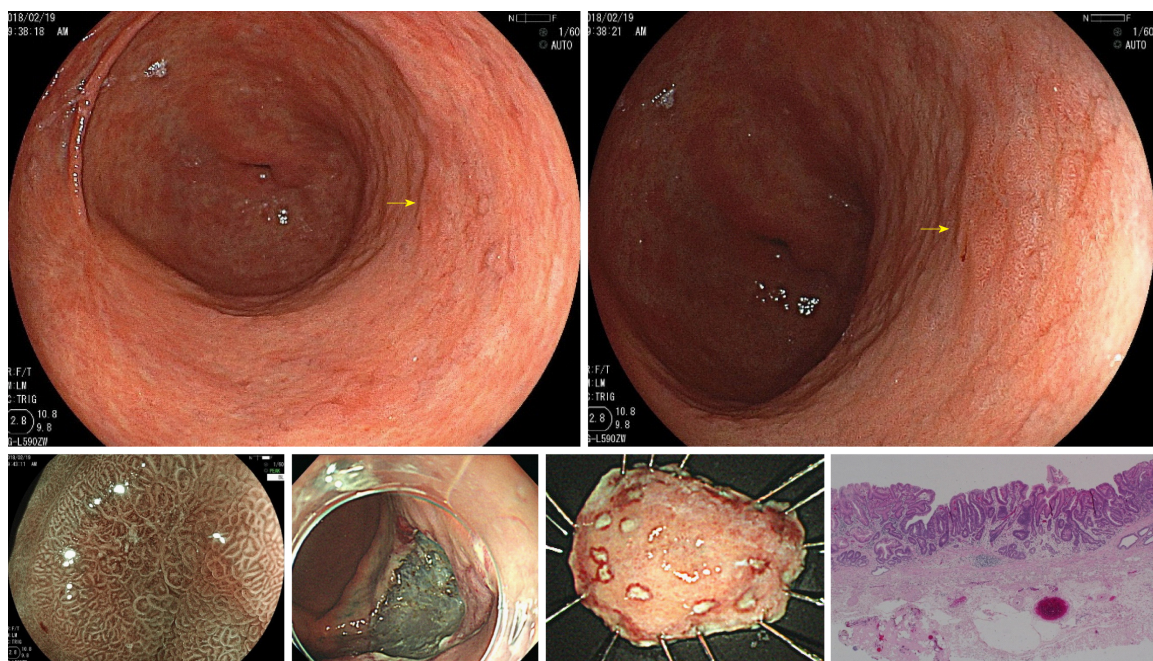


Figure 2 A patient with gastric cancer detected through the conventional endoscope. Endoscopic submucosal dissection scar on the anterior wall of the antrum and IIc lesion on the posterior wall. Results of endoscopic submucosal dissection: 5 mm × 5 mm, tubular adenocarcinoma, well-differentiated type, pT1a (M).

ARTICLE HIGHLIGHTS

Research background

An ultrathin endoscope has low luminous intensity, low image resolution, and difficulty in operation. However, the ultrathin endoscopy is a useful tool for screening endoscopy because of its low invasion.

Research motivation

Recently endoscopic technology has markedly advanced. The improvement of the diagnostic ability of ultrathin endoscope has also improved. Evaluating the diagnostic ability of the ultrathin endoscope is warranted.

Research objectives

In this study, early gastric cancer diagnostic ability of an ultrathin endoscope loaded with a laser light source was compared with that of the conventional endoscope.

Research methods

The study subjects were 375 consecutive patients who underwent endoscopy at our hospital for post-endoscopic submucosal dissection follow-up of gastric cancer from January to August 2018. During endoscopy, the ultrathin endoscope was used in 140 patients (37.3%), and the conventional endoscope was used in 235 patients (62.7%). Patient background was adjusted using the propensity score matching method, and gastric cancer detection ability was evaluated in the two groups.

Research results

The gastric cancer detection rate was 7.8% in the ultrathin endoscope group and 7.0% in the conventional endoscope group, and the mean intragastric observation time was 4.1 ± 1.7 min in the ultrathin endoscope group and 4.1 ± 1.9 min in the conventional endoscope group, showing no significant differences between the groups. Moreover, the biopsy implementation rate was 31.8% in the ultrathin endoscope group and 41.1% in the conventional endoscope group, and the biopsy prediction rate was 17.9% and 13.2%, respectively, showing no significant differences between the groups.

Research conclusions

The gastric cancer diagnostic ability of the ultrathin endoscope loaded with a laser light source was comparable to that of the conventional endoscope. The observation time was also comparable. Thus, endoscopy using the ultrathin endoscope loaded with the laser light source would be the first option in screening examinations of gastric cancer due to its low invasion.

REFERENCES

- 1 Oshima A, Hirata N, Ubukata T, Umeda K, Fujimoto I. Evaluation of a mass screening program for stomach cancer with a case-control study design. *Int J Cancer* 1986; **38**: 829-833 [PMID: 3793262 DOI: 10.1002/ijc.2910380608]
- 2 Fukao A, Tsubono Y, Tsuji I, Hisamichi S, Sugahara N, Takano A. The evaluation of screening for gastric cancer in Miyagi Prefecture, Japan: A population-based case-control study. *Int J Cancer* 1995; **60**: 45-48 [PMID: 7814150 DOI: 10.1002/ijc.2910600106]
- 3 Tsubono Y, Hisamichi S. Screening for gastric cancer in Japan. *Gastric Cancer* 2000; **3**: 9-18 [PMID: 11984703]
- 4 Nisizawa M. Present status and prospect for cancer screening (in Japanese). *J Gastroenterol Mass Surv* 1993; **78**: 100-103
- 5 Hamashima C, Ogoshi K, Okamoto M, Shabana M, Kishimoto T, Fukao A. A community-based, case-control study evaluating mortality reduction from gastric cancer by endoscopic screening in Japan. *PLoS One* 2013; **8**: e79088 [PMID: 24236091 DOI: 10.1371/journal.pone.0079088]
- 6 Matsumoto S, Yoshida Y. Efficacy of endoscopic screening in an isolated island: A case-control study. *Indian J Gastroenterol* 2014; **33**: 46-49 [PMID: 23996741 DOI: 10.1007/s12664-013-0378-2]
- 7 Brandt LJ. Patients' attitudes and apprehensions about endoscopy: How to calm troubled waters. *Am J Gastroenterol* 2001; **96**: 280-284 [PMID: 11232665 DOI: 10.1111/j.1572-0241.2001.03508.x]
- 8 Hart R, Classen M. Complications of diagnostic gastrointestinal endoscopy. *Endoscopy* 1990; **22**: 229-233 [PMID: 2147002 DOI: 10.1055/s-2007-1010734]
- 9 Bough EW, Meyers S. Cardiovascular responses to upper gastrointestinal endoscopy. *Am J Gastroenterol* 1978; **69**: 655-661 [PMID: 707460 DOI: 10.1016/S0016-5107(78)73508-X]
- 10 Amin MR, Postma GN, Setzen M, Koufman JA. Transnasal esophagoscopy: A position statement from the American Bronchoesophagological Association (ABEA). *Otolaryngol Head Neck Surg* 2008; **138**: 411-414 [PMID: 18359345 DOI: 10.1016/j.otohns.2007.12.032]
- 11 Yagi J, Adachi K, Arima N, Tanaka S, Ose T, Azumi T, Sasaki H, Sato M, Kinoshita Y. A prospective randomized comparative study on the safety and tolerability of transnasal esophagogastroduodenoscopy. *Endoscopy* 2005; **37**: 1226-1231 [PMID: 16329022 DOI: 10.1055/s-2005-921037]
- 12 Preiss C, Charton JP, Schumacher B, Neuhaus H. A randomized trial of unsedated transnasal small-caliber esophagogastroduodenoscopy (EGD) versus peroral small-caliber EGD versus conventional EGD. *Endoscopy* 2003; **35**: 641-646 [PMID: 12929057 DOI: 10.1055/s-2003-41513]
- 13 Mori A, Ohashi N, Maruyama T, Tatebe H, Sakai K, Shibuya T, Inoue H, Okuno M, Fushimi N, Asano T. Cardiovascular tolerance in upper gastrointestinal endoscopy using an ultrathin scope: Prospective randomized comparison between transnasal and conventional oral procedures. *Dig Endosc* 2008; **20**: 79-83 [DOI: 10.1111/j.1443-1661.2008.00780.x]
- 14 Nakata H, Oka M, Magari H, Inoue I, Iguchi M, Yanaoka K, Tamai H, Arai K, Ichinose M. Prospective study comparing transoral and transnasal upper gastrointestinal endoscopy on the cardiorespiratory parameter and tolerability (in Japanese). *Gastroenterol Endosc* 2007; **49**: 2684-2689 [DOI: 10.11280/gee1973b.49.2684]
- 15 Kawai T, Miyazaki I, Yagi K, Kataoka M, Kawakami K, Yamagishi T, Sofuni A, Itoi T, Moriyasu F, Osaka Y, Takagi Y, Aoki T. Comparison of the effects on cardiopulmonary function of ultrathin transnasal versus normal diameter transoral esophagogastroduodenoscopy in Japan. *Hepatogastroenterology* 2007; **54**: 770-774 [PMID: 17591059 DOI: 10.1111/j.1523-5378.2007.00489.x]
- 16 Tatsumi Y, Harada A, Matsumoto T, Tani T, Nishida H. Current status and evaluation of transnasal esophagogastroduodenoscopy. *Dig Endosc* 2009; **21**: 141-146 [PMID: 19691759 DOI: 10.1111/j.1443-1661.2009.00891.x]
- 17 Sorbi D, Gostout CJ, Henry J, Lindor KD. Unsedated small-caliber esophagogastroduodenoscopy (EGD) versus conventional EGD: A comparative study. *Gastroenterology* 1999; **117**: 1301-1307 [PMID: 10555555 DOI: 10.1053/gie.1999.117.1301]

- 10579971 DOI: [10.1016/S0016-5085\(99\)70280-5](https://doi.org/10.1016/S0016-5085(99)70280-5)
- 18 **Catanzaro A**, Faulx A, Isenberg GA, Wong RC, Cooper G, Sivak MV, Chak A. Prospective evaluation of 4-mm diameter endoscopes for esophagoscopy in sedated and unsedated patients. *Gastrointest Endosc* 2003; **57**: 300-304 [PMID: [12612506](https://pubmed.ncbi.nlm.nih.gov/12612506/) DOI: [10.1067/mge.2003.113](https://doi.org/10.1067/mge.2003.113)]
 - 19 **Murata A**, Akahoshi K, Sumida Y, Yamamoto H, Nakamura K, Nawata H. Prospective randomized trial of transnasal versus peroral endoscopy using an ultrathin videoendoscope in unsedated patients. *J Gastroenterol Hepatol* 2007; **22**: 482-485 [PMID: [17376037](https://pubmed.ncbi.nlm.nih.gov/17376037/) DOI: [10.1111/j.1440-1746.2006.04730.x](https://doi.org/10.1111/j.1440-1746.2006.04730.x)]
 - 20 **Yoshida Y**, Hayami Y, Matuoka M, Nakayama S. Comparison of endoscopic detection rate of early gastric cancer and gastric adenoma using transnasal EGD with that of transoral EGD. *Dig Endosc* 2008; **20**: 184-189 [DOI: [10.1111/j.1443-1661.2008.00804.x](https://doi.org/10.1111/j.1443-1661.2008.00804.x)]
 - 21 **Nakata H**, Enomoto S, Maekita T, Inoue I, Ueda K, Deguchi H, Shingaki N, Moribata K, Maeda Y, Mori Y, Iguchi M, Tamai H, Yamamichi N, Fujishiro M, Kato J, Ichinose M. Transnasal and standard transoral endoscopies in the screening of gastric mucosal neoplasias. *World J Gastrointest Endosc* 2011; **3**: 162-170 [PMID: [21954413](https://pubmed.ncbi.nlm.nih.gov/21954413/) DOI: [10.4253/wjge.v3.i8.162](https://doi.org/10.4253/wjge.v3.i8.162)]
 - 22 **Hayashi Y**, Yamamoto Y, Suganuma T, Okada K, Nego M, Imada S, Imai M, Yoshimoto K, Ueki N, Hirasawa T, Uragami N, Tsuchida T, Fujisaki J, Hoshino E, Takahashi H, Igarashi M. Comparison of the diagnostic utility of the ultrathin endoscope and the conventional endoscope in early gastric cancer screening. *Dig Endosc* 2009; **21**: 116-121 [PMID: [19691786](https://pubmed.ncbi.nlm.nih.gov/19691786/) DOI: [10.1111/j.1443-1661.2009.00840.x](https://doi.org/10.1111/j.1443-1661.2009.00840.x)]
 - 23 **Fukase K**, Kato M, Kikuchi S, Inoue K, Uemura N, Okamoto S, Terao S, Amagai K, Hayashi S, Asaka M; Japan Gast Study Group. Effect of eradication of *Helicobacter pylori* on incidence of metachronous gastric carcinoma after endoscopic resection of early gastric cancer: An open-label, randomised controlled trial. *Lancet* 2008; **372**: 392-397 [PMID: [18675689](https://pubmed.ncbi.nlm.nih.gov/18675689/) DOI: [10.1016/S0140-6736\(08\)61159-9](https://doi.org/10.1016/S0140-6736(08)61159-9)]

P- Reviewer: Christodoulidis G, Sitkin S

S- Editor: Yan JP **L- Editor:** Filipodia **E- Editor:** Huang Y



Retrospective Study

Clinical outcomes of ampullary neoplasms in resected margin positive or uncertain cases after endoscopic papillectomy

Arata Sakai, Masahiro Tsujimae, Atsuhiko Masuda, Takao Iemoto, Shigeto Ashina, Kohei Yamakawa, Takeshi Tanaka, Shunta Tanaka, Yasutaka Yamada, Ryota Nakano, Yu Sato, Manabu Kurosawa, Takuya Ikegawa, Seiji Fujigaki, Takashi Kobayashi, Hideyuki Shiomi, Yoshifumi Arisaka, Tomoo Itoh, Yuzo Kodama

ORCID number: Arata Sakai (0000-0003-1072-5243); Masahiro Tsujimae (0000-0001-9142-0702); Atsuhiko Masuda (0000-0002-2138-1207); Takao Iemoto (0000-0002-5829-1475); Shigeto Ashina (0000-0001-8167-301X); Kohei Yamakawa (0000-0001-8239-9913); Takeshi Tanaka (0000-0003-0490-3453); Shunta Tanaka (0000-0003-0640-4877); Yasutaka Yamada (0000-0002-3205-6872); Ryota Nakano (0000-0002-1844-2865); Yu Sato (0000-0002-0797-5973); Manabu Kurosawa (0000-0002-5144-108X); Takuya Ikegawa (0000-0002-8661-4593); Seiji Fujigaki (0000-0002-9433-1614); Takashi Kobayashi (0000-0002-9202-7643); Hideyuki Shiomi (0000-0002-7461-8538); Yoshifumi Arisaka (0000-0001-8535-5430); Tomoo Itoh (0000-0003-1498-5018); Yuzo Kodama (0000-0003-1223-7147).

Author contributions: Sakai A and Masuda A designed the study, analyzed the data, and drafted the manuscript; Tsujimae M and Iemoto T collected the data; Kodama Y gave the final approval of the manuscript; All the other authors revised the manuscript and approved the final version of the manuscript.

Institutional review board

statement: This study was conducted with the approval of the ethics committee of Kobe

Arata Sakai, Masahiro Tsujimae, Atsuhiko Masuda, Takao Iemoto, Shigeto Ashina, Kohei Yamakawa, Takeshi Tanaka, Shunta Tanaka, Yasutaka Yamada, Ryota Nakano, Yu Sato, Manabu Kurosawa, Takuya Ikegawa, Seiji Fujigaki, Takashi Kobayashi, Hideyuki Shiomi, Yoshifumi Arisaka, Yuzo Kodama, Division of Gastroenterology, Department of Internal Medicine, Kobe University Graduate School of Medicine, Kobe 650-0017, Japan

Takao Iemoto, Department of Gastroenterology, Kita-Harima Medical Center, Ono, Hyogo 675-1392, Japan

Yoshifumi Arisaka, Department of Gastroenterology, Nippon Life Hospital, Osaka 550-0006, Japan

Tomoo Itoh, Department of Diagnostic Pathology, Kobe University Graduate School of Medicine, Kobe 650-0017, Japan

Corresponding author: Atsuhiko Masuda, MD, PhD, Assistant Professor, Doctor, Division of Gastroenterology, Department of Internal Medicine, Kobe University Graduate School of Medicine, 7-5-1 Kusunoki-cho, Chuo-ku, Kobe, Hyogo 650-0017, Japan.

atmasuda@med.kobe-u.ac.jp

Telephone: +81-78-3826305

Fax: +81-78-3826309

Abstract

BACKGROUND

Endoscopic papillectomy (EP) for benign ampullary neoplasms could be a less-invasive alternative to pancreatoduodenectomy (PD). There are some problems and limitations with EP. The post-EP resection margins of ampullary tumors are often positive or uncertain because of the burning effect of EP. The clinical outcomes of resected margin positive or uncertain cases after EP remain unknown.

AIM

To investigate the clinical outcomes of resected margin positive or uncertain cases after EP.

METHODS

Between January 2007 and October 2018, all patients with ampullary tumors who

University Graduate School of Medicine, IRB No. 170057.

Informed consent statement:

Patients were not required to give informed consent to the study because this retrospective study used anonymous clinical data that were obtained after each patient agreed to treatment by written consent.

Conflict-of-interest statement:

There are no conflicts of interest.

Data sharing statement:

No additional data are available.

Open-Access:

This is an open-access article that was selected by an in-house editor and fully peer-reviewed by external reviewers. It is distributed in accordance with the Creative Commons Attribution Non Commercial (CC BY-NC 4.0) license, which permits others to distribute, remix, adapt, build upon this work non-commercially, and license their derivative works on different terms, provided the original work is properly cited and the use is non-commercial. See: <http://creativecommons.org/licenses/by-nc/4.0/>

Manuscript source: Invited manuscript

Received: December 13, 2018

Peer-review started: December 13, 2018

First decision: January 30, 2019

Revised: February 6, 2019

Accepted: February 15, 2019

Article in press: February 15, 2019

Published online: March 21, 2019

underwent EP at Kobe University Hospital were included in this study. The indications for EP were as follows: adenoma, as determined by preoperative endoscopic biopsy, without bile/pancreatic duct extension, according to endoscopic ultrasound or intraductal ultrasound. The clinical outcomes of resected margin positive or uncertain cases after EP were retrospectively investigated.

RESULTS

Of the 45 patients, 29 were male, and 16 were female. The mean age of the patients was 65 years old. Forty-one patients (89.5%) underwent *en bloc* resection, and 4 patients (10.5%) underwent piecemeal resection. After EP, 33 tumors were histopathologically diagnosed as adenoma, and 12 were diagnosed as adenocarcinoma. The resected margins were positive or uncertain in 24 patients (53.3%). Of these cases, 15 and 9 were diagnosed as adenoma and adenocarcinoma, respectively. Follow-up observation was selected for all adenomas and 5 adenocarcinomas. In the remaining 4 adenocarcinoma cases, additional PD was performed. Additional PD was performed in 4 cases, and residual carcinoma was found after the additional PD in 1 of these cases. In the follow-up period, local tumor recurrence was detected in 3 cases. Two of these cases involved primary EP-diagnosed adenoma. The recurrent tumors were also adenomas detected by biopsy. The remaining case involved primary EP-diagnosed adenocarcinoma. The recurrent tumor was also an adenocarcinoma. All of the recurrent tumors were successfully treated with argon plasma coagulation (APC). There was no local or lymph node recurrence after the APC. The post-APC follow-up periods lasted for 57.1 to 133.8 mo. No ampullary tumor-related deaths occurred in all patients.

CONCLUSION

Resected margin positive or uncertain cases after EP could be managed by endoscopic treatment including APC, even in cases of adenocarcinoma. EP could become an effective less-invasive first-line treatment for early stage ampullary tumors.

Key words: Ampullary neoplasm; Endoscopic papillectomy; Resected margin; Clinical outcome

©The Author(s) 2019. Published by Baishideng Publishing Group Inc. All rights reserved.

Core tip: In this study, we investigated the clinical outcomes of resected margin positive or uncertain cases after endoscopic papillectomy (EP). All of the recurrent tumors were successfully treated with argon plasma coagulation, even in cases of adenocarcinoma. There was no local or lymph node recurrence after the argon plasma coagulation. No ampullary tumor-related deaths occurred in all patients. In conclusion, resected margin positive or uncertain cases after EP could be managed by endoscopic treatment.

Citation: Sakai A, Tsujimae M, Masuda A, Iemoto T, Ashina S, Yamakawa K, Tanaka T, Tanaka S, Yamada Y, Nakano R, Sato Y, Kurosawa M, Ikegawa T, Fujigaki S, Kobayashi T, Shiomi H, Arisaka Y, Itoh T, Kodama Y. Clinical outcomes of ampullary neoplasms in resected margin positive or uncertain cases after endoscopic papillectomy. *World J Gastroenterol* 2019; 25(11): 1387-1397

URL: <https://www.wjgnet.com/1007-9327/full/v25/i11/1387.htm>

DOI: <https://dx.doi.org/10.3748/wjg.v25.i11.1387>

INTRODUCTION

Endoscopic papillectomy (EP) for benign ampullary neoplasms could be a less-invasive alternative to pancreatoduodenectomy (PD) because PD might be an excessively invasive treatment for benign neoplasms^[1,2]. The current standard treatment for ampullary tumor is PD, which is still associated with a high morbidity rate despite a recent reduction in the mortality rate to less than 5%^[3,4]. On the other

hand, the mortality after EP has been reported by high volume centers to be 0.4%. The overall complication rate of EP was reported between 8% and 35%, and the most common complications are pancreatitis (5%–15%) and bleeding (2%–16%). Most episodes of bleeding can be controlled by endoscopic hemostasis, and most episodes of pancreatitis are mild and resolved with conservative treatment^[5]. Surgical ampullectomy (SA) is another alternative to PD. Ceppa *et al*^[6] showed that EP was found to have equivalent efficacy when compared with SA. Moreover, EP had lower morbidity and identical mortality.

There are some problems and limitations with EP. The preoperative detection of tumor extension into a bile duct or the pancreatic duct is sometimes technically difficult, although the diagnostic ability of imaging studies, such as endoscopic ultrasonography (EUS), has recently markedly improved^[7,8]. In addition, the pathological evaluation of the margins of resected ampullary tumor specimens is often difficult because of the burning effect of EP^[9]. Therefore, we sometimes experience resected margin positive or uncertain cases and the management of those cases might be important clinical issue on performing this endoscopic treatment.

Recently, some studies have indicated that EP might be a useful treatment for early stage ampullary carcinoma with T1, in which the tumor is limited to the sphincter of Oddi^[10]. In cases involving T2, in which the tumor has invaded the duodenal wall, additional surgery is recommended because the frequency of lymph node metastasis was reported to range from 24%–45% in such cases^[11–14]. Furthermore, Yamamoto *et al*^[15] reported that there was no lymphovascular invasion or lymph node metastasis in any T1a cases, whereas one of four T1b cases exhibited lymphovascular invasion. Therefore, in cases of early stage ampullary carcinoma, distinguishing between T1a and T1b during preoperative diagnostic examinations might be extremely important for ensuring that the indications for EP are appropriate. However, unfortunately, there are no diagnostic tools for clearly detecting tumor invasion into the sphincter of Oddi. The identification of the sphincter of Oddi using EUS or intraductal ultrasound (IDUS) is still technically difficult in many cases. For these reasons, EP for early stage ampullary carcinoma is still challenging, and its indications might be restrictive.

Moreover, the post-EP resection margins of ampullary tumors are often positive or uncertain because of the burning effect of EP. The clinical outcomes of resected margin positive or uncertain cases after EP remains unknown. Decisions regarding the treatment course in such cases might differ among institutions and/or depend on each patient's condition. Therefore, in this study we investigated the clinical outcomes of ampullary neoplasms encountered at our hospital, including ampullary carcinomas that were diagnosed based on pathological evaluations of resected specimens, that exhibited positive or uncertain margins after EP.

MATERIALS AND METHODS

Patients

All patients with ampullary tumors who underwent EP at Kobe University Hospital between January 2007 and October 2018 were included in this study. Tumor staging and intraductal involvement were evaluated using computed tomography (CT) and EUS for all patients. IDUS was attempted for cases that were difficult to diagnose intraductal extension by EUS, because of the risk of pancreatitis. The main indication for EP was adenoma, as determined by a preoperative biopsy examination, without bile/pancreatic duct extension, according to EUS and/or IDUS (Figure 1). In the cases with evidence of ampullary carcinoma by the preoperative biopsy, PD was recommended. In some cases, such as those involving super-elderly patients or patients in a poor general condition, EP was performed when T2 invasion was not detected by preoperative imaging studies. Preoperative biopsy diagnosed as adenocarcinoma was only 4 patients in this study. In these cases, they were unfit for surgery because 1 patient was super-elderly (85 years old), and 3 patients were poor general condition with severe comorbidity. The clinical outcomes of each EP cases were retrospectively investigated. The study protocol was reviewed and approved by the ethical committee at Kobe University School of Medicine before the study (No. 170057). This study was conducted in accordance with the Declaration of Helsinki and the consolidated Good Clinical Practice guidelines. All authors had access to the study data, and they all reviewed and approved the final manuscript.

EP procedure and evaluation of resected specimens

EP was carried out with a standard polypectomy snare using a blended electrosurgical current. Even though it became piecemeal resection because of its size, the tumor was completely resected endoscopically in all cases. We tried to insert both

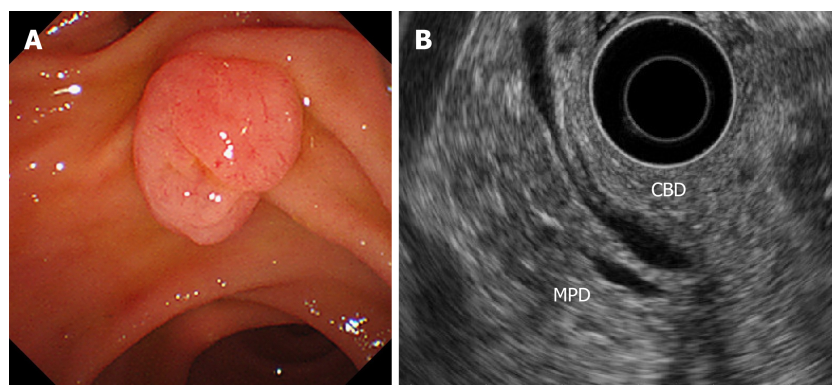


Figure 1 A case of ampullary adenoma that was indicated for endoscopic papillectomy. A: Duodenoscopy showed an ampullary tumor. The tumor was diagnosed as an adenoma based on an endoscopic biopsy. B: Endoscopic ultrasound did not show any bile/pancreatic duct invasion. CBD: Common bile duct; MPD: Main pancreatic duct.

bile duct and pancreatic duct stents after the EP procedure. Post-EP bleeding was defined as hematemesis and/or melena or a > 2 g/dL decrease in hemoglobin level (bleeding requiring hemostasis). Immediate bleeding was not defined as post-EP bleeding. Post-EP pancreatitis was defined as an increase in serum amylase/lipase to > 3 times the upper limit of normal, along with typical pancreatic-type pain. Experienced pathologists examined the resected specimens. The final depth of cancer invasion was recorded according to the Classification of Biliary Tract Carcinoma developed by the Japanese Society of Hepato-Biliary-Pancreatic Surgery as follows^[16]: carcinoma *in situ*, tumors limited to the mucosa, tumors limited to the sphincter of Oddi, and tumors that had invaded the duodenal wall were defined as Tis, T1a, T1b, and T2, respectively (Table 1). Horizontal margins (HM) and vertical margins (VM) were assessed as follows: positive (Figure 2A): involvement of the margin; uncertain (Figure 2B): involvement of the margin cannot be assessed; negative: margins were tumor-free. After examining the resected specimens, additional PD was recommended in the cases of adenocarcinoma. However, in the cases in which additional PD could not be performed based on the patient's wishes or condition, we chose to perform palliative endoscopic treatment or medical follow-up. In all cases of adenoma, medical follow-up was recommended, even though the resected tumor exhibited a positive or uncertain margin after EP.

Follow-up strategy after EP

The first follow-up session was scheduled for 3 mo after EP. Then, follow-up examinations were scheduled every 3 mo to 6 mo for 1 year, and yearly thereafter for 5 years. The follow-up examinations included blood tests (for transaminase, pancreatic enzyme, and tumor markers), duodenoscopy with biopsies, and contrast-enhanced CT scans. When a polypoid lesion that was suspected to be a recurrent tumor was detected on follow-up duodenoscopy, an endoscopic biopsy was performed. Additional management strategies, such as argon plasma coagulation (APC) or PD, were considered when the biopsy demonstrated a tumorous lesion. PD was recommended for all cases of recurrent cancer. However, patients who refused or were unfit for PD were considered for APC. APC was recommended for adenomas (Figure 3).

RESULTS

Baseline characteristics of this study

The characteristics of the patients are shown in Table 2. Of the 45 patients, 29 were male, and 16 were female. The mean age of the patients was 65.0 years old (65.0 ± 11.5). Six patients were over 80 years old (13.3%). Forty-one tumors (91.1%) were treated with *en bloc* resection, and 4 (8.9%) tumors were treated with piecemeal resection. Prophylactic both pancreatic and biliary stent was placed in 33 (73.3%) patients, only pancreatic stent was placed in 7 (15.6%) patients, and only biliary stent was placed in 4 (8.9%) patients, there was no stent placement in 1 (2.2%) case. Complications occurred in 42.2% of all patients. Hemorrhage occurred in 9 patients (20.0%), and pancreatitis occurred in 13 patients (28.9%). One of 9 post-EP hemorrhage cases was severe bleeding that needed transcatheter arterial embolization

Table 1 Histopathological findings of primary tumor invasion (according to the Classification of Biliary Tract Cancers established by the Japanese Society of Hepato-Biliary-Pancreatic Surgery: 3rd English edition)

Tis	Carcinoma <i>in situ</i>
T1a	Tumor limited to mucosa
T1b	Tumor limited to sphincter of Oddi
T2	Tumor invades duodenal wall
T3a	Tumor invades pancreas within 5 mm in depth
T3b	Tumor invades pancreas beyond 5 mm in depth
T4	Tumor invades peripancreatic soft tissues, or other adjacent organs or structures

(TAE). One of 13 post-EP pancreatitis cases was severe acute pancreatitis. Prophylactic pancreatic stent was placed in all post-EP pancreatitis patients. There were no complication related deaths. The mean hospital stay was 15.4 d. After EP, 33 (73.3%) tumors were histopathologically diagnosed as adenomas, and 12 (26.7%) were diagnosed as adenocarcinomas. The diagnostic accuracy of preoperative biopsy was 68.9% (31/45), with underestimated diagnosis in 2.2% (1/45) (Table 3). The resected margins were positive in 12 cases, uncertain in 12 cases, and negative in 21 cases. The HM were positive in 9 cases and uncertain in 10 cases. The VM were positive in 5 cases and uncertain in 9 cases. The median duration of the follow-up period was 27.1 mo (range: 3.0-133.4).

Clinical outcomes of resected margin positive or uncertain cases

Clinical outcomes of resected margin positive or uncertain cases are shown in Figure 4. The frequency of positive or uncertain margins after EP was 53.3% (24/45). Among these cases, 15 and 9 were diagnosed as adenoma and adenocarcinoma, respectively. In all cases of adenoma and 5 cases of adenocarcinoma, follow-up observation was selected. In 4 cases of adenocarcinoma, additional PD was performed. No residual tumors were found after additional PD in 3 cases, whereas residual carcinoma was detected after additional PD in the remaining case. In the latter case, the depth of the resected specimen after EP was suspected to be T1b, and the final pathological stage after PD was T1b without lymph node metastasis. In the follow-up period, local tumor recurrence was observed in 3 cases. In 2 of these cases, primary adenomas were diagnosed based on EP. After the EP, recurrent adenomas were diagnosed based on biopsy examinations. In the remaining case, a primary adenocarcinoma was diagnosed based on EP, and the recurrent tumor was also an adenocarcinoma. All of the recurrent tumors were successfully treated with APC. No local or lymph node recurrence was detected during the subsequent follow-up period (duration: 57.1 mo to 133.8 mo). No ampullary tumor-related deaths occurred in all patients.

Clinical outcomes of resected margin negative cases

The clinical outcomes of the resected margin-negative cases are shown in Figure 5. Among the cases that exhibited negative margins after EP, 18 cases were diagnosed as adenoma, 2 were diagnosed as Tis, and 1 was diagnosed as T1a. Follow-up observation was selected in all patients. In 1 of the cases of adenoma, local recurrence was detected. The recurrent tumor was also an adenoma and was detected during a biopsy examination. The recurrent tumor was treated with APC, and no local recurrence was detected during the subsequent follow-up period (duration: 71.0 mo).

Details of the cases involving post-EP recurrence

The clinical data of the cases involving recurrence after EP are shown in Table 4. There were 4 cases of recurrence after EP. In 20 follow-up cases of resected margin positive or uncertain cases, local recurrence was detected in 3 cases. In 21 resected margin negative cases, local recurrence was detected in 1 case. There was no significant difference in the local recurrence between resected margin positive /uncertain and negative cases ($P = 0.34$, 2-sided Fisher's exact test). In the local recurrent cases, 3 of the primary lesions were diagnosed as adenomas after EP, and 1 was diagnosed as an adenocarcinoma. There was no significant difference in the local recurrence between adenomas and adenocarcinomas ($P = 0.99$, 2-sided Fisher's exact test). The primary tumors ranged in size from 17 mm to 25 mm. The HM were positive and the VM were uncertain in 2 cases, the HM were positive and the VM were negative in 1 case, and both margins were negative in 1 case. There is no difference in the post-EP recurrence between the positive or uncertain HM and positive or uncertain VM. The duration of the period from EP to recurrence ranged

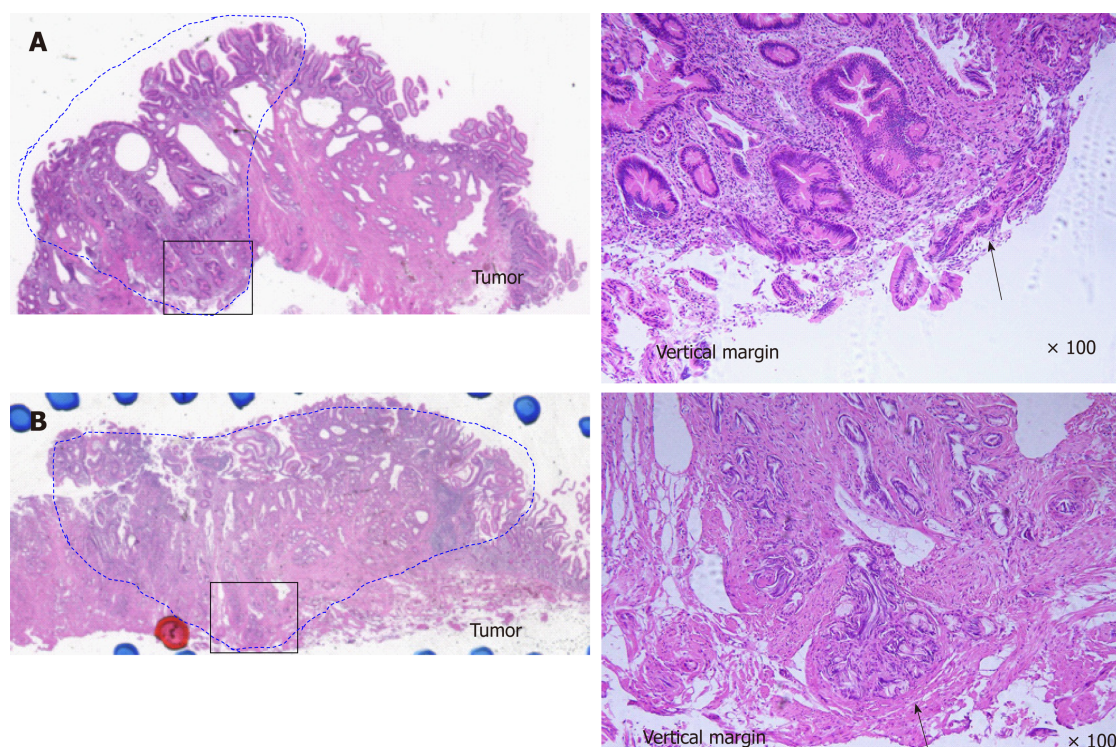


Figure 2 Ampullary adenoma. A: Ampullary adenoma with vertical margin positive. Tumor is present at resected vertical margin. (black arrow). (left) hematoxylin and eosin, loupe image. (right) hematoxylin and eosin $\times 100$. B: Ampullary adenoma with vertical margin uncertain. Tubular gland is present at resected vertical margin, but it cannot distinguish whether or not the tumor exists because of thermal denaturation (black arrow). (left) Hematoxylin and eosin, loupe image. (right) Hematoxylin and eosin $\times 100$.

from 1.0 mo to 6.3 mo. All of these cases were successfully treated with APC. The post-APC follow-up period lasted for 56.6 mo to 133.4 mo.

DISCUSSION

In this study, we investigated the clinical outcome of resected margin positive or uncertain cases after EP. EP for benign ampullary tumors is widely accepted as a less-invasive alternative to surgery. However, the pathological evaluation of resected margins was often difficult in the present study because of the burning effect of EP. Moreover, in some cases carcinoma was identified during post-EP pathological evaluations. There is no consistent evidence about the management of ampullary tumors that display positive or uncertain margins after EP.

The current study included 45 patients who underwent EP for ampullary tumors, and 24 (53.3%) of these cases exhibited positive or uncertain margins after EP. In previous studies, the frequency of incomplete EP-based resection varied from 10.6%-57.1%^[1,9,10,15,17]. However, the definitions of incomplete resection differed among these studies. In our study, the frequency of a positive or uncertain margin among resected ampullary tumors was relatively high. This was probably due to equivocal findings caused by the burning effect of EP producing uncertain diagnoses because there is a tendency for the pathologists at our hospital to avoid underestimation.

The recurrence rate of ampullary tumors after EP was reported to range from 10%-33% in previous studies^[18-21]. In our study, additional PD was performed in 4 of the 24 cases in which positive or uncertain margins were detected after the resection procedure. Of these 4 cases, a residual tumor was only found in 1 case. In the remaining 20 cases, follow-up observation was selected, and local tumor recurrence occurred in 15% (3/20) of these cases. Our results are similar to those of previous studies, despite the fact that our study included cases that exhibited positive or uncertain margins after EP. Among the cases that exhibited negative margins after EP, local tumor recurrence was found in 1 of 21 cases. In the literature of Ridditid *et al.*^[21], among patients with ampullary adenoma who had complete resection ($n = 107$), 16 patients (15%) developed recurrence up to 65 mo after resection. These results suggest that evaluating the margins of resected ampullary tumors after EP is sometimes difficult. Therefore, careful follow-up examinations are recommended after EP in all

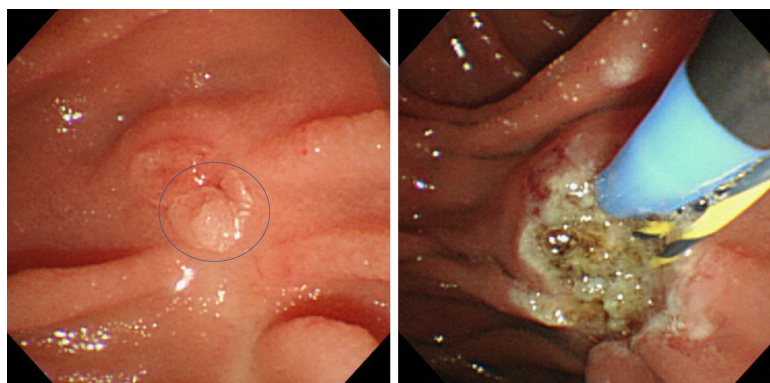


Figure 3 A recurrent tumor that was successfully treated with argon plasma coagulation.

cases of ampullary tumors. Established recommendation of follow-up protocol after EP has not been published. This point should be addressed in the future investigation.

APC is a type of non-contact thermal ablation in which a high-frequency current is applied to the target lesion, and it is widely used for the treatment of endoscopic hemostasis or additional treatment after endoscopic resection. APC has been reported to be useful for recurrent ampullary tumors that arise after EP^[4,9,15,17]. In our study, all of the recurrent tumors were successfully treated with APC, and there was no local or lymph node recurrence after APC (duration of the follow-up period: 56.6 mo to 133.4 mo). This indicates that APC is a reliable and feasible way of treating locally recurrent ampullary tumors that arise after EP. On the other hand, Nam *et al.*^[22] reported usefulness of APC subsequent to EP. In this literature, they concluded additional APC during EP might have a beneficial effect by decreasing bleeding rate without harmful effects but not have an effect of decreasing tumor recurrence.

Pancreatitis is the most common problematic complication of EP. Currently, several studies have shown that placement of a prophylactic pancreatic stent after EP reduces the risk of pancreatitis. A prospective, randomized, controlled trial showed that pancreatic duct stenting after EP significantly decreased the rate of post-EP pancreatitis^[23]. However, whether or not post EP pancreatic stenting can alleviate the rate of pancreatitis is still controversial. Some studies have shown no statistically significant benefit by prophylactic placement of a pancreatic stent during EP. In this study, post-EP pancreatitis occurred in 13 patients (28.9%). Prophylactic pancreatic stent had been placed in all post-EP pancreatitis patients. Further prospective controlled studies are required to evaluate the efficacy of prophylactic pancreatic stenting after EP for prevention of post-EP pancreatitis.

The present study had some limitations. First, it was affected by selection bias due to its retrospective nature. However, before performing EP we intensively examined the patients for bile/pancreatic duct invasion using EUS or IDUS. This resulted in good clinical courses being achieved, even in cases that exhibited positive or uncertain margins after EP. Second, the sample size was too small to allow the results to be generalized. A further large-scale prospective study will be needed in future. There is no consistent evidence about the management of ampullary tumors that exhibit positive or uncertain margins after being resected *via* EP. Our results might help to determine appropriate indications for EP, including for cases of early stage ampullary carcinoma.

In conclusion, resected margin positive or uncertain cases after EP could be managed by endoscopic treatment including APC, even in cases of adenocarcinoma. EP could become an effective less-invasive first-line treatment for early stage ampullary tumors.

Table 2 The characteristics of all patients

Number of all EP cases	45
Male/female	29/16
Age (yr, mean \pm SD)	65.0 \pm 11.5
Tumor size (mm, mean \pm SD)	21.1 \pm 6.2
<i>En-bloc</i> resection/piecemeal resection	41/4
Stent placement	
Both/pancreatic/biliary/none	33/7/4/1
Complications of EP	
Post-EP bleeding	9 (20.0%)
Post-EP pancreatitis	13 (28.9%)
Hospital stay (d, mean \pm SD)	15.4 \pm 8.5
Pathological diagnosis	
Adenoma/adenocarcinoma	33/12
Pathological evaluation of resected margin	
Positive/uncertain/negative	12/12/21
Horizontal margin	
Positive/uncertain	9/10
Vertical margin	
Positive/uncertain	5/9
Median observation period (mo, range)	27.1 (3.0-133.4)

EP: Endoscopic papillectomy.

Table 3 The diagnostic accuracy of endoscopic forceps biopsy before endoscopic papillectomy

Preoperative biopsy	Number	Final pathological diagnosis	
		Adenoma	Adenocarcinoma
Adenoma	30	28	2
Borderline	11	4	7
Adenocarcinoma	4	1	3

Table 4 Summary of the clinical data of the patients who developed recurrent tumors after endoscopic papillectomy

Age	Sex	Preoperative diagnosis	Final diagnosis	Size (mm)	Resection margin	Duration to recurrence (mo)	Additional treatment	Follow up periods after APC (mo)
75	Male	Adenoma	Adenoma	25	HM (+), VM (X)	1.0	APC	75.9
60	Female	Adenoma	Adenoma	17	HM (+), VM (X)	5.0	APC	133.4
73	Male	Borderline	Adenocarcinoma	22	HM (+), VM (-)	1.2	APC	56.6
74	Female	Adenoma	Adenoma	n/d	HM (-), VM (-)	6.3	APC	71.0

APC: Argon plasma coagulation.

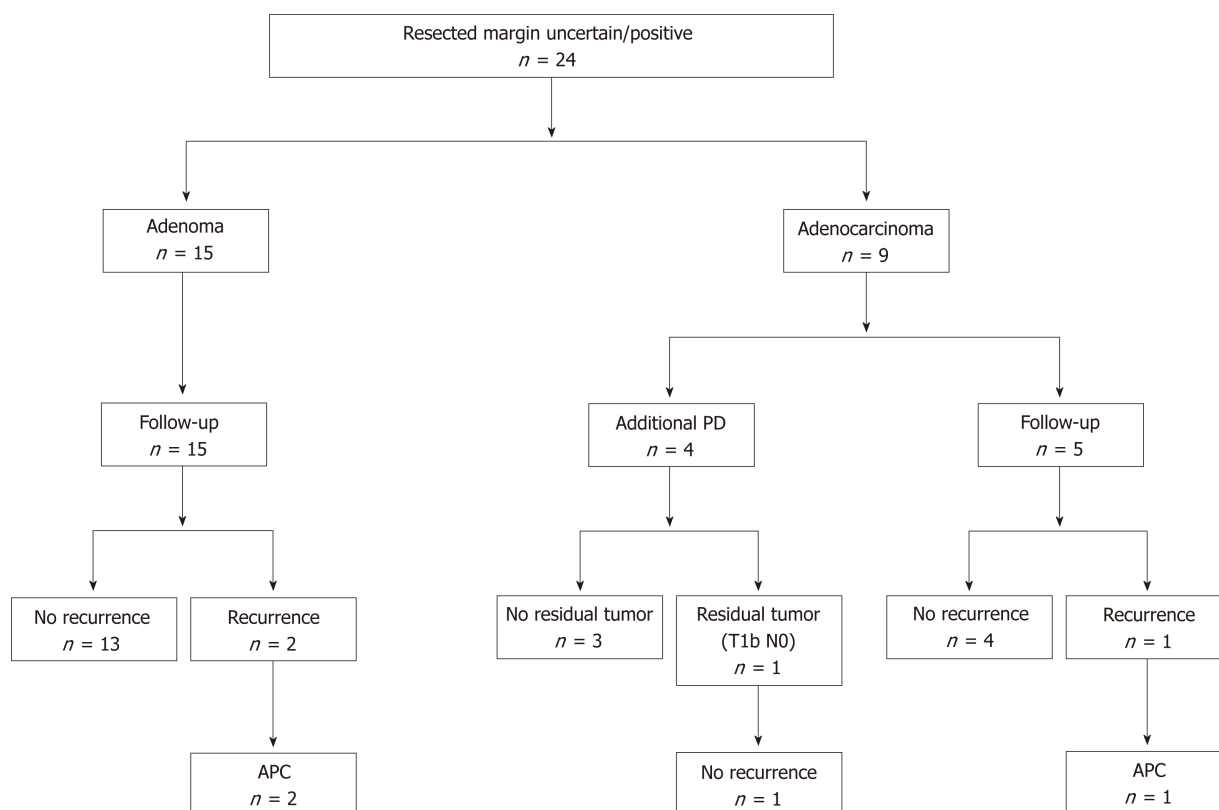


Figure 4 Clinical outcomes of resected margin positive or uncertain cases. APC: Argon plasma coagulation; PD: Pancreatoduodenectomy.

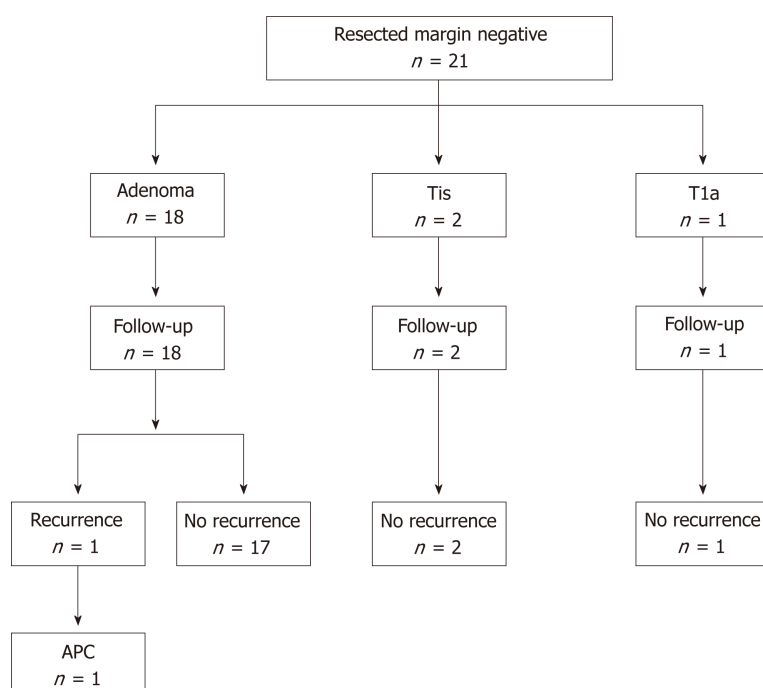


Figure 5 Clinical outcomes of resected margin negative cases. APC: Argon plasma coagulation.

ARTICLE HIGHLIGHTS

Research background

The clinical outcomes of resected margin positive or uncertain cases after endoscopic papillectomy (EP) remains unknown.

Research motivation

The post-EP resection margins of ampullary tumors are often positive or uncertain because of the burning effect of EP. The clinical outcomes of resected margin positive or uncertain cases after EP remains unknown. Decisions regarding the treatment course in such cases might differ among institutions and/or depend on each patient's condition.

Research objectives

To investigate the clinical outcomes of resected margin positive or uncertain cases after EP.

Research methods

Forty-one patients with ampullary tumors who underwent EP at Kobe University Hospital between January 2007 and October 2018 were included in this study. The clinical outcomes of each EP cases were retrospectively investigated.

Research results

The resected margins were positive or uncertain in 24 patients (53.3%). Of these cases, 15 and 9 were diagnosed as adenoma and adenocarcinoma, respectively. Local tumor recurrence was detected in 3 cases. All of the recurrent tumors were successfully treated with argon plasma coagulation (APC). There was no local or lymph node recurrence after the APC. The post-APC follow-up periods lasted for 57.1 mo to 133.8 mo. No ampullary tumor-related deaths occurred in all patients.

Research conclusions

In conclusion, resected margin positive or uncertain cases after EP could be managed by endoscopic treatment including APC, even in cases of adenocarcinoma.

Research perspectives

Our results might help to determine appropriate indications for EP, including for cases of early stage ampullary carcinoma. A further large-scale prospective study will be needed in the future.

REFERENCES

- 1 Li S, Wang Z, Cai F, Linghu E, Sun G, Wang X, Meng J, Du H, Yang Y, Li W. New experience of endoscopic papillectomy for ampullary neoplasms and other interventional techniques. *Surg Endosc* 2018; Epub ahead of print
- 2 De Palma GD, Luglio G, Maione F, Esposito D, Siciliano S, Gennarelli N, Cassese G, Persico M, Forestieri P. Endoscopic snare papillectomy: a single institutional experience of a standardized technique. A retrospective cohort study. *Int J Surg* 2015; **13**: 180-183 [PMID: 25498490 DOI: 10.1016/j.ijsu.2014.11.045]
- 3 Yeo CJ, Cameron JL, Sohn TA, Lillemoe KD, Pitt HA, Talamini MA, Hruban RH, Ord SE, Sauter PK, Coleman J, Zahurak ML, Grochow LB, Abrams RA. Six hundred fifty consecutive pancreaticoduodenectomies in the 1990s: pathology, complications, and outcomes. *Ann Surg* 1997; **226**: 248-57; discussion 257-60 [PMID: 9339931 DOI: 10.1097/0000658-199709000-00004]
- 4 Böttger TC, Junginger T. Factors influencing morbidity and mortality after pancreaticoduodenectomy: critical analysis of 221 resections. *World J Surg* 1999; **23**: 164-171; discussion 171-172 [PMID: 9880426]
- 5 Ardengh JC, Kemp R, Lima-Filho ER, Dos Santos JS. Endoscopic papillectomy: The limits of the indication, technique and results. *World J Gastrointest Endosc* 2015; **7**: 987-994 [PMID: 26265992 DOI: 10.4253/wjge.v7.i10.987]
- 6 Ceppa EP, Burbridge RA, Rialon KL, Omotosho PA, Emick D, Jowell PS, Branch MS, Pappas TN. Endoscopic versus surgical ampullectomy: an algorithm to treat disease of the ampulla of Vater. *Ann Surg* 2013; **257**: 315-322 [PMID: 23059497 DOI: 10.1097/SLA.0b013e318269d010]
- 7 Okano N, Igarashi Y, Hara S, Takuma K, Kamata I, Kishimoto Y, Mimura T, Ito K, Sumino Y. Endosonographic preoperative evaluation for tumors of the ampulla of Vater using endoscopic ultrasonography and intraductal ultrasonography. *Clin Endosc* 2014; **47**: 174-177 [PMID: 24765600 DOI: 10.5946/ce.2014.47.2.174]
- 8 Riditid W, Schmidt SE, Al-Haddad MA, LeBlanc J, DeWitt JM, McHenry L, Fogel EL, Watkins JL, Lehman GA, Sherman S, Coté GA. Performance characteristics of EUS for locoregional evaluation of ampullary lesions. *Gastrointest Endosc* 2015; **81**: 380-388 [PMID: 25293823 DOI: 10.1016/j.gie.2014.08.005]
- 9 Ito K, Fujita N, Noda Y, Kobayashi G, Obana T, Horaguchi J, Koshita S, Kanno Y, Ogawa T, Kato Y, Yamashita Y. Impact of technical modification of endoscopic papillectomy for ampullary neoplasm on the occurrence of complications. *Dig Endosc* 2012; **24**: 30-35 [PMID: 22211409 DOI: 10.1111/j.1443-1661.2011.01161.x]
- 10 Alvarez-Sanchez MV, Oria I, Luna OB, Píalat J, Gincul R, Lefort C, Bourdariat R, Fumex F, Lepilliez V, Scoazec JY, Salgado-Barreira A, Lemaistre AI, Napoléon B. Can endoscopic papillectomy be curative for early ampullary adenocarcinoma of the ampulla of Vater? *Surg Endosc* 2017; **31**: 1564-1572 [PMID: 27530895 DOI: 10.1007/s00464-016-5141-1]
- 11 Hornick JR, Johnston FM, Simon PO, Younkin M, Chamberlin M, Mitchem JB, Azar RR, Linehan DC, Strasberg SM, Edmundowicz SA, Hawkins WG. A single-institution review of 157 patients presenting with benign and malignant tumors of the ampulla of Vater: management and outcomes. *Surgery* 2011; **150**: 169-176 [PMID: 21801957 DOI: 10.1016/j.surg.2011.05.012]
- 12 Amini A, Miura JT, Jayakrishnan TT, Johnston FM, Tsai S, Christians KK, Gamblin TC, Turaga KK. Is local resection adequate for T1 stage ampullary cancer? *HPB (Oxford)* 2015; **17**: 66-71 [PMID: 25395092 DOI: 10.1111/hpb.12297]
- 13 You D, Heo J, Choi S, Choi D, Jang KT. Pathologic T1 subclassification of ampullary carcinoma with perisphincteric or duodenal submucosal invasion: Is it T1b? *Arch Pathol Lab Med* 2014; **138**: 1072-1076

- [PMID: 25076296 DOI: 10.5858/arpa.2013-0324-OA]
- 14 **Kawabata Y**, Ishikawa N, Moriyama I, Tajima Y. What is an adequate surgical management for Tis and pT1 early ampullary carcinoma? *Hepatogastroenterology* 2014; **61**: 12-17
 - 15 **Yamamoto K**, Itoi T, Sofuni A, Tsuchiya T, Tanaka R, Tonoizuka R, Honjo M, Mukai S, Fujita M, Asai Y, Matsunami Y, Kurosawa T, Yamaguchi H, Nagakawa Y. Expanding the indication of endoscopic papillectomy for T1a ampullary carcinoma. *Dig Endosc* 2018; Epub ahead of print [PMID: 30161275 DOI: 10.1111/den.13265]
 - 16 **Miyazaki M**, Ohtsuka M, Miyakawa S, Nagino M, Yamamoto M, Kokudo N, Sano K, Endo I, Unno M, Chijiwa K, Horiguchi A, Kinoshita H, Oka M, Kubota K, Sugiyama M, Uemoto S, Shimada M, Suzuki Y, Inui K, Tazuma S, Furuse J, Yanagisawa A, Nakanuma Y, Kijima H, Takada T. Classification of biliary tract cancers established by the Japanese Society of Hepato-Biliary-Pancreatic Surgery: 3(rd) English edition. *J Hepatobiliary Pancreat Sci* 2015; **22**: 181-196 [PMID: 25691463 DOI: 10.1002/jhbp.211]
 - 17 **Kang SH**, Kim KH, Kim TN, Jung MK, Cho CM, Cho KB, Han JM, Kim HG, Kim HS. Therapeutic outcomes of endoscopic papillectomy for ampullary neoplasms: retrospective analysis of a multicenter study. *BMC Gastroenterol* 2017; **17**: 69 [PMID: 28558658 DOI: 10.1186/s12876-017-0626-5]
 - 18 **Catalano MF**, Linder JD, Chak A, Sivak MV, Rajman I, Geenen JE, Howell DA. Endoscopic management of adenoma of the major duodenal papilla. *Gastrointest Endosc* 2004; **59**: 225-232 [PMID: 14745396 DOI: 10.1016/S0016-5107(03)02366-6]
 - 19 **Cheng CL**, Sherman S, Fogel EL, McHenry L, Watkins JL, Fukushima T, Howard TJ, Lazzell-Pannell L, Lehman GA. Endoscopic snare papillectomy for tumors of the duodenal papillae. *Gastrointest Endosc* 2004; **60**: 757-764 [PMID: 15557951 DOI: 10.1016/S0016-5107(04)02029-2]
 - 20 **Bohnacker S**, Seitz U, Nguyen D, Thonke F, Seewald S, deWeerth A, Ponnudurai R, Omar S, Soehendra N. Endoscopic resection of benign tumors of the duodenal papilla without and with intraductal growth. *Gastrointest Endosc* 2005; **62**: 551-560 [PMID: 16185970 DOI: 10.1016/j.gie.2005.04.053]
 - 21 **Riditid W**, Tan D, Schmidt SE, Fogel EL, McHenry L, Watkins JL, Lehman GA, Sherman S, Coté GA. Endoscopic papillectomy: risk factors for incomplete resection and recurrence during long-term follow-up. *Gastrointest Endosc* 2014; **79**: 289-296 [PMID: 24094466 DOI: 10.1016/j.gie.2013.08.006]
 - 22 **Nam K**, Song TJ, Kim RE, Cho DH, Cho MK, Oh D, Park DH, Lee SS, Seo DW, Lee SK, Kim MH, Baek S. Usefulness of argon plasma coagulation ablation subsequent to endoscopic snare papillectomy for ampullary adenoma. *Dig Endosc* 2018; **30**: 485-492 [PMID: 29288506 DOI: 10.1111/den.13008]
 - 23 **Harewood GC**, Pochron NL, Gostout CJ. Prospective, randomized, controlled trial of prophylactic pancreatic stent placement for endoscopic snare excision of the duodenal ampulla. *Gastrointest Endosc* 2005; **62**: 367-370 [PMID: 16111953 DOI: 10.1016/j.gie.2005.04.020]

P- Reviewer: Haraldsson E, Luglio G, Ramia JM, Yang Z

S- Editor: Ma RY **L- Editor:** Filipodia **E- Editor:** Huang Y





Retrospective Study

Serum Mac-2 binding protein glycosylation isomer level predicts hepatocellular carcinoma development in E-negative chronic hepatitis B patients

Lung-Yi Mak, Wai-Pan To, Danny Ka-Ho Wong, James Fung, Fen Liu, Wai-Kay Seto, Ching-Lung Lai, Man-Fung Yuen

ORCID number: Lung-Yi Mak

(0000-0002-2266-3935);

Danny Ka-Ho Wong

(0000-0001-9078-5005); James Fung

(0000-0002-1286-8902);

Wai-Kay Seto

(0000-0002-9012-313X); Ching-Lung

Lai (0000-0002-5927-2436); Man-

Fung Yuen (0000-0001-7985-7725).

Author contributions: Mak LY and To WP were involved in drafting the manuscript. Wong DKH was involved in performing laboratory tests and collecting the data. Fung J was involved in data acquisition, statistical analysis, and language editing of the manuscript. Seto WK was involved in interpretation of the data and critical revision of the manuscript. Lai CL was involved in critical revision of the manuscript. Yuen MF was involved in study concept and design, analysis and interpretation of data, critical revision of manuscript, and overall study supervision. All authors have approved the final draft submitted.

Institutional review board

statement: This study was reviewed and approved by the Institutional Review Board/ Ethics Committee of the University of Hong Kong and the Hong Kong West Cluster of Hospital Authority.

Informed consent statement:

Patients were not required to give informed consent to the study because the analysis used

Lung-Yi Mak, Wai-Pan To, James Fung, Department of Medicine, Queen Mary Hospital, Hong Kong, China

Danny Ka-Ho Wong, Fen Liu, Wai-Kay Seto, Ching-Lung Lai, Man-Fung Yuen, Department of Medicine, The University of Hong Kong, Hong Kong, China

Danny Ka-Ho Wong, James Fung, Wai-Kay Seto, Ching-Lung Lai, Man-Fung Yuen, State Key Laboratory for Liver Research, The University of Hong Kong, Hong Kong, China

Corresponding author: Man-Fung Yuen, DSc, FRCP (C), MBBS, MD, MRCP, PhD, Professor, Department of Medicine, Queen Mary Hospital, The University of Hong Kong, Pokfulam Road 102, Hong Kong, China. mfyuen@hkucc.hku.hk

Telephone: +86-852-22553994

Fax: +86-852-28162863

Abstract

BACKGROUND

Liver cirrhosis is a major risk factor for hepatocellular carcinoma (HCC) development in chronic hepatitis B (CHB). Serum Mac-2 binding protein glycosylation isomer (M2BPGi) is a novel serological marker for fibrosis. The role of M2BPGi in prediction of HCC is unknown.

AIM

To examine the role of serum M2BPGi in predicting HCC development in hepatitis B e antigen (HBeAg)-negative patients.

METHODS

Treatment-naïve CHB patients with documented spontaneous HBeAg seroconversion were recruited. Serum M2BPGi was measured at baseline (within 3 years from HBeAg seroconversion), at 5 years and 10 years after HBeAg seroconversion and expressed as cut-off index (COI). Multivariate cox regression was performed to identify predictors for HCC development. ROC analysis was used to determine the cut-off value of M2BPGi.

RESULTS

Among 207 patients (57% male, median age at HBeAg seroconversion 40 years old) with median follow-up of 13.1 (11.8-15.5) years, the cumulative incidence of

anonymous clinical data and stored serum samples that were obtained after each patient agreed to such storage for clinical research by informed consent in previous studies.

Conflict-of-interest statement: All authors declare no conflicts-of-interest related to this article.

Data sharing statement: No additional data are available.

Open-Access: This is an open-access article that was selected by an in-house editor and fully peer-reviewed by external reviewers. It is distributed in accordance with the Creative Commons Attribution Non Commercial (CC BY-NC 4.0) license, which permits others to distribute, remix, adapt, build upon this work non-commercially, and license their derivative works on different terms, provided the original work is properly cited and the use is non-commercial. See: <http://creativecommons.org/licenses/by-nc/4.0/>

Manuscript source: Unsolicited manuscript

Received: December 15, 2018

Peer-review started: December 17, 2018

First decision: January 6, 2019

Revised: January 22, 2019

Accepted: January 26, 2019

Article in press: January 26, 2019

Published online: March 21, 2019

HCC at 15 years was 7%. Median M2BPGi levels were significantly higher in patients with HCC compared to those without HCC (baseline: 1.39 COI *vs* 0.38 COI, $P < 0.001$; 5-year: 1.45 COI *vs* 0.47 COI, $P < 0.001$; 10-year: 1.20 COI *vs* 0.55 COI, $P = 0.001$). Multivariate analysis revealed age at HBeAg seroconversion [odds ratio (OR) = 1.196, 95% confidence interval (CI): 1.034-1.382, $P = 0.016$] and baseline M2BPGi (OR = 4.666, 95% CI: 1.296-16.802, $P = 0.018$) were significant factors predictive of HCC. Using a cut-off value of 0.68 COI, baseline M2BPGi yielded AUROC of 0.883 with 91.7% sensitivity and 80.8% specificity.

CONCLUSION

High serum M2BPGi within 3 years after HBeAg seroconversion was a strong predictor for subsequent HCC development in treatment-naïve HBeAg-negative CHB patients.

Key words: Hepatocellular carcinoma; Hepatitis B; Liver fibrosis; Mac-2 binding protein glycosylation isomer; Biomarker

©The Author(s) 2019. Published by Baishideng Publishing Group Inc. All rights reserved.

Core tip: Serum Mac-2 binding protein glycosylation isomer (M2BPGi) is a novel marker to assess severity of liver disease. The aim of this study was to assess its role in prediction of incident hepatocellular carcinoma (HCC) in patients with chronic hepatitis B who were prospectively followed-up for a median duration of 13.1 years. High serum M2BPGi increased HCC risk by 4-5 folds. If M2BPGi is below the threshold (0.68 cut-off index), there is > 99% chance that the patient will not develop liver cancer in the subsequent 15 years.

Citation: Mak LY, To WP, Wong DKH, Fung J, Liu F, Seto WK, Lai CL, Yuen MF. Serum Mac-2 binding protein glycosylation isomer level predicts hepatocellular carcinoma development in E-negative chronic hepatitis B patients. *World J Gastroenterol* 2019; 25(11): 1398-1408

URL: <https://www.wjgnet.com/1007-9327/full/v25/i11/1398.htm>

DOI: <https://dx.doi.org/10.3748/wjg.v25.i11.1398>

INTRODUCTION

As of year 2015, chronic hepatitis B virus infection (CHB) affects 257 million persons worldwide^[1]. It accounts for 50%-80% of all cases of hepatocellular carcinoma (HCC) globally^[2,3], which is the 5th most common cancer worldwide and still demonstrates rising incidence^[4,4]. Up to 15%-40% of hepatitis B virus (HBV) carriers will develop cirrhosis and/or HCC in their lifetime^[5,6]. Identifying CHB patients with high risk for HCC is essential for implementation of preventive measures, including initiation of antiviral therapy and regular surveillance for HCC.

Known risk factors for HCC in CHB patients include both host factors [*e.g.*, older age, male gender, genetic polymorphism, family history, presence of cirrhosis, co-existing chronic liver diseases, co-infection with hepatitis C virus (HCV) or human immunodeficiency virus (HIV)] and viral factors [*e.g.*, high HBV DNA levels, core promoter mutations]^[7-12]. Risk stratification models for prediction of HCC risk in CHB patients have been developed and validated, namely the REACH-B, GAG-HCC and CU-HCC^[13-15]. Common variables among these prediction scores include age, gender, HBV DNA, cirrhosis, liver biochemistries. Among these factors, diagnosis of cirrhosis is particularly prone to inter-observer variability due to the nature of qualitative assessment by imaging. Improving diagnostic accuracy of cirrhosis without histological assessment could be achieved by non-invasive means. Quantitative assessment with imaging-based (*e.g.*, liver stiffness measurement) or serum-based tests is increasingly used in estimating the severity of liver fibrosis for risk stratification.

Serum Mac-2 binding protein glycosylation isomer (M2BPGi), also known as Wisteria floribunda agglutinin positive Mac-2 binding protein (WFA⁺-M2BP), is a novel glycan-based marker for assessment of liver fibrosis^[16]. The sugar chain structure of M2BP changes correspondingly to progression of hepatic fibrosis. WFA, a

lectin used to recognize the altered glycan parts of M2BP, is detected by a lectin-antibody sandwich immunoassay and liver fibrosis can thus be quantified. Serum M2BPGi has recently been shown to be a reliable marker for diagnosing advanced liver fibrosis and cirrhosis in various liver diseases^[17-19]. The predictive value of M2BPGi for risk of HCC development has also been demonstrated in CHB patients^[20-23]. However, these studies were mostly retrospective with a relatively short duration of follow-up of ≤ 5 years. In addition, the patient population was heterogeneous, including both treatment-naïve and treatment-experienced patients. In the only study evaluating M2BPGi in treatment-naïve patients, serum M2BPGi higher than a pre-defined cut-off [≥ 2.0 cut-off index (COI)] was associated with higher risk of HCC^[22]. However, the serum M2BPGi levels in CHB patients may differ between populations with different ethnicity and disease stage and the cut-off values should be properly defined for each. Moreover, as the majority of HCC in CHB is diagnosed in Hepatitis B e antigen (HBeAg) negative patients^[24], the predictive value of M2BPGi in HBeAg negative patients should be investigated in a well-defined cohort. Therefore, the aim of this longitudinal study was to examine the relationship between serum M2BPGi and the development of HCC in treatment-naïve HBeAg-negative patients, and to define an optimal cut-off value for prediction of subsequent HCC development.

MATERIALS AND METHODS

Patients

The present study recruited CHB patients who were aged ≥ 18 years old and were managed in the Liver Clinics in Queen Mary Hospital, Hong Kong. All recruited patients had persistent positivity for serum HBV surface antigen (HBsAg) ≥ 6 mo, and were positive for HBeAg on presentation with subsequent documented spontaneous HBeAg seroconversion between year 2000-2007. Patients were excluded for the following conditions: co-infection with chronic HCV, HIV, excessive alcohol intake (≥ 30 g/d for male, ≥ 20 g/d for female), other chronic liver diseases (*e.g.*, primary biliary cholangitis, autoimmune hepatitis, Wilson's disease), history of treatment with antiviral agents, history of HCC, or other major medical comorbidities, *e.g.*, heart failure and pulmonary disease. Patients with incomplete clinical data or without retrievable serum samples were also excluded. A total of 207 patients were recruited for this study. All patients were treatment-naïve at recruitment. Subsequent antiviral therapy consisting of nucleos(t)ide analogues were initiated for either hepatitis flare [defined as alanine aminotransferase (ALT) > 2 times the upper limit of normal with serum HBV DNA > 2000 IU/mL] or development of liver-related complications (cirrhosis or HCC)^[25]. This study population was also examined for the role of hepatitis B core-related antigen (HBcrAg) on the HCC development in a previous study^[26]. The study protocol was approved by the Institutional Review Board/ Ethics Committee of the University of Hong Kong and the Hong Kong West Cluster of Hospital Authority. **Figure 1** depicts the patient disposition.

Clinical data and laboratory assessment

All recruited patients had regular clinic visits every 6 months or more frequently if clinically indicated. For the purpose of this study, the date of HBeAg seroconversion was defined as the start of follow-up. The end of follow-up was defined as the date of diagnosis of HCC, or the date of last clinic visit for patients without HCC development. Clinical parameters including age at presentation, age at HBeAg seroconversion and gender were documented. Blood tests including liver biochemistry and alpha-feto-protein (AFP) were measured at the time of HBeAg seroconversion and subsequent visits. Serum HBV DNA levels were measured at baseline by Cobas Taqman (Roche Diagnostics, Branchburg, NJ, United States) with lower limit of detection of 20 IU/mL.

Measurement of serum M2BPGi

Serum M2BPGi was measured using a chemiluminescent enzyme-linked immunoassay by two-step sandwich method and the details of the test were reported elsewhere^[18]. Briefly, serum M2BPGi was measured by HISCL M2BPGi reagent kit (Sysmex, Hyogo, Japan) on an automatic immunoanalyzer HISCL-800 (Sysmex, Hyogo, Japan). Serum M2BPGi level was expressed as COI. Serum M2BPGi level was measured at 3 time points: at baseline (defined as within 3 years after HBeAg seroconversion), at 5 years and at 10 years after HBeAg seroconversion.

Radiological assessment

Regular 6 monthly ultrasonography of the hepatobiliary system was advised to all

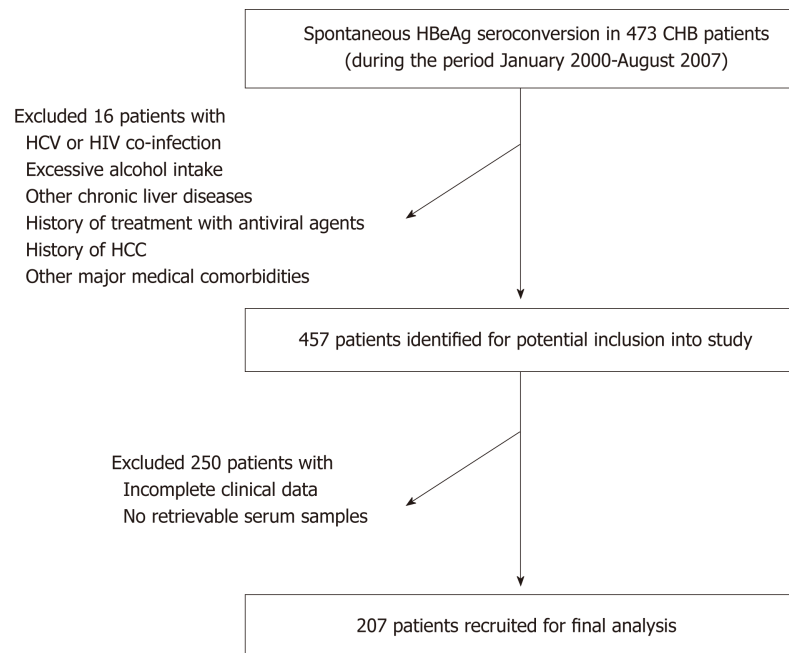


Figure 1 Patient disposition. CHB: Chronic hepatitis B; HCC: Hepatocellular carcinoma; HCV: Hepatitis C virus; HBeAg: Hepatitis B e antigen; HIV: Human immunodeficiency virus.

patients and AFP levels were measured regularly at the interval of 3–6 mo. For those with abnormal AFP levels and/or abnormal ultrasound findings, contrast-enhanced imaging, either computerized tomography or magnetic resonance imaging would be arranged. HCC was diagnosed by the typical features of arterial phase hyper-enhancement and porto-venous washout of contrast, with or without histological proof. Cirrhosis was diagnosed in the presence of small nodular liver, splenomegaly or ascites.

Liver stiffness measurement

Liver stiffness measurement (LSM) was performed using Fibroscan (Echosens®, Paris, France). Liver stiffness (LS) was expressed as the median value of ≥ 10 successful acquisitions in units of kilopascals (kPa). LSM was only considered reliable with a success rate of $\geq 60\%$, combined with an interquartile range of $< 30\%$. The operator received prior formal training from Echosens® and had performed at least 500 transient elastography procedures. As the Fibroscan machine was only available in our centre since year 2006, LSM was performed at year 5 from HBeAg seroconversion. Advanced fibrosis was defined as $LS \geq 9$ kPa according to the European Association for Study of Liver, Asociación Latinoamericana para el Estudio del Hígado clinical guidelines^[27].

Statistical analysis

Continuous variables were expressed as median [interquartile range (IQR), as specified]. Mann-Whitney *U* test was used for comparison of median between 2 groups. Categorical variables, expressed as proportions, were compared using Chi-square test and Fisher's Exact test when appropriate. Pearson's correlations were performed to evaluate the relationship between LS and serum M2BPGi. To determine whether factors were independently associated with subsequent HCC development, variables with a $P < 0.05$ in univariate analyses were entered into multivariate analysis performed by binary logistic regression, with odds ratio (OR) and 95% confidence interval (CI) calculated. To evaluate the diagnostic performance of serum M2BPGi in predicting subsequent HCC development, receiver-operating characteristic (ROC) curve analysis was carried out. Diagnostic accuracy was expressed as the specificity, sensitivity, positive predictive value (PPV), negative predictive value (NPV), and area under the ROC curve (AUROC). The optimal cut-off values were obtained by maximizing the Youden's index. Kaplan-Meier survival analysis was used to compare the incidence of HCC using the derived M2BPGi cut-off value. A two-tailed P value of < 0.05 was considered statistically significant. All statistical analysis was performed using Statistical package for Social Sciences (SPSS) version 20.0 (SPSS Inc, Chicago, IL, United States). The statistical review of the study was performed by a biomedical statistician.

RESULTS

Baseline characteristics of the patients

The baseline characteristics of 207 enrolled patients were shown in Table 1. One-hundred and eighteen (57%) were male. The median age at HBeAg seroconversion was 40 (IQR: 34-45) years old. The median follow-up duration was 13.1 (IQR: 11.8-15.5) years. The median HBV DNA was 4.0 (IQR: 3-5.4) log IU/mL and the median ALT was 32 (IQR: 21-50) U/L. Seven patients (3.6%) had HBsAg seroclearance after a median duration of 6.4 years and none of them developed HCC. Subsequent antiviral therapy was initiated in 102 (49.3%) patients after a median duration of 5.5 years due to hepatitic flare or diagnosis of liver-related complications including cirrhosis and HCC. The details of the antiviral therapy are listed in Supplementary Table 1.

Markers of liver fibrosis and cirrhosis

The median serum M2BPGi at baseline, 5-year and 10-year was 0.42 (IQR: 0.27-0.68), 0.5 (IQR: 0.29-0.68) and 0.56 (0.38-0.76) COI, respectively. Cirrhosis was present in 35 (16.9%) patients at the end of follow-up. Compared to non-cirrhotic group, the median serum M2BPGi levels in the cirrhotic group were significantly higher at all 3 time points (0.38 COI *vs* 0.95 COI, 0.47 COI *vs* 1.23 COI, 0.54 COI *vs* 0.98 COI, respectively, $P < 0.001$ for all time points) (Figure 2). Among 167 patients with 5-year LSM, the median LS was 6.5 (5-8.8) kPa. Advanced fibrosis was present in 39 (23.4%) patients. The median LS at 5-year was significantly higher in the cirrhotic group than the non-cirrhotic group (14.4 kPa *vs* 6.1 kPa, $P < 0.001$). Serum M2BPGi at baseline and 5-year demonstrated linear correlations with LSM at 5-year ($r = 0.232$, $P = 0.009$ and $r = 0.563$, $P < 0.001$, respectively). Baseline serum M2BPGi level was significantly higher in patients with subsequent LSM at 5-year showing advanced fibrosis compared to those without (0.61 COI *vs* 0.37 COI, $P = 0.008$).

Since almost half patients were eventually started on antiviral therapy, it would be impractical to exclude these patients from subsequent analysis. Previous report stated that antiviral therapy would lead to decline in serum M2BPGi level and reduction in histological fibrosis^[18]. To address this issue, we performed additional analysis to compare the serum M2BPGi levels at 5-year and 10-year between those who were subsequently initiated with antiviral therapy. The median serum M2BPGi levels in patients requiring treatment compared to patients not requiring treatment were 0.50 (IQR: 0.37-0.71) COI *vs* 0.50 (IQR: 0.28-0.64) COI and 0.66 (IQR: 0.43-0.95) COI *vs* 0.52 (IQR: 0.34-0.62) COI at 5-year ($P = 0.167$) and 10-year ($P < 0.001$), respectively.

Factors associated with HCC development

Among 207 patients, HCC developed in 14 patients (6.8%) at a median of 4.7 (IQR: 2.7-8.9) years at median age of 59.1 years. The 5-year, 10-year and 15-year cumulative incidences of HCC were 3.9%, 5.9% and 7%, respectively.

Compared to patients without HCC development, HCC patients were older at HBeAg seroconversion (median age: 40 years old *vs* 52 years old, $P < 0.001$). HCC patients had higher baseline serum aspartate aminotransferase (AST, 44 U/L *vs* 24 U/L, $P = 0.002$), alanine aminotransferase (ALT, 61 U/L *vs* 27 U/L, $P = 0.007$), and gamma glutamyl transferase (GGT, 59 U/L *vs* 22 U/L, $P = 0.003$). The proportion of patients with cirrhosis was higher in the HCC group compared to non-HCC group (92.8% *vs* 11.4%, $P < 0.001$). The median serum M2BPGi at baseline, 5-year and 10-year were significantly higher in HCC group compared to non-HCC group (1.39 COI *vs* 0.38 COI, 1.45 COI *vs* 0.47 COI and 1.20 COI *vs* 0.55 COI, respectively; $P < 0.001$, $P < 0.001$ and $P = 0.001$, respectively) (Figure 3). The 5-year LS was significant higher in HCC group compared to non-HCC group (12.6 kPa *vs* 6.4 kPa, $P = 0.028$) (Table 2).

As more than half of HCC cases in this cohort developed between baseline and 5-year, multivariate analysis was only performed on baseline variables for association with subsequent HCC development. Multivariate analysis showed that age at HBeAg seroconversion (OR = 1.196, 95%CI: 1.034-1.382, $P = 0.016$) and baseline serum M2BPGi (OR = 4.666, 95%CI: 1.296-16.802, $P = 0.018$) were independent factors associated with HCC development (Table 2).

Performance characteristics of serum M2BPGi in prediction of HCC development

The AUROC of baseline serum M2BPGi for predicting subsequent HCC development was 0.883 (95%CI: 0.771-0.995, $P < 0.001$). The optimal cut-off value was 0.685 COI, which predicted HCC development with 91.7% sensitivity and 80.8% specificity. The PPV and NPV were 25.8% and 99.3%, respectively (Supplementary Figure 1).

The cumulative incidence of HCC at 15-year of follow-up was significantly higher in patients with baseline M2BPGi ≥ 0.68 COI compared to < 0.68 COI (29% *vs* 0.9%, respectively, $P < 0.001$) (Figure 4).

Table 1 Baseline demographics of the 207 patients

Characteristics	Value
Gender (male, %)	118 (57%)
Age of HBeAg seroconversion (yr)	40 (34-45) ¹
Follow-up duration (yr)	13.1 (11.8-15.5) ¹
Liver biochemistry	
Bilirubin (μmol/L)	12 (9-16) ¹
ALP (U/L)	69 (57-82) ¹
AST (U/L)	29 (23-37) ¹
ALT (U/L)	32 (21-50) ¹
GGT (U/L)	23 (16-36) ¹
Albumin (g/dL)	43 (41-45) ¹
Globulin	34 (31-36) ¹
AFP (ng/mL)	4 (3-7) ¹
HBV DNA (log IU/mL)	4 (3-5.4) ¹
Baseline M2BPGi	0.42 (0.27-0.68) ¹

¹Median and values in brackets represented interquartile range. AFP: Alpha feto protein; ALP: Alkaline phosphatase; ALT: Alanine aminotransferase; AST: Aspartate aminotransferase; GGT: Gamma glutamyl transferase; HBV: Hepatitis B virus; HBeAg: Hepatitis B e antigen; M2BPGi: Mac-2 binding protein glycosylation isomer.

DISCUSSION

The present longitudinal study investigated a homogenous CHB patient population with a well-defined time point of HBeAg seroconversion, with a median follow-up length of 13.1 years representing a relatively long duration of follow up in the existing literature regarding risk prediction for HCC development in such a population. HCC development was shown to be highly predictable by baseline serum M2BPGi (OR = 4.666). Serum M2BPGi provides an objective quantitative assessment of liver fibrosis, rather than qualitative sonographic features. In comparison, sonographic diagnosis of cirrhosis was not a significant factor for HCC development upon multivariate analysis ($P = 0.239$), highlighting the limitations of qualitative assessment. Although 5-year LSM and 5-year M2BPGi were not included in the multivariate analysis, they showed good linear correlation with each other ($r = 0.563$, $P < 0.001$). Baseline M2BPGi also dictated advanced liver fibrosis at subsequent 5-year LSM ($P = 0.008$). It would be of great interest for future studies to determine whether a combined M2BPGi and fibroscan measurement at baseline would further enhance the predictability for HCC development.

The cut-off value of baseline serum M2BPGi was derived by established statistical methods with an excellent performance (AUROC = 0.883). Using a cut-off value of 0.68 COI, the sensitivity and specificity was > 90% and > 80%, respectively, with very high NPV (99.3%). The low PPV (25.8%) was mainly related to the relatively low incidence of HCC in this HBeAg negative cohort and is not unexpected from their inactive disease profile. In view of such, serum M2BPGi would be useful to exclude patients with low risk of HCC. As LSM has been incorporated into HCC prediction scores^[28], combining other markers for liver fibrosis, like M2BPGi, into risk prediction models should also be explored.

Apart from baseline M2BPGi, older age at HBeAg seroconversion (OR = 1.196) was another independent factor associated with the development of HCC. This is consistent with previous reports that the risk of HCC was higher if spontaneous HBeAg seroconversion occurred at an older age^[29,30]. As HBeAg seroconversion marks the transition from immune active phase to residual low replicative phase of CHB^[31,32], patients with late HBeAg seroconversion might experience more cumulative liver insult from more active viral replication during the longer HBeAg positive immune active phase compared to patients who had HBeAg seroconversion at a younger age.

In this study, a few known risk factors were not statistically significant variables for subsequent HCC development. The patients in this study were all treatment-naïve at the time of recruitment, implying a relatively inactive disease profile. Expectantly, both groups (HCC and non-HCC) had relatively low viral load at the time of HBeAg seroconversion (HBV DNA 4.6 and 4.0 log IU/mL, respectively). Similarly, serum albumin in both groups were in the normal range (43 and 44 g/L, respectively),

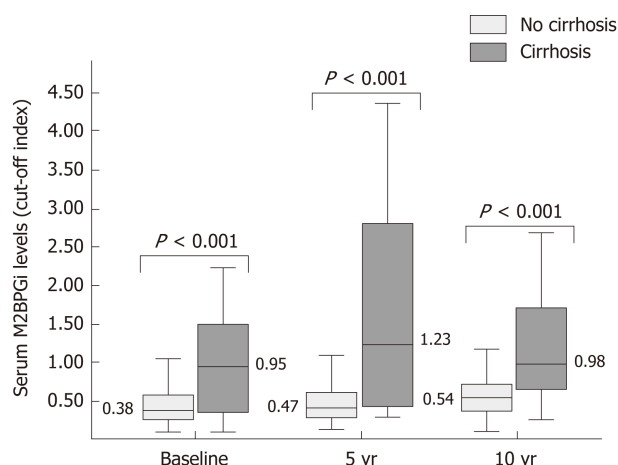


Figure 2 Serum Mac-2 binding protein glycosylation isomer levels at baseline, 5 years and 10 years after hepatitis B e antigen seroconversion according to presence of cirrhosis. Boxplot: Horizontal lines, colored bars and error bars represent median, interquartile range and 95% confidence interval, respectively. M2BPGi: Mac-2 binding protein glycosylation isomer.

indicating preserved liver synthetic function in this selected population. The lack of statistical significance for male gender in this study might be related to the small sample size and low number of patients with HCC. A higher proportion of patients who subsequently developed HCC were initiated with antiviral therapy compared to patients who did not develop HCC (71.4% *vs* 47.7% for non-HCC, $P = 0.102$). Although statistical significance was not reached, those that did not need antiviral therapy may intrinsically have a better disease profile with more favourable virological and biochemical characteristics^[30], which accounted for an apparently lower risk of HCC in those who do not require antiviral therapy.

Antiviral treatment cannot be withheld if treatment indications were reached, including not only hepatitic flare but also development of cirrhosis or HCC. Therefore, 49.3% of patients in this study eventually received treatment at a median duration of 5.5 years. We showed that subsequent antiviral therapy did not significantly change the serum M2BPGi levels at 5-year, probably related to the short duration of treatment. Paradoxically, the median M2BPGi level was significantly higher at 10-year in those requiring antiviral treatment compared to those who did not (0.66 *vs* 0.52, $P < 0.001$). This reflects the intrinsically more advanced liver disease in those requiring antiviral treatment. As the timing of antiviral therapy initiation was heterogenous (IQR: 2.7-8.6 years after recruitment), it is difficult to assess the effect of antiviral therapy on fibrosis regression, taking into consideration the differences in the severity of liver disease accumulated at the timing of therapy. Therefore, the differences in serum M2BPGi levels between HCC and non-HCC group at 5-year and 10-year could not be explained by antiviral therapy alone.

There are a few limitations in the present study. Firstly, platelet counts were not available, precluding the use of other serum-based indices for fibrosis assessment (*e.g.*, FIB-4, APRI). Secondly, viral factors including HBV genotype and specific mutations - known risk factors for HCC development - were not included in the analysis. Thirdly, due to the low number of HCC cases at 5-year ($n = 8$) and 10-year ($n = 3$), 5-year and 10-year serum M2BPGi as well as 5-year LS were not included in multivariate analysis. Larger scale studies including more patients would be needed to evaluate the role of longitudinal assessment of these markers in HCC risk prediction.

In summary, serum M2BPGi accurately predicted subsequent HCC development in treatment-naïve HBeAg-negative CHB patients across a long-term follow-up duration. The derived cut-off value of serum M2BPGi would be a valuable tool for risk stratification regarding HCC risk prediction.

Table 2 Factors associated with development of hepatocellular carcinoma in 207 treatment-naïve chronic hepatitis B patients

	Univariate analysis			Multivariate analysis		
	HCC (<i>n</i> = 14)	No HCC (<i>n</i> = 193)	<i>P</i> value	OR	95%CI	<i>P</i> value
Gender (being male, %)	10 (71.4%)	108 (56%)	0.403			
Age of HBeAg seroconversion (yr)	53	39	< 0.001	1.196	1.034-1.382	0.016
Bilirubin (μmol/L)	11	10	0.797			
ALP (U/L)	74	58	0.177			
AST (U/L)	44	24	0.002	1.042	0.906-1.199	0.564
ALT (U/L)	61	27	0.007	1.030	0.969-1.094	0.347
GGT (U/L)	59	22	0.003	0.981	0.932-1.033	0.471
Albumin (g/L)	43	44	0.427			
Globulin	36	34	0.157			
AFP (ng/mL)	4	3	0.587			
HBV DNA (log IU/mL)	4.6	4.0	0.446			
Baseline M2BPGi (COI)	1.39	0.38	< 0.001	4.666	1.296-16.802	0.018
5-year M2BPGi (COI)	1.45	0.47	< 0.001			
10-year M2BPGi (COI)	1.2	0.55	0.001			
5-year LS (kPa)	12.6	6.4	0.028			
Cirrhosis (%)	13 (92.8%)	22 (11.4%)	< 0.001	7.142	0.270-188.693	0.239
Treatment after HBeAg seroconversion	10 (71.4%)	92 (47.7%)	0.102			
HBsAg seroclearance (%)	0 (0%)	7 (3.6%)	0.608			

AFP: Alpha feto protein; ALP: Alkaline phosphatase; ALT: Alanine aminotransferase; AST: Aspartate aminotransferase; CI: Confidence interval; GGT: Gamma glutamyl transferase; HCC: Hepatocellular carcinoma; HBV: Hepatitis B virus; HBeAg: Hepatitis B e antigen; HBsAg: Hepatitis B surface antigen; LS: Liver stiffness; M2BPGi: Mac-2 binding protein glycosylation isomer; OR: Odds ratio.

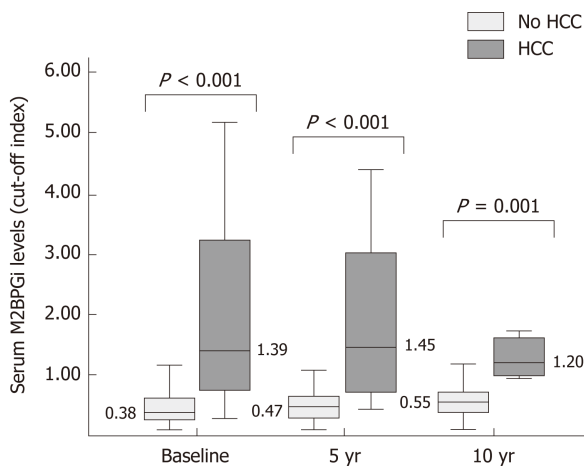


Figure 3 Serum Mac-2 binding protein glycosylation isomer levels at baseline, 5 years and 10 years after hepatitis B e antigen seroconversion in patients with or without subsequent development of hepatocellular carcinoma. Boxplot: Horizontal lines, colored bars and error bars represent median, interquartile range and 95% confidence interval, respectively. HCC: Hepatocellular carcinoma; M2BPGi: Mac-2 binding protein glycosylation isomer.

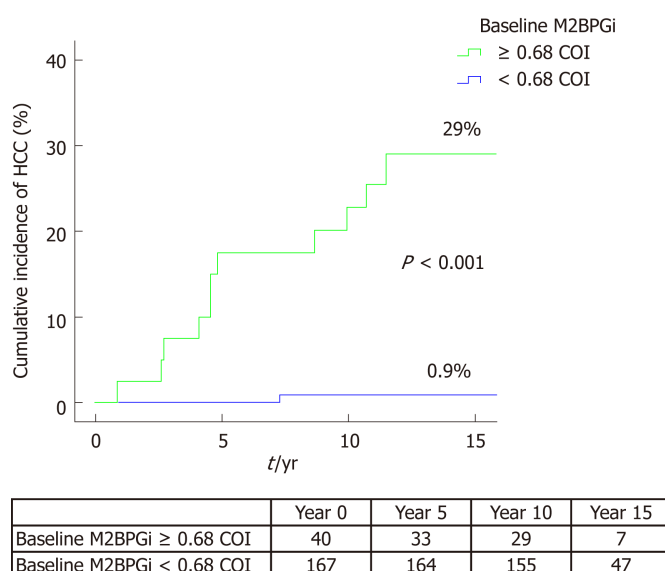


Figure 4 Cumulative incidence of hepatocellular carcinoma according to baseline serum Mac-2 binding protein glycosylation isomer level. COI: Cut-off index; HCC: Hepatocellular carcinoma; M2BPGi: Mac-2 binding protein glycosylation isomer.

ARTICLE HIGHLIGHTS

Research background

Hepatocellular carcinoma (HCC) is the most dreadful complication of chronic hepatitis B infection (CHB). Recent research showed that serum Mac-2 binding protein glycosylation isomer (M2BPGi) is a novel biomarker for liver fibrosis and cirrhosis, and preliminary studies reported its potential role in predicting risk of HCC in both untreated and treated patients.

Research motivation

The current literature has limited data on the role of serum M2BPGi in predicting risk of HCC in patients with hepatitis B e antigen (HBeAg) seroconversion (HBeAg-negative disease), and studies with long-term follow-up are lacking.

Research objectives

We would like to know if serum M2BPGi can predict subsequent HCC development in untreated CHB patients who underwent HBeAg seroconversion.

Research methods

This is a retrospective study by a tertiary center in Hong Kong. Treatment-naïve patients with documented spontaneous HBeAg seroconversion were recruited. Serum M2BPGi was measured at baseline, at 5-years and 10-years from HBeAg-seroconversion. We investigated the relationship between serum M2BPGi levels and subsequent HCC development.

Research results

The cumulative HCC incidence at 15 years was 7% among 207 recruited patients (median follow-up of 13.1 years). Serum M2BPGi was significantly higher in patients with HCC compared to those without HCC at all 3 time points (all $P < 0.01$). Baseline serum M2BPGi was significantly associated with HCC development (odds ratio of 4.666, $P = 0.018$). The area under the receiver operating characteristics curve for baseline M2BPGi was 0.883, with sensitivity and specificity of 91.7% and 80.8%, respectively, when the derived cut-off value of 0.68 cut-off index was used to predict HCC development.

Research conclusions

High serum M2BPGi level at HBeAg seroconversion was a strong predictor for subsequent HCC development in CHB patients.

Research perspectives

The derived cut-off value of serum M2BPGi would be a valuable tool for risk stratification regarding HCC risk prediction. Further validation studies are warranted.

REFERENCES

- 1 Lam YF, Seto WK, Wong D, Cheung KS, Fung J, Mak LY, Yuen J, Chong CK, Lai CL, Yuen MF. Seven-Year Treatment Outcome of Entecavir in a Real-World Cohort: Effects on Clinical Parameters,

- HBsAg and HBcrAg Levels. *Clin Transl Gastroenterol* 2017; **8**: e125 [PMID: 29072673 DOI: 10.1038/ctg.2017.51]
- 2 **Yuen MF**, Hou JL, Chutaputti A; Asia Pacific Working Party on Prevention of Hepatocellular Carcinoma. Hepatocellular carcinoma in the Asia pacific region. *J Gastroenterol Hepatol* 2009; **24**: 346-353 [PMID: 19220670 DOI: 10.1111/j.1440-1746.2009.05784.x]
 - 3 **Parkin DM**. The global health burden of infection-associated cancers in the year 2002. *Int J Cancer* 2006; **118**: 3030-3044 [PMID: 16404738 DOI: 10.1002/ijc.21731]
 - 4 **Petrick JL**, Kelly SP, Altekruse SF, McGlynn KA, Rosenberg PS. Future of Hepatocellular Carcinoma Incidence in the United States Forecast Through 2030. *J Clin Oncol* 2016; **34**: 1787-1794 [PMID: 27044939 DOI: 10.1200/JCO.2015.64.7412]
 - 5 **Fattovich G**, Stroffolini T, Zagni I, Donato F. Hepatocellular carcinoma in cirrhosis: incidence and risk factors. *Gastroenterology* 2004; **127**: S35-S50 [PMID: 15508101]
 - 6 **Lok AS**. Chronic hepatitis B. *N Engl J Med* 2002; **346**: 1682-1683 [PMID: 12037146 DOI: 10.1056/NEJM200205303462202]
 - 7 **Yuen MF**, Yuan HJ, Wong DK, Yuen JC, Wong WM, Chan AO, Wong BC, Lai KC, Lai CL. Prognostic determinants for chronic hepatitis B in Asians: therapeutic implications. *Gut* 2005; **54**: 1610-1614 [PMID: 15871997 DOI: 10.1136/gut.2005.065136]
 - 8 **Yuen MF**, Tanaka Y, Shinkai N, Poon RT, But DY, Fong DY, Fung J, Wong DK, Yuen JC, Mizokami M, Lai CL. Risk for hepatocellular carcinoma with respect to hepatitis B virus genotypes B/C, specific mutations of enhancer II/core promoter/precore regions and HBV DNA levels. *Gut* 2008; **57**: 98-102 [PMID: 17483190 DOI: 10.1136/gut.2007.119859]
 - 9 **Varbobitis I**, Papatheodoridis GV. The assessment of hepatocellular carcinoma risk in patients with chronic hepatitis B under antiviral therapy. *Clin Mol Hepatol* 2016; **22**: 319-326 [PMID: 27729632 DOI: 10.3350/cmh.2016.0045]
 - 10 **Chen CJ**, Yang HI, Su J, Jen CL, You SL, Lu SN, Huang GT, Iloeje UH; REVEAL-HBV Study Group. Risk of hepatocellular carcinoma across a biological gradient of serum hepatitis B virus DNA level. *JAMA* 2006; **295**: 65-73 [PMID: 16391218 DOI: 10.1001/jama.295.1.65]
 - 11 **Zhang H**, Zhai Y, Hu Z, Wu C, Qian J, Jia W, Ma F, Huang W, Yu L, Yue W, Wang Z, Li P, Zhang Y, Liang R, Wei Z, Cui Y, Xie W, Cai M, Yu X, Yuan Y, Xia X, Zhang X, Yang H, Qiu W, Yang J, Gong F, Chen M, Shen H, Lin D, Zeng YX, He F, Zhou G. Genome-wide association study identifies 1p36.22 as a new susceptibility locus for hepatocellular carcinoma in chronic hepatitis B virus carriers. *Nat Genet* 2010; **42**: 755-758 [PMID: 20676096 DOI: 10.1038/ng.638]
 - 12 **El-Serag HB**. Hepatocellular carcinoma. *N Engl J Med* 2011; **365**: 1118-1127 [PMID: 21992124 DOI: 10.1056/NEJMra1001683]
 - 13 **Yang HI**, Yuen MF, Chan HL, Han KH, Chen PJ, Kim DY, Ahn SH, Chen CJ, Wong VW, Seto WK; REACH-B Working Group. Risk estimation for hepatocellular carcinoma in chronic hepatitis B (REACH-B): development and validation of a predictive score. *Lancet Oncol* 2011; **12**: 568-574 [PMID: 21497551 DOI: 10.1016/S1470-2045(11)70077-8]
 - 14 **Yuen MF**, Tanaka Y, Fong DY, Fung J, Wong DK, Yuen JC, But DY, Chan AO, Wong BC, Mizokami M, Lai CL. Independent risk factors and predictive score for the development of hepatocellular carcinoma in chronic hepatitis B. *J Hepatol* 2009; **50**: 80-88 [PMID: 18977053 DOI: 10.1016/j.jhep.2008.07.023]
 - 15 **Wong VW**, Chan SL, Mo F, Chan TC, Loong HH, Wong GL, Lui YY, Chan AT, Sung JJ, Yeo W, Chan HL, Mok TS. Clinical scoring system to predict hepatocellular carcinoma in chronic hepatitis B carriers. *J Clin Oncol* 2010; **28**: 1660-1665 [PMID: 20194845 DOI: 10.1200/JCO.2009.26.2675]
 - 16 **Kuno A**, Sato T, Shimazaki H, Unno S, Saitou K, Kiyohara K, Sogabe M, Tsuruno C, Takahama Y, Ikehara Y, Narimatsu H. Reconstruction of a robust glycodiagnostic agent supported by multiple lectin-assisted glycan profiling. *Proteomics Clin Appl* 2013; **7**: 642-647 [PMID: 23640794 DOI: 10.1002/prca.201300010]
 - 17 **Kuno A**, Ikehara Y, Tanaka Y, Ito K, Matsuda A, Sekiya S, Hige S, Sakamoto M, Kage M, Mizokami M, Narimatsu H. A serum "sweet-doughnut" protein facilitates fibrosis evaluation and therapy assessment in patients with viral hepatitis. *Sci Rep* 2013; **3**: 1065 [PMID: 23323209 DOI: 10.1038/srep01065]
 - 18 **Mak LY**, Wong DK, Cheung KS, Seto WK, Lai CL, Yuen MF. Role of serum M2BPGi levels on diagnosing significant liver fibrosis and cirrhosis in treated patients with chronic hepatitis B virus infection. *Clin Transl Gastroenterol* 2018; **9**: 163 [PMID: 29915243 DOI: 10.1038/s41424-018-0020-9]
 - 19 **Toshima T**, Shirabe K, Ikegami T, Yoshizumi T, Kuno A, Togayachi A, Gotoh M, Narimatsu H, Korenaga M, Mizokami M, Nishie A, Aishima S, Maehara Y. A novel serum marker, glycosylated Wisteria floribunda agglutinin-positive Mac-2 binding protein (WFA(+)-M2BP), for assessing liver fibrosis. *J Gastroenterol* 2015; **50**: 76-84 [PMID: 24603981 DOI: 10.1007/s00535-014-0946-y]
 - 20 **Kim SU**, Heo JY, Kim BK, Park JY, Kim DY, Han KH, Ahn SH, Kim HS. Wisteria floribunda agglutinin-positive human Mac-2 binding protein predicts the risk of HBV-related liver cancer development. *Liver Int* 2017; **37**: 879-887 [PMID: 27973711 DOI: 10.1111/liv.13341]
 - 21 **Cheung KS**, Seto WK, Wong DK, Mak LY, Lai CL, Yuen MF. Wisteria floribunda agglutinin-positive human Mac-2 binding protein predicts liver cancer development in chronic hepatitis B patients under antiviral treatment. *Oncotarget* 2017; **8**: 47507-47517 [PMID: 28537900 DOI: 10.18632/oncotarget.17670]
 - 22 **Liu J**, Hu HH, Lee MH, Korenaga M, Jen CL, Batrla-Utermann R, Lu SN, Wang LY, Mizokami M, Chen CJ, Yang HI. Serum Levels of M2BPGi as Short-Term Predictors of Hepatocellular Carcinoma in Untreated Chronic Hepatitis B Patients. *Sci Rep* 2017; **7**: 14352 [PMID: 29085039 DOI: 10.1038/s41598-017-14747-5]
 - 23 **Heo JY**, Kim SU, Kim BK, Park JY, Kim DY, Ahn SH, Park YN, Ahn SS, Han KH, Kim HS. Use of Wisteria Floribunda Agglutinin-Positive Human Mac-2 Binding Protein in Assessing Risk of Hepatocellular Carcinoma Due to Hepatitis B Virus. *Medicine (Baltimore)* 2016; **95**: e3328 [PMID: 27922546 DOI: 10.1097/MD.0000000000003328]
 - 24 **Yuen MF**, Lai CL. Natural history of chronic hepatitis B virus infection. *J Gastroenterol Hepatol* 2000; **15** Suppl: E20-E24 [PMID: 10921377]
 - 25 **European Association for the Study of the Liver, European Association for the Study of the Liver**. EASL 2017 Clinical Practice Guidelines on the management of hepatitis B virus infection. *J Hepatol* 2017; **67**: 370-398 [PMID: 28427875 DOI: 10.1016/j.jhep.2017.03.021]
 - 26 **To WP**, Wong DK, Mak LY, Cheung KS, Yue Y, Fung J, Lai CL, Yuen MF. Relationship between hepatitis B core-related antigen and chronic hepatitis B outcome in HBeAg negative patients: a 10-year longitudinal study. *J Hepatol* 2018; **68** Suppl 1: S478 [DOI: 10.1016/S0168-8278(18)31206-6]

- 27 **European Association for Study of Liver, Asociacion Latinoamericana para el Estudio del Hgado.** EASL-ALEH Clinical Practice Guidelines: Non-invasive tests for evaluation of liver disease severity and prognosis. *J Hepatol* 2015; **63**: 237-264 [PMID: [25911335](#) DOI: [10.1016/j.jhep.2015.04.006](#)]
- 28 **Wong GL**, Chan HL, Wong CK, Leung C, Chan CY, Ho PP, Chung VC, Chan ZC, Tse YK, Chim AM, Lau TK, Wong VW. Liver stiffness-based optimization of hepatocellular carcinoma risk score in patients with chronic hepatitis B. *J Hepatol* 2014; **60**: 339-345 [PMID: [24128413](#) DOI: [10.1016/j.jhep.2013.09.029](#)]
- 29 **Chen YC**, Chu CM, Liaw YF. Age-specific prognosis following spontaneous hepatitis B e antigen seroconversion in chronic hepatitis B. *Hepatology* 2010; **51**: 435-444 [PMID: [19918971](#) DOI: [10.1002/hep.23348](#)]
- 30 **Fung J**, Cheung KS, Wong DK, Mak LY, To WP, Seto WK, Lai CL, Yuen MF. Long-term outcomes and predictive scores for hepatocellular carcinoma and hepatitis B surface antigen seroclearance after hepatitis B e-antigen seroclearance. *Hepatology* 2018; **68**: 462-472 [PMID: [29534307](#) DOI: [10.1002/hep.29874](#)]
- 31 **Hsu YS**, Chien RN, Yeh CT, Sheen IS, Chiou HY, Chu CM, Liaw YF. Long-term outcome after spontaneous HBeAg seroconversion in patients with chronic hepatitis B. *Hepatology* 2002; **35**: 1522-1527 [PMID: [12029639](#) DOI: [10.1053/jhep.2002.33638](#)]
- 32 **Yuen MF**, Lai CL. Treatment of chronic hepatitis B. *Lancet Infect Dis* 2001; **1**: 232-241 [PMID: [11871510](#) DOI: [10.1016/S1473-3099\(01\)00118-9](#)]

P- Reviewer: Lee CL, Namisaki T

S- Editor: Ma RY **L- Editor:** A **E- Editor:** Huang Y





Observational Study

Gluten immunogenic peptide excretion detects dietary transgressions in treated celiac disease patients

Ana Florencia Costa, Emilia Sugai, María de la Paz Temprano, Sonia Isabel Niveloni, Horacio Vázquez, María Laura Moreno, M. Remedios Domínguez-Flores, Alba Muñoz-Suano, Edgardo Smecuol, Juan Pablo Stefanolo, Andrea F González, Angel Cebolla-Ramirez, Eduardo Mauriño, Elena F Verdú, Julio César Bai

ORCID number: Ana Florencia Costa (0000-0002-0082-5630); Emilia Sugai (0000-0002-9408-4369); María de la Paz Temprano (0000-0003-2357-7858); Sonia Isabel Niveloni (0000-0002-1534-1604); Horacio Vázquez (0000-0002-9641-3437); María Laura Moreno (0000-0002-0120-8789); M. Remedios Domínguez-Flores (0000-0002-3931-7457); Alba Muñoz-Suano (0000-0003-2332-5943); Edgardo Smecuol (0000-0002-4451-819X); Juan Pablo Stefanolo (0000-0003-0679-3470); Andrea F González (0000-0003-1773-0694); Angel Cebolla-Ramirez (0000-0002-6976-4522); Eduardo Mauriño (0000-0002-2450-3839); Elena F Verdú (0000-0002-304-7077); Julio César Bai (0000-0003-4159-0185).

Author contributions: Costa AF contributed with patient enrolment and analysis of data; Sugai E performed biochemical tests, data analysis and interpretation; Temprano MdIP contributed to patient enrolment, dietary reports and assessment of compliance; Niveloni SI contributed to study design and patient enrolment; Vázquez H contributed to statistical analysis and data interpretation; Moreno ML contributed to patient enrolment and data analysis. Domínguez-Flores MR contributed with reagents; Muñoz-Suano A contributed with reagents; Smecuol E contributed to the study design

Ana Florencia Costa, Emilia Sugai, María de la Paz Temprano, Sonia Isabel Niveloni, Horacio Vázquez, María Laura Moreno, Edgardo Smecuol, Juan Pablo Stefanolo, Andrea F González, Eduardo Mauriño, Julio César Bai: Small Bowel Section, Department of Medicine, Dr. C. Bonorino Udaondo Gastroenterology Hospital, Buenos Aires 1263, Argentina

M. Remedios Domínguez-Flores, Alba Muñoz-Suano, Angel Cebolla-Ramirez, Department of Immunology, Biomedal S.L., Sevilla 41092, Spain

Elena F Verdú, Farncombe Family Digestive Health Research Institute, McMaster University, Hamilton, ON L8S4L8, Canada

Julio César Bai, Research Institutes, Universidad del Salvador, Buenos Aires 1050, Argentina

Corresponding author: Julio César Bai, MD, Professor Emeritus, Small Bowel Section, Department of Medicine, Dr. C. Bonorino Udaondo Gastroenterology Hospital, Av. Caseros 2061, Buenos Aires 1264, Argentina. jbai@intramed.net

Telephone: +54-11-43041018

Fax: +54-11-43041018

Abstract

BACKGROUND

Life-long removal of gluten from the diet is currently the only way to manage celiac disease (CeD). Until now, no objective test has proven useful to objectively detect ingested gluten in clinical practice. Recently, tests that determine consumption of gluten by assessing excretion of gluten immunogenic peptides (GIP) in stool and urine have been developed. Their utility, in comparison with conventional dietary and analytical follow-up strategies, has not been fully established.

AIM

To assess the performance of enzyme-linked immunosorbent assay (ELISA) and point-of-care tests (PoCTs) for GIP excretion in CeD patients on gluten-free diet (GFD).

METHODS

We conducted an observational, prospective, cross-sectional study in patients following a GFD for at least two years. Using the Gastrointestinal Symptom

and patient enrolment; Stefanolo JP contributed to data analysis; González A contributed to dietary reports and assessment of compliance; Cebolla-Ramírez A contributed to study design and development of GIP tests; Mauriño E contributed to study design and critical review of the manuscript; Verdú EF contributed to language editing and critical revision of the manuscript for intellectual content; Bai JC contributed to study concept and design, analysis and interpretation of data, study direction and manuscript writing; All authors read and approved the final manuscript.

Institutional review board

statement: The study was approved by Local Institutional Review Committees for Research and Ethics.

Informed consent statement: All patients signed a written informed consent approved by the Local Ethics Committee.

Conflict-of-interest statement:

Authors from Biomedal S.L. did not participate in the study design, data analysis and writing of the manuscript. The remaining authors have no conflicts to disclose.

STROBE statement: The authors have read and checked the STROBE checklist.

Open-Access: This is an open-access article that was selected by an in-house editor and fully peer-reviewed by external reviewers. It is distributed in accordance with the Creative Commons Attribution Non Commercial (CC BY-NC 4.0) license, which permits others to distribute, remix, adapt, build upon this work non-commercially, and license their derivative works on different terms, provided the original work is properly cited and the use is non-commercial. See: <http://creativecommons.org/licenses/by-nc/4.0/>

Manuscript source: Invited manuscript

Received: December 14, 2018

Peer-review started: December 14, 2018

First decision: December 28, 2018

Revised: January 8, 2019

Accepted: January 14, 2019

Article in press: January 14, 2019

Published online: March 21, 2019

Rating Scale questionnaire, patients were classified at enrollment as asymptomatic or symptomatic. Gluten consumption was assessed twice by 3-d dietary recall and GIP excretion (by ELISA in stool and PoCTs (commercial kits for stool and urine) in two consecutive samples. These samples and dietary reports were obtained 10 day apart one from the other. Patients were encouraged to follow their usual GFD during the study period.

RESULTS

Forty-four patients were enrolled, of which 19 (43.2%) were symptomatic despite being on a GFD. Overall, 83 sets of stool and/or urine samples were collected. Eleven out of 44 patients (25.0%) had at least one positive GIP test. The occurrence of at least one positive test was 32% in asymptomatic patients compared with 15.8% in symptomatic patients. GIP was concordant with dietary reports in 65.9% of cases (*Cohen's kappa*: 0.317). PoCT detected dietary indiscretions. Both ELISA and PoCT in stool were concordant (concomitantly positive or negative) in 67 out of 74 (90.5%) samples. Excretion of GIP was detected in 7 (8.4%) stool and/or urine samples from patients considered to be strictly compliant with the GFD by dietary reports.

CONCLUSION

GIP detects dietary transgressions in patients on long-term GFD, irrespective of the presence of symptoms. PoCT for GIP detection constitutes a simple home-based method for self-assessment of dietary indiscretions.

Key words: Celiac disease; Follow-up; Gluten-free diet; Gluten immunogenic peptide excretion; Rapid tests

©The Author(s) 2019. Published by Baishideng Publishing Group Inc. All rights reserved.

Core tip: Excreted gluten immunogenic peptides (GIPs) in stool and urine are specific indicators of gluten consumption in patients with celiac disease. GIP tests detect dietary indiscretions in treated celiac patients, irrespective of the presence of symptoms. GIPs were detected in stool and/or urine samples of patients considered to be strictly compliant with the gluten-free diet according to dietary reports. Point-of-care tests for GIP detection constitute simple home-based methods for self-assessment of dietary indiscretions.

Citation: Costa AF, Sugai E, Temprano MLP, Niveloni SI, Vázquez H, Moreno ML, Domínguez-Flores MR, Muñoz-Suano A, Smecuol E, Stefanolo JP, González AF, Cebolla-Ramírez A, Mauriño E, Verdú EF, Bai JC. Gluten immunogenic peptide excretion detects dietary transgressions in treated celiac disease patients. *World J Gastroenterol* 2019; 25(11): 1409-1420

URL: <https://www.wjgnet.com/1007-9327/full/v25/i11/1409.htm>

DOI: <https://dx.doi.org/10.3748/wjg.v25.i11.1409>

INTRODUCTION

Life-long removal of gluten from the diet is currently the only way to manage celiac disease (CeD)^[1]. In most patients, strict gluten avoidance results in symptomatic, serologic and histological remission. Adherence to the gluten-free diet (GFD) is associated with a reduction and/or normalization of the risk for associated disorders or complications^[2]. While the majority of treated patients who are compliant with the GFD are asymptomatic, up to 40% of treated patients remain symptomatic or experience symptom relapse^[3]. In this context, the persistence of gluten consumption, or accidental antigen exposure, is considered the main underlying factor^[4-6]. Asymptomatic patients on a GFD who have normal serology are not always assessed for adherence to the diet. Furthermore, most guidelines do not reinforce the necessity for monitoring GFD compliance. Until now, there was no objective test to reveal ingested gluten in clinical practice, and evaluations have relied on the presence of symptoms, dietary questionnaires by dietitians and/or serology^[7-9].

Quantitative enzyme-linked immunosorbent assays (ELISA) (stool) and quantitative immunocromatography (urine) tests that determine consumption of gluten by assessing the excretion of gluten immunogenic peptides (GIP) have recently been developed^[10,11]. These tests are based on the detection of GIP in stool and urine by monoclonal antibodies (anti-33merα-gliadin peptide G12). Previous studies have shown that a positive result constitutes specific evidence of dietary indiscretions. In addition to these, point-of-care tests (PoCT) (both for stool and urine) have been recently developed to simplify their use by patients at home. It is not currently known how these newly developed tests perform compared with laboratory tests for GIP, such as ELISA, traditional dietary assessment and serology. It is also unknown whether PoCT can help in the identification of transgressions in asymptomatic patients on GFD, in whom gluten contamination is not suspected^[9].

Thus, our aims were: (1) to assess the performance of ELISA and PoCT for detecting GIP excretion in stool and urine in patients on GFD for more than two years; and (2) to explore the potential association of dietary transgressions with symptoms in CeD patients on long-term GFD.

MATERIALS AND METHODS

Patients

CD patients (> 18 years old) attending the Celiac Disease Clinic of the “C. Bonorino Udaondo” Gastroenterology Hospital were offered to participate in the study. Inclusion criteria were: (1) a well-established histological and serological diagnosis of CeD; (2) self-reported adherence to the GFD for more than two years; and (3) ability to complete dietary reports, and collect and transport samples to our institution per the protocol. The diagnosis of CeD was based on positive specific serology and concomitant duodenal biopsy showing villous atrophy (Marsh’s 3 damage)^[1-4]. Patients not willing to participate, unable to complete dietary diary recall, having concomitant disorders (*e.g.*, type I diabetes, hypothyroidism, *etc*), type II refractory CeD, or unable to collect and deliver the required samples, were excluded. Serum samples were obtained at the time of enrollment for the determination of CeD-specific antibodies, although levels of serologic tests did not limit patient enrollment.

Study design

The study followed an observational, cross-sectional design, and prospectively assessed adult CeD patients on a GFD. Patients fulfilling the inclusion and exclusion criteria were invited to enroll in the study after signing a written informed consent. At baseline, patients were assessed for the presence of GI symptoms by the Gastrointestinal Symptom Rating Scale (GSRS) questionnaire^[12]. A patient was classified as symptomatic if reporting ≥ 3 points for individual syndromes or, ≥ 2 points in the average score of the five syndromes^[13]. Patients were encouraged to follow their usual GFD during the study period (2 wk) (Figure 1).

The first step of the study consisted of a self-written 3-d recall diary on food consumption, as previously described^[14]. The following morning, patients delivered a random sample of stool and urine (first morning urine) to the specialized laboratory within 4 h after collection. After a 1-wk clearance period during which patients remained on a GFD to prevent confounding results from potential contaminations prior to the study^[5-7], patients completed a second recall diary. Stool and urine samples were collected the consecutive morning, as explained previously^[10,11] (Figure 1). The second collection of samples was performed to investigate whether dietary transgressions were isolated or frequent events.

Analytical methods and test sensitivity

Details on detection limits, lapse of time from consumption to detection, time for clearance of stool and urine, and the quantity of gluten consumption required for detection, are detailed in Table 1.

Blood, stool and urine sample collection and storage

After collection, blood samples were stored at -20°C until tested. Patients were instructed to collect three sets of 2-4 g of stool from the first morning deposition, and to place them immediately into sealed containers at both time points. Stool samples were transported to the lab within 4 h of collection. Stool samples were kept frozen until GIP quantitative ELISA tests were performed. The urine and stool samples were also used for PoCT detection of GIP, and both determinations were evaluated as soon as they arrived in the lab to prevent any peptide degradation. The manufacturer reported sufficient GIP stability in urine for at least 24 h at room temperature (Cebolla-Ramirez A; personal communication/unpublished).

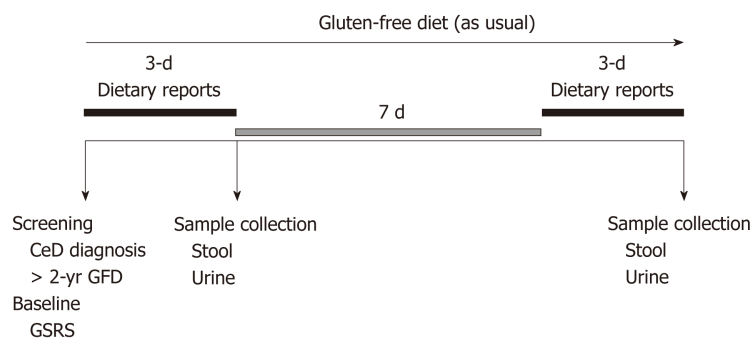


Figure 1 Study design. GFD: Gluten-free diet; GSRS: Gastrointestinal Symptom Rating Scale.

Quantitative GIP detection in stool by ELISA

Testing was performed according to instructions from manufacturers. Briefly, GIP excretion was quantified by a sandwich ELISA kit (iVYLISA GIP-S®, Biomedal S.L.; Sevilla, Spain) designed to detect and quantify GIPs (containing similar epitopes to those found in the immunodominant α -gliadin 33-mer peptide) in samples. Stool samples were incubated for 60 min at 50°C with gentle agitation in 9 mL of Universal Gluten Extraction Solution (UGES; Biomedal S.L.; Seville, Spain) per gram of stool to release the GIP from the stool matrix. The extracted sample was then added to a plate coated with A1/G12 monoclonal antibodies that specifically detect the epitopes of wheat prolamins (gliadin), rye (secalin) and barley (hordein). Details on analytics and detection limit are shown in Table 1^[10].

GIP in stools and urine by PoCT

PoCT in stool and urine samples was performed by lateral flow immunoassays (GlutenDetect®; Biomedal S.L., Spain). First, 2 mL urine samples were mixed with 0.7 mL of the manufacturer solution. If gluten peptides are present, they react with the conjugated antibodies (monoclonal antibodies A1 and G12) previously fixed in the lateral flow strip, producing a red line in the result window. A control antibody-antigen reaction is generated to confirm the correct flow and conditions for antibody binding, which generates a green line to indicate correct test performance. Positive results are revealed by two lines (red and green) and negative results are indicated by a single green line. The limits of quantification in stool and urine are shown in Table 1.

CeD serology tests

CeD-related serology included: (1) IgA a-tTG (QUANTA Lite TM, h-tTG IgA, INOVA Diagnostic Inc.; San Diego, CA, United States) by ELISA; and (2) IgA deamidated gliadin peptide (IgA DGP) antibodies, both by ELISA. Cut-off for both antibodies was 20 IU/mL. Characteristics of the serologic test have been reported in previous studies^[14].

Estimation of gluten intake by dietary recall

During the 3-d dietary recall, patients were encouraged to be explicit about foods, brands consumed, management strategies and food processing. However, patients were asked to avoid major changes to their usual GFD, and eventual modifications were not determined. A second expert dietitian, blinded to clinical and laboratory results, determined the potential gluten consumption for each dietary report. The degree of adherence was estimated as follows: (1) patients with no evidence of transgression; and (2) patients non-adherent to the diet, which included voluntary or inadvertent transgression with known sources containing gluten, and patients with intake of gluten traces (when hidden gluten or cross contamination was not controlled)^[15].

Statistical analysis

The study was approved by the Institutional Ethical Committee (CEI) and the Local Research Committee (CODEI) from Dr. C. Bonorino Udaondo Gastroenterology Hospital. A written consent was obtained from all patients. Data were analyzed using MedCalc (ver. 11.2.1.0; MedCalc Software; bvba). Comparison between GIP excretion tests and degree of compliance with the GFD was estimated, without considering the existence of a gold standard test. Data are reported as mean and standard deviation or median and range, according to distribution. The proportion (%) of positive or negative tests was established. Results were analyzed using *t*-tests, Mann-Whitney

Table 1 Characteristics of tests for detecting gluten immunogenic peptides in stool and urine

Method	Type of sample	Limit of detection	Time to be excreted ¹	Time of GIP clearance ¹	Detectable levels of gluten intake
ELISA					
LFIA; PoCT	Stool	60-150 µg/g	2 d	2-7 d	>40 mg/d
LFIA; PoCT	Urine	2-3 ng/mL	1-12 h	24-48 h	40-500 mg/d ²

¹Time after gluten intake;²The ingestion of 50mg of gluten per day can be detected in urine with a sensitivity of 15%, and the ingestion of 500mg gluten per day can be detected with a sensitivity of 90% when analyzing the first urine in the morning^[24]. GIP: Gluten immunogenic peptides; ELISA: Enzyme-linked immunosorbent assay; LFIA: Lateral-flow immunochromatographic assay; PoCT: Point-of-care test.

tests or Fisher exact tests as appropriate, according to data distribution. Concordance between dietary reports and GIP excretion was determined by using the *Cohen's kappa*.

RESULTS

Patient characteristics

A total of 62 CeD patients were screened and 44 patients were enrolled. Based on the GRSR questionnaire, 19 (43.2%) patients were symptomatic and 25 asymptomatic (Figure 2). Median age was 50 years (range: 25-82). Median time on a GFD was 8 years (range: 2-48). There were no differences in the median time spent on a GFD, age, or median body mass index between patients identified as symptomatic or asymptomatic (*p*NS) (Table 2). As expected, the symptomatic subpopulation had a significantly higher global GRSR score than asymptomatic patients (*P*<0.00001) (Table 1). This was also true for individual syndromes (*P*<0.04 to *P*< 0.0001) (data not shown).

Serology was performed on the 42 patients at enrollment (42 for IgA tTG and 40 for IgA DGP). Overall, 21/42 (50.0%) patients had antibody concentrations above the upper limit of normality (ULN) for at least one test. Median serum concentrations (range) for IgA tTG were borderline for the UNL [17.9 AU/mL (2-78) and 21.4(2->100) for IgA DGP]. Nine out of 42 (21.4%) and 18/40 (45.0%) had positive serum concentrations of IgA tTG and IgA DGP, respectively. However, only four had serum antibody concentrations 3X above ULN. In three of them, serum concentrations were concomitantly abnormal for both antibodies. The remaining patients with abnormal serologic values had concentrations below <3X the ULN arbitrary threshold (Tables 3 and 4).

GIP excretion in stool and urine

Forty-four patients returned 83 sets of dietary reports and/or stool and urine samples. Five other patients did not return complete sets and thus were excluded from analysis (Tables 3 and 4). We determined GIP excretion by ELISA in 82 stool samples, and by PoCT in 74 stool samples and in 78 urine samples. Only 73/83 complete sets of samples were returned. Considering both sets of determinations, 11/ 44 patients (25.0%) had at least one positive GIP test, of which 32% were asymptomatic and 15.8% were symptomatic. Ten samples were positive for ELISA in stool, five were positive for PoCT in stool (two of which were the only positive tests) and three were positive for PoCT in urine (one of which was the only positive test). Three samples were positive for both ELISA and PoCT in stool, and one sample was concomitantly positive in the three tests. Stool tests (both ELISA and PoCT) were concordant (concomitantly positive or negative) in 67/74 (90.5%) samples (Table 2). Only two patients who were asymptomatic with negative serology had positive GIP in both sets of samples.

Dietary assessment using a 3-d recall diary

Blinded estimation of the degree of adherence with the GFD using 3-d recall diaries estimated that 53/83 reports (63.9%) showed no evidence of transgressions (strict GFD), while 30/83 (36.1%) reports indicated non-adherence by consumption of foods with potential gluten sources or traces (Tables 3 and 4).

Comparison of GIP excretion tests, dietary assessment and serology

Overall, there was concordance between the estimation of dietary adherence and determinations of GIP excretion in 54/82 (65.9%) samples, while 28/82 (34.1%) cases

Table 2 Demography, clinical and biochemical characteristics and results of the 3-d dietary reports of the complete population according to clinical characterization at enrollment

Parameter	Asymptomatic	Symptomatic
Number of individuals (females)	25 (21)	19 (19)
Age at enrollment, median (range)	50 (29-82)	51 (25-59)
Years on a GFD, median (range)	8 (2-48)	9 (4-27)
Body mass index, median (range)	25 (19-32)	25 (19-38)
GSRS, median score (range)	1.16 (0.2-2)	2.44 (2-3.6) ^a
Serology		
Serum IgA tTG		
Median concentration (range)	11 (2-100)	8 (3-200)
Number of patients with normal tests (%)	19/24 (79.2)	14/18 (77.8)
Serum IgA DGP		
Median concentration (range)	19 (2-78)	12 (200-5)
Number of patients with normal tests (%)	12/22 (54.5)	10/18 (55.6)
Excretion of GIP (stool and urine)		
N of positive samples (%)	10/47 (21.3)	3/36 (8.3)
3-d dietary recall (completed)	(47)	(36)
Strict adherence		
Number of patients (%)	26 (55.3)	27 (75.0)
No adherents		
Number of patients (%)	21 (44.7)	9 (25.0)

^a*P* <0.0001. GFD: Gluten-free diet; GIP: Gluten immunogenic peptides; GSRS: Gastrointestinal Symptom Rating Scale; DGP: Deamidated gliadin peptide.

were discordant (*Cohen's kappa*: 0.317). Positive GIP excretion was present in 7/82 (8.4%) cases that were estimated to be strictly adherent by dietary assessment, and in 5/28 (17.9%) that were considered non-adherent by sources or traces. Dietary assessment estimated the consumption of gluten in only 50% of samples that were also positive for GIP.

IgA tTG and IgA DGP were positive in 3/12 and 6/12 cases excreting GIP, respectively. Interestingly, three of those cases with high antibody concentrations (above 3X UNL) had positive excretion of GIP in one or more determinations (Tables 3 and 4).

Comparison between asymptomatic and symptomatic patients

Presence of GIP in stool and/or urine was detected in at least one of two determinations in 9/25 (36.0%) asymptomatic patients (Table 3). Although GIP excretion was shown in only 3/19 (15.8%) symptomatic patients (Table 4), the difference did not reach statistical significance (*P*=0.22). Similarly, no differences were found in subgroup analysis comparing estimation of the degree of adherence with the diet, IgA tTG and IgA DGP antibody mean concentrations, or proportion of patients with normal serology (Table 2). The low number of patients with values above 3X UNL produced no statistically significant results. The median serum concentration for IgA DGP antibodies was very close to the UNL (Table 2).

DISCUSSION

Strict adherence to the GFD improves or normalizes growth, ameliorates most symptoms, reduces the risk of intestinal and extra-intestinal complications, normalizes immunological reactivity, and heals enteropathy in both pediatric and adult populations^[1-4]. Monitoring compliance with the GFD is a key aspect of patient follow-up. Unfortunately, strict adherence is limited by the lack of availability of gluten-free foods, cost, social isolation and frequent cross-contamination^[16]. Therefore, caregivers and patients are often confronted with questions regarding the best method for detecting dietary indiscretions. This is the population that requires strict follow-up of the frequency at which these measurements should be performed.

Our first objective compared GIP excretion in urine and feces using laboratory tests,

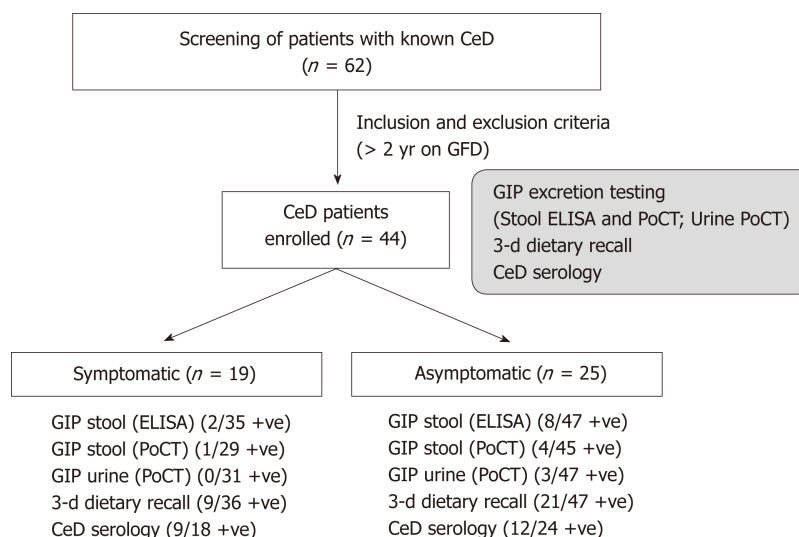


Figure 2 Summary of outcome of patients enrolled, and samples received and analyzed according to clinical status. GFD: Gluten-free diet; GIP: Gluten immunogenic peptides; CeD: Celiac disease; PoCT: Point-of-care tests; ELISA: Enzyme-linked immunosorbent assay.

which detect A1 and G12 epitopes similar to those of the gliadin 33-mer peptide^[10,11] with the newly developed PoCT. These tests were designed to simplify GIP excretion measurement in stool and/or urine. In 25% of patients who considered themselves compliant with the GFD, we detected GIP excretion in at least one of two different determinations, performed 10 d apart. Although there were no statistical differences in terms of the presence or absence of symptoms, the majority of these patients were asymptomatic. A former study showed that the diagnostic sensitivity of the fecal ELISA test was 98.5% and its specificity 100%, with positive and negative predictive values of 100% and 91.7%, respectively^[11,17,18]. Furthermore, the specificity for the new PoCT tests have also been previously explored, and were determined to be specific for detecting most of the immunoactivity of gluten peptides in an *in vitro* research context^[19] (Cebolla-Ramirez A, unpublished data). Here we show that these tests can detect gluten contaminations that do not cause symptoms.

In 90.5% of the samples, PoCT and ELISA from stool were concordantly positive or negative. There was lack of concordance in seven pairs of stool samples in which at least one test was positive (ELISA was the only positive test in five stool samples, while PoCT was the only positive fecal test in the remaining two samples). Lack of concordance between stool tests could be related to: intrinsic test factors associated with different extraction quality, the non-homogeneous distribution of GIP in stool, or different sensitivities of the methods in relation to the quantity of gluten ingested, especially in patients subjected to strict protocol procedures. Discordance between tests was more prominent in urine samples compared with detections in stool. GIP in urine was detected in three sets of samples, two of which were in concordance with excretion in stool. The time of gluten intake prior to sample collection (different times to be cleared for detection compared with stool tests) (see Table 1), the degree of urine dilution (related to levels of water consumption), the amount of gluten ingested, and the potential role of deamidation (which decreases antibody reactivity) are all possible reasons for these results. Another explanation is the fact that gluten intake could be below 500 mg/d, since volunteers improve their diets when they are monitored. Interestingly, the urine test has a window of detection ranging from 2-16 or 48 h after gluten intake. Recent unpublished results showed that the performance of PoCT in urine from healthy people consuming regular gluten and CeD patients with strictly controlled GFD had sensitivity, specificity, PPV and NPV of 91%, 99%, 99% and 95%, respectively (Cebolla-Ramirez A, personal communication). Overall, the results suggest that the use of more than one test may enhance the global assessment during patient follow-up.

We also studied the performance of these tests according to symptom presentation. Recent articles suggested that the most common reason for non-responsive CeD is persistent gluten exposure^[15,20]. Indeed, a strategy employed in clinical practice with symptomatic patients is the recommendation of a “natural” GFD that, in the majority of cases, resolves symptoms^[21]. Although no gold standard is available, the estimation of dietary adherence by dietitians is, in general, quick, simple and mostly recommended^[1,3]. However, this method has the setback of being subjective and

Table 3 Serology, dietary adherence (3-d recall) and gluten immunogenic peptide excretion tests in samples from patients with celiac disease responding to the gluten-free diet (asymptomatic cases)

Patient No.	Serology		First set of determinations				Second set of determinations			
	IgAtTG AU/mL	IgADGPAU /mL	Dietary report	GIP in stool ELISA µg/g	GIP in stool PoCT	GIP in urine PoCT	Dietary report	GIP in stool ELISA µg/g	GIP in stool PoCT	GIP in urine PoCT
1	12	10	Strict	< 0.16	-ve	-ve	Strict	< 0.16	-ve	-ve
2	11	36	NA	0.19	ND	-ve	NA	< 0.16	ND	-ve
3	14	13	Strict	< 0.16	-ve	-ve	Strict	< 0.16	-ve	-ve
4	5	7	Strict	< 0.16	-ve	-ve	Strict	< 0.16	-ve	-ve
5	17	22	Strict	< 0.16	-ve	-ve	Strict	< 0.16	+ve	-ve
6	32	58	NA	< 0.16	-ve	-ve	NA	ND	ND	ND
7	16	41	Strict	< 0.16	-ve	-ve	Strict	< 0.16	-ve	-ve
8	6	11	NA	< 0.16	-ve	+ve	NA	< 0.16	-ve	-ve
9	33	18	NA	< 0.16	-ve	-ve	NA	< 0.16	-ve	-ve
10	2	2	NA	0.38	+ve	-ve	NA	0.75	+ve	-ve
11	40	23	Strict	< 0.16	-ve	-ve	Strict	< 0.16	-ve	-ve
12	12	6	NA	< 0.16	-ve	-ve	NA	< 0.16	-ve	-ve
13	8	20	Strict	< 0.16	-ve	-ve	Strict	< 0.16	-ve	-ve
14	8	25	Strict	< 0.16	-ve	-ve	Strict	< 0.16	-ve	-ve
15	9	ND	NA	< 0.16	-ve	-ve	NA	< 0.16	-ve	-ve
16	10	25	NA	< 0.16	-ve	-ve	NA	0.66	+ve	+ve
17	15	ND	Strict	0.26	-ve	-ve	Strict	< 0.16	-ve	-ve
18	32	16	Strict	< 0.16	-ve	-ve	Strict	< 0.16	-ve	-ve
19	ND	ND	NA	< 0.16	-ve	-ve	NA	< 0.16	-ve	-ve
20	11	21	Traces	< 0.16	-ve	-ve	NA	ND	ND	ND
21	6	13	Traces	< 0.16	-ve	-ve	NA	< 0.16	-ve	-ve
22	100	78	ND	0.66	-ve	+ve	ND	ND	ND	ND
23	8	8	Strict	0.26	-ve	-ve	Strict	0.75	-ve	-ve
24	17	22	Strict	< 0.16	-ve	-ve	Strict	< 0.16	-ve	-ve
25	6	6	Strict	< 0.16	-ve	-ve	Strict	< 0.16	-ve	-ve

Dietary assessments were categorized as “strict” (patients with no transgression detected) or no adherence (by sources: transgression by foods with potential gluten sources or by traces: patients with potential intake of gluten traces). Gluten immunogenic peptides in stool by enzyme-linked immunosorbent assay <0.156: no gluten excretion detected. NA: No adherence; ND: Not determined and excluded from analysis; -ve: Negative result; +ve: Positive result; DGP: Deamidated gliadin peptide; GIP: Gluten immunogenic peptides; ELISA: Enzyme-linked immunosorbent assay; PoCT: Point-of-care test.

training-dependent. In this study, food dietary reports were recorded by trained patients and blindly analyzed by an expert nutritionist. We detected a 65.9% concordance between dietary reports and objective evidence of GIP in stool and/or urine samples (*Cohen kappa*: 0.317). Notably, 13.2% of dietary reports that had estimated “strict” GFD adherence showed evidence of gluten consumption, as assessed by GIP excretion in stool and/or urine.

GIP excretion was more prevalent in asymptomatic versus symptomatic patients, although this difference was not statistically significant, which was likely due to the low number of cases enrolled. Interestingly, dietary reports and specific serology were also similar between both subgroups (Tables 2-4). The present study thus confirms the limitations of dietary assessment, since this method failed to detect gluten consumption in 7/13 samples that were positive for GIP excretion. In contrast, dietary reports suggested transgressions in 15 samples in which GIP tests were negative. This could be explained by possible intentional omission in dietary reports by patients. Another possibility is the fact that some foods may contain traces of gluten that could not be detected by GIP excretion tools, despite being labeled as gluten-free^[22,23], among other factors. Therefore, dietary indiscretions may not explain all cases of persistent symptoms in CeD patients on long-term diets. The consumption of FODMAPs could be a potential explanation for symptom persistence^[24]. Additional factors, such as alterations in small bowel microbiota, as previously suggested, may explain some persistent symptomatic cases^[25].

Table 4 Celiac serology, dietary adherence assessed by dietary report and gluten immunogenic peptide excretion tests in samples from patients with celiac disease not responding to the gluten-free diet (symptomatic cases)

Patient No.	Serology		First set of determinations				Second set of determinations			
	IgAtTG AU/mL	IgADGPAU /mL	Dietary report	GIP in stool ELISA µg/g	GIP in stool PoCT	GIP in urine PoCT	Dietary report	GIP in stool ELISA µg/g	GIP in stool PoCT	GIP in urine PoCT
1	3	5	Strict	< 0.16	ND	ND	NA	< 0.16	-ve	ND
2	15	9	NA	< 0.16	ND	ND	Strict	< 0.16	ND	ND
3	30	75	Strict	0.38	ND	ND	Strict	< 0.16	ND	-ve
4	77	> 200	NA	< 0.16	-ve	-ve	NA	< 0.16	-ve	-ve
5	8	1	Strict	< 0.16	-ve	-ve	Strict	< 0.16	-ve	-ve
6	4	6	Strict	< 0.16	-ve	-ve	NA	< 0.16	-ve	-ve
7	3	13	Strict	< 0.16	-ve	-ve	Strict	< 0.16	-ve	-ve
8	27	11	Strict	ND	ND	-ve	Strict	< 0.16	-ve	-ve
9	3	39	Strict	< 0.16	ND	-ve	Strict	< 0.16	-ve	-ve
10	5	4	Strict	< 0.16	-ve	-ve	Strict	< 0.16	-ve	-ve
11	> 200	67	Strict	< 0.16	-ve	-ve	Strict	0.42	-ve	-ve
12	8	10	Strict	< 0.16	-ve	-ve	Strict	< 0.16	-ve	-ve
13	3	35	NA	< 0.16	-ve	-ve	Strict	< 0.16	+ve	-ve
14	ND	ND	NA	< 0.16	-ve	-ve	NA	< 0.16	-ve	-ve
15	12	12	Strict	< 0.16	-ve	-ve	Strict	< 0.16	-ve	-ve
16	14	25	Strict	< 0.16	-ve	-ve	ND	ND	ND	ND
17	8	9	Strict	< 0.16	-ve	-ve	ND	ND	ND	ND
18	17	36	Strict	< 0.16	-ve	-ve	Strict	< 0.16	-ve	-ve
19	8	24	NA	< 0.16	-ve	-ve	Strict	< 0.16	-ve	-ve

Dietary assessments were categorized as “strict” (patients with no transgression detected) or no adherence (by sources: transgression by foods with potential gluten sources or by traces: patients with potential intake of gluten traces). Gluten immunogenic peptides in stool by enzyme-linked immunosorbent assay < 0.156: no gluten excretion detected. NA: No adherence; ND: Not determined and excluded from analysis; -ve: Negative result; +ve: Positive result; DGP: Deamidated gliadin peptide; GIP: Gluten immunogenic peptides; ELISA: Enzyme-linked immunosorbent assay; PoCT: Point-of-care test.

Former studies and guidelines have suggested that periodic testing for IgA anti-tTG or IgA anti-DGP is a non-invasive method for monitoring compliance during the initiation of the GFD^[1-4]. The decline in serum antibody concentrations is considered a useful indicator of compliance with the diet^[26]. However, while highly increased concentrations are strongly associated with continued gluten challenge, serology tests do not identify minor dietary indiscretions^[2,3]. In contrast, normal titers are not sensitive enough for ongoing gluten exposure or the persistence of enteropathy^[27]. Our study suggests that most patients with abnormal serum antibody values had mildly elevated concentrations. Only in four cases were levels above 3X ULN, which is considered to be the best cut-off to discriminate transgressions. In two of these, there was objective evidence of gluten intake. We confirmed that the most frequently positive test was the IgA DGP antibody, a finding that is in agreement with previous observations^[26].

Limitations of this study include the relatively low number of patients, the lack of reliable gold standard testing to monitor real-time adherence with the GFD for comparing with new tests, potential discrepancies between the direct detection of the toxic agent by lab testing and real-time home tests that remain speculative, the subjective essence of dietary reports, and the fact that serology cannot be directly compared with tests that measure real-time consumption. Despite these limitations, our study highlights the difficulties emerging in clinical practice for assessing adherence to the GFD, even in patients who consider themselves compliant.

In conclusion, the study confirms former observations showing that GIP detection in stool and urine are useful adjuvant tools for monitoring adherence to the GFD in real-life conditions of treated CeD patients. It expands this knowledge by showing GIP in stool and urine can also be detected by simple, easy-to-perform PoCT tools. An interesting observation relates to the analysis of asymptomatic patients, in whom it is assumed that dietary adherence is high, and consequently will not be subjected to follow-up. The presence of GIP in the stool and/or urine of patients considered

compliant with the diet highlights the limitations of only using dietary estimations. Other factors, such as changes in small intestinal microbiome structure, methods for using these tests, or ways to determine very low gluten consumption, should be explored.

ARTICLE HIGHLIGHTS

Research background

Until now, there was no objective test to reveal objectively ingested gluten in clinical practice. Recently developed stool and urine laboratory tests based on monoclonal antibody technology specifically determine consumption of gluten by assessing the excretion of gluten immunogenic peptides (GIP). These tests were proposed to help in the monitoring of adherence to the gluten-free diet (GFD). More recently, point-of-care tests (PoCT) for stool and urine have been developed that may encourage patient self-monitoring and better compliance with disease management.

Research motivation

Despite recent research, there are at least three unsolved issues regarding the use of objective tests to detect gluten consumption. (1) The utility of GIP excretion tests, in patients with CeD who consider themselves adherent to the GFD, has not been compared with conventional monitoring methods in a real-life-scenario; (2) It is unknown whether consumption of gluten as measured by GIP excretion is different in symptomatic and asymptomatic CeD patients while on GFD; and (3) It is unclear how the new PoCT tests compare with laboratory-performed GIP tests.

Research objectives

We assessed (1) the performance of enzyme-linked immunosorbent assays (ELISA) and point-of-care (PoCTs) GIP excretion tests in patients with CeD on GFD; and (2) its relation to the presence of symptoms.

Research methods

We conducted an observational, prospective, cross-sectional study in CeD patients on a GFD for at least two years. Patients were categorized as asymptomatic or symptomatic at enrollment, using the Gastrointestinal Symptom Rating Scale questionnaire. Gluten consumption was assessed by 3-d dietary recall and GIP excretion in stool by ELISA, and by PoCTs in stool and urine using commercial kits.

Research results

Forty-four of the sixty-two screened CeD patients were enrolled; nineteen (43.2%) were symptomatic despite being on a GFD. Overall, 83 sets of stool and/or urine samples were collected. At least one positive GIP test was detected in 11 out of the total 44 (25.0%) patients, 32% of whom were asymptomatic. GIP was concordant with dietary reports in 65.9% of cases (*Cohen's kappa*: 0.317). PoCT tests detected dietary indiscretions. Excretion of GIP was detected in 7 (8.4%) stool and/or urine samples from patients considered to be strictly compliant with the GFD by dietary reports.

Research conclusions

Our study shows that GIP determination in stool and urine detects dietary transgressions in patients on long-term GFD who are unaware of gluten consumption. Our data also suggest that PoCT for GIP detection in stool and urine constitutes simple home-based methods that may aid in self-assessment of dietary indiscretions, especially inadvertent contaminations. GIP excretion is evident in treated patients, irrespective of the presence of symptoms. This observation confirms that patients should be assessed even when they are asymptomatic and/or have negative serology.

Research perspectives

The results support the use of specific GIP tests in stool and urine in conjunction with conventional strategies used to determine adherence to the GFD. One potential future research direction includes the use of these new tools to determine patterns of adherence in patients who believe to be adherent to the GFD. PoCT tests might encourage patients to be involved in self-monitoring and, thus, improve adherence to the diet.

REFERENCES

- 1 Green PH, Cellier C. Celiac disease. *N Engl J Med* 2007; **357**: 1731-1743 [PMID: 17960014 DOI: 10.1056/NEJMra071600]
- 2 Kelly CP, Bai JC, Liu E, Leffler DA. Advances in diagnosis and management of celiac disease. *Gastroenterology* 2015; **148**: 1175-1186 [PMID: 25662623 DOI: 10.1053/j.gastro.2015.01.044]
- 3 Ludvigsson JF, Bai JC, Biagi F, Card TR, Ciacci C, Ciclitira PJ, Green PH, Hadjivassiliou M, Holdaway A, van Heel DA, Kaukinen K, Leffler DA, Leonard JN, Lundin KE, McGough N, Davidson M, Murray JA, Swift GL, Walker MM, Zingone F, Sanders DS; BSG Coeliac Disease Guidelines Development Group; British Society of Gastroenterology. Diagnosis and management of adult coeliac disease:

- guidelines from the British Society of Gastroenterology. *Gut* 2014; **63**: 1210-1228 [PMID: [24917550](#) DOI: [10.1136/gutjnl-2013-306578](#)]
- 4 **Bai JC**, Ciacci C. World Gastroenterology Organisation Global Guidelines: Celiac Disease February 2017. *J Clin Gastroenterol* 2017; **51**: 755-768 [PMID: [28877080](#) DOI: [10.1097/MCG.0000000000000919](#)]
 - 5 **Leffler DA**, Dennis M, Hyett B, Kelly E, Schuppan D, Kelly CP. Etiologies and predictors of diagnosis in nonresponsive celiac disease. *Clin Gastroenterol Hepatol* 2007; **5**: 445-450 [PMID: [17382600](#) DOI: [10.1016/j.cgh.2006.12.006](#)]
 - 6 **Rubio-Tapia A**, Hill ID, Kelly CP, Calderwood AH, Murray JA; American College of Gastroenterology. ACG clinical guidelines: diagnosis and management of celiac disease. *Am J Gastroenterol* 2013; **108**: 656-76; quiz 677 [PMID: [23609613](#) DOI: [10.1038/ajg.2013.79](#)]
 - 7 **Moreno ML**, Rodríguez-Herrera A, Sousa C, Comino I. Biomarkers to Monitor Gluten-Free Diet Compliance in Celiac Patients. *Nutrients* 2017; **9** [PMID: [28067823](#) DOI: [10.3390/nu9010046](#)]
 - 8 **Mahadev S**, Murray JA, Wu TT, Chandan VS, Torbenson MS, Kelly CP, Maki M, Green PH, Adelman D, Lebwohl B. Factors associated with villus atrophy in symptomatic coeliac disease patients on a gluten-free diet. *Aliment Pharmacol Ther* 2017; **45**: 1084-1093 [PMID: [28220520](#) DOI: [10.1111/apt.13988](#)]
 - 9 **Lebwohl B**, Murray JA, Rubio-Tapia A, Green PH, Ludvigsson JF. Predictors of persistent villous atrophy in coeliac disease: a population-based study. *Aliment Pharmacol Ther* 2014; **39**: 488-495 [PMID: [24428688](#) DOI: [10.1111/apt.12621](#)]
 - 10 **Comino I**, Fernández-Bañares F, Esteve M, Ortigosa L, Castillejo G, Fambuenza B, Ribes-Koninckx C, Sierra C, Rodríguez-Herrera A, Salazar JC, Caunedo Á, Marugán-Miguelsanz JM, Garrote JA, Vivas S, Lo Iacono O, Nuñez A, Vaquero L, Vegas AM, Crespo L, Fernández-Salazar L, Arranz E, Jiménez-García VA, Antonio Montes-Cano M, Espín B, Galera A, Valverde J, Girón FJ, Bolonio M, Millán A, Cerezo FM, Guajardo C, Alberto JR, Rosinach M, Segura V, León F, Marinich J, Muñoz-Suano A, Romero-Gómez M, Cebolla Á, Sousa C. Fecal Gluten Peptides Reveal Limitations of Serological Tests and Food Questionnaires for Monitoring Gluten-Free Diet in Celiac Disease Patients. *Am J Gastroenterol* 2016; **111**: 1456-1465 [PMID: [27644734](#) DOI: [10.1038/ajg.2016.439](#)]
 - 11 **Moreno ML**, Cebolla Á, Muñoz-Suano A, Carrillo-Carrion C, Comino I, Pizarro Á, León F, Rodríguez-Herrera A, Sousa C. Detection of gluten immunogenic peptides in the urine of patients with coeliac disease reveals transgressions in the gluten-free diet and incomplete mucosal healing. *Gut* 2017; **66**: 250-257 [PMID: [26608460](#) DOI: [10.1136/gutjnl-2015-310148](#)]
 - 12 **Svedlund J**, Sjödin I, Dotevall G. GSRS--a clinical rating scale for gastrointestinal symptoms in patients with irritable bowel syndrome and peptic ulcer disease. *Dig Dis Sci* 1988; **33**: 129-134 [PMID: [3123181](#) DOI: [10.1007/BF01535722](#)]
 - 13 **Nachman F**, Mauriño E, Vázquez H, Sfoglia C, Gonzalez A, Gonzalez V, Plancer del Campo M, Smecuol E, Niveloni S, Sugai E, Mazure R, Cabanne A, Bai JC. Quality of life in celiac disease patients: prospective analysis on the importance of clinical severity at diagnosis and the impact of treatment. *Dig Liver Dis* 2009; **41**: 15-25 [PMID: [18602354](#) DOI: [10.1016/j.dld.2008.05.011](#)]
 - 14 **Sugai E**, Moreno ML, Hwang HJ, Cabanne A, Crivelli A, Nachman F, Vázquez H, Niveloni S, Argonz J, Mazure R, La Motta G, Caniggia ME, Smecuol E, Chopita N, Gómez JC, Mauriño E, Bai JC. Celiac disease serology in patients with different pretest probabilities: is biopsy avoidable? *World J Gastroenterol* 2010; **16**: 3144-3152 [PMID: [20593499](#) DOI: [10.3748/wjg.v16.i25.3144](#)]
 - 15 **Faulkner-Hogg KB**, Selby WS, Loblay RH. Dietary analysis in symptomatic patients with coeliac disease on a gluten-free diet: the role of trace amounts of gluten and non-gluten food intolerances. *Scand J Gastroenterol* 1999; **34**: 784-789 [PMID: [10499479](#) DOI: [10.1080/003655299750025714](#)]
 - 16 **Sugai E**, Vázquez H, Nachman F, Moreno ML, Mazure R, Smecuol E, Niveloni S, Cabanne A, Kogan Z, Gómez JC, Mauriño E, Bai JC. Accuracy of testing for antibodies to synthetic gliadin-related peptides in celiac disease. *Clin Gastroenterol Hepatol* 2006; **4**: 1112-1117 [PMID: [16860613](#) DOI: [10.1016/j.cgh.2006.05.004](#)]
 - 17 **Leffler D**, Kupfer SS, Lebwohl B, Bugin K, Griebel D, Lathrop JT, Lee JJ, Mulberg AE, Papadopoulos E, Tomaino J, Crowe SE. Development of Celiac Disease Therapeutics: Report of the Third Gastroenterology Regulatory Endpoints and Advancement of Therapeutics Workshop. *Gastroenterology* 2016; **151**: 407-411 [PMID: [27456385](#) DOI: [10.1053/j.gastro.2016.07.025](#)]
 - 18 **Morón B**, Cebolla A, Manyani H, Alvarez-Maqueda M, Megías M, Thomas Mdel C, López MC, Sousa C. Sensitive detection of cereal fractions that are toxic to celiac disease patients by using monoclonal antibodies to a main immunogenic wheat peptide. *Am J Clin Nutr* 2008; **87**: 405-414 [PMID: [18258632](#) DOI: [10.1093/ajcn/87.2.405](#)]
 - 19 **Moreno Mde L**, Cureton PA, Martin ML, Puppa EL, Fasano A, Muñoz-Suano A, López-Casado MÁ, Torres MI, Sousa C, Cebolla Á. Selective capture of most celiac immunogenic peptides from hydrolyzed gluten proteins. *Food Chem* 2016; **205**: 36-42 [PMID: [27006211](#) DOI: [10.1016/j.foodchem.2016.02.066](#)]
 - 20 **Hollon JR**, Cureton PA, Martin ML, Puppa EL, Fasano A. Trace gluten contamination may play a role in mucosal and clinical recovery in a subgroup of diet-adherent non-responsive celiac disease patients. *BMC Gastroenterol* 2013; **13**: 40 [PMID: [23448408](#) DOI: [10.1186/1471-230X-13-40](#)]
 - 21 **Leonard MM**, Cureton P, Fasano A. Indications and Use of the Gluten Contamination Elimination Diet for Patients with Non-Responsive Celiac Disease. *Nutrients* 2017; **9** [PMID: [29057833](#) DOI: [10.3390/nu9101129](#)]
 - 22 **Lee HJ**, Anderson Z, Ryu D. Gluten contamination in foods labeled as "gluten free" in the United States. *J Food Prot* 2014; **77**: 1830-1833 [PMID: [25285507](#) DOI: [10.4315/0362-028X.JFP-14-149](#)]
 - 23 **Syage JA**, Kelly CP, Dickason MA, Ramirez AC, Leon F, Dominguez R, Sealey-Voyksner JA. Determination of gluten consumption in celiac disease patients on a gluten-free diet. *Am J Clin Nutr* 2018; **107**: 201-207 [PMID: [29529159](#) DOI: [10.1093/ajcn/nqx049](#)]
 - 24 **Gibson PR**, Muir JG, Newnham ED. Other Dietary Confounders: FODMAPS *et al.* *Dig Dis* 2015; **33**: 269-276 [PMID: [25925934](#) DOI: [10.1159/000371401](#)]
 - 25 **Wacklin P**, Kaukinen K, Tuovinen E, Collin P, Lindfors K, Partanen J, Mäki M, Mättö J. The duodenal microbiota composition of adult celiac disease patients is associated with the clinical manifestation of the disease. *Inflamm Bowel Dis* 2013; **19**: 934-941 [PMID: [23478804](#) DOI: [10.1097/MIB.0b013e31828029a9](#)]
 - 26 **Nachman F**, Sugai E, Vázquez H, González A, Andrenacci P, Niveloni S, Mazure R, Smecuol E, Moreno ML, Hwang HJ, Sánchez MI, Mauriño E, Bai JC. Serological tests for celiac disease as indicators of long-term compliance with the gluten-free diet. *Eur J Gastroenterol Hepatol* 2011; **23**: 473-480 [PMID: [21537123](#) DOI: [10.1097/MEG.0b013e328346e0f1](#)]
 - 27 **Silvester JA**, Kurada S, Szwajczer A, Kelly CP, Leffler DA, Duerksen DR. Tests for Serum Transglutaminase and Endomysial Antibodies Do Not Detect Most Patients With Celiac Disease and

Persistent Villous Atrophy on Gluten-free Diets: a Meta-analysis. *Gastroenterology* 2017; **153**: 689-701.e1
[PMID: 28545781 DOI: 10.1053/j.gastro.2017.05.015]

P- Reviewer: Dutta AK, Rostami-Nejad M, Vorobjova T
S- Editor: MaRY **L- Editor:** Filipodia **E- Editor:** Huang Y





Randomized Clinical Trial

Khubchandani's procedure combined with stapled posterior rectal wall resection for rectocele

Yi Shao, Yong-Xing Fu, Qing-Fa Wang, Zhi-Qiang Cheng, Guang-Yong Zhang, San-Yuan Hu

ORCID number: Yi Shao (0000-0001-6333-4452); Yong-Xing Fu (0000-0001-8994-1007); Qing-Fa Wang (0000-0001-8737-3595); Zhi-Qiang Cheng (0000-0002-6916-747X); Guang-Yong Zhang (0000-0002-6497-1389); San-Yuan Hu (0000-0002-0546-9778).

Author contributions: Shao Y, Cheng ZQ, Zhang GY, and Hu SY designed the study, analyzed the data, and wrote the paper; Shao Y, Cheng ZQ, and Hu SY performed the surgery and treated the patients; Shao Y, Fu YX, and Wang QF did the follow-up and collected and analyzed the patient data; Hu SY approved the final manuscript.

Institutional review board statement: The study was reviewed and approved by the Ethics Committee of Scientific Research of Shandong University Qilu Hospital.

Clinical trial registration statement: This study is registered at Chinese Clinical Trial Registry, and the registration number is ChiCTR1900020992.

Informed consent statement: In this study, all involved participants or their legal guardian provided written informed consent before entering the trial.

Conflict-of-interest statement: No authors of this paper have conflicting interests.

Data sharing statement: No additional data are available.

CONSORT 2010 statement: The guidelines of the CONSORT 2010

Yi Shao, Zhi-Qiang Cheng, Guang-Yong Zhang, San-Yuan Hu, Department of General Surgery, Qilu Hospital of Shandong University, Jinan 250012, Shandong Province, China

Yong-Xing Fu, Qing-Fa Wang, Department of Neonatal Medicine, Yidu Central Hospital of Weifang, Weifang 262500, Shandong Province, China

Corresponding author: San-Yuan Hu, MD, PhD, Chief Doctor, Professor, Department of General Surgery, Qilu Hospital of Shandong University, No. 107, Wenhua Xi Road, Jinan 250012, Shandong Province, China. huan1962@hotmail.com

Telephone: +86-531-82166351

Fax: +86-531-82166351

Abstract

BACKGROUND

Obstructed defecation syndrome (ODS) is a widespread disease in the world. Rectocele is the most common cause of ODS in females. Multiple procedures have been performed to treat rectocele and no procedure has been accepted as the gold-standard procedure. Stapled transanal rectal resection (STARR) has been widely used. However, there are still some disadvantages in this procedure and its effectiveness in anterior wall repair is doubtful. Therefore, new procedures are expected to further improve the treatment of rectocele.

AIM

To evaluate the efficacy and safety of a novel rectocele repair combining Khubchandani's procedure with stapled posterior rectal wall resection.

METHODS

A cohort of 93 patients were recruited in our randomized clinical trial and were divided into two different groups in a randomized manner. Forty-two patients (group A) underwent Khubchandani's procedure with stapled posterior rectal wall resection and 51 patients (group B) underwent the STARR procedure. Follow-up was performed at 1, 3, 6, and 12 mo after the operation. Preoperative and postoperative ODS scores and depth of rectocele, postoperative complications, blood loss, and hospital stay of each patient were documented. All data were analyzed statistically to evaluate the efficiency and safety of our procedure.

RESULTS

In group A, 42 patients underwent Khubchandani's procedure with stapled posterior rectal wall resection and 34 were followed until the final analysis. In

Statement have been adopted.

Open-Access: This article is an open-access article which selected by an inhouse editor and fully peer-reviewed by external reviewers. It distributed in accordance with the Creative Commons Attribution Non Commercial (CC BY-NC 4.0) license, which permits others to distribute, remix, adapt, build upon this work non-commercially, and license their derivative works on different terms, provided the original work is properly cited and the use is non-commercial. See: <http://creativecommons.org/licenses/by-nc/4.0/>

Manuscript source: Unsolicited manuscript

Received: January 30, 2019

Peer-review started: January 30, 2019

First decision: February 13, 2019

Revised: February 17, 2019

Accepted: February 22, 2019

Article in press: February 22, 2019

Published online: March 21, 2019

group B, 51 patients underwent the STARR procedure and 37 were followed until the final analysis. Mean operative duration was 41.47 ± 6.43 min (group A) *vs* 39.24 ± 6.53 min (group B). Mean hospital stay was 3.15 ± 0.70 d (group A) *vs* 3.14 ± 0.54 d (group B). Mean blood loss was 10.91 ± 2.52 mL (group A) *vs* 10.14 ± 1.86 mL (group B). Mean ODS score in group A declined from 16.50 ± 2.06 before operation to 5.06 ± 1.07 one year after the operation, whereas in group B it was 17.11 ± 2.57 before operation and 6.03 ± 2.63 one year after the operation. Mean depth of rectocele decreased from 4.32 ± 0.96 cm (group A) *vs* 4.18 ± 0.95 cm (group B) preoperatively to 1.19 ± 0.43 cm (group A) *vs* 1.54 ± 0.82 cm (group B) one year after operation. No other serious complications, such as rectovaginal fistula, perianal sepsis, or deaths, were recorded. After 12 mo of follow-up, 30 patients' (30/34, 88.2%) final outcomes were judged as effective and 4 (4/34, 11.8%) as moderate in group A, whereas in group B, 30 (30/37, 81.1%) patients' outcomes were judged as effective, 5 (5/37, 13.5%) as moderate, and 2 (2/37, 5.4%) as poor.

CONCLUSION

Khubchandani's procedure combined with stapled posterior rectal wall resection is an effective, feasible, and safe procedure with minor trauma to rectocele.

Key words: Rectocele; Rectal prolapse; Obstructed defecation syndrome; Khubchandani's procedure; Stapled posterior rectal wall resection; Stapled transanal rectal resection

©The Author(s) 2019. Published by Baishideng Publishing Group Inc. All rights reserved.

Core tip: Rectocele is one of most common causes of obstructed defecation syndrome (ODS) in females. A diversity of procedures has been performed to treat rectocele. Stapled transanal rectal resection (STARR) is more often used among all the procedures for its simpleness. However, it is not the gold-standard procedure since its effect of anterior wall repair is doubted. We performed a novel procedure combining Khubchandani's procedure and stapled posterior wall resection to treat rectocele. We compared the ODS score, rectocele depth, and complications between our procedure and STARR. Our procedure was proved to be safe and effective for treating rectocele.

Citation: Shao Y, Fu YX, Wang QF, Cheng ZQ, Zhang GY, Hu SY. Khubchandani's procedure combined with stapled posterior rectal wall resection for rectocele. *World J Gastroenterol* 2019; 25(11): 1421-1431

URL: <https://www.wjgnet.com/1007-9327/full/v25/i11/1421.htm>

DOI: <https://dx.doi.org/10.3748/wjg.v25.i11.1421>

INTRODUCTION

Obstructed defecation syndrome (ODS), which is more common in females^[1], is one of the most widespread diseases in the world. The symptoms, such as difficult evacuation, prolonged or infrequent defecation, sense of incomplete evacuation, difficult evacuation without hand assistance, and perineal heaviness, significantly lower the life quality of ODS patients. The etiology of ODS can be functional disorders or rectal anatomy abnormality such as rectocele with or without rectal prolapse^[2]. Although the incidence of rectocele is still illusive, approximately 30%-71% females suffer from the disease^[3]; rectocele, pelvic floor^[4] disease, and rectal mucosal prolapse are the most common causes of ODS in approximately 80% of female patients^[5]. Approximately 54% of ODS patients suffer from both mucosal prolapse and rectocele. Several procedures for rectocele resection have been reported during the past years^[6-10], and among them stapled transanal rectal resection (STARR) procedure was more often used. However, the STARR procedure still has its disadvantages^[11,12], and no surgical technique has been widely adopted as the gold-standard procedure for treatment of rectocele^[13-16], as well as rectocele combined with rectal prolapse. Our department developed a new procedure that combined Khubchandani's procedure^[10] with stapled posterior rectal wall resection (KSPRWR) in 42 female patients with ODS caused by rectocele combined with or without rectal mucosal prolapse to evaluate

and compare its safety and effectiveness with the STARR procedure.

MATERIALS AND METHODS

Inclusion criteria

From January 2014 to January 2017, 93 consecutive female patients who suffered from ODS caused by rectocele underwent surgery at Qilu Hospital of Shandong University. Their median age was 48.56 ± 13.22 (mean \pm standard deviation, ranging from 22 to 79) years and their average duration of constipation was 2.27 ± 1.02 (6 mo to 4 years) years. They had an ODS score > 10 ^[17] with a rectocele depth > 2 cm, and failed to respond to conservative measures, such as diet therapy, laxatives, prokinetic medicine, or biofeedback therapy^[18]. All patients were randomly divided into two groups with ODS score and rectocele depth paired. Forty-two patients underwent KSPRWR (group A) and 51 patients underwent the STARR procedure (group B). All symptoms coincided with Rome III diagnostic criteria^[19]. All patients signed a medical consent form before entering the trial.

Exclusion criteria

Patients had a rectocele depth > 2.0 cm and an ODS score > 10 but had not received any medical treatment, or patients did not undergo operation due to health or personal reason were excluded from our trial. Defecography, colonoscopy, transmission test, and rectal and canal manometry were performed to exclude slow transit constipation, rectal or colorectal carcinoma, complete rectal prolapse, enterocoele, inflammatory bowel disease, severe fecal incontinence, and pelvic floor dyssynergia. Patients with an ODS score < 10 or a depth of rectocele < 2.0 cm, which was shown on defecography, were not recruited in our study. Patients who failed to perform the follow-up were not take into the final analysis.

Surgical procedure

Preoperative procedure: An enema was administered the night before the surgery and another on the morning of the surgery. Other preoperative preparations included perioperative antibiotics and insertion of a urinary catheter.

KSPRWR procedure: The patients received spinal anesthesia and were placed in the prone jackknife position. The procedure comprised two steps. Step 1 included performing stapled posterior rectal wall resection, as follows: We placed a circular anal dilator to loosen the anal canal and then inserted a half-purse string suture, which only included the mucosa and the submucosa, clockwise from 8 o'clock to 4 o'clock using a 2-0 absorbable suture at about 4 cm above the dentate line on the posterior wall of the anus. We placed the anvil of the stapling instrument (EEATM Auto SutureTM Hemorrhoid and Prolapse Stapler with DST SeriesTM Technology, 3.3-3.5 mm) above the half-purse string and inserted a small intestinal spatula into the anus with the distant edge above the half-purse string to protect the anterior wall. The stapler was adjusted until the half-purse string lay on the shaft of the stapler. We then closed and fired the stapler and held it closed for 15 s to aid hemostasis. The stapler was opened to its maximum and withdrawn. The posterior rectal wall was resected as a half circle. In step 2, we performed the procedure as reported by Khubchandani^[20]: 1:1000 adrenaline was injected into the mucosa of the anterior rectal wall to aid hemostasis. A transverse incision was made at the dentate line with a length of 2-3 cm but not too close to the staple line, and at the edge of the transverse incision two vertical incisions were made and extended into the anus for about 7 cm. It is very important that the incision reaches the muscular layer. Thus, a U-shaped mucomuscular flap was obtained and the flap was freed from the mucosal layer with meticulous hemostasis. Furthermore, three to five interrupted transverse sutures, which started from the dentate line to the edge of the flap using 3-0 polyglycolic acid absorbable stitches, were placed at the mucosal layer to plicate the flabby rectovaginal septum, thus strengthening the anterior wall. Then two vertical sutures, which started at the proximal and ended at the distal points of the incision, were made to plicate the anterior rectal wall. During suturing, the guidance of the finger into the vagina was essential to prevent penetration of the suture into the vaginal mucosa. Most part of the flap was resected to further strengthen the anterior wall and the transverse and vertical incisions were sewed using interrupted sutures (Figure 1).

STARR procedure: Posterior wall repair was the same as that for the KWPRWR procedure. The same method was used to repair the anterior rectal wall. The staple line of the posterior wall was 1-2 cm deeper into the anus than that of the anterior wall (Figure 2).

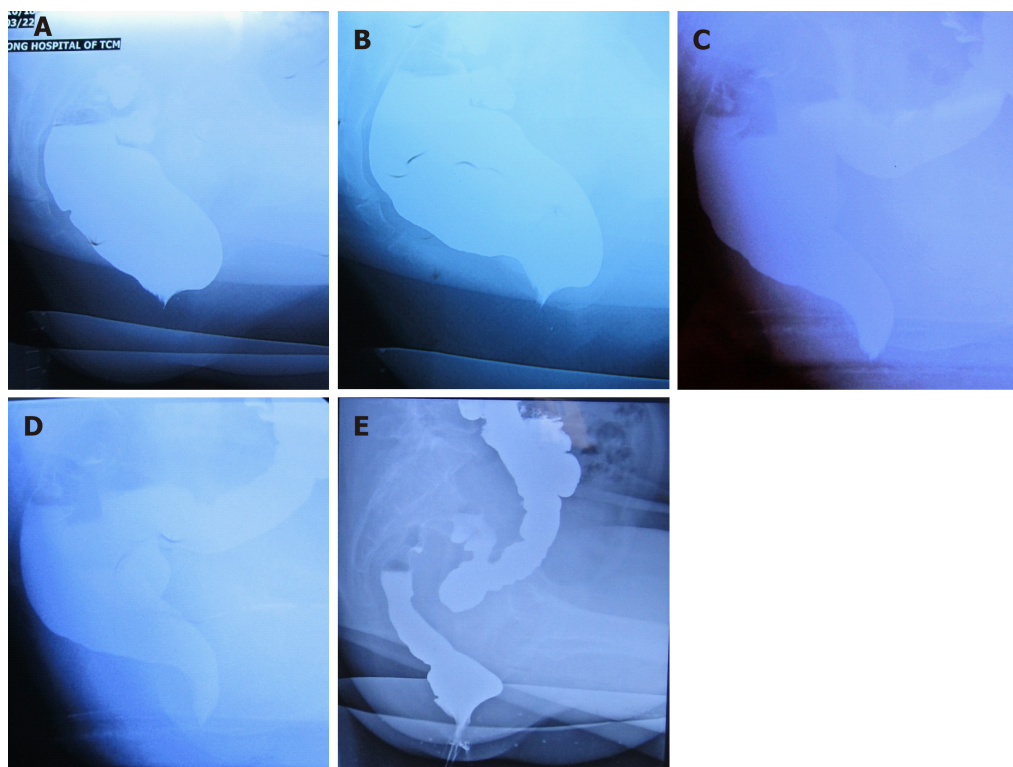


Figure 1 Defecography images for rectocele patients. A: Preoperative defecography for a patient in group A; B: Preoperative defecography for a patient in group B; C: Postoperative defecography for the patient in group A; D: Postoperative defecography for the patient in group B; E: Defecography image of rectocele recurrence.

Postoperative procedure: A drainage tube circled by three layers of Vaseline pledget was inserted into the anus as an anal plug for hemostasis and was removed on the second day after operation. The urinary catheter was removed on the second day after operation.

Follow-up

The complications of the operation (*e.g.*, postoperative bleeding, anal fissure, rectal stricture, incontinence to flatus, persistent pain, *etc.*), the depth of the rectocele, and the ODS scores were recorded before and after operation. The follow-up was performed at 1, 3, 6, and 12 mo after operation. Follow-up was discontinued in the following situations: unable to return for a check-up at the follow-up time point, severe diseases, mental illness, postoperative operation, and death.

Evaluation of procedure effectiveness

After 12 mo of follow-up, procedure effectiveness in patients with an ODS score < 10 and a depth of rectocele < 2.0 cm, but without other complications that were included in Rome III diagnostic criteria (*e.g.*, incontinence to flatus) was considered effective. Procedure effectiveness in patients with complications in Rome III diagnostic criteria but having an ODS score < 10 and a depth of rectocele < 2.0 cm was considered moderate, and procedure effectiveness in patients with an ODS score > 10 or a depth of rectocele > 2.0 cm was considered poor.

Statistical analysis

All data are expressed as the mean \pm standard deviation. Statistical analyses were performed using paired *t*-test with SPSS 22.0, and the level of statistical significance was set at $P < 0.05$.

RESULTS

In group A, eight patients failed to perform our follow-up program; therefore, there were 34 patients in the final analysis with at least 12 mo of follow-up. In group B, there were 37 patients in the final analysis. All females suffered from rectocele, and 23 (23/34, 67.6%) patients in group A and 24 (24/37, 64.9%) in group B suffered from both rectocele and rectal prolapse. Mean operative time was 41.47 ± 6.43 min (group A) *vs* 39.24 ± 6.53 (group B). Mean hospital stay was 3.15 ± 0.70 d (group A) *vs* $3.14 \pm$

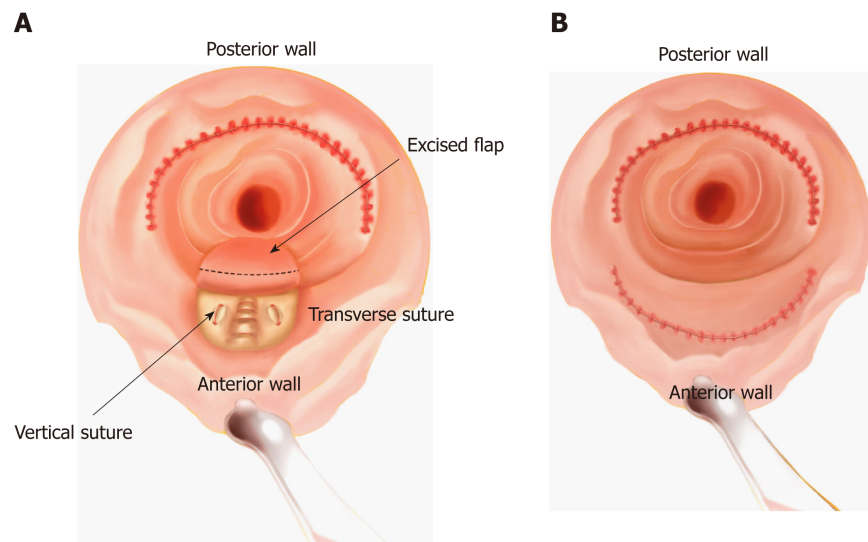


Figure 2 Sketch of the operation. A: Khubchandani's procedure with stapled posterior rectal wall resection. Stapled posterior wall repair is performed. Subsequently, a U-shape flap is freed, and three to five transverse and two vertical sutures are made in the muscular layer. Then, most part of the U-shape flap is excised and sutured; B: Stapled transanal rectal resection. Stapled rectal wall repair is performed in both the anterior and posterior wall.

0.54 d (group B), and mean blood loss was 10.91 ± 2.52 mL (group A) *vs* 10.14 ± 1.86 mL (group B). No significant differences were found regarding operative time, hospital stay, or blood loss between the two groups (Table 1).

The minimum follow-up duration was 12 mo. At this follow-up, ODS scores, depth of rectocele, and complications of operation were recorded. Mean ODS score before the operation was 16.50 ± 2.06 (group A) *vs* 17.11 ± 2.57 (group B) (Figure 3A). Mean ODS score 1 mo after operation (1MT), 3 mo after operation (3MT), 6 mo after operation (6MT), and 1 year after operation (12MT) in groups A and B were 4.62 ± 2.03 *vs* 4.76 ± 1.98 , 5.38 ± 2.34 *vs* 5.68 ± 2.03 , 4.94 ± 2.09 *vs* 5.78 ± 2.64 , and 5.06 ± 1.07 *vs* 6.03 ± 2.63 , respectively. Compared with the preoperative ODS scores, ODS scores at 1MT, 3MT, 6MT, and 12MT all had significant differences in both groups A and B ($P < 0.05$) (Table 2). In the pairwise comparison of postoperative groups (1MT, 3MT, 6MT, and 12MT) in each group, there were no significant differences ($P > 0.05$). There was a statistical difference in 12MT ODS scores between groups A and B. The ODS scores of two patients were over 10 at 12MT in group B.

Mean preoperative depth of rectocele was 4.32 ± 0.96 cm (group A) *vs* 4.18 ± 0.95 cm (group B) (Figure 3B). Mean ODS scores at 1MT, 3MT, 6MT, and 12MT were 1.15 ± 0.31 cm (group A) *vs* 1.13 ± 0.42 cm (group B), 1.20 ± 0.35 cm *vs* 1.25 ± 0.50 cm, 1.14 ± 0.44 cm *vs* 1.33 ± 0.42 cm, and 1.19 ± 0.43 cm *vs* 1.54 ± 0.82 cm, respectively. Compared with the preoperative rectocele depth, rectocele depth at 1MT, 3MT, 6MT, and 12MT all showed statistically significant differences in both groups A and B ($P < 0.05$) (Table 2). There were no significant differences ($P > 0.05$) in the pairwise comparison of the postoperative groups (1MT, 3MT, 6MT, and 12MT) in each group. A statistical difference was found in 12MT depth of rectocele between the two groups. One patient's rectocele depth was over 2 cm at 12MT (Figure 1E).

In group A, five (5/34, 14.7%) patients had vaginal discomfort in the first week after operation (Table 3). Retention of urine after removal of the ureter was seen in three (3/34, 8.8%) patients. Postoperative bleeding occurred in one (1/34, 2.9%) patient after the anal plug was removed, but blood loss was approximately less than 5 mL and stopped spontaneously. The other complications that occurred in the first week after operation were nausea (7/34, 20.6%), anal fissures (7/34, 20.6%), incontinence to flatus (2/34, 5.9%), defecatory urgency (2/34, 5.9%), and persistent pain (13/34, 38.2%). One patient felt defecatory urgency after surgery and relieved at 6MT, while three patients complained about defecatory urgency since 6MT and did not relieve at 12MT. No occurrence of staple line dehiscence, rectal stricture, rectovaginal fistula, or perianal sepsis was recorded. No deaths were reported 12 mo after operation.

In group B, nine (9/37, 24.3%) patients had nausea after operation and no postoperative bleeding occurred (Table 4). The most common complications in the first week after operation in group B was persistent pain (12/37, 32.4%), and two (2/37, 5.4%) patients continued to experience anal pain 12 mo after operation. The other complications that occurred in the first week after operation were retention of

Table 1 Patients' clinical characteristics

	n/mean \pm SD	
	KSPRWR	STARR
Age (yr)	46.59 \pm 9.41	50.38 \pm 15.86
Gender	Female	Female
Combined with rectal prolapse	23	24
History of disease (yr)	2.35 \pm 0.93	2.20 \pm 1.11
Procedure (in final analysis)	34	37
Operative time (min)	41.47 \pm 6.43	39.24 \pm 6.53
Estimated blood loss (mL)	10.91 \pm 2.52	10.14 \pm 1.86
Hospital stay (d)	3.15 \pm 0.70	3.14 \pm 0.54

KSPRWR: Khubchandani's procedure with stapled posterior rectal wall resection; STARR: Stapled transanal rectal resection.

urine after urinary catheter removal (1/37, 2.7%), anal fissures (5/37, 13.5%), incontinence to flatus (2/37, 5.4%), and defecatory urgency (2/37, 5.4%). No occurrence of staple line dehiscence, rectal stricture, rectovaginal fistula, or perianal sepsis was recorded. No deaths were reported 12 mo after operation. One patient had the feeling of incontinence to flatus and another patient felt defecatory urgency until 3 mo after surgery and they all relieved at 6MT. Two patients had incontinence to flatus and defecatory urgency since 6MT, which further worsened at 12MT. The follow-up revealed that their ODS scores were more than 10. The rectocele depth in one of the patients was more than 2.0 cm. Thus, recurrence was reported in these two patients.

After 12 mo of follow-up, 30 patients' (30/34, 88.2%) final outcomes were judged as effective and 4(4/34, 11.8%) as moderate in group A, whereas in group B, 30 (30/37, 81.1%) patients' outcomes were judged as effective, 5 (5/37, 13.5%) as moderate, and 2 (2/37, 5.4%) as poor.

DISCUSSION

Rectocele is one of the most common causes of female ODS^[21,22]. The reason for the high morbidity of rectocele might be that the internal anal sphincter is shorter and formed distally in the anterior upper anal canal, which might weaken the anorectal junction that is devoid of support structure in females^[23]. A substantial number of procedures *via* the vagina^[24,25], perineum^[26], anus^[6,27], or abdomen^[28,29] have been reported to repair the rectocele through different routes, and none of the methods were adopted as the gold-standard operation^[25]. Longo^[6,7] performed STARR, which has been ameliorated and used owing to its simple, easy, and fast operation^[30-32] since the past years. The STARR procedure aims to rebuild the rectal volume and strengthen the anterior rectal wall through linear resection and suturing of the frail rectal mucosa, submucosa, and superficial muscular layer^[7]. The entire procedure requires two staplers and is simple to perform. Moreover, it effectively rebuilds the rectal volume by resection of the prolapsed tissue. However, there is an ongoing debate between the supporters and the opponents of STARR as multiple postoperative complications have been reported^[31,33-37] after STARR. Some long-term follow-up studies^[11,38] revealed that the ODS score of patients who underwent the STARR procedure had a smooth increase after operation. Moreover, the effectiveness of anterior wall repair using the STARR procedure has been questioned by some opponents^[2,39]. They argue that the resection of the muscular layer in the STARR procedure is not adequate to strengthen the anterior rectal wall; thus, recurrence can be expected in the future. Some supporters of the STARR procedure also admitted that, so several modified STARR procedures were invented^[34,35] to ensure the effectiveness of anterior wall repair. However, none of these modified procedures has been accepted as a gold-standard procedure as the long-term curative effect is not clear.

Khubchandani *et al*^[10,20] reported his procedure of rectocele repair with satisfactory outcomes. This procedure strengthens the anterior rectal wall through transverse suturing in the muscular layer. However, rectal prolapse combined with rectocele, with morbidity ranging from 24% to 54%^[5,11,18], was not considered in their procedure. Moreover, Khubchandani *et al*^[20] found that isolated anterior rectal wall repair in the

Table 2 Comparisons of obstructed defecation syndrome scores and rectocele depth

		ODS score		Rectocele depth	
		Group A	Group B	Group A	Group B
Comparison within group	a	$P < 0.05$	$P < 0.05$	$P < 0.05$	$P < 0.05$
	b	$P < 0.05$	$P < 0.05$	$P < 0.05$	$P < 0.05$
	c	$P < 0.05$	$P < 0.05$	$P < 0.05$	$P < 0.05$
	d	$P < 0.05$	$P < 0.05$	$P < 0.05$	$P < 0.05$
	e	$P > 0.05$	$P > 0.05$	$P > 0.05$	$P > 0.05$
	f	$P > 0.05$	$P > 0.05$	$P > 0.05$	$P > 0.05$
	g	$P > 0.05$	$P > 0.05$	$P > 0.05$	$P > 0.05$
	h	$P > 0.05$	$P > 0.05$	$P > 0.05$	$P > 0.05$
	i	$P > 0.05$	$P > 0.05$	$P > 0.05$	$P > 0.05$
	j	$P > 0.05$	$P > 0.05$	$P > 0.05$	$P > 0.05$
Comparison between groups	k	$P > 0.05$		$P > 0.05$	
	l	$P > 0.05$		$P > 0.05$	
	m	$P > 0.05$		$P > 0.05$	
	n	$P > 0.05$		$P > 0.05$	
	o	$P < 0.05$		$P < 0.05$	

a: 1MT *vs* Preoperative; b: 3MT *vs* Preoperative; c: 6MT *vs* Preoperative; d: 12MT *vs* Preoperative; e: 1MT *vs* 3MT; f: 1MT *vs* 6MT; g: 1MT *vs* 12MT; h: 3MT *vs* 6MT; i: 3MT *vs* 12MT; j: 6MT *vs* 12MT; k: Group A preoperative *vs* Group B preoperative; l: Group A 1MT *vs* Group B 1MT; m: Group A 3MT *vs* Group B 3MT; n: Group A 6MT *vs* Group B 6MT; o: Group A 12MT *vs* Group B 12MT. ODS: Obstructed defecation syndrome; 1MT: 1 mo after operation; 3MT: 3 mo after operation; 6MT: 6 mo after operation; 12MT: 1 year after operation.

rectocele without rectal prolapse may cause hypotonus of the posterior wall, which may induce posterior rectal wall intussusception after operation. As the effect of rebuilding the rectal volume of STARR procedure is clear, we decided to combine the two procedures. We used Khubchandani's procedure for anterior wall repair to strengthen the rectal wall and stapled posterior rectal wall resection to resect the potentially or already existing excessive tissue of the posterior wall to restore anatomy and correct the tension of posterior rectal wall in rectocele patients with or without rectal prolapse.

There were no significant differences in hospital stay, operative time, or blood loss between the two groups, which indicated that the trauma and difficulty of the two operations have no significant difference. The most common postoperative complication of STARR was persistent anal pain because of the staple line. In our research, one patient had persistent pain at 12MT in group A and two patients had persistent pain at 12MT in group B. Nausea was the second most common complication in both groups, especially in women aged 45-55 years. All episodes of nausea occurred in the first three days after operation and all were relieved one week after the operation, which might be related to hormonal standard^[37]. Rectal vaginal fistula is a very serious complication in both procedures, but no rectal vaginal fistula was recorded in both groups. Our experience was that while performing anterior wall repair, a guidance of the finger into the vagina is essential to prevent the damage. No occurrence of staple line dehiscence, rectal stricture, or perianal sepsis was recorded in our research. Vagina discomfort is a rare but annoying complication in Khubchandani's procedure^[20], which is probably due to the suture in the rectovaginal septum. In our study, five patients experienced vagina discomfort in the first week after operation, and the discomfort was relieved at 3MT. Anal fissure is another common complication after rectocele surgery^[11,38,40,41], especially using the STARR procedure. More patients suffered anal fissure in group A in the first week after operation, but the number became the same after that. No anal fissure was recorded at 12MT in either group.

In our study, the mean ODS score of the patients who underwent the STARR procedure significantly dropped to a normal level at 1MT. However, although the ODS scores of the STARR group remained within normal levels, they continued to increase smoothly from 3MT to 12MT. Accompanied with the increasing ODS score, the depth of the rectocele also increased from 3MT to 12MT. However, in patients who underwent our procedure, the ODS score and rectocele depth dropped to normal

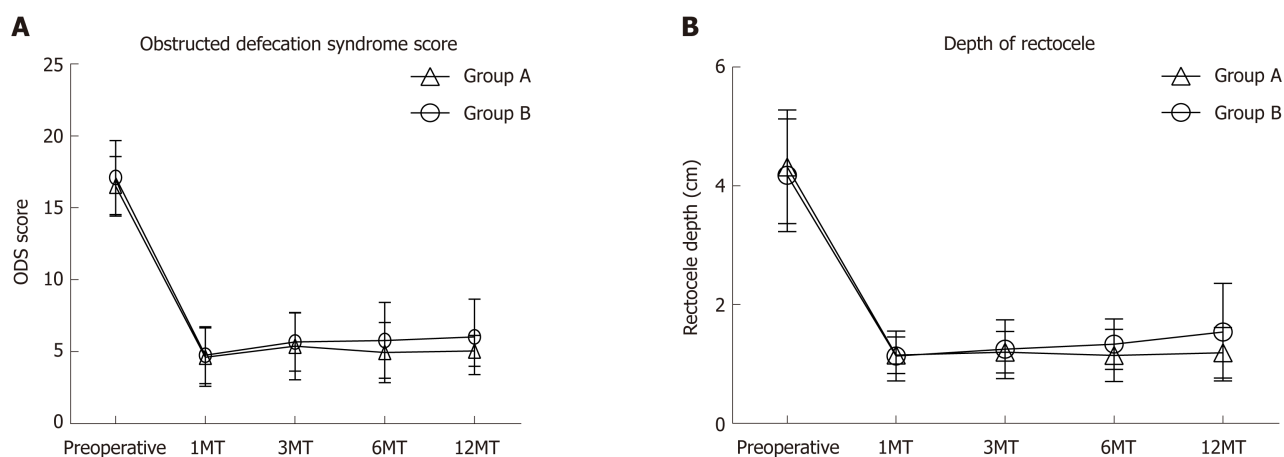


Figure 3 Preoperative and postoperative obstructed defecation syndrome scores and rectocele depth. A: Obstructed defecation syndrome score. There was a statistical difference between groups A and B at 1 year after operation; B: Rectocele depth. There was a statistical difference between groups A and B at 1 year after operation. ODS: Obstructed defecation syndrome; 1MT: 1 mo after operation; 3MT: 3 mo after operation; 6MT: 6 mo after operation; 12MT: 1 year after operation.

levels after surgery, remained at a certain level at 3MT and 6MT, and slightly increased within normal standard at 12MT. Recurrence did not occur in any patient in group A, but two patients in group B had recurrence at 12 MT. Defecography showed that the rectocele depth of one patient was more than 2 cm. Interestingly, these two patients both had deep preoperative rectocele which was around 5.5 cm in depth, thus indicating that the STARR procedure might have a less effect than expected in anterior wall repair in the patients with deep rectocele. Furthermore, defecatory urgency and incontinence to flatus were the most common complaints after operation^[9,39,42,43]. More patients in group B experienced these symptoms at 12MT than those in group A. Moreover, although the mean ODS score and rectocele depth were within normal levels in both groups, they were significantly lower in group A than in group B at 12MT, thus indicating that the patients who underwent our procedure might have a better outcome in the mid-long period.

In this research, we gained initial experience of the new procedure. There are four key points of successfully carrying out this operation. The first one was to make sure that the transverse and vertical suture in the anterior wall was in the muscular layer. This can ensure the effectiveness of anterior wall repair. The second key point was that the vertical edge of the U-shaped flap should not overlap with the stapler suture on the posterior wall in the case of postoperative rectal stricture. The third key point was excising most part but not all of the U-shape flap and leaving proper part of the flap. This was significant to avoid rectal stricture. The last key point of the procedure was using the finger as guidance in the vagina to prevent damage. As we suture the anterior wall, there is a possibility of hurting the vagina; therefore, the guidance is quite important. This requires skill and practice.

Although our procedure was not less effective than the STARR procedure in a short to middle term, there were still some limitations in our research. We did not perform any procedure or treatment on the recurrent patients since we lost the contact with them after the last check-up, thus we could not explore if our procedure would be effective for recurrent rectocele. Besides, we need more experience on selecting a more suitable type of stitch for suture in rectal vaginal septum so that less vagina discomfort would happen after our surgery. Furthermore, we did not set subgroups to analyze different outcomes of the two procedures in patients with different rectocele depth or ODS scores. A larger number of patients, a multiple center study, and a longer-term follow-up are needed to further prove its effectiveness and safety.

In conclusion, Khubchandani's procedure combined with stapled posterior rectal wall resection is an effective and safe procedure with minor trauma, short hospital stay, and low cost for rectocele treatment, especially for rectocele combined with rectal prolapse. It is not less effective compared with the STARR procedure, which may be an optional procedure in the treatment of rectocele with rectal prolapse. We plan to perform a longer period follow-up and recruit larger number of patients in a multiple center, which aims at determining long-term postoperative quality of life in female patients, to further verify the safety and effectiveness of the procedure in the future.

Table 3 Complications of group A

Complication	First week	1 mo after operation	3 mo after operation	6 mo after operation	12 mo after operation
Nausea	7 (20.6%)	0	0	0	0
Retention of urine after urinary catheter removal	3 (8.8%)	0	0	0	0
Anal fissure	7 (20.6%)	5 (14.7%)	2 (5.9%)	0	0
Incontinence to flatus	2 (5.9%)	1 (2.9%)	0	0	0
Postoperative bleeding	1 (2.9%)	0	0	0	0
Defecatory urgency	2 (5.9%)	1 (2.9%)	1 (2.9%)	3 (8.8%)	3 (8.8%)
Persistent pain	13 (38.2%)	4 (11.8%)	2 (5.9%)	2 (5.9%)	1 (2.9%)
Vagina discomfort	5 (14.7%)	2 (5.9%)	0	0	0
Recurrence	0	0	0	0	0

Table 4 Complications of group B

Complication	First week	1 mo after operation	3 mo after operation	6 mo after operation	12 mo after operation
Nausea	9 (24.3%)	0	0	0	0
Retention of urine after urinary catheter removal	1 (2.7%)	0	0	0	0
Anal fissure	5 (13.5%)	5 (13.5%)	2 (5.4%)	0	0
Incontinence to flatus	2 (5.4%)	1 (2.7%)	1 (2.7%)	3 (8.1%)	4 (10.8%)
Postoperative bleeding	0	0	0	0	0
Defecatory urgency	2 (5.4%)	1 (2.7%)	1 (2.7%)	2 (5.4%)	3 (8.1%)
Persistent pain	12 (32.4%)	3 (8.1%)	2 (5.4%)	2 (5.4%)	2 (5.4%)
Vagina discomfort	0	0	0	0	0
Recurrence	0	0	0	0	2 (5.4%)

ARTICLE HIGHLIGHTS

Research background

Obstructed defecation syndrome (ODS) has a serious influence on health and life quality of patients. Rectocele is one of the main causes of ODS, which has an approximate incidence of 30%-71%. Multiple procedures have been performed to treat rectocele, but no one has been considered as the gold-standard treatment.

Research motivation

Stapled transanal rectal resection (STARR) has been quite popular in treating rectocele for its simpleness. However, debate on STARR has never stopped. Opponents doubted its effectiveness in anterior wall repair and declared that multiple serious postoperative complications occurred. Khubchandani performed his procedure for rectocele with a satisfying effect, but it did not take rectal prolapse into consideration and may potentially induce rectal prolapse in posterior rectal wall. Therefore, we combined Khubchandani's procedure and stapled posterior rectal wall resection together.

Research objectives

In this study, we evaluated the efficacy and safety of a novel rectocele repair which combined Khubchandani's procedure with stapled posterior rectal wall resection. The results of the study will guide the treatment for rectocele in future.

Research methods

From January 2014 to January 2017, 93 patients were recruited into our randomized clinical trial and divided into two different groups in a randomized manner. Forty-two patients (group A) underwent Khubchandani's procedure with stapled posterior rectal wall resection (KSPRWR) and 51 patients (group B) underwent the stapled transanal rectal resection (STARR) procedure. Follow-up was performed at 1, 3, 6, and 12 mo after the operation. Preoperative and postoperative ODS scores and depth of rectocele, postoperative complications, blood loss, and hospital stay of each patient were documented. All data were analyzed statistically to evaluate the efficiency and safety of our procedure.

Research results

No significant differences were found in blood loss, hospital stay, or operative time. Compared with preoperative ODS scores and rectocele depth, postoperative ODS scores and rectocele depth in the two groups were statistically lower, which proved the effectiveness of our procedure. There were significant differences when comparing the ODS score and rectocele depth 1 year after operation, which were significantly lower in group A than in group B, thus indicating that group A might have better outcomes in future.

Research conclusions

KSPRW is an effective and safe procedure with minor trauma, short hospital stay, and low cost for rectocele treatment, especially for rectocele combined with rectal prolapse. It should be considered as an alternative operation for rectocele.

Research perspectives

A long-term follow-up, a larger number of patients, and a multiple center clinical trial are expected in the future to further prove the effectiveness and safety of this procedure.

REFERENCES

- 1 Heaton KW, Radvan J, Cripps H, Mountford RA, Braddon FE, Hughes AO. Defecation frequency and timing, and stool form in the general population: A prospective study. *Gut* 1992; **33**: 818-824 [PMID: 1624166 DOI: 10.1136/gut.33.6.818]
- 2 Mustain WC. Functional Disorders: Rectocele. *Clin Colon Rectal Surg* 2017; **30**: 63-75 [PMID: 28144214 DOI: 10.1055/s-0036-1593425]
- 3 Schmidlin-Enderli K, Schuessler B. A new rectovaginal fascial plication technique for treatment of rectocele with obstructed defecation: A proof of concept study. *Int Urogynecol J* 2013; **24**: 613-619 [PMID: 22890282 DOI: 10.1007/s00192-012-1911-z]
- 4 Zbar AP, Lienemann A, Fritsch H, Beer-Gabel M, Pescatori M. Rectocele: Pathogenesis and surgical management. *Int J Colorectal Dis* 2003; **18**: 369-384 [PMID: 12665990 DOI: 10.1007/s00384-003-0478-z]
- 5 Pescatori M, Spyrou M, Pulvirenti d'Urso A. A prospective evaluation of occult disorders in obstructed defecation using the 'iceberg diagram'. *Colorectal Dis* 2006; **8**: 785-789 [PMID: 17032326 DOI: 10.1111/j.1463-1318.2006.01138.x]
- 6 Longo A. Treatment of hemorrhoids disease by reduction of mucosa and hemorrhoidal prolapse with a circular suturing device: A new procedure; Proceedings of the 6th World Congress of Endoscopic Surgery; 1998 Jun 3-6; Rome, Italy. Bologna: Monduzzi Publishing 1998; 777-784
- 7 Longo A. Obstructed defecation because of rectal pathologies 2004
- 8 Bresler L, Rauch P, Denis B, Grillot M, Tortuyaux JM, Regent D, Boissel P, Grosdidier J. [Treatment of sub-levator rectocele by transrectal approach. Value of the automatic stapler with linear clamping]. *J Chir (Paris)* 1993; **130**: 304-308 [PMID: 8408332]
- 9 Hasan HM, Hasan HM. Stapled transanal rectal resection for the surgical treatment of obstructed defecation syndrome associated with rectocele and rectal intussusception. *ISRN Surg* 2012; **2012**: 652345 [PMID: 22577584 DOI: 10.5402/2012/652345]
- 10 Khubchandani IT, Sheets JA, Stasik JJ, Hakki AR. Endorectal repair of rectocele. *Dis Colon Rectum* 1983; **26**: 792-796 [PMID: 6641461 DOI: 10.1007/BF02554752]
- 11 Pescatori M, Gagliardi G. Postoperative complications after procedure for prolapsed hemorrhoids (PPH) and stapled transanal rectal resection (STARR) procedures. *Tech Coloproctol* 2008; **12**: 7-19 [PMID: 18512007 DOI: 10.1007/s10151-008-0391-0]
- 12 Schiano di Visconte M, Nicoli F, Pasquali A, Bellio G. Clinical outcomes of stapled transanal rectal resection for obstructed defaecation syndrome at 10-year follow-up. *Colorectal Dis* 2018; **20**: 614-622 [PMID: 29363847 DOI: 10.1111/codi.14028]
- 13 Beck DE, Allen NL. Rectocele. *Clin Colon Rectal Surg* 2010; **23**: 90-98 [PMID: 21629626 DOI: 10.1055/s-0030-1254295]
- 14 Bruscianno L, Limongelli P, Tolone S, del Genio GM, Martellucci J, Docimo G, Lucido F, Docimo L. Technical Aspect of Stapled Transanal Rectal Resection. From PPH-01 to Contour to Both: An Optional Combined Approach to Treat Obstructed Defecation? *Dis Colon Rectum* 2015; **58**: 817-820 [PMID: 26163963 DOI: 10.1097/DCR.0000000000000381]
- 15 Ellis CN, Essani R. Treatment of obstructed defecation. *Clin Colon Rectal Surg* 2012; **25**: 24-33 [PMID: 23449341 DOI: 10.1055/s-0032-1301756]
- 16 Wexner SD. Reaching a Consensus for the Stapled Transanal Rectal Resection Procedure. *Dis Colon Rectum* 2015; **58**: 821 [PMID: 26163964 DOI: 10.1097/DCR.0000000000000380]
- 17 Altomare DF, Spazzafumo L, Rinaldi M, Dodi G, Ghiselli R, Piloni V. Set-up and statistical validation of a new scoring system for obstructed defaecation syndrome. *Colorectal Dis* 2008; **10**: 84-88 [PMID: 17441968 DOI: 10.1111/j.1463-1318.2007.01262.x]
- 18 Lembo A, Camilleri M. Chronic constipation. *N Engl J Med* 2003; **349**: 1360-1368 [PMID: 14523145 DOI: 10.1056/NEJMr020995]
- 19 Rome Foundation. Guidelines--Rome III Diagnostic Criteria for Functional Gastrointestinal Disorders. *J Gastrointest Liver Dis* 2006; **15**: 307-312 [PMID: 17203570]
- 20 Khubchandani IT, Clancy JP, Rosen L, Riether RD, Stasik JJ. Endorectal repair of rectocele revisited. *Br J Surg* 1997; **84**: 89-91 [PMID: 9043465 DOI: 10.1046/j.1365-2168.1997.02463.x]
- 21 Bozkurt MA, Kocataş A, Karabulut M, Yürgin H, Kalaycı MU, Ahiş H. Two Etiological Reasons of Constipation: Anterior Rectocele and Internal Mucosal Intussusception. *Indian J Surg* 2015; **77**: 868-871 [PMID: 27011472 DOI: 10.1007/s12262-014-1042-5]
- 22 Stewart JR, Hamner JJ, Heit MH. Thirty Years of Cystocele/Rectocele Repair in the United States. *Female Pelvic Med Reconstr Surg* 2016; **22**: 243-247 [PMID: 26825407 DOI: 10.1097/SPV.0000000000000240]
- 23 Fritsch H, Höttinger H. Tomographical anatomy of the pelvis, visceral pelvic connective tissue, and its

- compartments. *Clin Anat* 1995; **8**: 17-24 [PMID: 7697508 DOI: 10.1002/ca.980080103]
- 24 **Shafik AA**, El Sibai O, Shafik IA. Rectocele repair with stapled transvaginal rectal resection. *Tech Coloproctol* 2016; **20**: 207-214 [PMID: 26711102 DOI: 10.1007/s10151-015-1410-6]
 - 25 **Stojkovic SG**, Balfour L, Burke D, Finan PJ, Sagar PM. Does the need to self-digitate or the presence of a large or nonemptying rectocele on proctography influence the outcome of transanal rectocele repair? *Colorectal Dis* 2003; **5**: 169-172 [PMID: 12780908 DOI: 10.1046/j.1463-1318.2003.00427.x]
 - 26 **Watson SJ**, Loder PB, Halligan S, Bartram CI, Kamm MA, Phillips RK. Transperineal repair of symptomatic rectocele with Marlex mesh: A clinical, physiological and radiologic assessment of treatment. *J Am Coll Surg* 1996; **183**: 257-261 [PMID: 8784320]
 - 27 **Maurel J**, Gignoux M. [Surgical treatment of supralevator rectocele. Value of transanal excision with automatic stapler and linear suture clips]. *Ann Chir* 1993; **47**: 326-330 [PMID: 8352510]
 - 28 **Fox SD**, Stanton SL. Vault prolapse and rectocele: Assessment of repair using sacrocolpopexy with mesh interposition. *BJOG* 2000; **107**: 1371-1375 [PMID: 11117764 DOI: 10.1111/j.1471-0528.2000.tb11650.x]
 - 29 **Thornton MJ**, Lam A, King DW. Laparoscopic or transanal repair of rectocele? A retrospective matched cohort study. *Dis Colon Rectum* 2005; **48**: 792-798 [PMID: 15785902 DOI: 10.1007/s10350-004-0843-1]
 - 30 **Lenisa L**, Schwandner O, Stuto A, Jayne D, Pigot F, Tuech JJ, Scherer R, Nugent K, Corbisier F, Espin-Basany E, Hetzer FH. STARR with Contour Transtar: Prospective multicentre European study. *Colorectal Dis* 2009; **11**: 821-827 [PMID: 19175625 DOI: 10.1111/j.1463-1318.2008.01714.x]
 - 31 **Liu WC**, Wan SL, Yaseen SM, Ren XH, Tian CP, Ding Z, Zheng KY, Wu YH, Jiang CQ, Qian Q. Transanal surgery for obstructed defecation syndrome: Literature review and a single-center experience. *World J Gastroenterol* 2016; **22**: 7983-7998 [PMID: 27672293 DOI: 10.3748/wjg.v22.i35.7983]
 - 32 **Ribaric G**, D'Hoore A, Schiffhorst G, Hempel E; TRANSTAR Registry Study Group. STARR with CONTOUR® TRANSTAR™ device for obstructed defecation syndrome: One-year real-world outcomes of the European TRANSTAR registry. *Int J Colorectal Dis* 2014; **29**: 611-622 [PMID: 24554148 DOI: 10.1007/s00384-014-1836-8]
 - 33 **Arroyo A**, González-Argenté FX, García-Domingo M, Espin-Basany E, De-la-Portilla F, Pérez-Vicente F, Calpena R. Prospective multicentre clinical trial of stapled transanal rectal resection for obstructive defaecation syndrome. *Br J Surg* 2008; **95**: 1521-1527 [PMID: 18942056 DOI: 10.1002/bjs.6328]
 - 34 **Lin HC**, Chen HX, He QL, Huang L, Zhang ZG, Ren DL. A Modification of the Stapled TransAnal Rectal Resection (STARR) Procedure for Rectal Prolapse. *Surg Innov* 2018; **25**: 578-585 [PMID: 30117358 DOI: 10.1177/1553350618793415]
 - 35 **Ren XH**, Yaseen SM, Cao YL, Liu WC, Shrestha S, Ding Z, Wu YH, Zheng KY, Qian Q, Jiang CQ. A transanal procedure using TST STARR Plus for the treatment of Obstructed Defecation Syndrome: 'A mid-term study'. *Int J Surg* 2016; **32**: 58-64 [PMID: 27345262 DOI: 10.1016/j.ijsu.2016.06.039]
 - 36 **Tjandra JJ**, Ooi BS, Tang CL, Dwyer P, Carey M. Transanal repair of rectocele corrects obstructed defecation if it is not associated with anismus. *Dis Colon Rectum* 1999; **42**: 1544-1550 [PMID: 10613472 DOI: 10.1007/BF02236204]
 - 37 **Vahabi S**, Abaszadeh A, Yari F, Yousefi N. Postoperative pain, nausea and vomiting among pre- and postmenopausal women undergoing cystocele and rectocele repair surgery. *Korean J Anesthesiol* 2015; **68**: 581-585 [PMID: 26634082 DOI: 10.4097/kjae.2015.68.6.581]
 - 38 **Naldini G**. Serious unconventional complications of surgery with stapler for haemorrhoidal prolapse and obstructed defaecation because of rectocele and rectal intussusception. *Colorectal Dis* 2011; **13**: 323-327 [PMID: 20002689 DOI: 10.1111/j.1463-1318.2009.02160.x]
 - 39 **Titu LV**, Riyad K, Carter H, Dixon AR. Stapled transanal rectal resection for obstructed defecation: A cautionary tale. *Dis Colon Rectum* 2009; **52**: 1716-1722 [PMID: 19966603 DOI: 10.1007/DCR.0b013e3181b550bf]
 - 40 **Boccasanta P**, Venturi M, Roviato G. What is the benefit of a new stapler device in the surgical treatment of obstructed defecation? Three-year outcomes from a randomized controlled trial. *Dis Colon Rectum* 2011; **54**: 77-84 [PMID: 21160317 DOI: 10.1007/DCR.0b013e3181e8aa73]
 - 41 **Zhang B**, Ding JH, Zhao YJ, Zhang M, Yin SH, Feng YY, Zhao K. Midterm outcome of stapled transanal rectal resection for obstructed defecation syndrome: A single-institution experience in China. *World J Gastroenterol* 2013; **19**: 6472-6478 [PMID: 24151367 DOI: 10.3748/wjg.v19.i38.6472]
 - 42 **Bock S**, Wolff K, Marti L, Schmied BM, Hetzer FH. Long-term outcome after transanal rectal resection in patients with obstructed defecation syndrome. *Dis Colon Rectum* 2013; **56**: 246-252 [PMID: 23303154 DOI: 10.1097/DCR.0b013e31827619aa]
 - 43 **Guttadauro A**, Chiarelli M, Maternini M, Bainsi M, Pecora N, Gabrielli F. Value and limits of stapled transanal rectal repair for obstructed defecation syndrome: 10 years-experience with 450 cases. *Asian J Surg* 2018; **41**: 573-577 [PMID: 28693959 DOI: 10.1016/j.asjsur.2017.05.002]

P- Reviewer: Boeckxstaens GE, Fernandez JM, Mulvihill SJ, Schmidt J

S- Editor: Yan JP **L- Editor:** Wang TQ **E- Editor:** Huang Y





Published By Baishideng Publishing Group Inc
7041 Koll Center Parkway, Suite 160, Pleasanton, CA 94566, USA
Telephone: +1-925-2238242
Fax: +1-925-2238243
E-mail: bpgoffice@wjgnet.com
Help Desk: <http://www.f6publishing.com/helpdesk>
<http://www.wjgnet.com>

